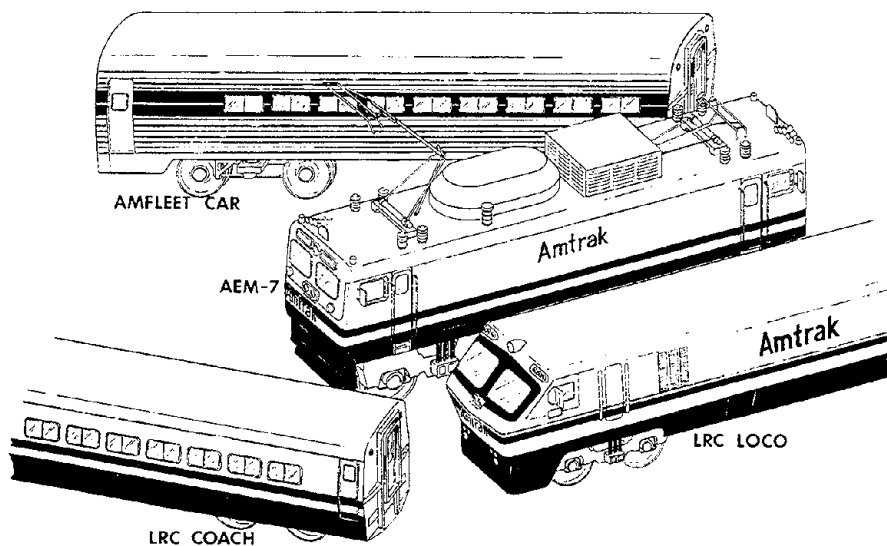


HIGH CANT DEFICIENCY TESTING OF THE LRC TRAIN, THE AEM-7 LOCOMOTIVE, AND THE AMCOACH

PATRICK L. BOYD - ROBERT E. SCOFIELD - JOSEPH P. ZAIKO

ENSCO, INC.
TRANSPORTATION TECHNOLOGY ENGINEERING DIVISION
5400 Port Royal Road
Springfield, VA 22151



Document is available to the U.S. public through the
National Technical Information Service,
Springfield, Virginia 22161

JANUARY 1982

REPRODUCED BY
U.S. DEPARTMENT OF COMMERCE
NATIONAL TECHNICAL
INFORMATION SERVICE
SPRINGFIELD, VA 22161

Prepared for:



U.S. DEPARTMENT OF TRANSPORTATION
Federal Railroad Administration
Office of Freight & Passenger Systems
400 Seventh Street, S.W.
Washington, DC 20590



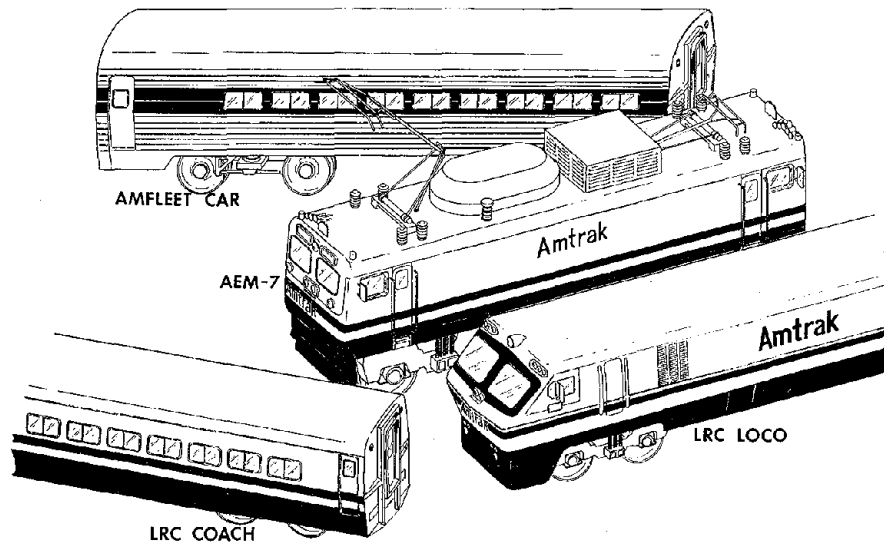
AMTRAK
400 North Capitol St. N.W.
Washington, DC 20001

1. Report No.	2. Government Accession No.	3. Recipient's Catalog No. PB82 213018	
4. Title and Subtitle HIGH CANT DEFICIENCY TESTING OF THE LRC TRAIN, THE AEM-7 LOCOMOTIVE AND THE AMCOACH		5. Report Date January 1982	6. Performing Organization Code 1444-207
7. Author(s) P. L. Boyd, R. E. Scofield, and J. P. Zaiko		8. Performing Organization Report No. DOT-FR-81-06	
9. Performing Organization Name and Address ENSCO, INC. Transportation Technology Engineering Division 5400 Port Royal Road Springfield, VA 22151		10. Work Unit No. (TRAIS)	11. Contract or Grant No. DTFR53-80-C-00002
12. Sponsoring Agency Name and Address * U.S. Department of Transportation Federal Railroad Administration Office of Passenger and Freight Systems Washington, DC 20590		13. Type of Report and Period Covered FINAL REPORT	
15. Supplementary Notes *Co-Sponsored by: AMTRAK 400 North Capitol Street NW Washington, DC 20001		14. Sponsoring Agency Code	
16. Abstract Increasing the speed of passenger trains in existing curves has been proposed as an alternative to changing curve radii for the purpose of reducing trip times on the Northeast Corridor. This test evaluates safety at high cant deficiency by comparing direct wheel/rail force measurements to safety criteria from world-wide sources. Tests were performed on the advanced LRC train with banking coaches and the modern but conventional AEM-7 Locomotive and Amcoach. The criteria concerning safety against vehicle overturning set the cant deficiency limits of all four vehicles, and the crosswind allowance set lower limits for coaches than for locomotives. A typical curve limited to 60 mph by the current 3 inch cant deficiency limit could be negotiated by the LRC train at up to approximately 79 mph (9 inches cant deficiency) while holding the steady state lateral acceleration below the AAR ride comfort criterion of 0.1g. A conventional train with standard Amcoaches towed by an AEM-7 locomotive could negotiate the same curve safely at up to about 76 mph (8 inches cant deficiency), but the steady state lateral acceleration in the coach would increase to about 0.15g. This level of lateral acceleration is acceptable by the SNCF (French National Railway) criterion, but it is considered "strongly noticeable" by the AAR.			
17. Key Words Cant Deficiency Curving Safety High Speed Curving Instrumented Wheels LRC, AEM-7, Amcoach		18. Distribution Statement This document is available to the public through the National Technical Information Service, Springfield, VA 22161	
19. Security Classif. (of this report) Unclassified	20. Security Classif. (of this page) Unclassified	21. No. of Pages	22. Price

HIGH CANT DEFICIENCY TESTING OF THE LRC TRAIN, THE AEM-7 LOCOMOTIVE, AND THE AMCOACH

PATRICK L. BOYD - ROBERT E. SCOFIELD - JOSEPH P. ZAIKO

ENSCO, INC.
TRANSPORTATION TECHNOLOGY ENGINEERING DIVISION
5400 Port Royal Road
Springfield, VA 22151



Document is available to the U.S. public through the
National Technical Information Service,
Springfield, Virginia 22161

JANUARY 1982



U.S. DEPARTMENT OF TRANSPORTATION
Federal Railroad Administration
Office of Freight & Passenger Systems
400 Seventh Street, S.W.
Washington, DC 20590

Prepared for:



AMTRAK
400 North Capitol St. N.W.
Washington, DC 20001

i. a



TABLE OF CONTENTS

<u>Section</u>	<u>Title</u>	<u>Page</u>
1.0	EXECUTIVE SUMMARY	1-1
2.0	INTRODUCTION	2-1
3.0	PRINCIPAL MEASUREMENTS	3-1
3.1	Wheel/Rail Forces	3-1
3.1.1	Description of Strain Gage Bridges	3-2
3.1.2	Primary Sensitivity and Crosstalk	3-6
3.1.3	Ripple	3-9
3.1.4	Load Point Sensitivity	3-11
3.1.5	Thermal and Centrifugal Effects and Other Sources of Drift	3-13
3.1.6	Sensitivity to Longitudinal Force	3-13
3.1.7	Comparison of Wheel/Rail Forces Between Wayside (Rail) and Wheelset Measurements	3-15
3.2	Angle-of-Attack (AOA)	3-16
3.2.1	Sensor Coils	3-23
3.2.2	Sensor Oscillator	3-23
3.2.3	Thermal Stabilizer	3-23
3.2.4	Discriminator	3-24
3.3	Other Transducers	3-24
3.3.1	Accelerometers	3-24
3.3.2	Displacement Transducers	3-24
3.3.3	Automatic Location Detection (ALD)	3-24
3.4	Data Acquisition System (DAS)	3-24
3.5	Data Reduction	3-30
4.0	TESTING PROCEDURES	4-1
4.1	General	4-1
4.2	Phase I Amcoach Test General Discussion	4-2
4.3	Phase II LRC Train Test	4-14
4.4	Phase III AEM-7 Locomotive Test	4-16
4.5	Test Consist	4-17

TABLE OF CONTENTS (Cont'd)

<u>Section</u>	<u>Title</u>	<u>Page</u>
5.0	SAFETY AND COMFORT CRITERIA	5-1
5.1	Vehicle Overturning Criteria	5-1
	5.1.1 Overturning Criteria in Use	5-4
	5.1.2 Comparison of Overturning Criteria	5-15
5.2	Wheel Climb Criteria	5-18
5.3	Rail Rollover Criteria	5-23
5.4	Lateral Track Shift Criteria	5-27
5.5	Ride Quality Criteria	5-31
5.6	Recommended Safety and Ride Comfort Criteria	5-37
6.0	RESULTS OF TESTING THE LRC TRAIN AT HIGH CANT DEFICIENCY	6-1
6.1	Vehicle Overturning	6-1
	6.1.1 Wind Speed Effect	6-2
	6.1.2 Steady State Measurements	6-2
	6.1.3 Transient (Peak) Measurements	6-4
6.2	Rail Rollover	6-21
6.3	Lateral Track Shift	6-23
6.4	Wheel Climb	6-24
6.5	Ride Comfort	6-27
6.6	Maximum Operational Cant Deficiency	6-27
6.7	Comparison of Test Results to Simple Quasistatic Predictions	6-29
7.0	RESULTS OF TESTING THE AMCOACH AT HIGH CANT DEFICIENCY	7-1
7.1	Vehicle Overturning	7-1
	7.1.1 Wind Speed Effect	7-2
	7.1.2 Steady State Measurements	7-2
	7.1.3 Transient Measurements	7-5

TABLE OF CONTENTS (Cont'd)

<u>Section</u>	<u>Title</u>	<u>Page</u>
7.2	Rail Rollover	7-10
7.3	Lateral Track Shift	7-11
7.4	Wheel Climb	7-12
7.5	Ride Comfort	7-13
7.6	Maximum Operational Cant Deficiency	7-13
7.7	Comparison of Test Results to Simple Quasistatic Predictions	7-15
8.0	RESULTS OF TESTING THE AEM-7 LOCOMOTIVE AT HIGH CANT DEFICIENCY	8-1
8.1	Vehicle Overturning	8-1
	8.1.1 Wind Speed Effect	8-2
	8.1.2 Steady State Curving Measurements	8-2
	8.1.3 Transient Curving Measurements	8-4
	8.1.4 Transient Measurements at Tangent Switches	8-14
8.2	Rail Rollover	8-17
8.3	Lateral Track Shift	8-19
8.4	Wheel Climb	8-20
8.5	Ride Comfort	8-23
8.6	Maximum Operational Cant Deficiency	8-25
8.7	Comparison of Test Results to Simple Quasistatic Predictions	8-25
9.0	GENERAL CONCLUSIONS	9-1
10.0	REFERENCES	10-1
APPENDICES		
APPENDIX A	- Test Data Summary	A-1
APPENDIX B	- Quasistatic Curving Model	B-1
APPENDIX C	- Vehicle Characteristics	C-1
APPENDIX D	- Summary Report on Wayside Measurements (Battelle)	D-1

LIST OF ILLUSTRATIONS

<u>Figure Number</u>	<u>Title</u>	<u>Page</u>
1-1	Steady State Weight Transfer Characteristics of Test Vehciles (Using Least Favorable Curving Direction)	1-5
2-1	Cant Deficiency	2-2
3-1	Vertical Force Measurement Bridge	3-3
3-2	Triangular Output and "A+B" Processing	3-4
3-3	Lateral Force Strain Distribution	3-5
3-4	Lateral Force Measurement Bridge	3-7
3-5	Typical Wheelset Calibration Constants	3-10
3-6	Typical Uncorrected Variability	3-12
3-7	Longitudinal Force Strain Distribution	3-14
3-8	Typical Comparison of Wheelset and Wayside Lateral Force Measument at Curve 67 Eastbound	3-17
3-9	AOA Configuration	3-19
3-10	AOA Sensor in Free Space	3-20
3-11	AOA Sensor Centered Over Rail	3-21
3-12	AOA Sensor Displaced Laterally Over Rail	3-22
3-13	Instrumentation Layout	3-27
3-14	Accelerometer Configuration	3-28
3-15	DAS Configuration	3-29
3-16	DAS/CPU Configuration	3-31
3-17	Effect of Processing Filtering on Peak Vector Intercept	3-33
3-18	Effect of Processing Filtering on Peak Lateral Intercept	3-40
3-19	Effect of Processing Filtering On Peak Wheel L/V	3-41
3-20	Effect of Processing Filtering on Lateral Acceleration	3-42

LIST OF ILLUSTRATIONS (Cont'd)

<u>Figure Number</u>	<u>Title</u>	<u>Page</u>
5-1	General Vehicle Overturning Model	5-1
5-2	Freebody Diagram, Overturning Moment Criteria	5-6
5-3	Freebody Diagram for Weight Transfer Due to General Overturning Moment	5-10
5-4	Freebody Diagram, Vertical Load Reduction Ratio Criteria	5-14
5-5	Comparison of Various Overturning Safety Criteria for LRC Coach	5-16
5-6	Comparison of Various Overturning Safety Criteria for LRC Locomotive	5-17
5-7	Interpretation of Instantaneous L/V Measurements	5-21
5-8	Comparison of Various Wheel Climb Criteria	5-22
5-9	Cross Section Geometric Resistance to Rail Rollover	5-24
5-10	Rail Rollover Criteria, AEM-7 Specifications	5-26
5-11	Comparison of Various Lateral Track Shift Criteria	5-30
5-12	Relation of Subjective Comfort Rating to Carbody Lateral Acceleration for AAR Experiment	5-33
5-13	Features of Carbody Lateral Acceleration Referenced to Location on Curve	5-35
5-14	Typical "Transient Response Diagram" of "Carbody Vibration"	5-36
5-15	Suspension Frequency Response to Steady Sinusoidal Lateral Perturbation	5-38
6-1	Weight Vector Intercept Measurement (Zero Wind) vs. Allowed Lateral Wind Speed for LRC Locomotive and Coach Based on JNR Recommended Load Ratios	6-3
6-2	Steady State Measurement of LRC Coach Overturning Safety	6-5
6-3	Steady State Measurement of LRC Locomotive Overturning Safety	6-6

LIST OF ILLUSTRATIONS (Cont'd)

<u>Figure Number</u>	<u>Title</u>	<u>Page</u>
6-4	Comparison of Peak Weight Vector Intercept of Locomotive at Right Hand to Overturning Safety Criteria	6-7
6-5	Comparison of Peak Weight Vector Intercept of LRC Coach (Banking) at Right Hand Test Curve to Overturning Safety Criteria	6-8
6-6	Comparison of Peak Measurements of Weight Vector Intercept for Curves in NEC Test Zone to Maximum Peaks for Curves Limited by Steady State Overturning Criteria-LRC Coach, Left Curves, East	6-10
6-7	Comparison of Peak Measurements of Weight Vector Intercept for Curves in NEC Test Zone to Maximum Peaks for Curves Limited by Steady State Overturning Criteria-LRC Coach, Right Curves, East	6-11
6-8	Comparison of Peak Measurements of Weight Vector Intercept for Curves in NEC Test Zone to Maximum Peaks for Curves Limited by Steady State Overturning Criteria-LRC Coach, Left Curves, West	6-12
6-9	Comparison of Peak Measurements of Weight Vector Intercept for Curves in NEC Test Zone to Maximum Peaks for Curves Limited by Steady State Overturning Criteria-LRC Coach, Right Curves, West	6-13
6-10	Comparison of Peak Measurements of Weight Vector Intercept for Curves in NEC Test Zone to Maximum Peaks for Curves Limited by Steady State Overturning Criteria-LRC Locomotive, Left Curves, East	6-14
6-11	Comparison of Peak Measurements of Weight Vector Intercept for Curves in NEC Test Zone to Maximum Peaks for Curves Limited by Steady State Overturning Criteria-LRC Locomotive, Right Curves, East	6-15
6-12	Comparison of Peak Measurements of Weight Vector Intercept for Curves in NEC Test Zone to Maximum Peaks for Curves Limited by Steady State Overturning Criteria-LRC Locomotive, Left Curves, West	6-16

LIST OF ILLUSTRATIONS (Cont'd)

<u>Figure Number</u>	<u>Title</u>	<u>Page</u>
6-13	Comparison of Peak Measurements of Weight Vector Intercept for Curves in NEC Test Zone to Maximum Peaks for Curves Limited by Steady State Overturning Criteria-LRC Locomotive, Right Curves, West	6-17
6-14	Peak Truck L/V Ratios of the LRC Vehicles as Functions of Cant Deficiency Measured at Right and Left Test Curves	6-22
6-15	Comparison of Peak Lateral Force Measurements of Lead Wheel and Truck Side of LRC Vehicles to Track Shift Criteria	6-25
6-16	Peak Wheel L/V Ratio of LRC Vehicles as a Function of Cant Deficiency at the More Severe of Right and Left Test Curves	6-26
6-17	Steady State Lateral Acceleration of LRC Vehicles Compared to a Vehicle with Zero Roll Angle	6-28
6-18	Comparison of Steady State Weight Vector Intercept Predictions to Test Results for LRC Coach in Left Hand Curve	6-31
6-19	Comparison of Steady State Weight Vector Intercept Predictions to Test Results for LRC Coach in Right Hand Curve	6-32
6-20	Comparison of Steady State Carbody Lateral Acceleration Predictions to Test Results for LRC Coach in Left Hand Curve	6-33
6-21	Comparison of Steady State Carbody Lateral Acceleration Predictions to Test Results for LRC Coach in Right Hand Curve	6-34
6-22	Comparison of Steady State Net Truck Lateral Force Predictions to Test Measurements of High Rail Side Truck Lateral Force for LRC Coach in Left Hand Curve	6-35
6-23	Comparison of Steady State Net Truck Lateral Force Predictions to Test Measurements of High Rail Side Truck Lateral Force for LRC Coach in Right Hand Curve	6-36

LIST OF ILLUSTRATIONS (Cont'd)

<u>Figure Number</u>	<u>Title</u>	<u>Page</u>
6-24	Comparison of Steady State Weight Vector Intercept Predictions to Test Results for LRC Locomotive in Left Hand Curve	6-37
6-25	Comparison of Steady State Weight Vector Intercept Predictions to Test Results for LRC Locomotive in Right Hand Curve	6-38
6-26	Comparison of Steady State Carbody Lateral Acceleration Predictions to Test Results for LRC Locomotive in Left Hand Curve	6-39
6-27	Comparison of Steady State Carbody Lateral Acceleration Predictions to Test Results for LRC Locomotive in Right Hand Curve	6-40
6-28	Comparison of Steady State Net Truck Lateral Force Predictions to Test Measurements of High Rail Side Truck Lateral Force for LRC Locomotive in Left Hand Curve	6-41
6-29	Comparison of Steady State Net Truck Lateral Force Predictions to Test Measurements of High Rail Side Truck Lateral Force for LRC Locomotive in Left Hand Curve	6-42
7-1	Weight Vector Intercept Measurement (Zero Wind) vs. Allowed Lateral Wind Speed for Unloaded Amcoach Based on JNR Recommended Load Ratios	7-3
7-2	Steady State Measurement of Amcoach Overturning Safety	7-4
7-3	Comparison of Peak Measurements of Weight Vector Intercept for Curves in NEC Test Zone to Maximum Peaks for Curves Limited by Steady State Overturning Criteria-Amcoach, Right Curves, East	7-6
7-4	Comparison of Peak Measurements of Weight Vector Intercept for Curves in NEC Test Zone to Maximum Peaks for Curves Limited by Steady State Overturning Criteria-Amcoach, Right Curves, West	7-7

LIST OF ILLUSTRATIONS (Cont'd)

<u>Figure Number</u>	<u>Title</u>	<u>Page</u>
7-5	Comparison of Peak Measurements of Weight Vector Intercept for Curves in NEC Test Zone to Maximum Peaks for Curves Limited by Steady State Overturning Criteria-Amcoach, Left Curves, East	7-8
7-6	Comparison of Peak Measurements of Weight Vector Intercept for Curves in NEC Test Zone to Maximum Peaks for Curves Limited by Steady State Overturning Criteria-Amcoach, Left Curves, West	7-9
7-7	Steady State Lateral Acceleration of an Amcoach Compared to a Vehicle with Zero Roll and to a Tilting Coach	7-14
7-8	Comparison of Steady State Weight Vector Intercept Predictions to Test Results for Amcoach in Right Hand Curve	7-16
7-9	Comparison of Steady State Weight Vector Intercept Predictions to Test Results for Amcoach in Left Hand Curve	7-17
7-10	Comparison of Steady State Carbody Lateral Acceleration Predictions to Test Results for Amcoach in Right Hand Curve	7-18
7-11	Comparison of Steady State Carbody Lateral Acceleration Predictions to Test Results for Amcoach in Left Hand Curve	7-19
7-12	Comparison of Steady State Net Truck Lateral Force Predictions to Test Measurements of High Rail Side Truck Lateral Force for Amcoach in Right Hand Curve	7-20
7-13	Comparison of Steady State Net Truck Lateral Force Predictions to Test Measurements of High Rail Side Truck Lateral Force for Amcoach in Left Hand Curve	7-21
8-1	Weight Vector Intercept Measurement (Zero Wind) vs. Allowed Lateral Wind Speed for AEM-7 Locomotive Based on JNR Recommended Load Ratios	8-3
8-2	Steady State Measurement of AEM-7 Locomotive Overturning Safety	8-5

LIST OF ILLUSTRATIONS (Cont'd)

<u>Figure Number</u>	<u>Title</u>	<u>Page</u>
8-3	Comparison of Peak Weight Vector Intercept Measured on Entry Spiral of Left Hand Test Curve to Projected Maximum Peaks for Curves Limited by Steady State Overturning Criteria	8-6
8-4	Comparison of Peak Measurements of Weight Vector Intercept for Curves in NEC Test zone to Maximum Peaks for Curves Limited by Steady State Overturning Criteria-AEM-7, Left Curves, West	8-8
8-5	Comparison of Peak Measurements of Weight Vector Intercept for Curves in NEC Test Zone to Maximum Peaks for Curves Limited by Steady State Overturning Criteria-AEM-7, Right Curves, East	8-9
8-6	Comparison of Peak Measurements of Weight Vector Intercept for Curves in NEC Test Zone to Maximum Peaks for Curves Limited by Steady State Overturning Criteria-AEM-7, Left Curves, East	8-10
8-7	Comparison of Peak Measurements of Weight Vector Intercept for Curves in NEC Test Zone to Maximum Peaks for Curves Limited by Steady State Overturning Criteria-AEM-7, Right Curves, West	8-11
8-8	Comparison of Peak Measurements of Weight Vector Intercept at Switches in the NEC Test Zone to the Vehicle Overturning Safety Criteria	8-15
8-9	Comparison of Peak Measurements of Weight Vector Intercept at Switches in the NEC Test Zone to the Vehicle Overturning Safety Criteria	8-16
8-10	Peak Truck L/V Ratio of the AEM-7 Locomotive as a Function of Cant Deficiency Measured at Right and Left Test Curves	8-18
8-11	Comparison of Peak Lateral Force Measurements of Lead Wheel and Truck Side of the AEM-7 Locomotive to Track Shift Criteria	8-21
8-12	Peak Wheel L/V Ratio of the AEM-7 Locomotive as a Function of Cant Deficiency Measured at Right and Left Test Curves	8-22
8-13	Steady State Lateral Acceleration of the AEM-7 Locomotive Compared to a Vehicle with Zero Roll Angle	8-24

LIST OF ILLUSTRATIONS (Cont'd)

<u>Figure Number</u>	<u>Title</u>	<u>Page</u>
8-14	Comparison of Steady State Weight Vector Intercept Predictions to Test Results for AEM-7 Locomotive in Left Hand Curve	8-27
8-15	Comparison of Steady State Weight Vector Intercept Predictions to Test Results for AEM-7 Locomotive in Right Hand Curve	8-28
8-16	Comparison of Steady State Carbody Lateral Acceleration Predictions to Test Results for AEM-7 Locomotive in Left Hand Curve	8-29
8-17	Comparison of Steady State Carbody Lateral Acceleration Predictions to Test Results for AEM-7 Locomotive in Right Hand Curve	8-30
8-18	Comparison of Steady State Net Truck Lateral Force Predictions to Test Measurements of High Rail Side Truck Lateral Force for AEM-7 Locomotive in Left Hand Curve	8-31
8-19	Comparison of Steady State Net Truck Lateral Force Predictions to Test Measurements of High Rail Side Truck Lateral Force for AEM-7 Locomotive in Right Hand Curve	8-32

LIST OF TABLES

<u>Table Number</u>	<u>Title</u>	<u>Page</u>
1-1	Summary of Safety Parameter Limits for Specific Test Vehicles	1-6
1-2	Summary of Test Results	1-8
3-1	Comparison of Force Measurements Between LRC Locomotive Instrumented Wheelset (IW) and Wayside Instrumented Rail (IR) Curve 67 Eastbond (8/1/80)	3-18
3-2	LRC Data Channel Assignments	3-25
3-3	Unfiltered Chart Peaks vs. Computer Data Reduction - LRC Locomotive - Curve 67 East (8/26/80) Weight Vector Crossing	3-35
3-4	Unfiltered Strip Chart Peaks vs. Computer Data Reduction - LRC Locomotive - Curve 67 East (8/26/80) Lead Wheel Lateral Force	3-36
3-5	Unfiltered Strip Chart Peaks vs. Computer Data Reduction LRC Locomotive - Curve 67 East (8/26/80) Lead Wheel L/V Ratio	3-37
4-1	Phase I Test Summary	4-3
4-2	Description of Curves Between Providence, RI (MP 180) and New Haven, CT (MP 73)	4-4
4-3	Phase II Test Summary	4-15
4-4	Phase III Test Summary	4-16
4-5	Description of Curves Between New York (MP 11) and Washington (MP 132-from Philadelphia)	4-18
5-1	Lateral Acceleration Ride Comfort Criteria	5-34
6-1	Curves at Which the LRC Coach Peak Vector Weight Intercept was High in Relation to Cant Deficiency	6-19
6-2	Curves at Which the LRC Locomotive Peak Weight Vector Intercept was High in Relation to Cant Deficiency	6-20
8-1	Curves at Which the Peak Weight Vector Intercept was High in Relation to Cant Deficiency for AEM-7 Locomotives	8-12

1.0 EXECUTIVE SUMMARY

This report describes high speed curving tests performed by ENSCO under a joint FRA/Amtrak project. Tests on the LRC locomotive, the LRC banking coach, the standard Amcoach and the AEM-7 locomotive measured high speed curving dynamics and developed data to support petitions for modifications of the FRA curving speed regulations applicable to these vehicles.

To perform the required high speed curving tests, the vehicles were equipped with instrumented wheels, carbody accelerometers, and displacement transducers. Safety limits were established based on a review of world wide safety research studies. The measurements from instrumented wheels and other transducers were processed in real time by the data acquisition system. The measurements were displayed on charts for constant safety monitoring and were collected on magnetic tape for detailed post processing and analysis.

The instrumented vehicles were first tested at a curve site equipped with force sensing rail instrumentation. The instrumentation techniques and calibration of the new instrumented wheels were confirmed by excellent agreement with the independent way-side measurements and by laboratory calibrations.

The first type of test of each vehicle consisted of repetitive runs at increasing speed over the same two curves to investigate steady state curving performance. In the repetitive runs the Amcoach was tested at up to nine inches of cant deficiency and the LRC train was tested at up to 15 inches of cant deficiency. Fifteen inches of cant deficiency corresponds to 105 mph at a test curve ordinarily limited to 70 mph. (See Figure 2-1 and page 2-1 for definitions of the relationship between speed and cant deficiency.) Similar repetitive runs were also performed on the AEM-7 locomotive at a test site located on the Philadelphia-Harrisburg line equipped with the required electrification. The AEM-7 was tested at over 11 inches of cant deficiency.

The second type of tests were "over-the-road" runs. In these tests the vehicles were run on a large sample of curves at high cant deficiency. The object was to investigate the transient performance of the vehicles over a wide range of typical perturbations. For the Amcoach and LRC equipment the "over-the-road" tests were run on the main line track between New Haven and Providence. The "over-the-road" tests on the AEM-7 locomotive were performed on the main line NEC track between Washington, DC and New York City.

In addition to the two test series described above, demonstration runs were performed on each of the test consists. For the demonstration run the results of the first two types of testing were reviewed and a target speed was chosen. The target speed was selected in terms of cant deficiency and the demonstration was conducted under a speed profile which appeared to be feasible for high cant deficiency operation.

The results of the repetitive tests and the over-the-road tests were processed using statistical routines. The primary objective of the data reduction was to organize the data so that the results could be compared to safety and comfort criteria.

Most of the data analysis effort was concentrated on the following principal numerics:

- o Speed
- o Carbody Lateral Acceleration
- o High Rail Lead Wheel Lateral Force
- o Low Rail Lead Wheel Vertical Force
- o High Rail Lead Wheel Vertical Force
- o High Rail Side Truck Lateral Force
- o High Rail Lead Wheel L/V Ratio
- o High Rail Side Truck L/V Ratio
- o Weight Vector Intercept

When time consuming examination of analog strip charts is used to identify peak data, the level which was exceeded for no more than 40 milliseconds is a good indication of the intensity of transient phenomena. The analog strip chart data from the repetitive runs on the same curve were compared to the results obtained from the computer derived statistical data reduction. The comparison showed that the 95th percentile level from the statistical analysis (95% of the data points are less than this value) agreed closely with the peaks (40 ms exceedance) identified by chart readings. Therefore, the 95th percentile statistical level was used for comparison to safety criteria where peak measurements were appropriate.

European, Japanese and U.S. safety criteria were reviewed and the following criteria were chosen for judging safety at high cant deficiency.

Vehicle Overturning - source: JNR load ratio standards expressed as weight vector intercept

$$\begin{array}{l} \text{Steady State} \\ \text{Vector Intercept} \end{array} \leq 18 - (.0153V^2 Sh_{cp}/W) \text{ inches}$$

and

$$\begin{array}{l} \text{Peak Vector} \\ \text{Intercept} \end{array} \leq 24 - (.0153V^2Sh_{cp}/W) \text{ inches}$$

where:

V is the lateral wind speed in mph

S is the lateral surface area of the vehicle in ft²

h_{cp} is the height of the center of wind pressure in ft

W is one half of the unloaded weight of the vehicle in pounds

Wheel Climb - source: Amtrak Acceptance specification of AEM-7 locomotive

$$\text{Peak Wheel (L/V)} < 0.056T^{-0.927} \quad \text{for } T < 50 \text{ ms}$$

$$\text{and, Peak Wheel (L/V)} \leq 0.90 \quad \text{for } T \leq 50 \text{ ms}$$

where L and V are simultaneous lateral and vertical wheel forces.

Rail Rollover - source: AAR

$$\text{Peak truck (L/V)} \leq 0.5 + 2300/P_w$$

where the high rail side of the truck is considered and P_w is the nominal single wheel vertical load. Higher values are permitted for durations less than 50 ms.

Track Panel Shift - source: SNCF criteria with correction factors for lateral wind force, internal thermal forces of CWR and typical U.S. tie spacing.

For typical NEC track:

Maximum Lateral Axle force,

$$F_{\max} = .61P + 5800 - 1.28 \times 10^{-3}SV^2$$

and maximum lateral truck force,

$$F_{\max} (\text{truck}) = .7N[.61P + 5800 - (1.28/.7N)10^{-3}SV^2]$$

where P is the vertical axle load, S is the lateral surface area of the vehicle, V is the lateral wind speed and N is the number of axles per truck.

Comparisons to peak wheel and truck side forces result in the most conservative conclusions concerning track panel shift.

When the weight, surface area, and shape of the specific test vehicles and the maximum wind speed* are considered, critical values of the safety parameters can be calculated as listed in Table 1-1.

Conclusions

All of the test vehicles were similar in that they were light weight and had two axle trucks with suspension systems advanced to the state-of-the-art or better. They were also similar in that the cant deficiency limit of each was set by the vehicle overturning safety criteria.

The allowance for 56 mph crosswinds is more restrictive for coaches than for locomotives due to their lower weight and greater body side area. Therefore, the coach will limit the operational cant deficiency of the train. The weight distribution of the instrumented truck of each vehicle deviated slightly from symmetry (c.g. up to 1-1/8 inches from the centerline). The steady state weight vector intercept for curving in the unfavorable direction (Figure 1-1) was used to determine the tentative limit on safe cant deficiency.

The peak weight vector intercepts were considered against the second overturning criteria. It was found that the cant deficiency was limited by steady state weight transfer except at a few special curves (see Tables 6-1, 6-2 and 8-1). Most of these special cases were curves with bridges or switches. Therefore,

*The wind speed at 15 ft. above ground level at Boston for a 10 year mean recurrence interval is 56 mph.

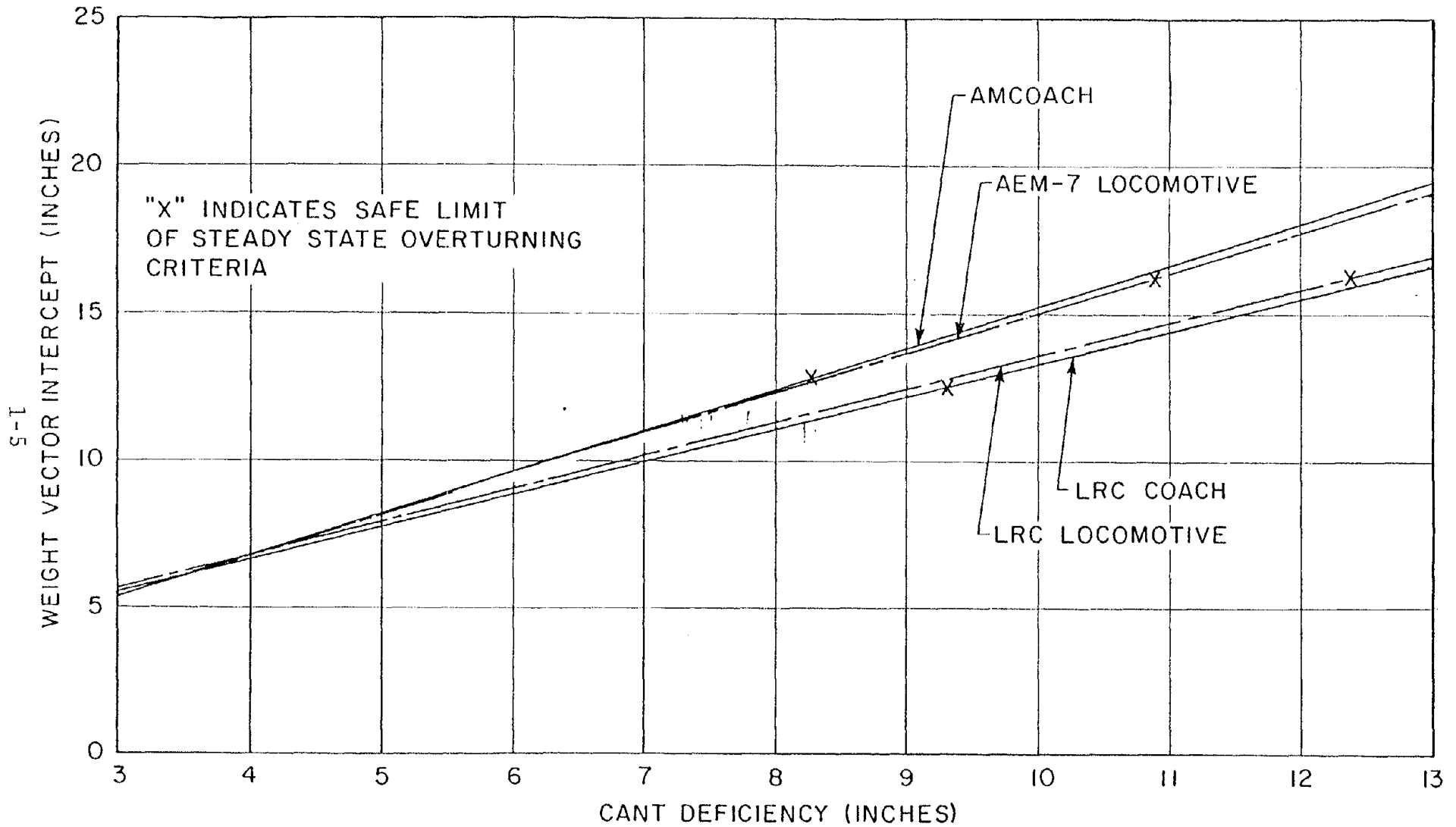


FIGURE I-1

STEADY STATE WEIGHT TRANSFER CHARACTERISTICS OF TEST VEHICLES
(USING LEAST FAVORABLE CURVING DIRECTION)

TABLE 1-1
SUMMARY OF SAFETY PARAMETER LIMITS FOR SPECIFIC TEST VEHICLES

<u>Hazard</u>	<u>Parameter</u>	<u>Limiting Value for Still Air Measurements</u>			
		<u>LRC</u> <u>Locomotive</u>	<u>LRC</u> <u>Coach</u>	<u>AEM-7</u> <u>Locomotive</u>	<u>Amcoach</u>
Vehicle Overturning	Steady State Weight Vector Intercept	16.3 in.	12.5 in	16.2 in.	12.8 in.
	Peak Weight Vector Intercept	22.3 in.	18.5 in	22.2 in	18.8 in.
Wheel Climb	Peak Wheel (L/V) T ≥50 ms	0.9	0.9	0.9	0.9
Rail Rollover	Peak Truck Side (L/V) T ≥50 ms	0.57	0.65	0.59	0.65
Track Panel Shift	Peak Lateral Axle Force	41,300 lb	18,200 lb	34,000 lb	18,700 lb
	Peak Lateral Truck Force	58,900 lb	26,900 lb	48,400 lb	27,300 lb

speed profiles to make use of the maximum recommended safe cant deficiency would require separate qualification of curves with switches and bridges. Speed restrictions at these curves may be unavoidable because of possible seasonal geometry perturbations due to track stiffness variations.

Table 1-2 summarizes the test results. The cant deficiency at the steady state weight vector intercept limit is given for each vehicle. The recommended maximum safe cant deficiency is based largely on steady state overturning because exceptional curves (without switches, bridges or grade crossings) are so few that remedial maintenance is practical. Also given is the cant deficiency limit based on peak weight vector intercept for the worst exceptional curve tested. Estimates of the other safety parameters at the maximum safe cant deficiency are listed, and they are well below the critical levels in Table 1-1. The steady state lateral acceleration at the maximum safe cant deficiency is given as an indication of ride comfort. It should be noted that the rougher test zone for the AEM-7 may be responsible for its higher peak (L/V) ratios and that high speed "S" curves should be checked for reaction with the tilt coach banking system before using maximum cant deficiency.

The maximum safe cant deficiency for a train is set by the coach. Table 1-2 suggests that LRC Train can run at 9 inches of cant deficiency while maintaining less than .1g steady state lateral acceleration by banking the coaches and that a train consisting of the AEM-7 locomotive and standard Amcoaches with Pioneer III trucks can run safely at 8 inches of cant deficiency at the expense of "strongly noticeable" steady state lateral acceleration.

TABLE 1-2
SUMMARY OF TEST RESULTS

	<u>LRC Locomotive</u>	<u>LRC Coach</u>	<u>AEM-7 Locomotive</u>	<u>Amcoach</u>
Recommended Maximum Operating Cant Deficiency	12 in.	9 in.	10 in	8 in.
Cant Deficiency at Steady State Weight Vector Intercept Limit	12.2 in	9.3 in	10.5 in.	8.3 in
Cant Deficiency at Worst Exceptional Curve for Peak Weight Vector Intercept Limit (curve in need of maintenance)*	10.6 in	8.7 in	8.5 in	8.5 in
<u>Estimated At Maximum Operating Cant Deficiency</u>				
Peak Wheel (L/V) Ratio	.60	.60	.75	.60
Peak Truck Side (L/V) ratio	.40	.40	.50	.40
Peak Lateral Truck Force	33,000 lb	15,000 lb	32,000 lb	18,000 lb
Steady State Lateral Acceleration	0.25g	0.09g	0.18g	0.15g

*Excluding curves with switches or bridges, which must be considered separately.

2.0 INTRODUCTION

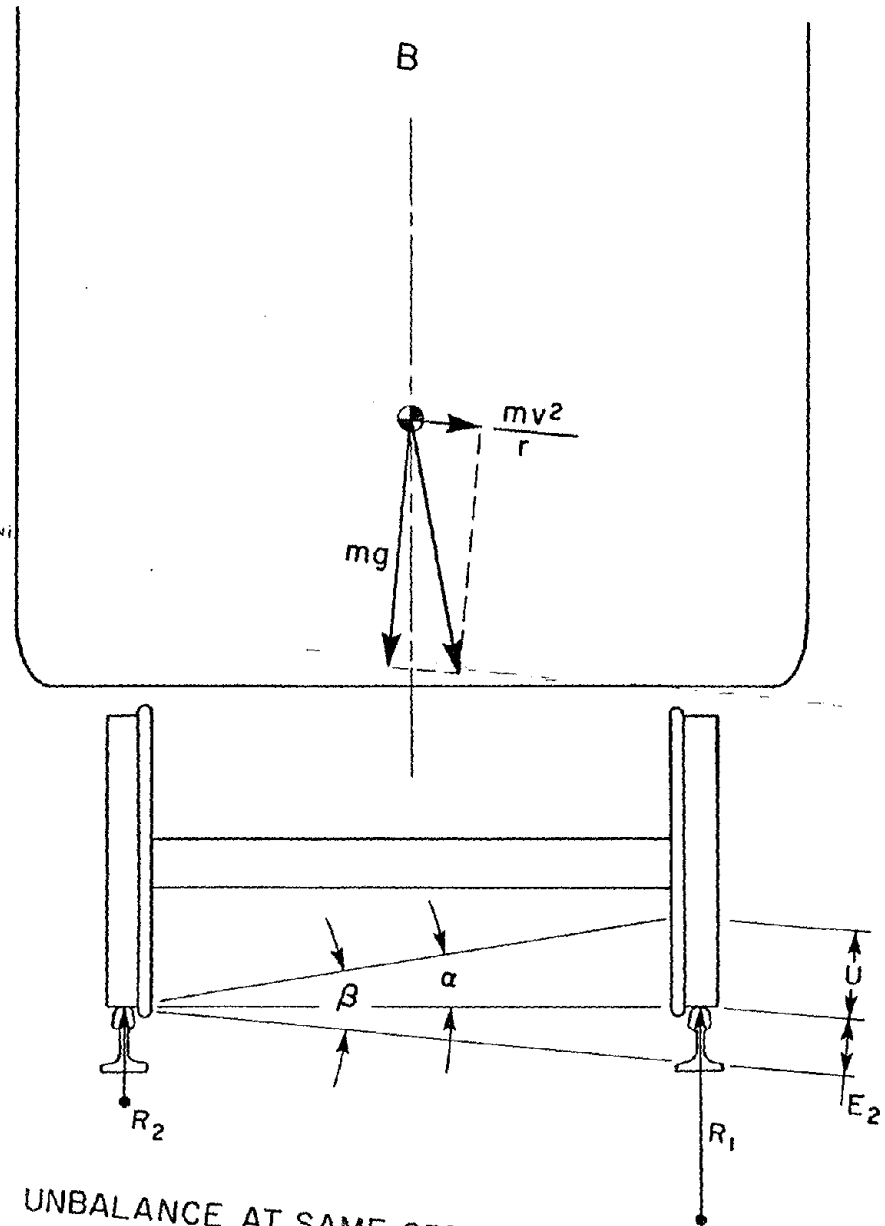
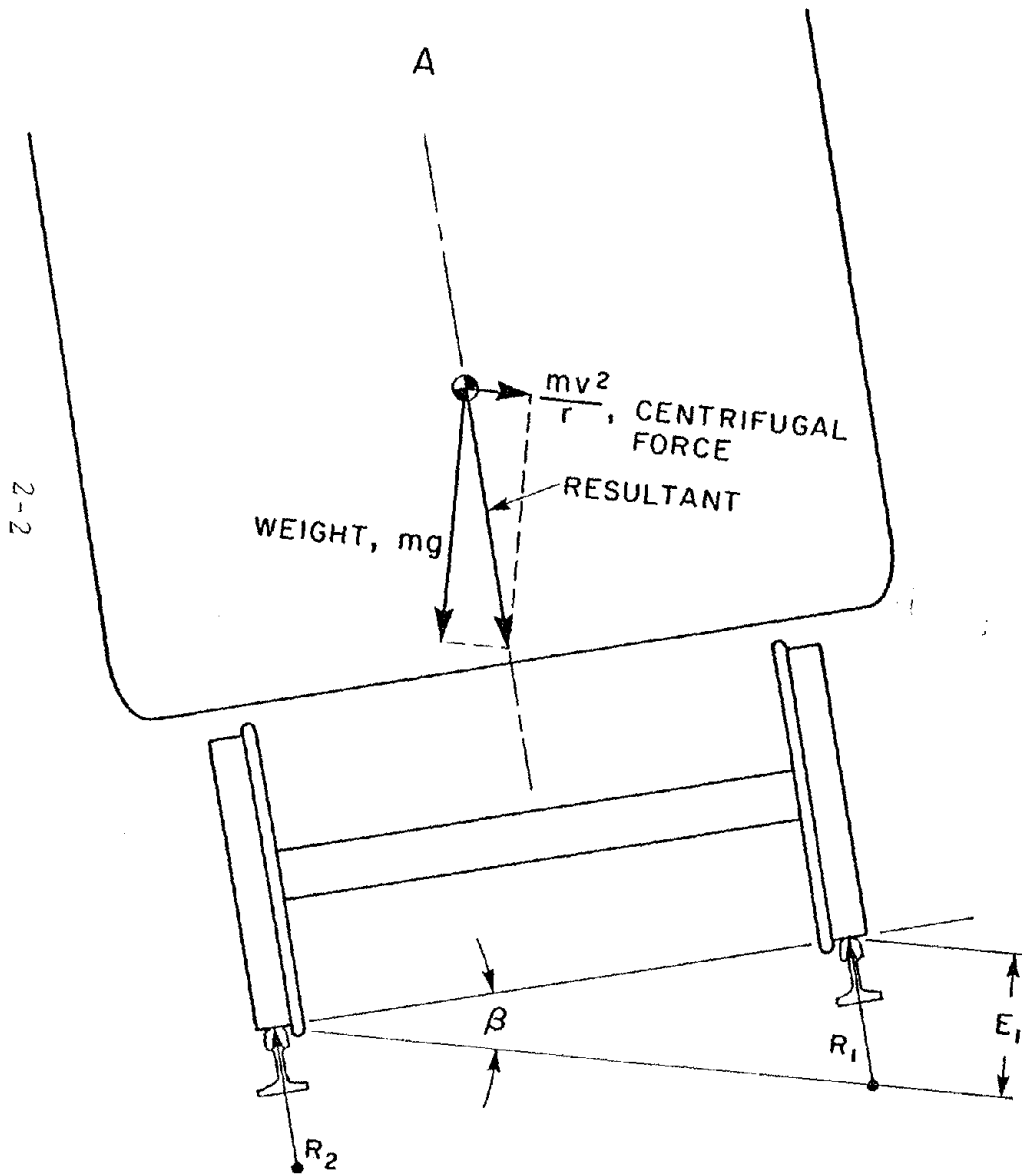
An efficient way to increase the average speed of passenger trains operating in the Northeast Corridor is to run faster through curves. At present, the maximum curving speeds are defined by the FRA Track Safety Standards based on maintaining conservative ride comfort standards for passengers and worst case safety considerations more applicable to freight cars.

Most other nations allow both tilt body and nontilting passenger trains to operate at higher speeds in curves. The Cant Deficiency Test Program described in this report provided extensive data supporting the argument for increasing allowable curving speeds for corridor trains. Analysis of the data indicates that modern passenger equipment is capable of negotiating curves at higher speeds without compromising passenger comfort or safety. This report describes the results of high speed curving tests which were performed on the LRC train, the standard Amcoach and the AEM-7 locomotive.

The LRC train (Light Rapid and Comfortable) was used for this test because the coaches are equipped with banking systems which tilt the coach bodies so that the passengers are not subjected to high centrifugal lateral forces. The use of tilt body coaches allows the train to operate at higher curving speeds without impairing passenger comfort. The LRC train and train systems operating in Japan and Europe have demonstrated that tilting coaches are an attractive solution for reducing the lateral accelerations resulting from increased curve speeds.

The test program focused on measurements required for the evaluation of safety and comfort at higher curving speeds. The measurements were recorded as functions of cant deficiency in order to compare the results at many curves. Cant deficiency expresses the intensity of curving by considering the curve radius and banking as well as vehicle speed. Figure 2-1 illustrates cant deficiency in the simplified case where the vehicle center of gravity is fixed on the track center line. In Figure 2-1A the track has sufficient crosslevel (or cant), E_1 , so that the resultant of the weight and centrifugal force vectors lies along the centerline of the track. Therefore, the rail forces, R_1 and R_2 are equal, and curving is said to be balanced with zero cant deficiency. In Figure 2-1B the weight vector, mg , and the centrifugal force vector, mv^2/r , are the same as in Figure 2-1A. The quantity, m , is the vehicle mass; g , the gravitational acceleration; v , the vehicle speed; and r , the curve radius. However, in Figure 2-1B the crosslevel, E_2 , is less. The resultant no longer lies on the center line, and the outer rail force is larger than the inner. The cant deficiency is U , the difference between the crosslevel for balance and the actual crosslevel.

CANT DEFICIENCY



BALANCE CONDITION AT SPEED v AND CROSSLEVEL E_1
 (VERTICAL RAIL FORCES R_1 AND R_2 ARE EQUAL)

UNBALANCE AT SAME SPEED AND CROSSLEVEL E_2
 CANT DEFICIENCY IS EQUALS $E - E_1$

This paper expresses cant deficiency in inches according to the American convention. The European convention is to express cant deficiency by the angle, α .

An evaluation of operating safety addresses the risks of vehicle overturning, wheel climb, rail rollover and track panel shift due to increased wheel/rail forces at higher curving speed. To obtain the required track and wheel forces and associated acceleration and displacement data, a detailed test plan was developed. The planning group included members from FRA, Amtrak, Battelle, ENSCO and Bombardier. This plan, implemented by ENSCO, required the development of three pairs of instrumented wheelsets capable of making continuous vertical and lateral force measurements. Since the equipment had to be operated at speeds well above the track speed permitted by current regulations, it was vital to have the capability of monitoring key parameters during the test.

To satisfy this requirement, a digital acquisition system was developed which recorded test data on digital tapes and computed real-time wheel/rail forces, vehicle roll over indicators and truck and wheel lateral to vertical force ratios, and displayed them on strip charts. In addition, a major part of the success of this test was the development of instrumented wheels for the LRC locomotive, the standard Amcoach and the LRC coach. The strain gaging techniques used by ASEA/SJ and EMD were reviewed, and the best features of these state-of-the-art wheels were considered in the design and construction of the FRA instrumented wheels. The gaging technique included empirical strain mapping at realistic loads, and computer aided selection of strain gage bridges for optimum sensitivity and crosstalk.

The testing was divided into three phases:

- Phase I - LRC locomotive and Amcoach as test vehicles
- Phase II - LRC locomotive and LRC coach as test vehicles
- Phase III - AEM-7 locomotive and LRC coach as test vehicles

The train consist for each test phase consisted of a test locomotive, a test coach, a data acquisition coach, and one or two additional coaches. The lead truck of the test locomotive and test coach were instrumented with force sensing wheels and other sensors.

Each phase of testing was divided into two parts. Part one consisted of repetitive runs on selected right and left hand curves at increasing speeds. Part two consisted of over-the-road testing on long Northeast Corridor routes at higher cant deficiencies.

The data acquisition system used to record data and monitor safety during testing was also used to perform post processing of the recorded data, including statistical analysis and graphic displays. The test program provided, for the first time, data concerning behavior of a variety of rail vehicles at high cant deficiency and specific evidence in the consideration of curving speed waivers for these and similar vehicles.

3.0 PRINCIPAL MEASUREMENTS

Measurements of wheel/rail forces, body accelerations at several locations, selected displacements of suspension and banking components, and wheel angle of attack to the rail were made at various levels of cant deficiency. The wheel/rail forces and the lateral acceleration at the floor of the vehicle provides direct comparison to criteria for safety and comfort performance. Wheel/rail forces were measured by special force sensing wheels on both axles of the lead truck of each vehicle, and wayside measurements were made at a selected site using an instrumented rail section. A data acquisition system was developed to process the various sensor outputs to produce measurements in engineering units, to display data in real time on strip charts, to make permanent digital tape recordings, and to perform statistical post processing.

3.1 WHEEL/RAIL FORCES

The instrumented wheelset is unsurpassed in obtaining accurate measurement of wheel/rail forces. The instrumented wheelset can provide accurate continuous measurements of lateral and vertical wheel/rail forces. It can measure frequencies up to 100 Hz or more, limited only by the fundamental resonant frequencies of the wheelset. Since the measurement is made in close proximity to the rail contact point (i.e., the wheelplate), the error introduced by inertial forces beyond the measurement point is negligible.

The objective of the design of force measuring wheels is to obtain adequate primary sensitivity for low signal/noise ratio and high resolution while controlling crosstalk, load point sensitivity, ripple, and the effects of heat, centrifugal force and longitudinal forces. The design philosophy is to choose strain gage bridge configurations which inherently minimize as many extraneous influences as possible and which are responsive to the general strain patterns expected in any rail wheel subjected to vertical and lateral forces. Such bridge configurations can be adapted to the standard production wheels of the desired test vehicles, eliminating problems of supply, mechanical compatibility, and possible alterations of vehicle behavior due to special wheels. The radial locations of the strain gages is optimized for each wheel size and shape while their angular locations are fixed by the chosen bridge configurations. The LRC locomotive, LRC coach, and Amcoach wheels have a large variation in tread diameter and wheelplate shape and yet were instrumented successfully using the same general procedures. Cast freight car wheels (70 ton) instrumented similarly for another FRA project will be included in the following discussion to illustrate the general applicability of the techniques.

3.1.1 DESCRIPTION OF STRAIN GAGE BRIDGES

The vertical force measuring bridges follow a concept used by ASEA/SJ (Ref. 18). Each bridge consists of eight strain gages arranged in a wheatstone bridge having two gages per leg. Each leg of the bridge has one strain gage on the field side and one strain gage on the gage side of the wheel. The four legs are evenly spaced 90° apart on the wheel as shown in Figure 3-1. The general strain distribution in a typical rail wheel plate due to a purely vertical load is characterized by maximum strains which are compressive and highly localized in the wheelplate above the point of rail contact. As the pair of gages in each leg of the bridge consecutively passes over the rail contact point, two negative and two positive peak bridge outputs occur per revolution. By correctly choosing the radial position of the gages, the bridge output as a function of rotational position of the wheel can be made to resemble a triangular waveform having two cycles per revolution. The purpose of having gages on both sides of the wheelplate in each leg is to cancel the effect of changes in the bending moments in the wheelplate due to lateral force and the change of axial tread/rail contact point.

When two triangular waveforms equal in amplitude and out of phase by one-fourth the wavelength, are rectified and added, the sum is a constant equal to the peak amplitude of the individual waveforms. In order to generate a strain signal proportional to vertical force and independent of wheel rotational position, the outputs of two identical vertical bridges out of phase by 45° of wheel arc are rectified and summed as shown in Figure 3-2. Since the bridge outputs do not have the sharp peaks of true triangular waveforms, the sum of one bridge peak and one bridge null is lower than that of two concurrent intermediate bridge outputs. In order to reduce the ripple or variation in force channel output with wheel rotation, the bridge sum is scaled down between the dips coinciding with the rounded bridge peaks. By taking as the force channel output the greatest of either individual bridge output or the scaled down sum of both bridges, the scaling down is applied selectively to the part of the force channel output between the dips as shown in Figure 3-2.

The general strain distribution of a typical rail wheelplate due to a purely lateral flange force is characterized by two components as shown in Figure 3-3. One component is a function of radius only because the wheelplate acts as a symmetric diaphragm in opposing the lateral force at the axle. The second component results from the moment about the hub caused by the flange force, and it tends to vary at a given radius with the cosine of the angular distance from the wheel/rail contact point. The strain distributions on the gage and field sides of the wheelplate are similar in magnitude, but opposite in sign (compression or tension).

VERTICAL FORCE MEASUREMENT BRIDGE

"A + B" TRIANGULAR OUTPUT (ASEA/SJ)

- TWO BRIDGES
- GAGES ON BOTH SIDES OF WHEELPLATE
- TRIANGULAR WAVEFORMS - 2 - CYCLES PER REVOLUTION
- $OUTPUT = MAX \{ |A|, |B|, K(|A| + |B|) \}$

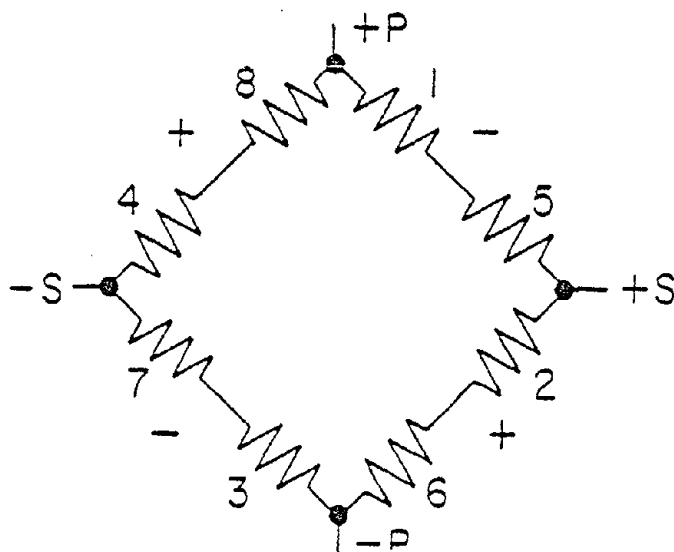
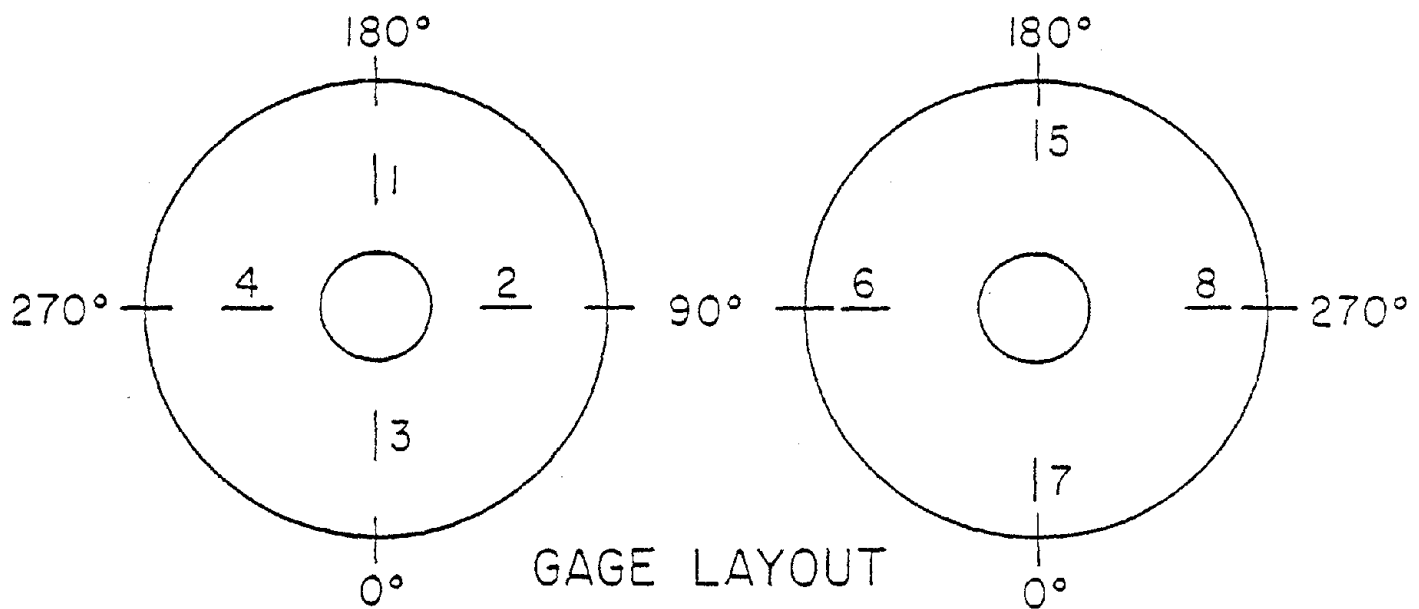


Figure 3-1
3-3

TRIANGULAR OUTPUT AND "A + B" PROCESSING

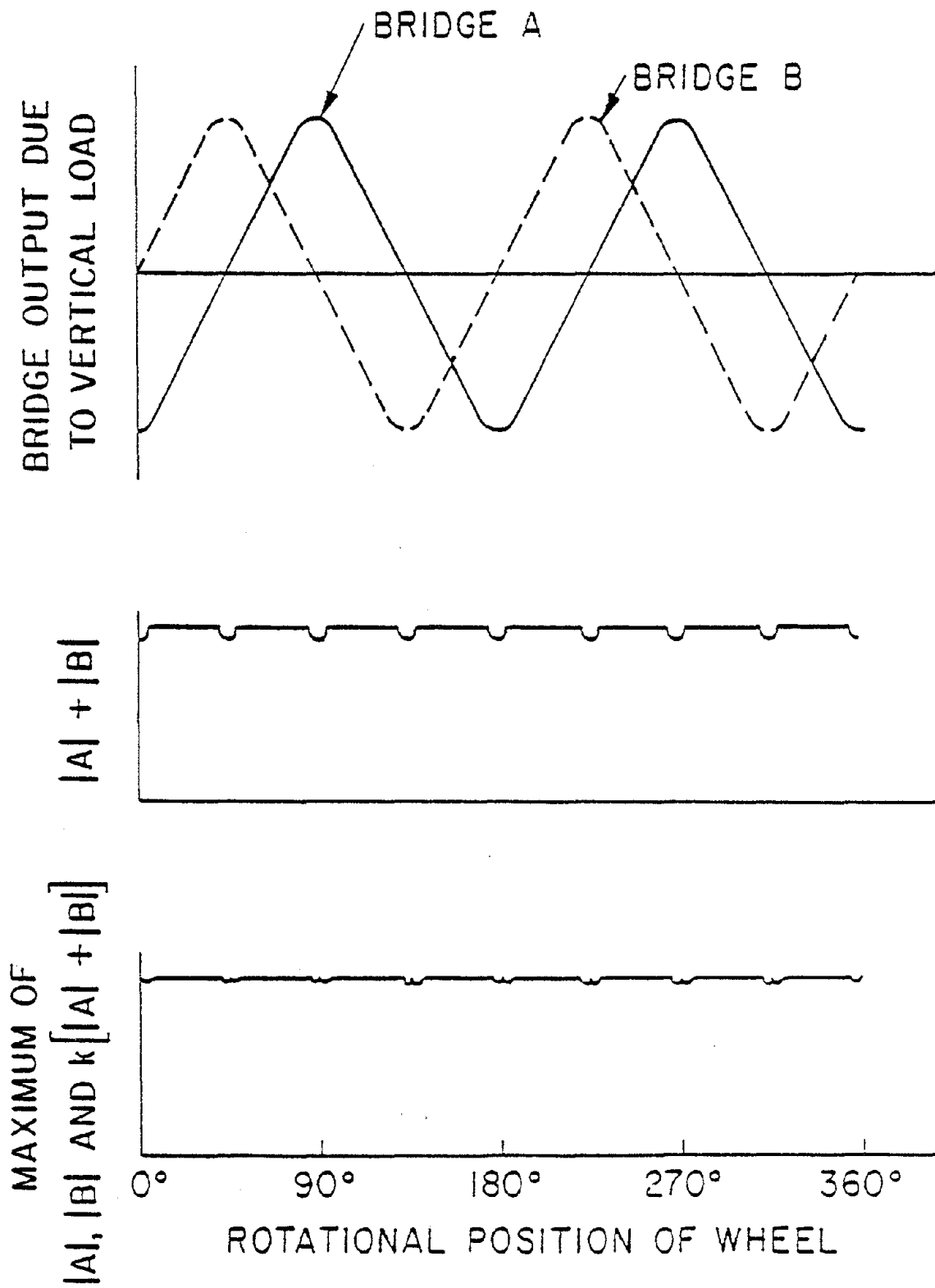
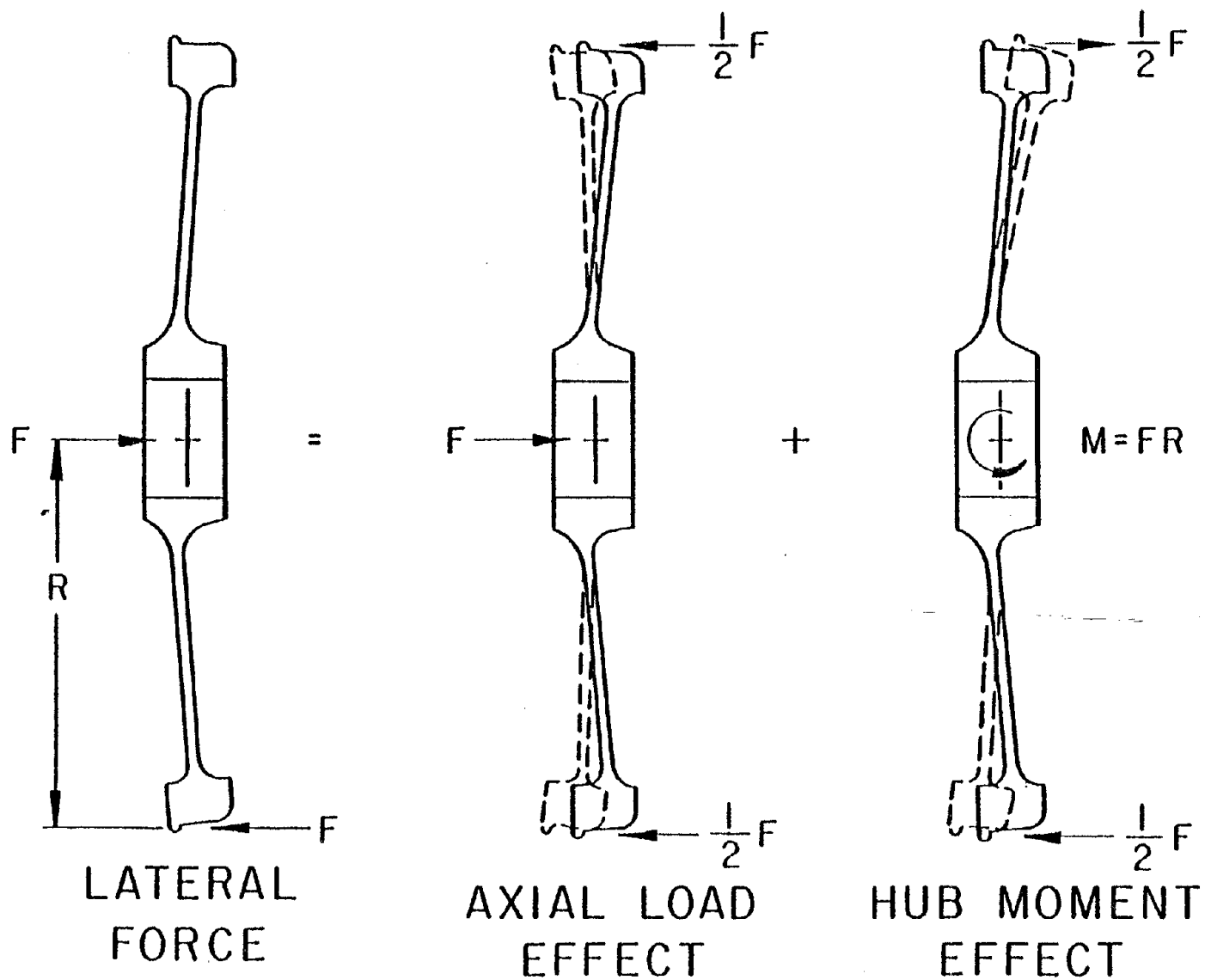


Figure 3-2

LATERAL FORCE STRAIN DISTRIBUTION



3-5

Figure 3-3

Lateral force measuring bridges, which follow a concept advanced by EMD (Ref. 19), take advantage of the general strain distribution in a standard rail wheelplate. As shown in Figure 3-4, each bridge is composed of eight gages evenly spaced around the field side of the wheelplate at the same radius. The first four adjacent gages are placed in legs of the bridge that cause a positive bridge output for tensile strain. The next four gages are placed in legs causing a negative bridge output for tensile strain. The resulting bridge cancels out the strain due to the axial load as all eight gages are at the same radius with four causing positive and four causing negative bridge outputs. However, the bridge is very sensitive to the sinusoidal strain component associated with the hub moment due to the flange force since the tensile strains and the compressive strains above and below the axle are fully additive in bridge output twice each revolution (once as a positive peak and once as a negative peak). Radial gage locations may be chosen such that the bridge output varies sinusoidally with one cycle per wheel revolution. Two identical bridges 90° out of phase are used to obtain a force channel output independent of wheel rotational position as a consequence of the geometric identity:

$$\sqrt{(L\sin\theta) + (L\sin\{\theta + 90^\circ\})} = L \text{ for any } \theta$$

3.1.2 PRIMARY SENSITIVITY AND CROSSTALK

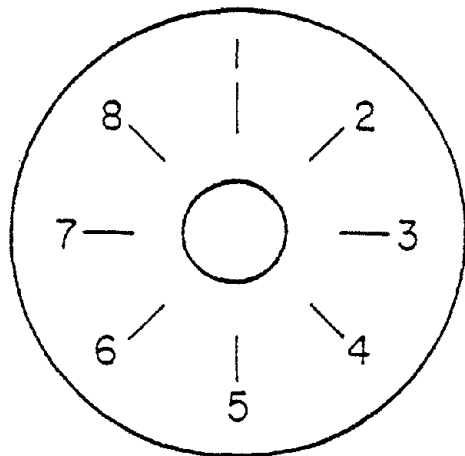
The first step in the production of instrumented wheels is the machining of all wheels in a production group to an identical contour. The contour is dictated by the minimum allowable wheelplate thickness and by the production variation of the available sample of wheels. The machining contour is usually close to the original design shape but at a minimum thickness. The thinning of the wheelplate is the easiest step in maximizing sensitivity because it does not involve compromise with the other measurement properties of the wheel.

The most powerful tool in selecting the radial locations of the strain gages for the best compromise between primary sensitivity, crosstalk, ripple, and sensitivity to axial load point variation is a detailed empirical survey of the strains induced in the given wheelplate by the expected service loads. The use of wheels machined to an identical profile makes the empirical approach to wheelset instrumentation practical since the results of the strain survey may be applied to all wheels in the group. The calibration loads and the reference lateral position of the wheel on the rail should reflect the type of experiment in which the wheels will be used.

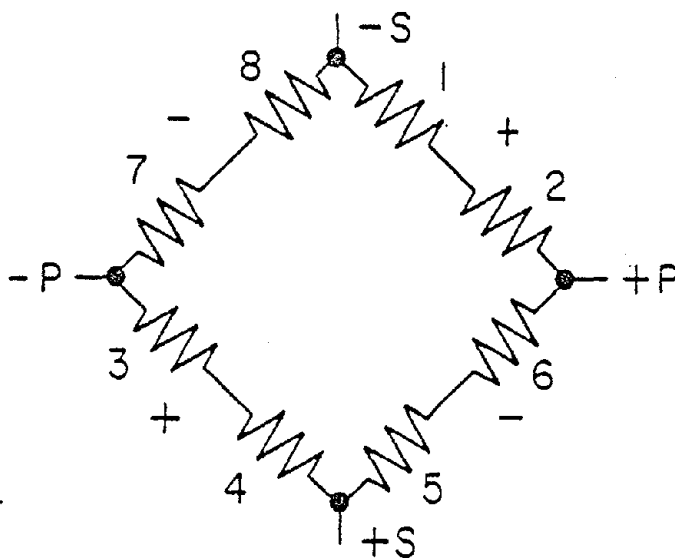
LATERAL FORCE MEASUREMENT BRIDGE

$\sqrt{\sin^2 + \cos^2}$ TECHNIQUE (EMD)

- TWO BRIDGES
- SINUSOIDAL OUTPUT
- 90° OUT OF-PHASE
- APPLIED AT SINGLE RADIUS TO ONE SIDE OF WHEELPLATE



GAGE LAYOUT



BRIDGE WIRING

Figure 3-4
3-7

For example, wheels destined to measure high speed curving forces should be loaded to about 1-1/2 times the nominal wheel load (to simulate load transfer) with the rail adjacent to the flange to determine the primary vertical sensitivity. Primary lateral sensitivity should be determined from a high lateral load (corresponding to expected L/V ratios) applied with a device which bears against the gage sides of two wheels on an axle at the tread radius and spreads the wheel apart. Loads applied in this manner create strains of equal magnitude and opposite sign to those produced by the hub moment effect of a flange load, but they eliminate the extraneous effect of the vertical load hub moment (treated as crosstalk) from the determination of primary lateral sensitivity. A combined vertical and lateral loading at the expected service L/V ratio level accomplished by forcing the wheelset laterally against a rail while maintaining a vertical load is necessary to select strain gage locations for minimal crosstalk. Vertical loadings at several points across the tread should be taken to evaluate the sensitivity to axial load point.

In the strain survey conducted on the FRA wheels strain gages were applied at intervals of one inch or less on both field and gage sides of the wheelplate along two radial lines separated by 180° of wheel arc. The calibration loads were repeated at every 15° of wheel arc until the strain along 24 equally spaced radial lines on both gage and field side was mapped for each load. This data was used in a computer program to predict the output of a force channel as a function of the radial locations of the gages in the companion bridges.

The vertical force measuring bridges of the FRA wheels have strain gages on both sides of the wheelplate. The simulation program allows the rapid trial of many combinations of gage and field side radii as potential strain gage locations. The maximum sensitivity possible, for a purely vertical load on a given wheel of a bridge actually producing the triangular waveform, is rapidly revealed. The "triangularity" of the waveform of a candidate bridge can be tested by adding its output at each angular load position to that at a load position advanced by 45° of wheel arc. This test determines the ripple expected of a force channel composed of two out of phase candidate bridges.

A lateral force effects the vertical bridge both by directly changing the strain pattern in the wheelplate and by moving the point of vertical load contact with the rail toward the flange. By using as a measurement of crosstalk the difference in bridge output caused by adding a lateral load to an existing vertical load, correction factors may be chosen which compensate for net lateral force crosstalk which includes direct lateral force crosstalk and the effect of vertical load point movement. It is desirable to identify vertical bridges in which the direct lateral force crosstalk and the effect of load point changes are

opposed and yield a minimum net crosstalk for flange forces in service. The accuracy of the highly loaded flanged wheel is enhanced by using a correction factor in processing based on the net lateral force crosstalk. Compromises in bridge selection are usually biased in favor of the flanged wheel because it generates the most vital data for vehicle dynamics or rail wear studies.

The primary sensitivities and crosstalk factors achieved for the cant deficiency test wheels and the freight car test wheels are shown in Figure 3-5. The vertical bridges were chosen from a detailed simulation with radial position increments of 0.1 inches on a basis of maximum primary sensitivity while holding the simulated crosstalk and ripple below 5% and minimizing sensitivity to axial load point. The primary sensitivity was observed to be linear within about 1% because the strains at each gage are low and the wheelplate behaves elastically. Primary vertical force sensitivity appears to be inversely proportional to tread diameter and wheelplate thickness for the several wheelplate shapes.

The lateral force measuring bridges of the FRA wheels have gages on only one side of the wheelplate, and the trial simulation of bridges is used to determine the most advantageous side of the wheel and the radial gage position. The primary sensitivity was determined from pure lateral loads applied with a spreader bar. The absolute value difference in lateral force indication between a combined vertical and lateral load on a rail and the pure lateral load with the spreader bar at the same lateral load is attributed to vertical force crosstalk. This method of crosstalk determination takes into account the vertical load point at the L/V ratios of interest. While a correction factor based on the vertical force crosstalk perfectly compensates a lateral force at the optimized L/V ratio, it is usually still accurate to about 2% of the lower lateral force at one-half the optimized L/V ratio.

Figure 3-5 gives the primary sensitivity and vertical force crosstalk actually achieved for several types of wheels. Lateral force measuring bridges of maximum sensitivity having less than 2% crosstalk and 5% ripple were sought in a simulation of possible bridges. Vertical load point sensitivity is not a great factor because the range of load points is narrow while lateral flange forces are being measured. The sensitivity of the sinusoidal lateral bridge is much greater than that of the triangular vertical bridge. Wheels of large tread diameter in general produce greater sensitivity.

3.1.3 RIPPLE

Ripple is caused by the failure of the bridges to produce the desired waveform and by deviation from the correct phase

TYPICAL WHEELSET CALIBRATION CONSTANTS

WHEEL DESCRIPTION	VERTICAL FORCE MEASUREMENT			LATERAL FORCE MEASUREMENT	
	SENSITIVITY	K	NET LATERAL FORCE CROSSTALK	SENSITIVITY	VERTICAL FORCE CROSSTALK
30" TREAD DIA., CONCAVE CONICAL WHEEL PLATE, 3/4" MIN. THICKNESS LRC COACH	$6 \frac{\mu\epsilon}{\text{kip}}$.94	2 %	$18 \frac{\mu\epsilon}{\text{kip}}$	1 1/2 %
33" TREAD DIA., CONCAVE CURVED WHEEL PLATE, 3/4" MIN. THICKNESS 70 TON FREIGHT CAR	$5 \frac{1}{2} \frac{\mu\epsilon}{\text{kip}}$.94	4 %	$16 \frac{1}{2} \frac{\mu\epsilon}{\text{kip}}$	3 %
36" TREAD DIA., CONVEX CONICAL WHEEL PLATE, 3/4" MIN. THICKNESS AMCOACH	$4 \frac{1}{4} \frac{\mu\epsilon}{\text{kip}}$.94	5 %	$17 \frac{\mu\epsilon}{\text{kip}}$	4 %
40" TREAD DIA., CONCAVE CONICAL WHEEL PLATE, 1" MIN. THICKNESS LRC LOCOMOTIVE	$3 \frac{1}{2} \frac{\mu\epsilon}{\text{kip}}$.92	1 1/2 %	$33 \frac{\mu\epsilon}{\text{kip}}$	1/2 %

3-10

Figure 3-5

relationship between the companion bridges which are processed together as a force channel.

The wheelplates are machined for uniformity to reduce ripple and a grid of radial and circumferential lines is scribed on the wheelplate to aid accurate gage placement. The massive computer aided simulation of trial bridges was used to determine gage locations of minimum inherent ripple. The ripple of the vertical force channel is reduced by attenuating the high bridge sums occurring between the rounded bridge peaks as shown in Figure 3-2. This method achieves a substantial reduction in ripple at a small cost in average sensitivity.

The lateral bridge output is inherently very sinusoidal. The requirement for two bridges at the same radius out of phase by 90° is in conflict with the 45° spacing between the gages in each bridge because theoretically both bridges should occupy the same space. Placing the gages side by side causes a deviation from the proper phase relationship which manifests itself as a ripple. Figure 3-6 gives the maximum ripple for each set of four wheels of four types. Larger wheels which have less phase deviation between lateral bridges also have less ripple. Combined loads caused greater ripple for both vertical and lateral channels because crosstalk produced distortions of the waveforms.

Ripple does not create as much error as might be supposed. Even the peak wheel forces measured during vehicle dynamics testing are averaged for 50 to 100 milliseconds. A 36-inch wheel makes a full revolution in 100 milliseconds at 64 mph, totally negating ripple in a 100 millisecond average wheel force. A single instantaneous measurement is rarely sought and any filtering has a mitigating influence on ripple.

3.1.4 LOAD POINT SENSITIVITY

The lateral bridge is sensitive to a lateral movement of the vertical load contact patch because it changes the hub moment. However, as shown in Figure 3-6, the vertical bridge is much more sensitive to load point than expected from the change in crosstalk due to the small change in lateral force measurement. The failure of the tread to transmit the moment due to load point offset uniformly into the wheelplate probably results in unusual changes to the local intense compressive strains in the wheelplate above the rail contact to which the vertical bridge is most sensitive. The high load point sensitivity of the 33-inch freight wheel having the thinnest tread supports this hypothesis.

The effect of load point sensitivity on measurements taken with the FRA wheels was minimized in two ways. Taking as the load

TYPICAL UNCORRECTED VARIABILITY

WHEEL DESCRIPTION	VERTICAL FORCE MEASUREMENT			LATERAL FORCE MEASUREMENT		
	SENSITIVITY TO AXIAL LOAD POINT	MAX. RIPPLE VERTICAL LOAD	MAX. RIPPLE COMBINED LOAD	SENSITIVITY TO AXIAL LOAD POINT	MAX. RIPPLE	MAX. RIPPLE COMBINED LOAD
30" TREAD DIA., CONCAVE CONICAL WHEEL PLATE, 3/4" MIN. THICKNESS LRC COACH	$+ 5.7 \frac{\%}{\text{inch}}$	$\pm 5 \%$	$\pm 8 \%$	$- 2.4 \frac{\%}{\text{inch}}$	$\pm 7 \%$	$\pm 7 \%$
33" TREAD DIA., CONCAVE CURVED WHEEL PLATE, 3/4" MIN. THICKNESS FREIGHT WHEEL	$+ 9.5 \frac{\%}{\text{inch}}$	$\pm 6 \%$	$\pm 6 \%$	$- 1 \frac{\%}{\text{inch}}$	$\pm 6 \%$	$\pm 7.5 \%$
36" TREAD DIA., CONVEX CONICAL WHEEL PLATE, 3/4" MIN. THICKNESS AMCOACH	$- 4.8 \frac{\%}{\text{inch}}$	$\pm 7 \%$	$\pm 10 \%$	$- 3.2 \frac{\%}{\text{inch}}$	$\pm 4 \%$	$\pm 6 \%$
40" TREAD DIA., CONCAVE CONICAL WHEEL PLATE, 1" MIN. THICKNESS LRC LOCOMOTIVE	$+ 4.7 \frac{\%}{\text{inch}}$	$\pm 5 \%$	$\pm 5 \%$	$- 3 \frac{\%}{\text{inch}}$	$\pm 4 \%$	$\pm 4 \%$

3-12

Figure 3-6

point for primary vertical sensitivity the wheel flange adjacent to the rail, causes the heavier loaded high rail wheel to deviate little from the calibrated load point. The additional movement of load point toward the flange under heavy lateral loading was accounted for in the net lateral force crosstalk correction factor. The lesser effect of vertical load point variation on lateral force was also accounted for in its crosstalk correction factor. The residual effect of load point variation is that load transfer from low rail wheel to high rail wheel in high cant deficiency curving is over estimated by about 5% because the low rail wheel is loaded at a less sensitive point on the tread.

3.1.5 THERMAL AND CENTRIFUGAL EFFECTS AND OTHER SOURCES OF DRIFT

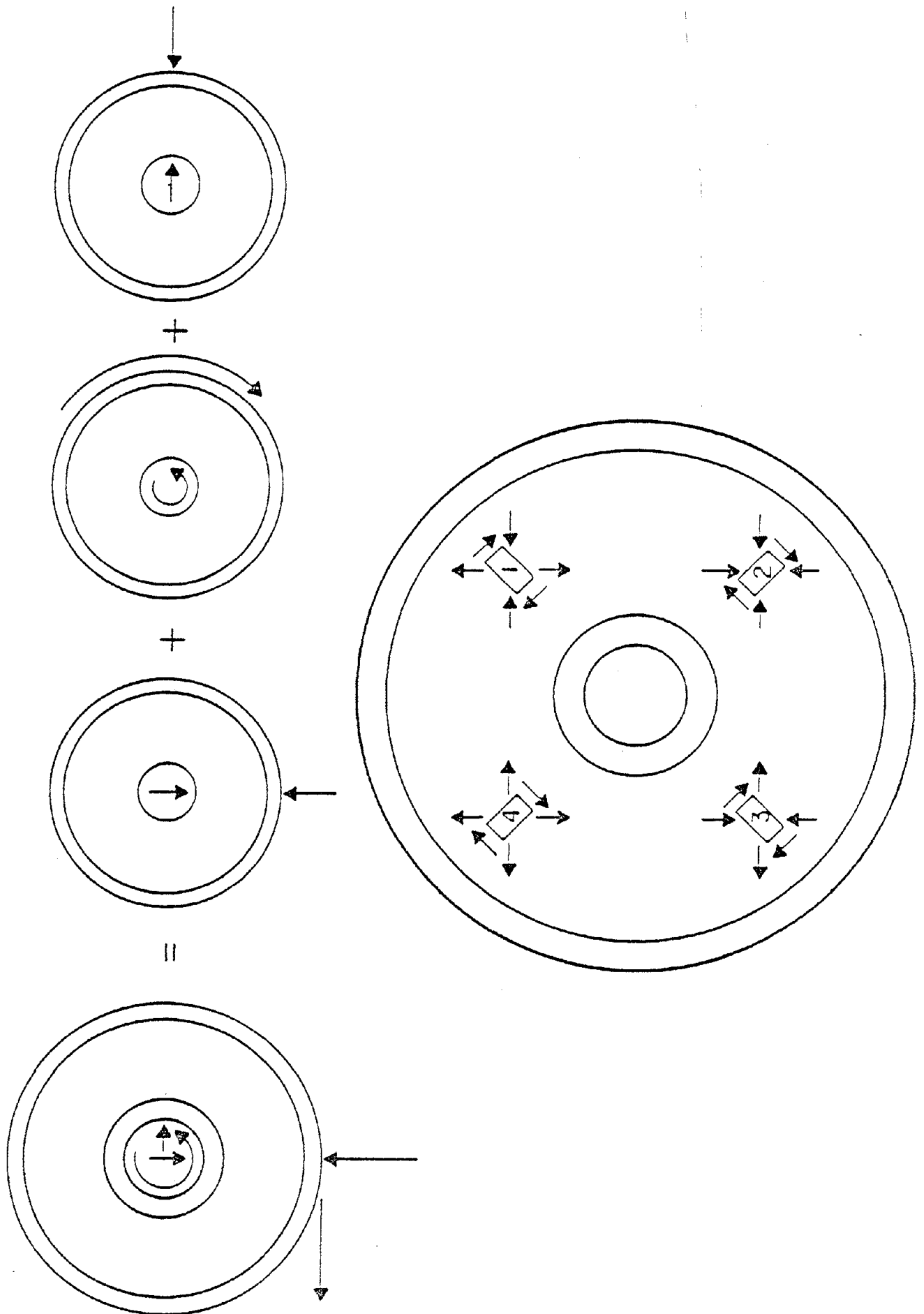
The vertical and lateral bridges used on the FRA wheelsets are particularly immune to drift by virtue of strain gage location and instrumentation technique. Strains induced by thermal change and centrifugal force are radially symmetric on each side of the wheelplate. The lateral bridge consists of eight gages at the same radius on the same side of the wheelplate positioned in the bridge so that four add and four subtract. A radially symmetric strain field is cancelled by the additions and subtractions. Similarly, the vertical bridges have four gages at the same radius on each side of the wheelplate. On each side two gages add and two subtract.

Each bridge generates a triangular or sinusoidal waveform as the wheel rotates under load. High pass filtering of the amplified bridge signals at 0.2 Hz does not attenuate the oscillating part of the signal but it forces the signal to oscillate about zero. High pass filtering eliminates gradual drift that could occur from thermal effects on the wheelset wiring and wheel to amplifier cabling and zero drift of the strain gage bridge amplifiers. It would also suppress thermal and centrifugal effects in bridges which do not self cancel them.

3.1.6 SENSITIVITY TO LONGITUDINAL FORCE

Longitudinal forces involved in braking and driving are extraneous influences on the vertical and lateral force measurement bridges. Brakes on instrumented wheelsets are usually disabled to avoid sensor damage caused by overheating and to avoid accidental flatspotting. However, instrumented wheelsets on self propelled vehicles must cope with driving forces. Figure 3-7 shows the strain distribution in a driven wheel. The longitudinal force may be resolved into a torque about the axle and a horizontal force perpendicular to the axle. The similarity between the horizontal force component and the vertical force suggests an error source.

LONGITUDINAL FORCE STRAIN DISTRIBUTION



The vertical force measuring bridges on the FRA wheelsets are configured in such a way as to cancel the effect of longitudinal forces. Figure 3-7 shows the strain components at four gage positions on one side of the wheelplate due to vertical and driving forces. The bridge is shown in the vertical null output position. Gages at 180° spacing add together in their contribution to the bridge summation. The vertical, horizontal and shear components of strain are opposite in sense for gages spaced 180° apart and cancel each other out retaining the null bridge output. The longitudinal force does not create an intense local strain aligned with the sensitive axis of a strain gage which stimulates the vertical bridge in any rotational position. The insensitivity of the vertical bridges to longitudinal force has also been verified experimentally.

The lateral bridges used on the FRA wheelsets are also insensitive to longitudinal forces. The symmetric gage pattern limits the effect of the shear strains, and the horizontal force has the effect of adding vectorially to the vertical force to produce crosstalk. Since the longitudinal force is limited by friction to about 1/4 the vertical load, the vector sum of forces is only about 3% higher than the vertical force alone. An increase in crosstalk of 3% of 4% (0.12%) is insignificant. If the measurement of driving force is desired, torque sensing bridges can be added to the axle between each wheel and the drive gear.

3.1.7 COMPARISON OF WHEEL/RAIL FORCES BETWEEN WAYSIDE (RAIL) AND WHEELSET MEASUREMENTS

The high rails of both Track 1 (westbound) and Track 2 (eastbound) of Curve 67 were instrumented for force measurement at six discrete sites each (see Appendix D for details). Comparisons between wayside measurements and instrumented wheelset measurements were made during Phase I and II of the test as an independent check of both methods.

The rail instrumentation produces a very sharp spike as the wheel rolls over an active strained gaged zone of about four inches at each site. The sites are placed about eight feet apart near the beginning of the curve body. The continuous wheel force measurement was displayed on a time based strip chart (equivalent to a distance based display at a constant curving speed). The locations of the wayside sites were indicated on a strip chart channel using an automatic location detection sensor (ALD) which produces voltage spikes in the proximity of sheet metal targets. The locomotive was parked with the lead axle at each site while a target was fastened to the tie under the ALD sensor located on the lead truck of the second coach so that the ALD sensor spikes marked the coincidence of the lead axle and each

wayside site. Figure 3-8 is an overlay of wheelsets and wayside lateral force data for a typical run on the wood tie track. Although lateral force gradients of over 2,500 pounds per foot of travel occur in the test zone the wayside and wheelset measurements correspond closely. The vertical forces have about the same gradient but lower total variation.

Table 3-1 compares vertical and lateral forces measured by the LRC locomotive lead wheel and by the instrumented high rail for runs at various speeds during the same day. The average force at each site compares within the variation that could be expected for a six-inch tolerance in ALD target placement. The standard deviation of the difference between wheelset and wayside measurements reflects a probable one-foot variability in matching continuous data to wayside sites due to draft gear movement and chart reading limitations. The good agreement between wayside and wheelset instrumentation and the ability to locate track features to within a foot relative to a continuous force measurement at over 80 mph are significant.

3.2 ANGLE-OF-ATTACK (AOA) SENSOR

Wheel angle-of-attack was provided by an eddy-current system developed by ENSCO Inc. Figure 3-9 shows the AOA system configuration for Phases I and II. Figures 3-10 to 3-12 viewed in sequence illustrate the principle of operation of the AOA sensor. The magnetic lines of flux are sketched at a particular instant in time to show how their patterns are influenced by the rail, but the send coils are actually subjected to ac excitation and it is the sequence of rise and decay of the magnetic field that induces an ac voltage response in the pick-up coil. The sensor moves laterally with the wheel but it is held far enough away that the steel wheel does not alter its operation. In the case of the Amcoach the sensors were placed to measure truck angle-of-attack because of mounting restrictions.

The angle-of-attack sensor is considerably more stable than most eddy current sensors because it separates the excitation coil from the sensing coil, and it employs a direct frequency modulation technique. Most eddy current sensors use the same coil to send the exciting field and to receive the reflected field. This has the disadvantage that the exciting current makes a small drift in the coil impedance, due to temperature or humidity changes, which appears the same as a reflected field. Because excitation and sensing is accomplished by different coils this effect is eliminated, and in addition, the circuit impedance can be chosen to minimize other coil impedance affects.

Amplitude drift and offset voltage severely limits the practical resolutions of most analog detection and data transmission

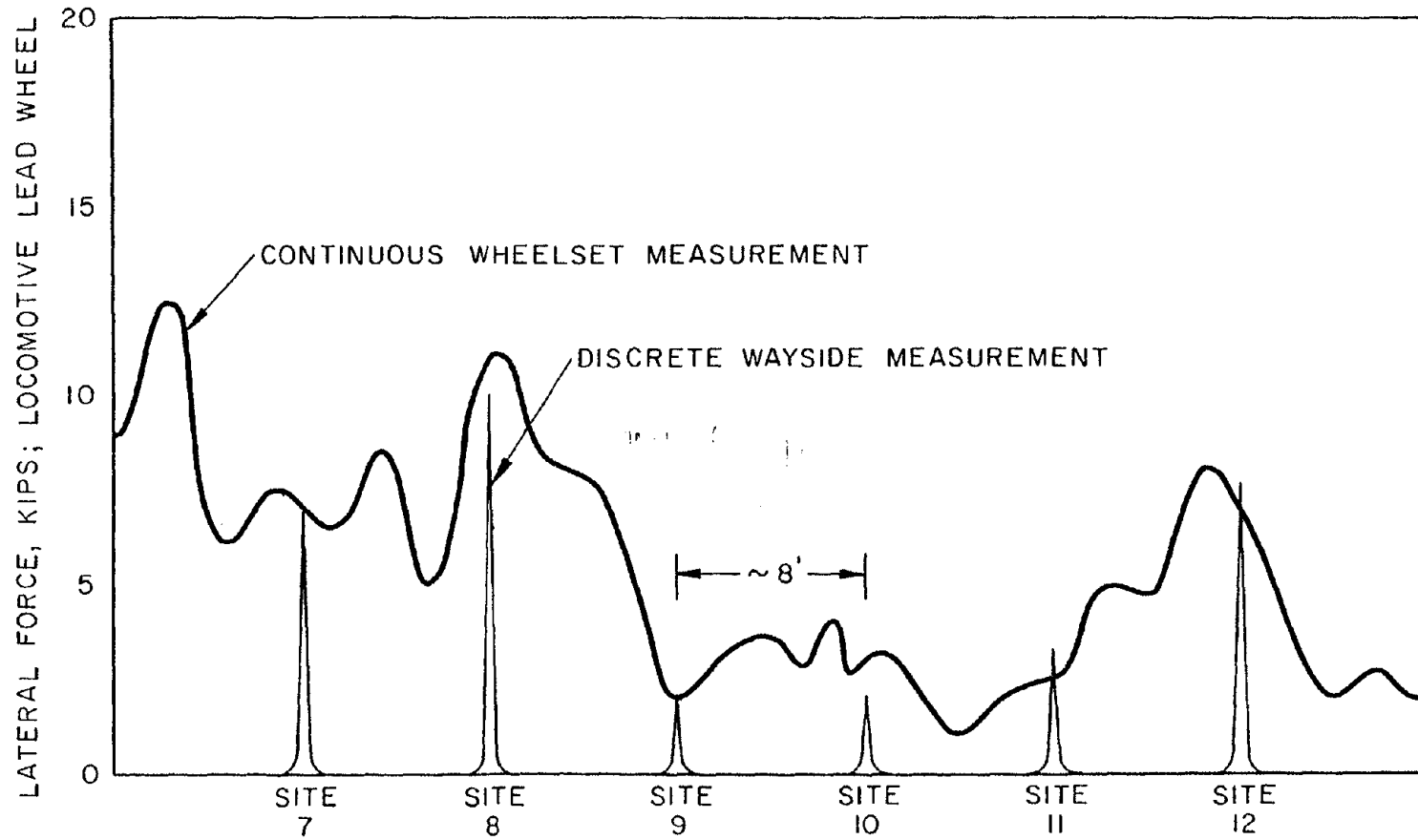


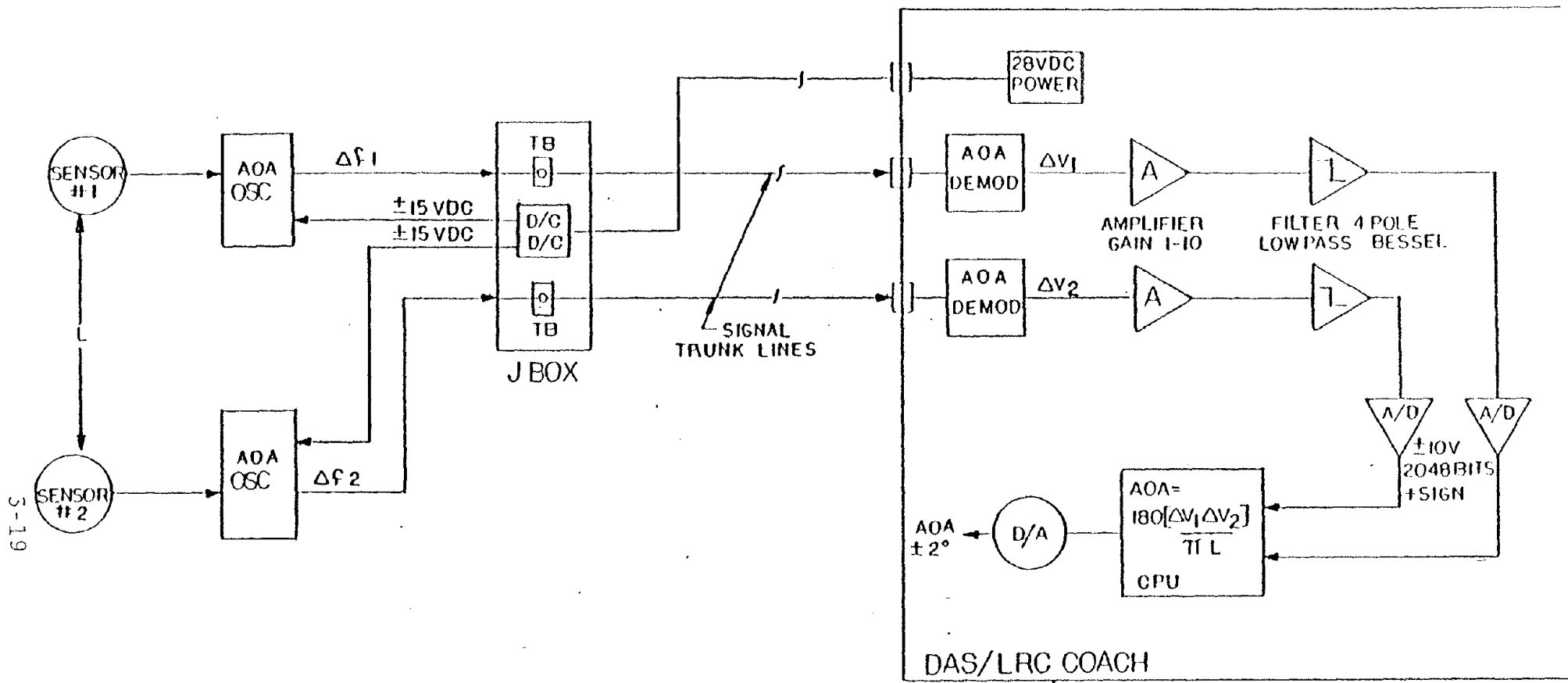
Figure 3-8. Typical Comparison of Wheelset and Wayside Lateral Force Measurement at Curve 67 Eastbound

TABLE 3-1

COMPARISON OF FORCE MEASUREMENTS BETWEEN LRC LOCOMOTIVE INSTRUMENTED
WHEELSET (IW) AND WAYSIDE INSTRUMENTED RAIL (IR) CURVE 67 EASTBOUND (8/1/80)

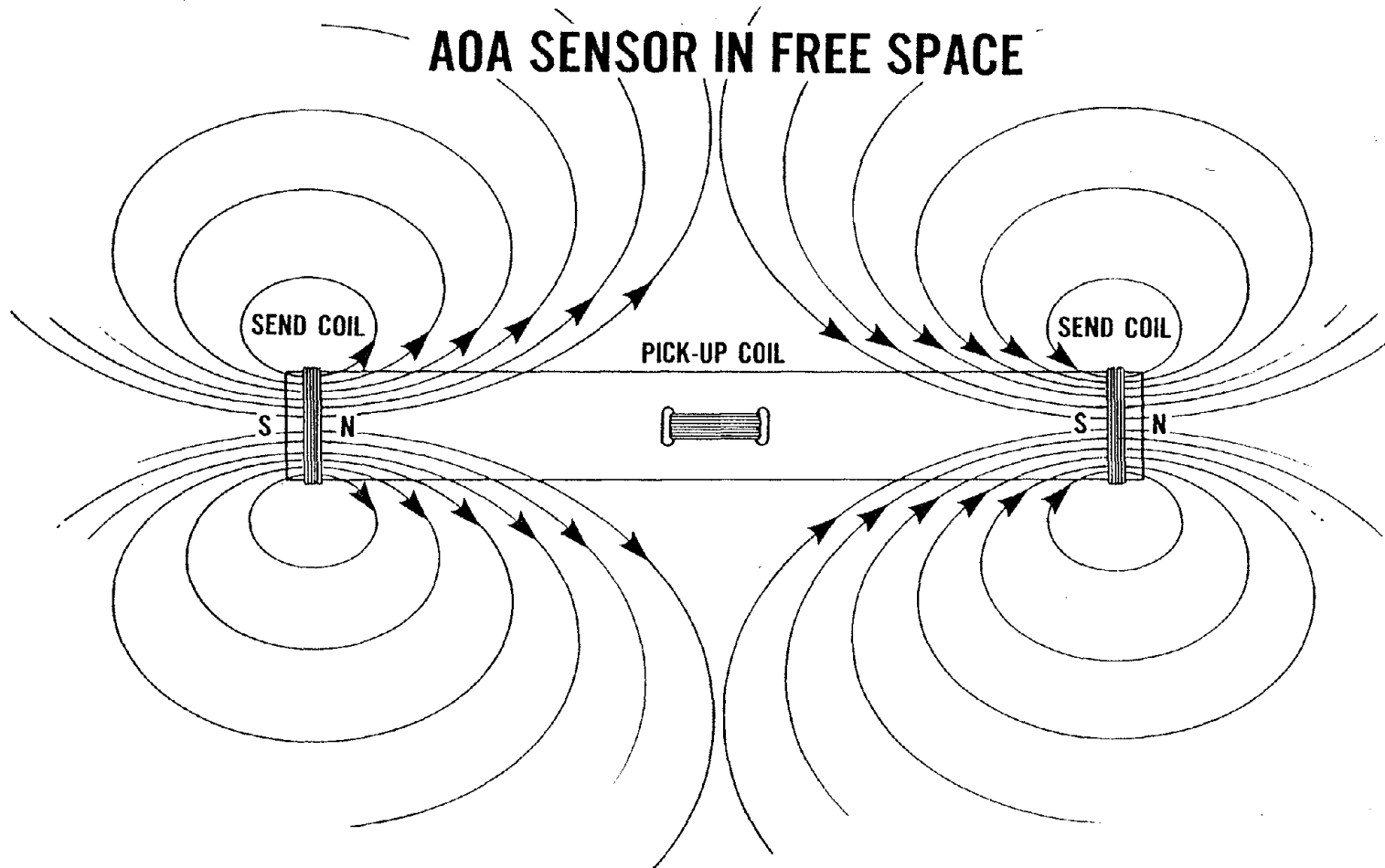
Run	Source	Lateral Force, Kips						Vertical Force, Kips						
		7	8	Site			7	8	Site			10	11	12
				9	10	11			12	9	10			
#1	IW	10.0	9.0	1.0	4.0	3.0	9.0	40.0	40.0	34.0	36.0	40.0	35.0	
80	IR	11.4	11.1	1.2	-	0.9	7.8	37.0	39.0	35.0	-	36.5	35.0	
mph	Δ	-1.4	-2.1	-0.2	-	2.1	2.2	3.0	1.0	-1.0	-	3.5	0.0	
#2	IW	10.5	13.0	2.0	3.5	2.0	5.5	40.0	42.0	40.0	38.0	42.0	36.0	
89	IR	8.4	14.7	3.3	-	1.8	3.3	36.5	41.0	40.5	-	42.5	35.0	
mph	Δ	2.1	-1.7	-1.3	-	0.2	2.2	3.5	1.0	-0.5	-	-0.5	1.0	
#3	IW	5.0	11.0	3.0	1.0	2.0	4.0	36.0	39.0	37.0	36.0	38.0	34.0	
85	IR	5.4	9.0	4.2	-	2.4	5.4	35.5	39.5	38.5	-	39.0	34.0	
mph	Δ	-0.4	2.0	-1.2	-	-0.4	-1.4	0.5	-0.5	-1.5	-	-1.00	0.0	
#4	IW	8.0	9.0	1.5	2.5	2.0	7.0	39.0	40.0	38.0	38.0	40.0	38.0	
87	IR	9.9	9.9	1.8	-	3.0	9.3	3.7	39.5	39.5	-	40.5	37.0	
mph	Δ	-1.9	-0.9	-0.3	-	-1.0	-2.3	2.0	0.5	-1.0	-	-0.5	1.0	
#5	IW	10.0	10.0	2.5	2.5	1.5	8.0	44.0	40.0	38.0	38.0	44.0	40.0	
88	IR	10.2	14.1	3.6	-	1.5	5.7	37.0	41.0	41.5	-	41.5	35.5	
mph	Δ	-2.0	-4.1	-1.1	-	0.0	-2.3	7.0	-1.0	-3.5	-	2.5	4.5	
Avg	IW	8.7	10.4	2.0	2.7	2.1	7.3	39.8	40.2	37.4	37.2	40.8	36.6	
	IR	9.1	11.8	2.8	-	1.9	6.0	36.6	40.0	38.9	-	40.0	35.3	
	Δ	-0.4	-1.4	-0.8	-	0.2	1.3	3.2	0.2	-1.5	-	0.8	1.3	
s.d. of Δ		1.5	2.2	0.5	-	1.2	3.2	2.4	0.9	1.2	-	2.0	1.9	

SI-5



AOA SYSTEM

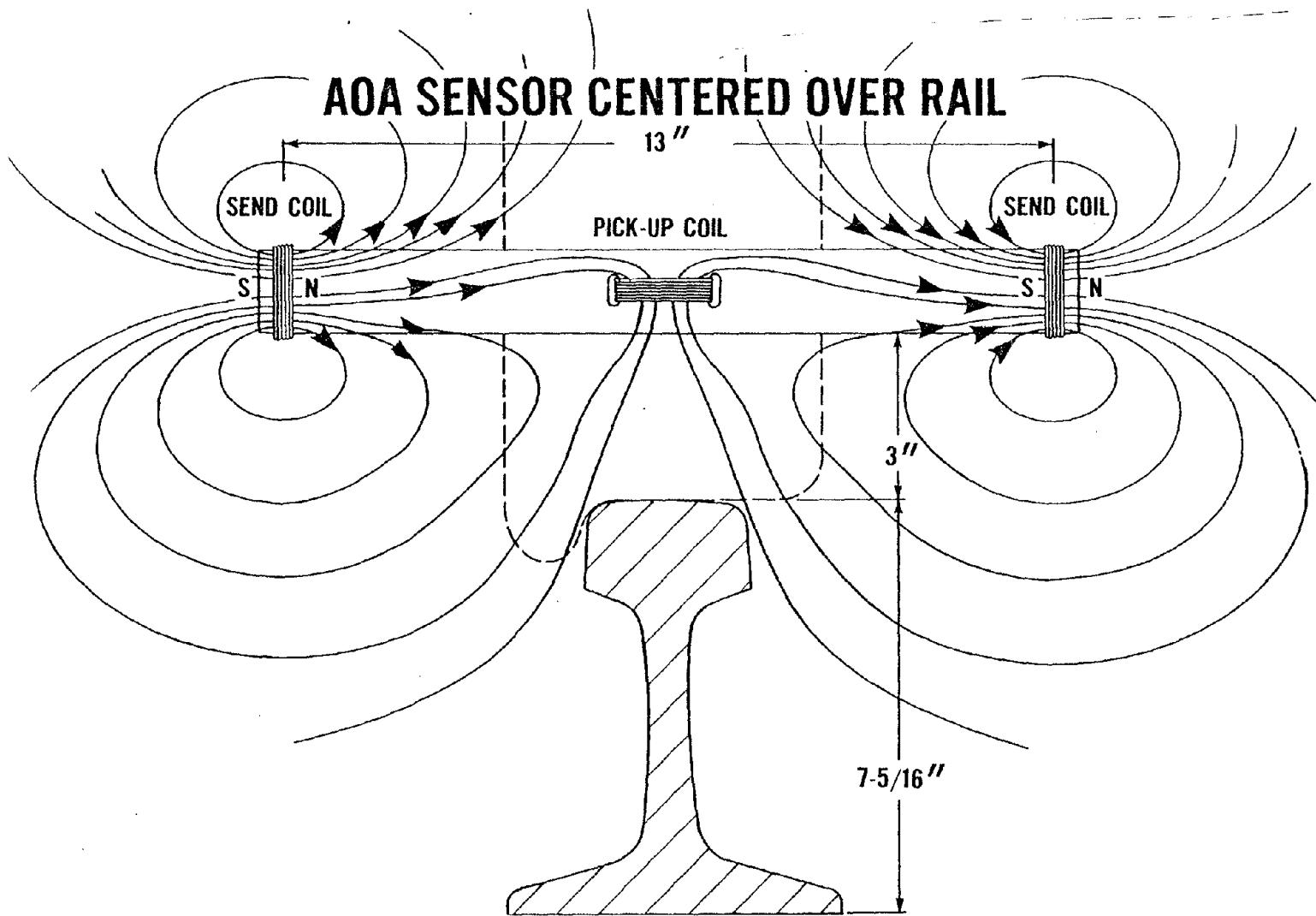
Figure 3-9. AOA Configuration



PICK-UP COIL IS NOT INFLUENCED BY SEND COIL FIELDS.

Figure 3-10

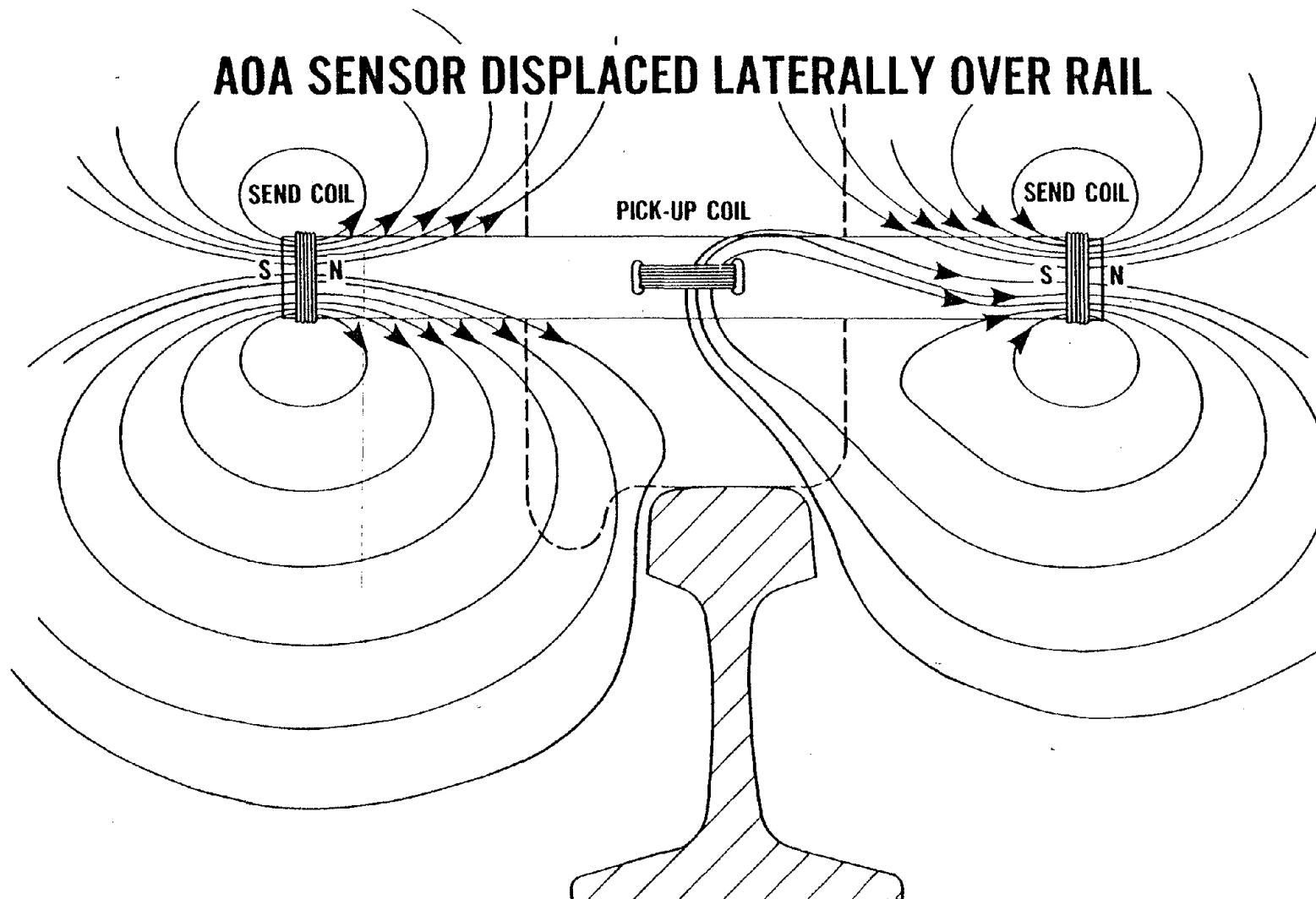
AOA SENSOR CENTERED OVER RAIL



3-21

THE MAGNETIC FIELDS OF EACH SEND COIL ARE DISTORTED BY THE PRESENCE OF THE CONDUCTIVE RAIL SURFACE BUT THE INDUCED VOLTAGE OF THE PICK-UP COIL IS ZERO BECAUSE IT INTERCEPTS EQUAL AND OPPOSITE LINES OF FLUX.

Figure. 3-11



THE PICK-UP COIL IS INFLUENCED PREDOMINANTLY BY THE MAGNETIC FIELD OF THE SEND COIL WHOSE FIELD HAS BEEN MORE DISTORTED BY THE PRESENCE OF THE CONDUCTIVE RAIL SURFACE. THE INDUCED VOLTAGE OF THE PICK-UP COIL IS PROPORTIONAL TO THE LATERAL DISPLACEMENT.

Figure 3-12

systems. By directly converting the amplitude of the sensor's feeble reflected signal to a frequency channel, these problems can be avoided by employing digital techniques of data transmission and demodulation.

3.2.1 SENSOR COILS

The angle-of-attack sensor coils are shunt tuned and connected to low impedance points in the oscillator circuit. This means that the returned signal is always 90° out of phase with the excitation voltage. Since the excitation coils are wound at right angles to the sensor coil, the returned signal may be either leading or lagging, depending on the target location. The coils are phased to null the returned signal when the sensor is centered over the railhead. This allows the sensor to be relatively insensitive to its distance above the railhead (about an optimum height as determined by the coil spacing) and give an approximately linear response to the lateral position relative to the railhead. Since the oscillator circuit demonstrates some sensitivity to the tuning of the receiving coil, a temperature compensating capacitor has been added directly across this coil to stabilize its tuning over a wide temperature range.

The oscillator for the angle-of-attack sensor must be located within a few feet of the sensor. This is because the amplifiers must have a very wide response in order to maintain good phase shift stability at the operating frequency. If the sensor wires are too long, they will act as tuned waveguides within the response range of the amplifiers, and spurious oscillations will result.

3.2.2 SENSOR OSCILLATOR

The oscillator consists of three basic sections: the passive tuning network, the summing amplifier and the limiting power amplifier. The overall functions of the oscillators are to produce a frequency that is stable with respect to time, temperature, etc., but is clearly related to the small coupling coefficient induced between the sensor's coils.

3.2.3 THERMAL STABILIZER

The angle-of-attack sensor oscillator is basically very sensitive and stable. However, the signal from the sensor is necessarily feeble in order to fulfill the mechanical requirement of sensor location and cancellation of cross axis inputs. Therefore, the oscillator stability is enhanced by placing it in a thermally stable environment. This is accomplished by mounting the oscillator PC board on an aluminum plate and heating the plate to a controlled temperature.

3.2.4 DISCRIMINATOR

The signal from the oscillator is fed into a digital-type discriminator circuit where it is compared against a crystal controlled clock. The difference counts are then applied to a digital to analog converter. The output signal is then fed through a scaling amplifier and, after filtering, is recorded by the Data Acquisition System.

3.3 OTHER TRANSDUCERS

Table 3-2 lists the data channel numbers for the entire collection of sensors and for measurements derived from one or more sensors. Figure 3-13 indicates the location of the sensors.

3.3.1 ACCELEROMETERS

Servo accelerometers were mounted over each truck on the floor of the locomotives and coaches to provide vertical and lateral ride quality information. Figure 3-14 is a schematic of the accelerometer circuit.

3.3.2 DISPLACEMENT TRANSDUCERS

String pot type displacement transducers were mounted on the Amcoach to measure vertical and lateral suspension displacements and on the LRC coach to measure motion of the banking tilt cylinder.

3.3.3 AUTOMATIC LOCATION DETECTOR (ALD)


The ALD was mounted on the leading truck of the DAS/LRC coach. The ALD was a capacitive displacement system to mark reference target location and geographic track features. The sensor was mounted on a bracket, six inches from the top of the railhead and in approximately the center of the truck. The distance from the center of the sensor to the center of the instrumented axle was noted.

3.4 DATA ACQUISITION SYSTEM (DAS)

The DAS as shown in Figure 3-15 was developed and used for this test project. This system was used to process the strain gage signals from the instrumented wheels, to display the forces and force ratio data on real time strip charts used for monitoring the test safety, and for recording the data on digital magnetic tape. The DAS was installed on one of the LRC coaches on a false floor configuration.

TABLE 3-2

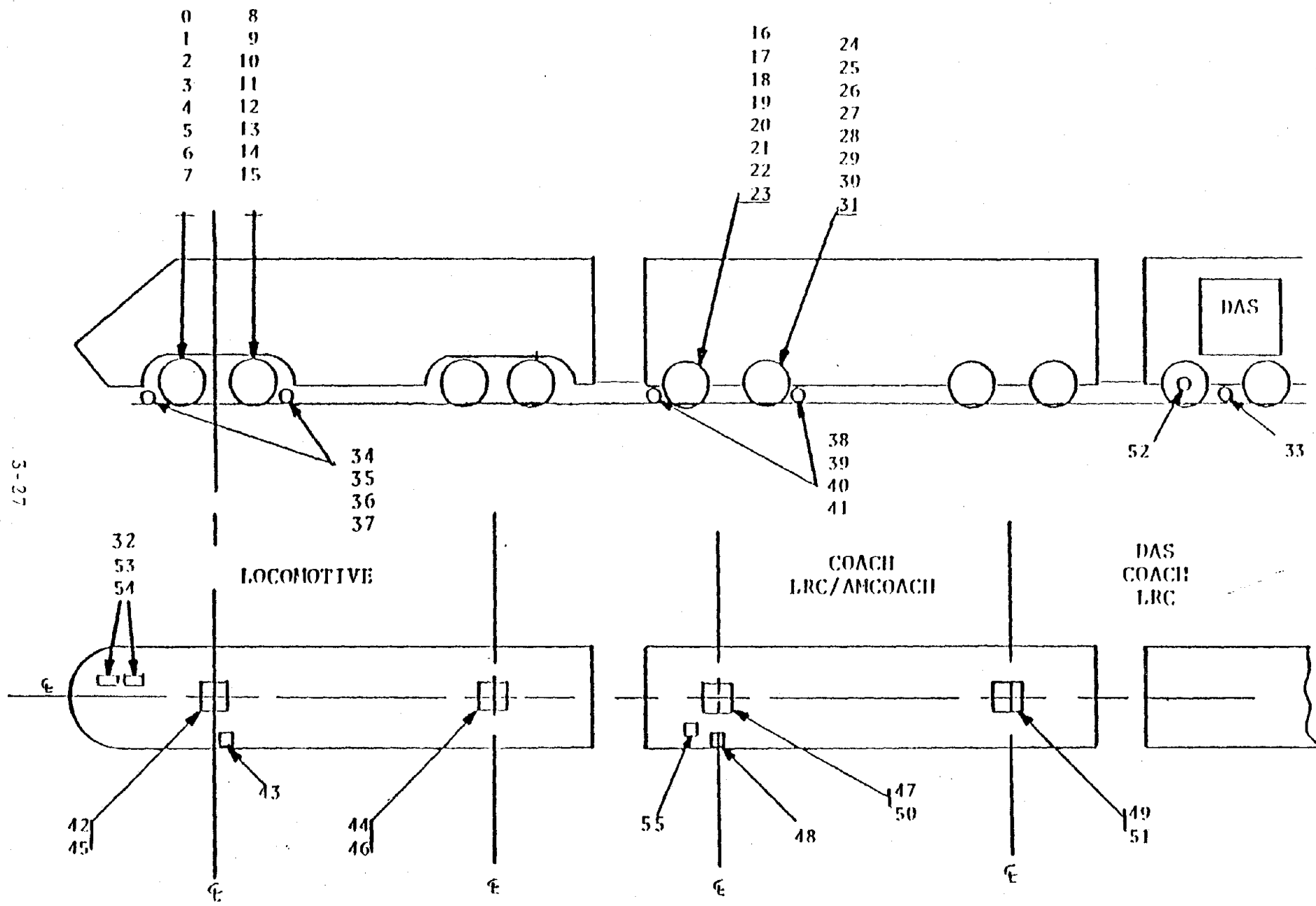
LRC DATA CHANNEL ASSIGNMENTS

Reproduced from
best available copy. 

CHN	MSR#	TYPE	LOCATION	SOURC	+10V RNG	UNITS	CTF	FRQ	EL CAL	PH CAL
0	11VA	VERTICAL A	LOCO.AXL.#1 LFT.	1-1VA	100.0	KIPS	85.0	5.39 V	0.00 V	0.00 V
1	11VB	VERTICAL B	LOCO.AXL.#1 LFT.	1-1VB	100.0	KIPS	85.0	5.35 V	0.00 V	0.00 V
2	11LA	LATERAL SINE	LOCO.AXL.#1 LFT.	1-1LA	50.0	KIPS	85.0	5.00 V	0.00 V	0.00 V
3	11LB	LATERAL COSINE	LOCO.AXL.#1 LFT.	1-1LB	50.0	KIPS	85.0	5.13 V	0.00 V	0.00 V
4	12VA	VERTICAL A	LOCO.AXL.#1 RHT.	1-2VA	100.0	KIPS	85.0	5.35 V	0.00 V	0.00 V
5	12VB	VERTICAL B	LOCO.AXL.#1 RHT.	1-2VB	100.0	KIPS	85.0	5.32 V	0.00 V	0.00 V
6	12LA	LATERAL SINE	LOCO.AXL.#1 RHT.	1-2LA	50.0	KIPS	85.0	5.03 V	0.00 V	0.00 V
7	12LB	LATERAL COSINE	LOCO.AXL.#1 RHT.	1-2LB	50.0	KIPS	85.0	5.03 V	0.00 V	0.00 V
8	21VA	VERTICAL A	LOCO.AXL.#2 LFT.	2-1VA	100.0	KIPS	85.0	5.32 V	0.00 V	0.00 V
9	21VB	VERTICAL B	LOCO.AXL.#2 LFT.	2-1VB	100.0	KIPS	85.0	5.28 V	0.00 V	0.00 V
10	21LA	LATERAL SINE	LOCO.AXL.#2 LFT.	2-1LA	50.0	KIPS	85.0	5.27 V	0.00 V	0.00 V
11	21LB	LATERAL COSINE	LOCO.AXL.#2 LFT.	2-1LB	50.0	KIPS	85.0	5.11 V	0.00 V	0.00 V
12	22VA	VERTICAL A	LOCO.AXL.#2 RHT.	2-2VA	100.0	KIPS	85.0	5.36 V	0.00 V	0.00 V
13	22VB	VERTICAL B	LOCO.AXL.#2 RHT.	2-2VB	100.0	KIPS	85.0	5.35 V	0.00 V	0.00 V
14	22LA	LATERAL SINE	LOCO.AXL.#2 RHT.	2-2LA	50.0	KIPS	85.0	5.23 V	0.00 V	0.00 V
15	22LB	LATERAL COSINE	LOCO.AXL.#2 RHT.	2-2LB	50.0	KIPS	85.0	5.23 V	0.00 V	0.00 V
16	51VA	VERTICAL A	COACHAXL.#1 LFT.	5-1VA	50.0	KIPS	85.0	0.00 V	0.00 V	0.00 V
17	51VB	VERTICAL B	COACHAXL.#1 LFT.	5-1VB	50.0	KIPS	85.0	0.00 V	0.00 V	0.00 V
18	51LA	LATERAL SINE	COACHAXL.#1 LFT.	5-1LA	50.0	KIPS	85.0	0.00 V	0.00 V	0.00 V
19	51LB	LATERAL COSINE	COACHAXL.#1 LFT.	5-1LB	50.0	KIPS	85.0	0.00 V	0.00 V	0.00 V
20	52VA	VERT A	COACHAXL.#1 RHT.	5-2VA	50.0	KIPS	85.0	0.00 V	0.00 V	0.00 V
21	52VB	VERTICAL B	COACHAXL.#1 RHT.	5-2VB	50.0	KIPS	85.0	0.00 V	0.00 V	0.00 V
22	52LA	LATERAL SINE	COACHAXL.#1 RHT.	5-2LA	50.0	KIPS	85.0	0.00 V	0.00 V	0.00 V
23	52LB	LATERAL COSINE	COACHAXL.#1 RHT.	5-2LB	50.0	KIPS	85.0	0.00 V	0.00 V	0.00 V
24	61VA	VERTICAL A	COACHAXL.#2 LFT.	6-1VA	50.0	KIPS	85.0	0.00 V	0.00 V	0.00 V
25	61VB	VERTICAL B	COACHAXL.#2 LFT.	6-1VB	50.0	KIPS	85.0	0.00 V	0.00 V	0.00 V
26	61LA	LATERAL SINE	COACHAXL.#2 LFT.	6-1LA	50.0	KIPS	85.0	0.00 V	0.00 V	0.00 V
27	61LB	LATERAL COSINE	COACHAXL.#2 LFT.	6-1LB	50.0	KIPS	85.0	0.00 V	0.00 V	0.00 V
28	62VA	VERTICAL A	COACHAXL.#2 RHT.	6-2VA	50.0	KIPS	85.0	0.00 V	0.00 V	0.00 V
29	62VB	VERTICAL B	COACHAXL.#2 RHT.	6-2VB	50.0	KIPS	85.0	0.00 V	0.00 V	0.00 V
30	62LA	LATERAL SINE	COACHAXL.#2 RHT.	6-2LA	50.0	KIPS	85.0	0.00 V	0.00 V	0.00 V
31	62LB	LATERAL COSINE	COACHAXL.#2 RHT.	6-2LB	50.0	KIPS	85.0	0.00 V	0.00 V	0.00 V
32	INOP	SAND	LOCO. CAB	SANDRLY	1.0	EVNT	20.0	0.00 V	0.00 V	0.00 V
33		CAPACITIVE ALD	COACH LEAD TRK.	ALD SNSR	1.0	EVNT	85.0	0.00 V	0.00 V	0.00 V
34	AOA1	WHL. RAIL POSIT.	LOC.AXL.#1LFT.FR	AOA SNSR	2.0	INCH	10.0	0.00 V	0.00 V	0.00 V
35	AOA2	WHL. RAIL POSIT.	LOC.AXL.#1LFT.RE	AOA SNSR	2.0	INCH	10.0	0.00 V	0.00 V	0.00 V
36	AOA3	WHL. RAIL POSIT.	LOC.AXL.#1RHT.FR	AOA SNSR	2.0	INCH	10.0	0.00 V	0.00 V	0.00 V
37	AOA4	WHL. RAIL POSIT.	LOC.AXL.#1RHT.RE	AOA SNSR	2.0	INCH	10.0	0.00 V	0.00 V	0.00 V
38	AOA5	WHL. RAIL POSIT.	COH.AXL.#1LFT.FR	AOA SNSR	2.0	INCH	10.0	0.00 V	0.00 V	0.00 V
39	AOA6	WHL. RAIL POSIT.	COH.AXL.#1LFT.RE	AOA SNSR	2.0	INCH	10.0	0.00 V	0.00 V	0.00 V
40	AOA7	WHL. RAIL POSIT.	COH.AXL.#1RHT.FR	AOA SNSR	2.0	INCH	10.0	0.00 V	0.00 V	0.00 V
41	AOA8	WHL. RAIL POSIT.	COH.AXL.#1RHT.RE	AOA SNSR	2.0	INCH	10.0	0.00 V	0.00 V	0.00 V
42	1536	VERT. ACCEL.	LOCO.LD.TRK.CTR	VERT.ACC	1.0	G.	40.0	0.00 V	1.00 V	0.00 V
43	1553	VERT. ACCEL.	LOCO.LD.TRK.SIDE	VERT.ACC	1.0	G.	40.0	0.00 V	1.00 V	0.00 V
44	1520	VERT.ACCEL.	LOCO.TR.TRK.CTR	VERT.ACC	1.0	G.	40.0	0.00 V	1.01 V	0.00 V
45	1577	LATERAL ACCEL.	LOCO.LD.TRK.CTR	LAT.ACC	1.0	G.	40.0	0.00 V	1.00 V	0.00 V

TABLE 3-2 (cont)
LRC DATA CHANNEL ASSIGNMENTS

CHN	MSR#	TYPE	LOCATION	SOURC	+10V RNG	UNITS	CTF	FRQ	EL CAL	PH CAL
46	1583	LATERAL ACCEL.	LOCO.TR.TRK.CTR.	LAT.ACC.	1.0	G.	40.0		0.00 V	1.00 V
47	1523	VERT. ACCEL.	COH.LD.TRK.CTR.	VERT.ACC	1.0	G.	40.0		0.00 V	.99 V
48	2773	VERT. ACCEL.	COH.LD.TRK.SIDE	VERT.ACC	1.0	G.	40.0		0.00 V	.99 V
49	2767	VERT. ACCEL.	COH.TR.TRK.CTR.	VERT.ACC	1.0	G.	40.0		0.00 V	1.00 V
50	1561	LATERAL ACCEL.	COH.LD.TRK.CTR.	LAT.ACC.	1.0	G.	40.0		0.00 V	1.00 V
51	1564	LATERAL ACCEL.	COH.TR.TRK.CTR.	LAT.ACC.	1.0	G.	40.0		0.00 V	1.00 V
52		SPEED	COACH LEAD TRK.	WABCO	150.0	MPH.	85.0		2.80 V	0.00 V
53	INOP	BRAKE PRESSURE	LOCOMOTIVE	CYLINDER	200.0	PSI.	85.0		0.00 V	0.00 V
54	INOP	TRCTN.MTR.CRRNT.	LOCOMOTIVE	SPECIAL	1.0		85.0		0.00 V	0.00 V
55		VERT.STRING POT	LFT.SIDECOACH	STRING	3.0	INCH	10.0		-5.22 V	0.00 V



5-27

Figure 3-15. Instrumentation Layout

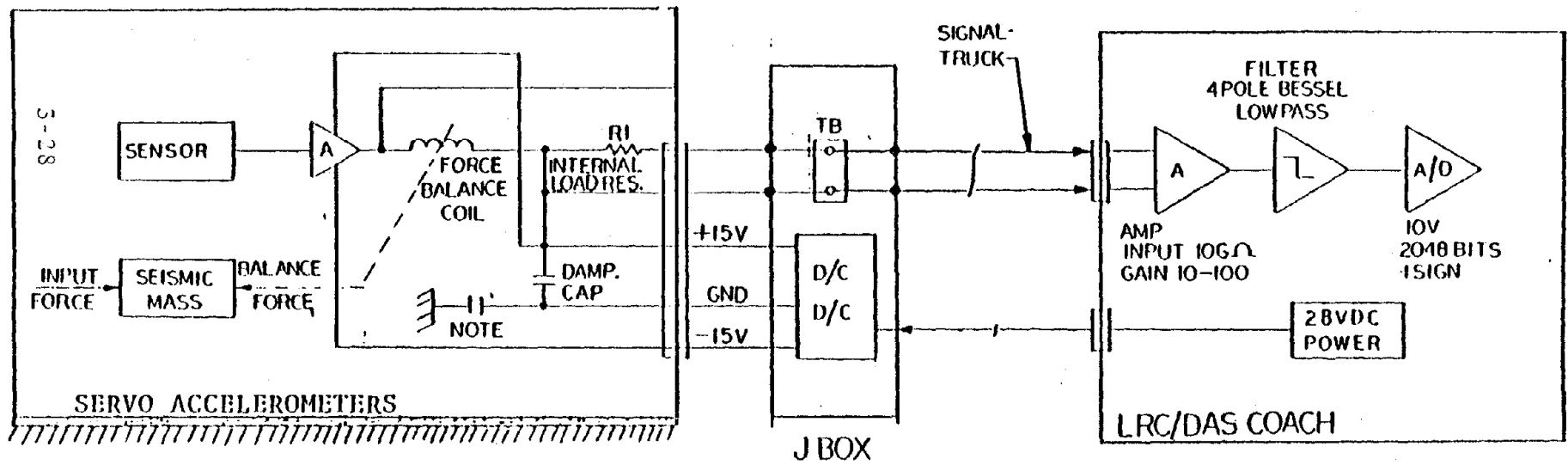


Figure 3-14. Accelerometer Configuration

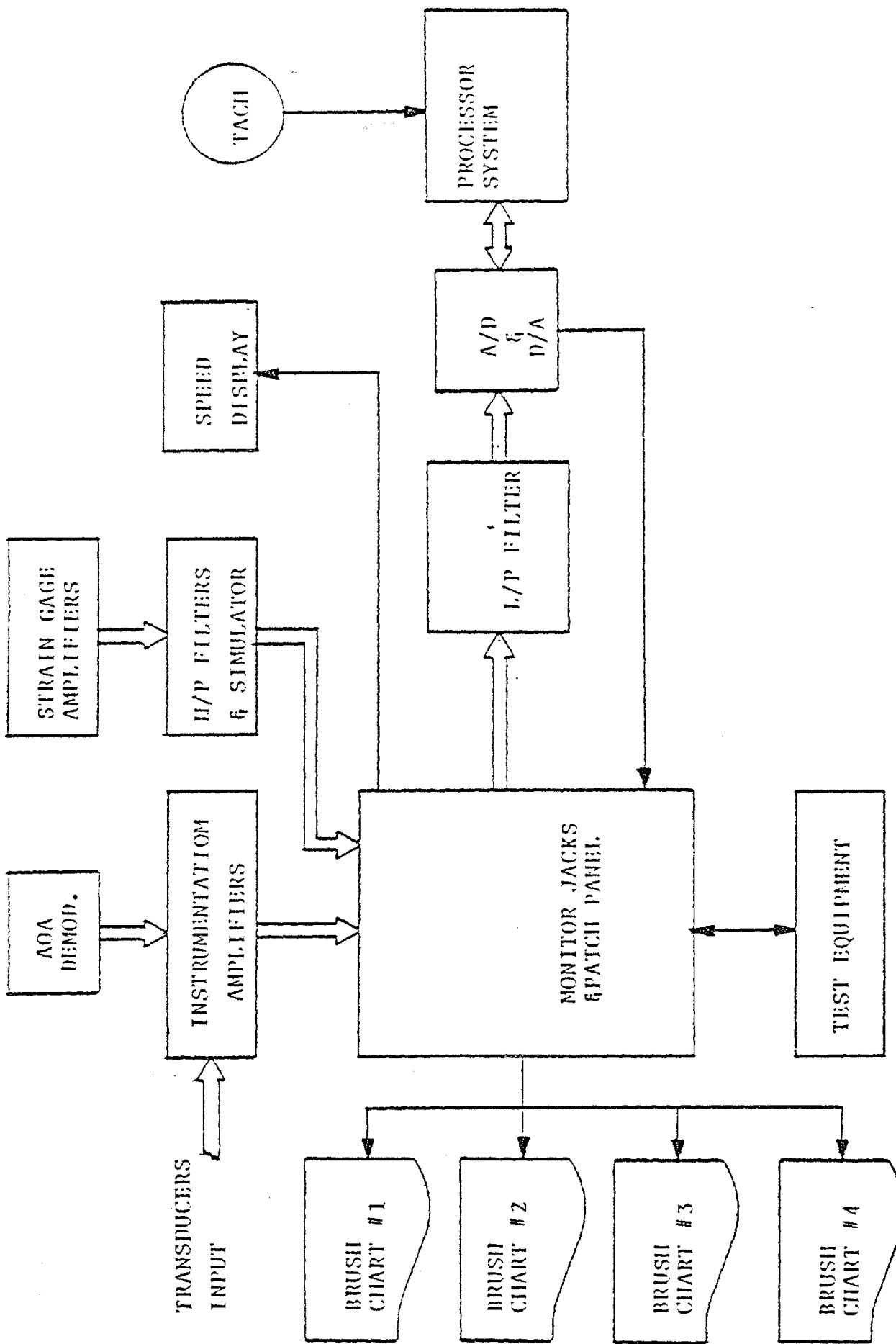


Figure 3-15. DAS Configuration

Reproduced from

 best available copy.

The heart of the DAS system was a HP-1000 series minicomputer. The configuration of the computer and associated peripheral equipment is shown in Figure 3-16. The instrumentation amplifiers used for this system were ENSCO Model 0531 and 0529 units. For these tests 10 high gain and 20 low gain amplifiers were required. In addition, a bank of carrier type Natel 2088 carrier amplifiers were used in conjunction with the ENSCO wheel simulator and associated filter unit Model 475.

The tachometer system converted the wheel tachometer output into logic signals which were fed to the programmable clock and used by the DAS for the distance base data. Programmable anti-aliasing four pole low base bessel active filters were set up so the 3 dB response for each filter was set as shown in Table 3-2. Selected data channels were displayed on Gould Model 260 6-channel ink recorders for real-time safety monitoring.

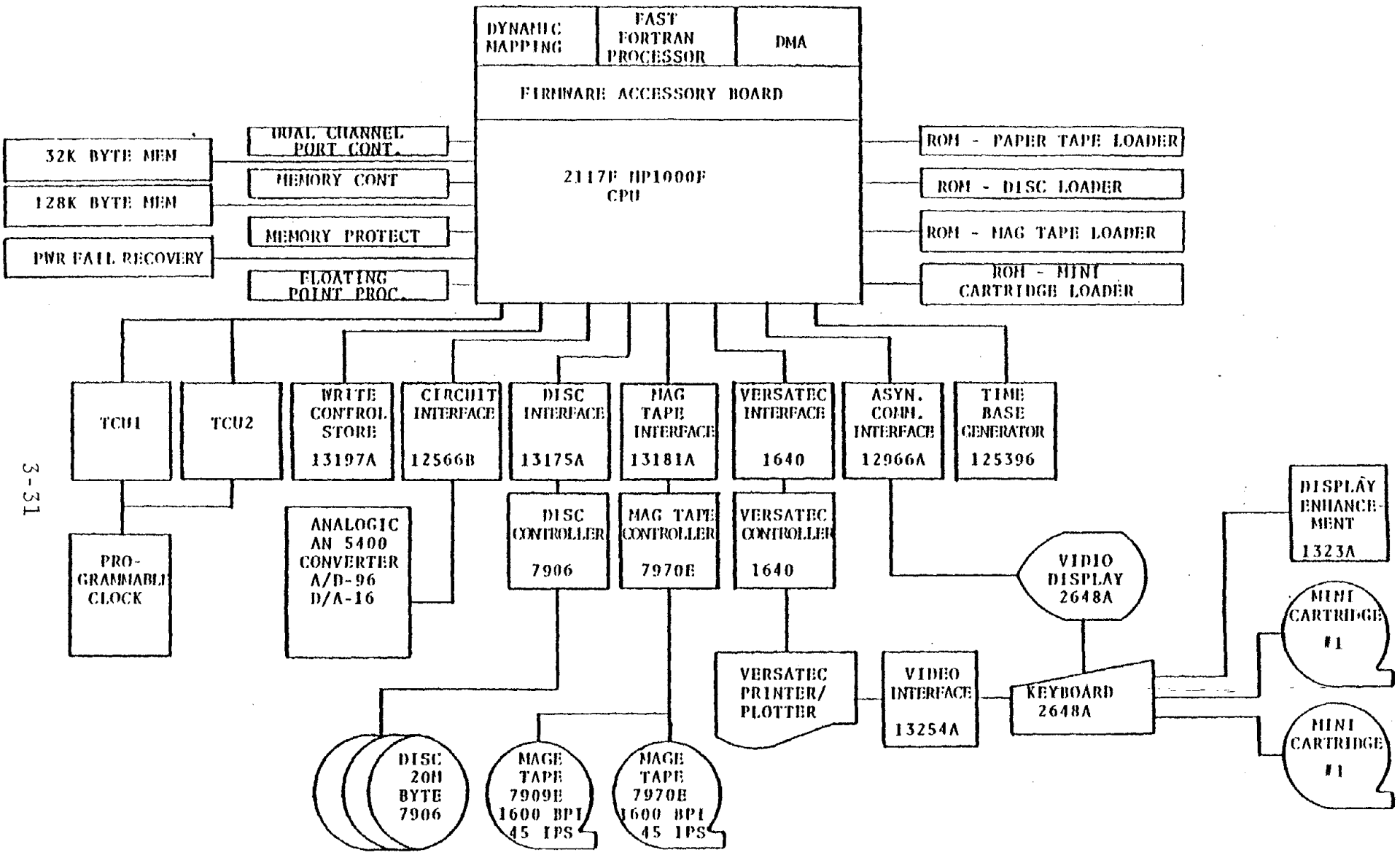
3.5 DATA REDUCTION

The primary object of the data reduction was to organize the measurements of the various sensors into a form suitable for comparison to safety and comfort criteria and for recognition of trends in the data. The factors considered in the safety criteria and observations during testing were the basis for selecting nine principal measurements for routine processing over every curve. The other channels were considered as supporting data to resolve any ambiguities in the principal measurements. The principal measurements which include both direct sensor outputs and qualities derived from several sensors are:

Speed - computed from decelostat pulses of the coach braking system.

Carbody Lateral Acceleration - measured by an accelerometer placed on the floor of the vehicle approximately over the center of the lead truck. The accelerometer senses lateral acceleration from gravity due to body roll and, in the case of the LRC coach, to deliberate tilting of the floor, lateral acceleration due to curving, and lateral accelerations due to carbody yaw and translation. The measurement reflects what the passengers would feel in the lateral direction.

High Rail Lead Wheel Lateral Force - This is usually the first wheel to make flange contact in a curve. High lateral wheel forces are considered to be related to derailment through rail panel shift, gage widening, rail rollover or wheel climb.



3-31

HP 1000 Series Processor System
 Figure-3-16. DAS/CPU Configuration

Low Rail Lead Wheel Vertical Force - This wheel is unloaded by weight transfer due to lateral acceleration, lateral body displacement relative to the truck, and body roll. Derailment by vehicle overturning can result after this wheel is fully unloaded.

High Rail Lead Wheel Vertical Force - not a safety criteria. It is used to indicate axle load transfer as a check on the weight vector crossing calculation.

High Rail Side Truck Lateral Force - the sum of lateral forces on the leading and trailing wheels of the lead truck on the high rail side. This parameter is a second indicator of the risk of rail panel shift, rail rollover or gage widening.

High Rail Lead Wheel L/V Ratio - determined by dividing the lateral force on the wheel by its vertical load. The high rail lead wheel is usually the first to reach high flange loads. The vertical load transfer to the high rail wheel tends to moderate this parameter. Wheel L/V ratio is the principal indication of the risk of derailment by wheel climb. The L/V ratio becomes critical at a lower level if the wheel angle of attack is high, causing maximum creep forces. However, the maximum angles of attack were measured at about 0.5 degree which does not saturate the creep force while most wheel climb criteria assume the maximum possible lateral creep force. Therefore, only the lead wheel L/V ratio is necessary for a conservative assessment of wheel climb risk over the large variety of conditions represented in the cant deficiency testing data base.

High Rail Side Truck L/V Ratio - determined by dividing the sum of lateral forces on the wheels on the high rail side of the lead truck by the sum of the vertical loads on those wheels. Truck side L/V ratios are used to evaluate the risk of rail rollover.

Weight Vector Crossing - the force vector which is the resultant of the vehicle mass being acted upon vertically by gravitational attraction and laterally by centrifugal acceleration in a curve may be visualized "piercing" the plane of the railheads. The distance between the center line of the track and the vector piercing point is called the weight vector intercept or vector crossing. It is the balancing point of the vertical wheel loads relative to the track center line and it was calculated from the vertical loads of the instrumented wheels. (See Section 5 for the equation.) The danger of vehicle overturning is indicated by the location of the weight vector intercept.

Both peak and steady state measurements of the above parameters are necessary for comparison with the various criteria. The average of a particular parameter over a section of the curve body is taken as an adequate approximation of the steady state value. The peak, however, has been defined in many ways, and the methodology and equipment used to gather and reduce the data frequently influence the definition. A good definition of the peak recognizes the frequency content of the data, the meaningful time duration of the event, and the characteristics of the data processing that influence repeatability. It is expressed in terms that allow comparison to peak values obtained by other means. Unfortunately many safety criteria do not specify what is meant by peak or worse yet only infer that peak data is being considered.

Several definitions of data peaks have been used to interpret the results of tests.

Single Point Peak - the highest point on an analog strip chart record or the highest digitized point of a digital tape is the most obvious peak. However, peaks obtained in this way are directly dependent on the frequency response of each piece of equipment involved in data collection, storage, and display. The method fails to distinguish between extraneous "noise" and meaningful dynamic information. It is doubtful that correct comparisons can be made between data from different studies if the peaks are collected in this manner.

Time Averaged Peaks - Examination of an analog strip chart recording for the highest average level over a given time segment solves some of the problems of the single point peak. The time segment may be established by convention for the comparison of data. It is usually large relative to the equipment frequency limitations because considerable energy rather than merely high force is required to influence a train. Most extraneous noise is either ac which is removed by averaging or of very short time duration relative to the segment being averaged. While a time averaged peak has clear intuitive meaning and removes most differences between test equipment it is sometimes difficult to apply repeatably by direct examination. It is not well suited to automated processing of great quantities of data. Time averaging of peaks is in one way equivalent to filtering at a very low frequency and recording the highest single point. An algorithm based on this interpretation may agree with the chart reading in many cases but the total loss of higher frequency content could cause lack of agreement in many others. The direct use of a moving average over the desired time segment is impractical for most small computers used for data acquisition when many simultaneous channels are required because of memory and operating time constraints.

Time Duration Peaks - Defining the peak value as the level which has been exceeded for a given time interval shares the advantages of the time averaged peaks although the magnitude is lower for a given time interval. The examination of strip charts is convenient and repeatable using this method and it was used during this test for onboard safety monitoring. It provides an intuitive measure of dynamic performance without sacrificing the frequency content, but it is an awkward definition for rapid automated processing of a great quantity of data.

Percentile Level Peak - A statistical analysis of a sample of digitized points for percentile levels is a common operation well suited for automated processing. It was used to process the curving data described in this test program. The peak descriptors resulting from this method are objective and consistent and were seen to compare well with those defined by the two previous methods. A percentile level does not measure the energy content of irregular peaks as intuitively as does the time averaged or time duration methods as it does not require the high digitized points to be consecutive. However, prefiltering at frequencies meant to eliminate noise without attenuating the response characteristics of the spring-mass systems involved seems to bring about an equivalency among the methods.

The frequency content of the data recorded on digital tape was limited only by the 85 Hz anti-aliasing filtering. But wheel forces and force ratios, which include primary suspension frequencies, were filtered at 25 Hz while carbody accelerations and weight vector intercept, which depend on lower secondary suspension frequencies, were filtered at 10 Hz before statistical analysis.

Tables 3-3 through 3-5 compare the time averaged, time duration and percentile level methods of peak data determination for runs at the highest test speeds on a rough wood tie curve. The 95th percentile level agrees well with the time duration peak (exceeded for 40 ms) for the several types of measurements taken. Although there is no mathematically derivable fixed relation between the 95th percentile level and the 40 ms time duration peak, the agreement was characteristic in general for the cant deficiency test data, and it may provide an intuitive dimension to the test results. A 40 ms peak is short enough to provide a high degree of conservativeness while requiring at least some energy content of the peak pulses. The 99th percentile peaks were deemed overly conservative and not as consistent due to the smaller number of points captured, and the single point peaks are dependent on filtering frequency.

TABLE 3-3

**UNFILTERED STRIP CHART PEAKS VS COMPUTER DATA REDUCTION
 LRC LOCOMOTIVE - CURVE 67 EAST 8/26/80
 - WEIGHT VECTOR CROSSING, INCHES**

ANALOG STRIP CHART

COMPUTER DATA REDUCTION

3-35

RUN

AVERAGE OVER		EXCEEDED FOR	
40ms	80ms	40ms	80ms
16 1/2	15 1/2	14	14
17	16	15 1/2	14 1/2
17	16 1/2	16	15 1/2
20 1/2	18 1/2	18	16
20	19 1/2	19 1/2	18
20 1/2	19 1/2	19 1/2	18 1/2

95%ile	99%ile	POINT SINGLE MAXIMUM
15.1	15.6	15.9
16.1	17.0	17.5
15.9	17.0	17.6
17.9	19.2	19.4
19.8	20.6	20.8
19.6	20.3	20.7

TABLE 3-4

UNFILTERED STRIP CHART PEAKS VS COMPUTER DATA REDUCTION
LRC LOCOMOTIVE - CURVE 67 EAST 8/26/80
- LEAD WHEEL LATERAL FORCE, KIPS

ANALOG STRIP CHART

COMPUTER DATA REDUCTION

3-56

RUN

	AVERAGE OVER		EXCEEDED FOR	
	40ms	80ms	40ms	80ms
1	13 1/2	13	12	10 1/2
2	13 1/2	13	13	10 1/2
4	14 1/2	12 1/2	12 1/2	9
5	15	13	13 1/2	8
6	17	16	16	11 1/2
7	16	15	14 1/2	12

95%ile	99%ile	SINGLE POINT MAXIMUM
12.5	15.2	16.0
12.7	13.7	14.5
12.7	14.9	15.4
13.8	15.7	16.3
16.3	17.6	18.0
15.8	17.0	18.4

TABLE 3-5

UNFILTERED STRIP CHART PEAKS VS COMPUTER DATA REDUCTION
LRC LOCOMOTIVE - CURVE 67 EAST 8/26/80
- LEAD WHEEL L/V RATIO

RUN	ANALOG STRIP CHART				COMPUTER DATA REDUCTION		
	AVERAGE OVER		EXCEEDED FOR		95%ile	99%ile	SINGLE POINT MAXIMUM
	40ms	80ms	40ms	80ms			
1	.31	.28	.26	.23	.301	.339	.348
2	.31	.29	.30	.25	.300	.321	.339
4	.36	.28	.31	.18	.291	.357	.377
5	.34	.28	.30	.16	.309	.335	.370
6	.34	.32	.31	.23	.333	.383	.421
7	.36	.32	.30	.22	.331	.382	.410

3-37

Consistency in locating the data interval relative to the curve body is required if percentile levels are used as peak descriptors. The data was arranged on the tape in records each containing 58 digitized points collected at a 256 Hz rate. The statistical analysis program could operate on intervals of up to 25 records. Before analysis, the data was displayed on strip charts which included a channel that counted tape record numbers and a channel that marked track location targets. With the aid of the auxiliary channels, the exact intervals of records which included the entry spiral, curve body, and exit spiral could be specified for separate analyses without the risk of skewing the percentile levels by including low level tangent data. For the over-the-road runs which emphasized peak rather than steady state measurements a record interval was chosen which included the peak area along with as much curve body as possible without dividing the curve into three regions. It is necessary to choose similar samples of data at each curve by examination of analog strip charts to use the percentile levels as true peak descriptors. The filtering prior to analysis should remove noise without attenuating data at the frequency of the event under study. Figures 3-17 through 3-20 which show the analysis of the same data sample after various levels of filtering indicate that those selected in this project achieved maximum noise suppression without attenuating the 95th percentile level for the various types of measurements.

EFFECT OF PROCESSING FILTERING

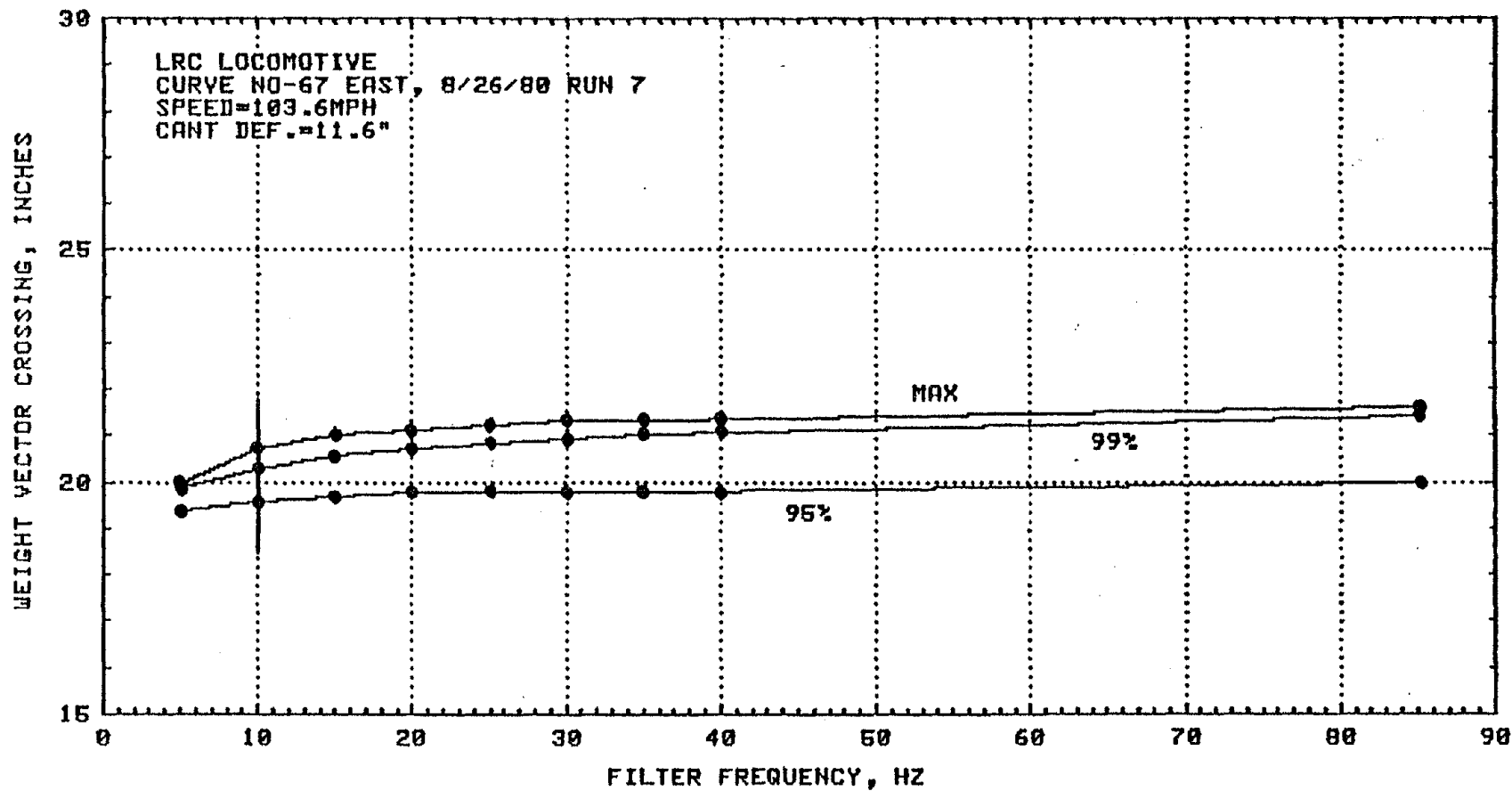


Figure 3-17

EFFECT OF PROCESSING FILTERING

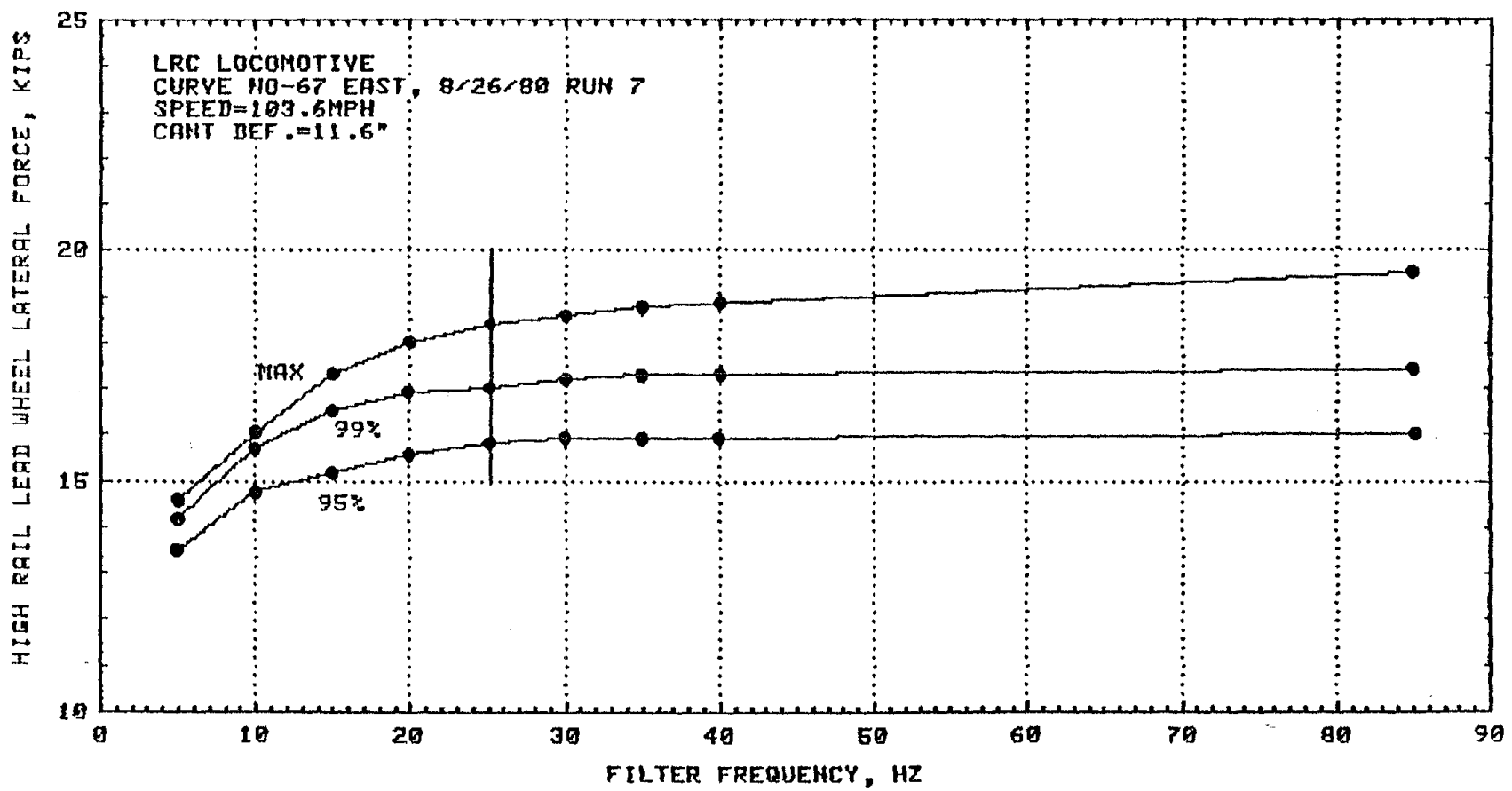
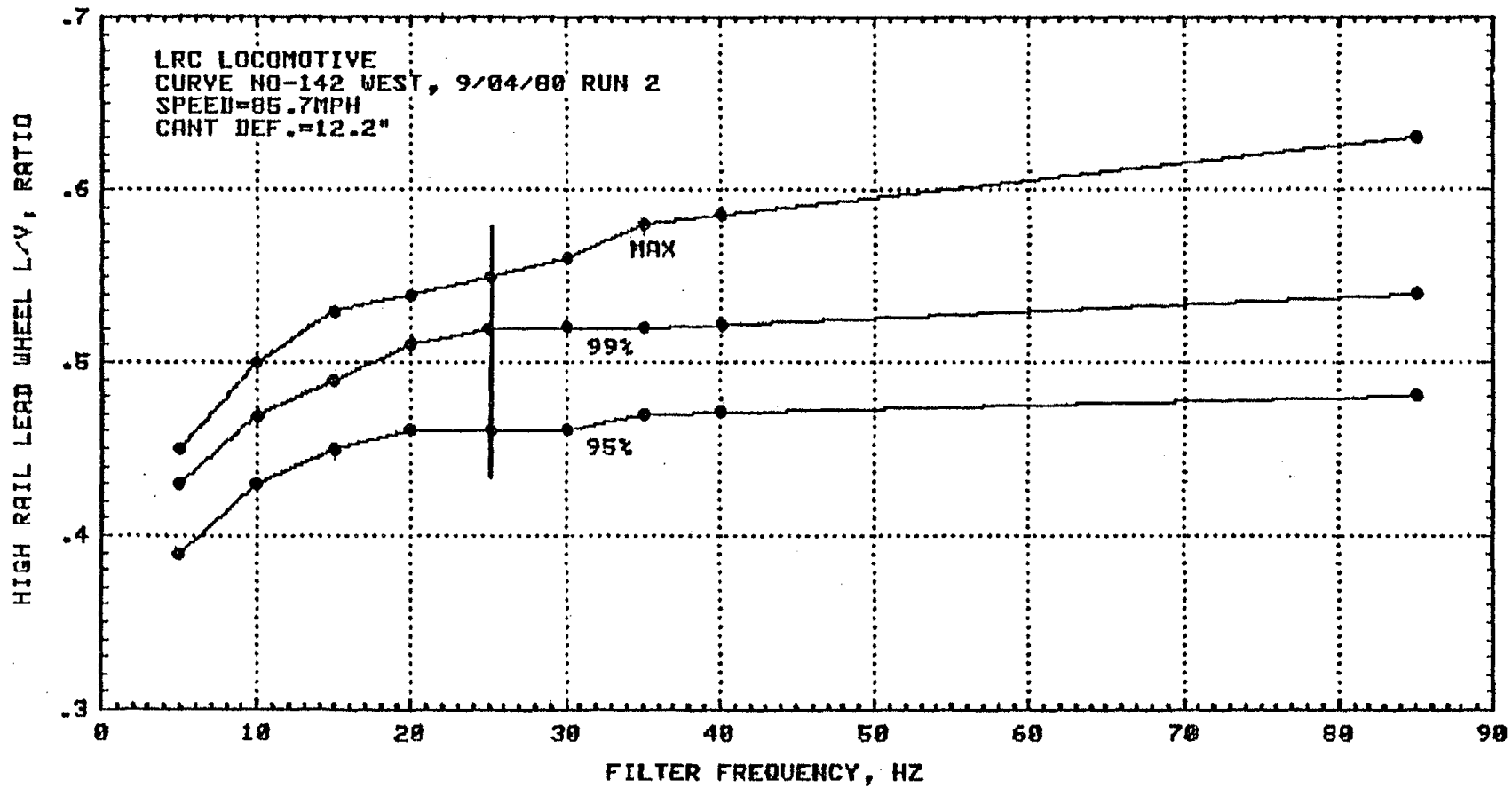


Figure 3-18

EFFECT OF PROCESSING FILTERING



3-41

Figure 3-19

EFFECT OF PROCESSING FILTERING

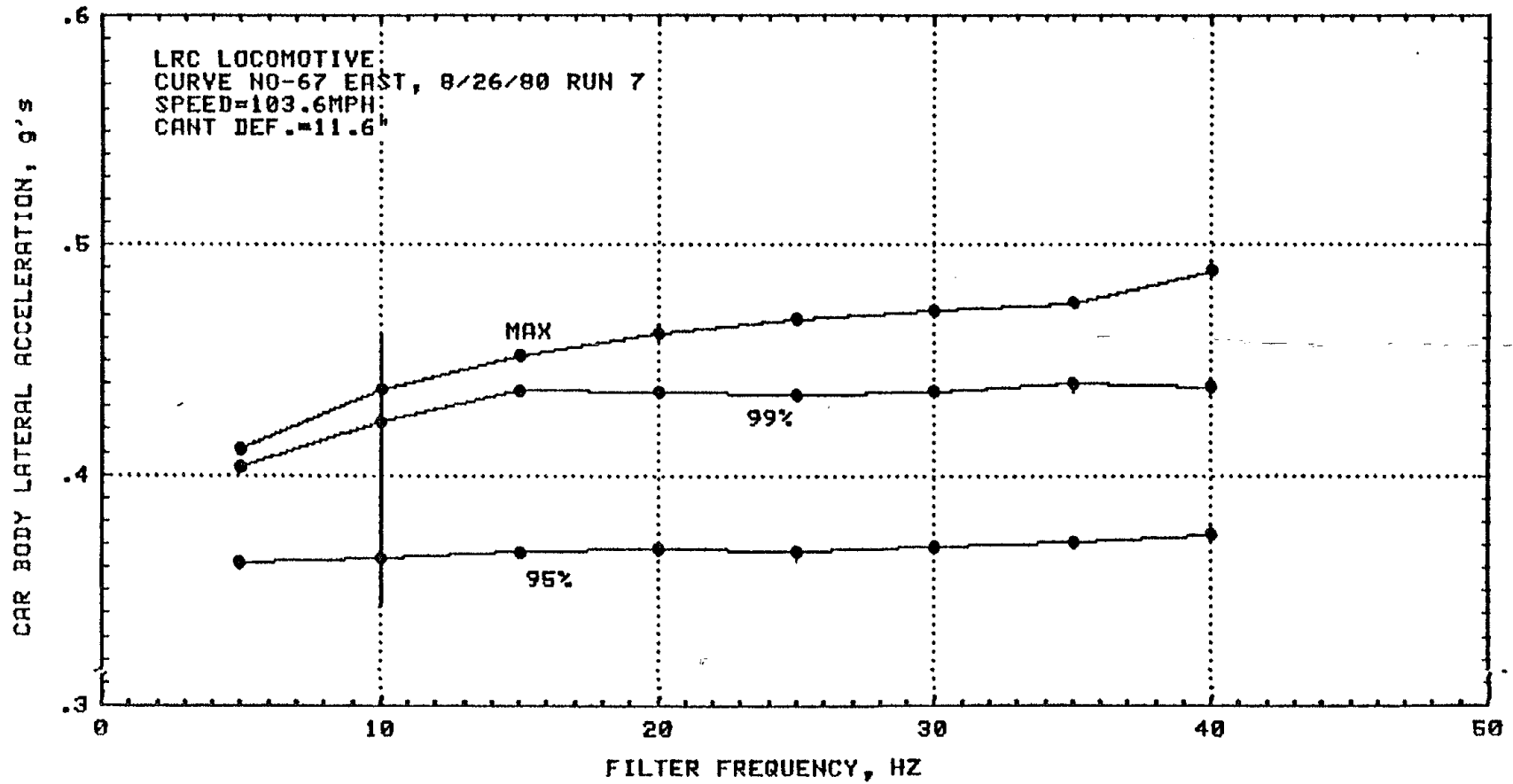


Figure 3-20

4.0 TESTING PROCEDURES

4.1 GENERAL

To accomplish the objectives of the cant deficiency test, the testing was performed in the following three phases:

- o Phase I tested an Amcoach car towed by the LRC Locomotive.
- o Phase II tested the LRC Locomotive and an LRC Coach.
- o Phase III tested the AEM-7 Locomotive.

For these tests instrumented wheels were installed on the lead truck of the locomotive and on the lead truck of the first coach. Accelerometers, displacement transducers and other sensors were installed on the locomotive and test coach.

A minicomputer based data acquisition system was used to perform real time processing of the wheel force signals, to display the force and acceleration data on monitors and to record the test data on magnetic tape. The data acquisition system was located in the second car in the consist. Three to five coaches were used for each of the tests.

The test was performed on mainline track at significantly higher than normal speeds which required extra care in the selection of the test site and the development of the operational plan. Detailed site selection consideration and criteria for the operations plans are described in the Test Plan (Ref. 22).

The system assembly and checkout was performed at the Amtrak shop facility in New Haven, CT. The instrumented wheelsets and special sensors were installed on the vehicles being tested and the data acquisition system was installed in one of the LRC coaches. The brakes were removed from the trucks equipped with instrumented wheels and the test coaches were ballasted.

After the system was installed, shake-down runs were conducted prior to the actual test runs. Each phase of the test was divided into four series of tests. The details of each of the tests will be discussed in the following paragraphs. The basic plan for each phase was to perform the following tests:

- o Repeated tests on a wood tie right-hand curve
- o Repeated test on a concrete tie left-hand curve
- o Repeated round trip runs over a selected set of curves
- o Repeated round trip over a selected route

Series 1 and 2 tests of Phase I and II were conducted on the instrumented curves 67 eastbound and 67 westbound. The repeated round trips for series 3 were run on the curves located between New Haven and Groton (Milepost 76 to 120) on the Northeast Corridor Track, and the repeated round trips of series 4 were made on the same tracks with the route extended to Providence. The Phase III test on the AEM-7 locomotive could not be run on the same test zone since this section is not electrified. All of the Phase III AEM-7 tests were conducted operating out of Amtrak's Philadelphia facility. Repeated runs at progressively higher speeds were conducted at MP 50 to 53 on the Harrisburg Line track. The Phase III over-the-road tests were performed on the mainline track from Washington to Philadelphia.

DYNAMIC CHECKOUT TEST

Prior to the formal test phases, a series of dynamic checkout tests were conducted. In Phase I and Phase II the checkout runs were made on Curve 67 and 68 located between Milepost 145 and 146. This curve was instrumented with track force and displacement measurement sensors. The force measurements from the instrumented wheels were compared to the similar data from the wayside measurement sensors. The wayside instrumentation was not used for the AEM-7 test (Phase III) but for all phases the wheelset data was checked for balance and repeatability and the results compared to the vehicle weight. The lateral forces were calibrated using the laboratory calibration data. The primary purpose of these tests was to confirm that the instrumentation systems were operational. The validation test consisted of repeated tests in tangent and curved sections of track and dynamic comparison checks with the track instrumentation installed by Battelle Columbus Laboratories.

The results from the wayside sites are contained in Appendix D. The repeated runs over this site confirmed that there was good agreement between the wayside measurements and the instrumented wheels and that the measurements from the instrumented wheels were repeatable and independent of rotational speed.

4.2 PHASE I AMCOACH TEST GENERAL DISCUSSION

The LRC locomotive and the test Amcoach were instrumented and arranged as described in Section 3. (Also see Section 3 and 5 of Ref. 22.) Table 4-1 summarizes the Phase I test runs.

PHASE I SERIES I

Series 1 of the Phase I test consisted of repeated passes over Curve 67 in both directions. This pair of curves was carefully selected based on a detailed review of train handling and safety requirements. The curve selection criteria is described in Reference 22. Both the eastbound and westbound tracks were instrumented with strain gage bridges and displacement measurement sensors as is described in Appendix D. The wayside instrumentation was used to determine that the most critical force levels were, in fact, experienced at the axles which had been instrumented with few exceptions.

For the Series 1 and 2 tests, two test runs were made at each predetermined speed; then the speed was increased in increments corresponding to steps in the cant deficiency. The absolute wheel forces, lateral to vertical forces ratios and other safety criteria were monitored. When any of the predetermined stop test levels were reached the test series was discontinued.

The series 1 tests were made at curve 67 eastbound on track 2. The curvature was $2^{\circ} 20'$ with 5.88 inches of crosslevel using wood ties and 133 lb/yard rail continuously welded. An unusual feature on this track was the presence of over four inches of crosslevel on the tangent section bordering the spirals. At the higher speeds, it tended to throw the vehicles at the end of the spiral. This produced overshoot in the vehicle response. Because of this overshoot in the vehicle response the series 1 tests eastbound were discontinued at speeds which corresponded to 7 inches of cant deficiency. After more experience had been acquired with the dynamic performance of the test vehicles the LRC coaches were run through this same curve at much higher speeds. This should not be interpreted to mean that the LRC coaches were found to be safer than the Amcoach car. The test on the Amcoach car was not scheduled to extend beyond 7 inches of cant deficiency so the tests were discontinued at speeds which corresponded to 7 inches of cant deficiency when the overshoot response was encountered. The basic Amcoach car does not tilt so the discontinuity in the crosslevel with respect to curvature produced relatively high lateral accelerations. For additional details on these runs, the test logs and maps of the data records are included in the Test Events Report (Ref. 23).

TABLE 4-1

PHASE I TEST SUMMARY

<u>Series</u>	<u>Date</u>	<u>Run No.</u>	<u>Max. Cant Def.</u>	<u>Route</u>	<u>Track</u>
1	7/29/80	1-6	4"	Curve 67	2 (East-wood ties)
1	7/31/80	1-3	5"	Curve 67	2
1	8/1/80	1-5	7"	Curve 67	2
2	8/2/80	1-9	9"	Curve 67	1 (West-conc.ties)
3	8/5/80	1	3"	N.H. to Groton	2
		2	3"	Groton to N.H.	1
		3	4"	N.H. to Groton	2
		4	5"	Groton to N.H.	1
3	8/6/80	1	5"	N.H. to Groton	2
		2	6"	N.H. to Groton	2
		3	6"	Groton to N.H.	1
4	8/7/80	1	7"	N.H. to Groton	2
			5"	Groton to Prov.	2
			5"	Prov. to Groton	1
		2	7"	Groton to N.H.	1
4	8/8/80	1	7"	N.H. to Prov.	2
		2	7"	Prov. to N.H.	1

PHASE 1 SERIES 2

The Series 2 tests of the Amcoach were run on Curve 67 westbound on Track 1. The curvature was $2^{\circ}36'$ with 5.25 inches of curvature using 133 lb/yd CWR and concrete ties. Crosslevel was not present on the preceding tangent. The Series 2 tests were performed at speeds which corresponded to cant deficiencies from 3 inches to over 9 inches. As shown in the results for the Phase 1 Series 2 test, the westbound curve has much better coordination between the crosslevel and curvature so the lateral accelerations and wheel forces in negotiating this curve were much lower.

PHASE 1 SERIES 3

The third series of the Phase 1 tests were performed between New Haven and Groton. The routes and run sequences are listed in Table 4-1 and the detailed records of the test are shown in the Test Events Report (Ref. 23). The first speed profile regulated cant deficiency at 3 inches and subsequent speed profiles included a maximum of up to 7 inches of cant deficiency.

The object of the third and fourth series of tests was to run a representative set of curves at higher speeds to collect peak data on the curving forces, accelerations and displacements. The test zone selected for the Phase 1 test was the set of curves between New Haven and Groton. The basic plan was to negotiate as many of these curves as possible or practical at increasingly higher speeds. Some of the curves in this territory had recently been reworked so the operations personnel were requested to restrict the speeds in any curves which had not accumulated at least 100,000 tons of traffic after being reworked. This restriction eliminated some curves in the test zone but the remaining set of curves producing discernable curving forces range from 4 degrees to about 0.5 degrees. The geometry of all the curves in the test zone is shown in Table 4-2. For the Series 3 and 4 tests this curve data was entered in the data acquisition computer and speed profile plots were developed showing the speed profile required to maintain a targeted constant cant deficiency. The speed profile maps were reviewed with the Amtrak train operations personnel and FRA officials. The speed profiles were modified to observe slow orders and to provide sufficient distance to make the required speed adjustments. An actual operating speed profile was generated and distributed to the Amtrak operations personnel, the road foreman of the locomotive, the FRA Test Director, and the ENSCO Test Director and Safety Director. These special profiles were used to monitor the test runs and for annotation of the data.

TABLE 4-2
 DESCRIPTION OF CURVES BETWEEN PROVIDENCE, RI
 (MP180) AND NEW HAVEN, CT (MP73)

Curve Number	Curve Location Westend MP + Feet		Total Length Feet	Track #1		Track #2	
				West Bound		East Bound	
			Curvature Degrees	Superelevation Inches	Curvature Degrees	Superelevation Inches	
47	180	2935	2720	+2.00	+6.25	-1.75	-5.30
48	180	1522	657	-1.00	-2.25	+1.00	+1.72
49	180	672	663	+1.00	+3.05	-0.92	-2.91
50	173	4371	2726	-1.50	-5.55	+1.50	+4.89
51	173	204	1456	+1.50	+6.00	-1.25	-4.98
52	172	3127	3403	+1.5 +1.6 +1.2	+3.70 +6.30 +5.75	-1.17	-4.61
4-5 53	170	3103	1232	-1.1	-4.30	+1.00	+4.12
54	168	900	300	+0.17	+1.00	-0.17	-1.00
55	167	4800	300	-0.18 +0.18	-1.00 +1.00	+0.18 -0.18	+1.00 -1.00
56	161	4800	600	-0.25	-1.50	+0.25	+1.50
57	161	3200	300	+0.25	+0.25	-0.25	-0.25
58	159	4063	3268	+1.10	+5.55	-1.00	-5.11
59	158	3630	400	+0.25	+1.15	-0.38	-1.06
60	158	2780	300	-0.25	-0.75	+0.32	+1.00
61	153	4893	1788	+2.10	+6.50	-1.92	-6.22

TABLE 4-2 (Cont'd).
 DESCRIPTION OF CURVES BETWEEN PROVIDENCE, RI
 (MP180) AND NEW HAVEN, CT (MP73)

Curve Number	Curve Location Westend MP + Feet		Total Length Feet	Track #1		Track #2	
				West Bound		East Bound	
			Curvature Degrees	Superelevation Inches	Curvature Degrees	Superelevation Inches	
62	153	509	2684	+1.60	+4.70	-0.83 -1.50	-3.44 -4.86
63	151	4902	3081	-2.30	-6.25	+2.17	+5.68
64	150	4127	1374	+2.00	+6.25	-1.75 -1.17	-5.75 -4.83
65	148	3246	4403	-1.30 -1.20 -1.70	-3.80 -4.10 -5.20	+1.17 +1.58	+4.11 +4.96
66	147	1571	3773	+1.1 +2.1 +1.1	+2.70 +5.50 +3.00	-1.00 -2.08 -1.17 -1.00 -0.75	-4.62 -6.07 -5.28 -4.35 -3.11
67	145	906	1038	-2.6	-5.60	+2.33	+5.88
68	144	626	2666	+2.0	+5.25	-1.92	-6.21
69	142	2542	888	+1.8	-3.75	-1.58	-3.26
70	141	4306	1647	-2.2	-6.00	+2.25	+5.98
71	140	4910	2750	-2.1	-4.80	+2.00	+4.29
72	139	2188	4704	+1.42 +1.00 +2.08	+3.26 +2.46 +5.04	-1.50 -1.00 -2.00	-4.61 -4.64 -6.15
73	138	2663	2620	-2.08	-5.38	+2.17	+6.38
74	138	1279	788	+1.42	+4.39	-1.58	-4.74

4-7

TABLE 4-2 (Cont'd)
 DESCRIPTION OF CURVES BETWEEN PROVIDENCE, -RI
 (MP180) AND NEW HAVEN, CT (MP75)

Curve Number	Curve Location Westend MP + Feet		Total Length Feet	Track #1		Track #2	
				West Bound		East Bound	
				Curvature Degrees	Superelevation Inches	Curvature Degrees	Superelevation Inches
75	136	1723	1295	+1.42	+1.85	-1.33	-3.50
75A	135	4943	2170	+3.50 +3.92	+4.59 +5.36	-3.75	-5.82
76	135	2390	1223	-2.92	-5.50	+3.00	+6.38
77	134	4783	1968	-3.00	-5.79	+2.58 +3.08	+5.66 +5.61
78	134	1407	1333	+2.42	+5.49	-2.42	-4.98
79	133	2819	1953	+3.58 +3.00	+5.34 +4.06	-3.58 -2.92	-5.23 -5.47
80	133	2036	498	+0.83	+1.38	-0.83	-1.65
81	132	676	2288	-4.00	-5.71	+3.92 +0.75	+5.27 +1.32
82	131	1417	3372	-1.0 -2.0	-2.47 -3.76	+0.33 +2.00 +1.00	+2.68 +3.53 +3.11
83	130	3059	1614	+1.58	+3.38	-1.50	-4.39
84	129	4612	1335	+2.67	+6.19	-2.67	-5.33
85	129	1777	2149	+3.42	+4.83	-2.00 -3.08 -3.17	-4.08 -5.61 -5.53
86	128	4841	1759	+2.17 +1.58	+3.19 +3.79	-1.50	-3.41

4-8

TABLE 4-2 (Cont'd)
 DESCRIPTION OF CURVES BETWEEN PROVIDENCE, RI
 (MP180) AND NEW HAVEN, CT (MP75)

Curve Number	Curve Location Westend MP + Feet		Total Length Feet	Track #1		Track #2	
				West Bound		East Bound	
			Curvature Degrees	Superelevation Inches	Curvature Degrees	Superelevation Inches	
87	127	85	2887	-0.92	-2.48	+1.00	+2.21
88	126	1148	1332	+3.67	+6.39	-3.58	-6.05
89	125	4754	1107	-2.25	-5.26	+2.25	+6.04
90	125	2009	1525	+4.67	+6.04	-4.58	-6.22
91	124	3579	3273	-2.58	-4.45	+2.42	+3.93
				-1.50	-4.03	+1.50	+4.03
				-1.92	-3.76	+1.83	+4.06
92	124	307	1234	-2.17	-3.16	+1.17	+2.87
				-3.83	-3.62	+4.25	+2.42
4-9 93	123	284	3534	-1.0	-1.68	+1.08	+0.93
						+6.08	+3.40
				-5.0	-3.20	+2.67	+2.87
94	122	3310	1773	+6.50	+2.87	-6.25	-3.00
				+9.42	+3.09	-9.58	-3.06
				+2.92	+2.85	-3.17	-1.15
95	122	1967	809	-7.25	-3.28	+7.25	+2.90
96	122	568	686	+2.17	+2.69	-2.08	-2.90
97	121	4314	558	+0.67	+2.00	-1.08	-1.78
98	120	3723	4350	+4.25	+5.46	-3.92	-5.03
				+3.83	+5.36	-1.33	-3.01
				+0.92	+1.77	-1.00	-1.95
				+1.75	+1.79	-1.58	-2.13
				+0.92	+1.79	-1.08	-2.10
				+1.75	+1.77	-1.42	-1.99

TABLE 4-2 (Cont'd)
 DESCRIPTION OF CURVES BETWEEN PROVIDENCE, RI
 (MP180) AND NEW HAVEN, CT (MP73)

Curve Number	Curve Location Westend MP + Feet		Total Length Feet	Track #1		Track #2	
				West Bound		East Bound	
			Curvature Degrees	Superelevation Inches	Curvature Degrees	Superelevation Inches	
99	119	3461	1801	-2.50	-5.72	+2.58	+5.67
100	118	4762	2165	-3.25 -2.92 -2.08	-6.53 -6.33 -4.88	+3.42 +3.00 +2.17	+6.00 +6.07 +4.79
101	118	3457	844	+3.00	+4.78	-3.08	-4.44
102	118	209	1927	+1.50 +3.08	+1.81 +6.51	-3.00	-6.04
103	117	421	2856	+3.08	+6.39	-3.00	-5.95
104	116	3951	1325	-2.25	-4.79	+2.25	+5.06
105	115	4207	4619	-1.58 -1.08 -0.50 -1.33	-3.27 -1.63 -1.50 -2.26	+1.50 +1.83 +0.83 +1.92 +1.08 +1.50	+4.24 +4.31 +3.92 +4.15 +3.91 +1.20
106	114	1564	1564	-1.92	-4.47	+1.92	+5.50
107	113	1902	2718	+2.08	+5.08	-2.00	-5.78
108	112	3542	884	-2.50	-3.89	+2.42	+3.29
109	112	2186	1198	+3.08	+5.38	-3.00	-4.73
110	112	756	1219	-3.25	-5.68	+3.17	+5.63
111	110	4485	1635	+2.08	+5.45	-2.08	-5.15
112	110	231	2446	+2.08	+5.25	-2.00	-5.32

4-10

TABLE 4-2 (Cont'd)
 DESCRIPTION OF CURVES BETWEEN PROVIDENCE, RI
 (MP180) AND NEW HAVEN, CT (MP75)

Curve Number	Curve Location Westend MP + Feet		Total Length Feet	Track #1		Track #2	
				West Bound		East Bound	
				Curvature Degrees	Superelevation Inches	Curvature Degrees	Superelevation Inches
113	109	3318	2027	-2.08	-5.26	+2.08	+4.83
114	108	370	4072	+0.83	+3.34	-1.00 -0.67 -0.42	-3.83 -2.86 -1.85
115	107	230	1775	-2.00 -2.08	-5.07 -4.95	+2.00	+4.76
116	106	1361	1446	-3.58	-3.60	+3.50	+3.63
117	105	1266	1049	+0.83 TC	+2.25 TC	-0.83	-1.76
118	103	3470	1111	+2.17	+5.56	-2.08	-5.62
119	103	502	266	+0.18 TC	+1.00 TC	-0.18 TC	-1.00 TC
120	102	58	994	+2.83	+5.04	-2.67	-5.81
121	100	3547	1442	-0.92	-2.48	+0.92	+2.34
121A	100	1279	2268	-1.92	-6.38	+1.92	+5.95
122	99	3722	1750	+1.24 +2.17	+3.84 +5.84	-1.25 -2.08	-2.36 -5.53
123	98	302	3884	+0.58 +1.33 +1.08	+2.43 +6.22 +4.30	-0.50 -1.08	-1.20 -2.93
124	97	1519	1408	-1.00	-2.43	+1.00	+2.41
125	96	976	1687	+0.92 +1.50	+2.00 +4.85	-1.42 -1.25	-4.53 -3.61

4-11

TABLE 4-2. (Cont'd)

DESCRIPTION OF CURVES BETWEEN PROVIDENCE, RI
(MP130) AND NEW HAVEN, CT (MP73)

Curve Number	Curve Location Westend MP + Feet		Total Length Feet	Track #1		Track #2	
				West Bound		East Bound	
				Curvature Degrees	Superelevation Inches	Curvature Degrees	Superelevation Inches
126	94	1917	2227	-2.25	-5.70	+2.08 +2.25	+6.12 +6.14
127	92	5178	1480	+1.50 +1.83	+2.79 +4.42	-1.33 -1.92	-4.10 -5.58
128	91	1509	1341	-0.92	-3.30	+0.92	+2.06
129	90	4569	325	+0.42	+1.03	-0.40	-1.00 TC
130	90	4067	321	-0.83	-0.43	+0.37 TC	+0.50 TC
131	90	1063	1151	-0.50	-2.26	+0.58	+0.29
132	89	200	300	+0.25 TC	+1.00 TC	-0.25 TC	-1.00 TC
133	87	5065	1738	-1.08	-3.92	+0.83 +1.08	+2.29 +2.78
134	87	797	1722	+2.42	+5.22	-2.33	-6.28
135	86	3424	503	+0.42	+1.34	-0.40	-0.50
136	86	1634	742	-1.08	-3.38	+1.08	+2.53
137	85	3227	1586	+2.17	+6.19	-2.00	-6.45
138	83	1063	2500	-1.0	-2.88	+1.00	+2.76
139	82	2512	1440	+0.83	+2.82	-0.75	-3.05
140	82	550	962	+0.58	+2.01	-1.42	-4.48
140A	81	4685	1145	+1.50	+4.60	-0.50	-1.64
141	81	2237	1541	-3.92	-6.11	+3.92	+5.75

TABLE 4-2 (Cont'd)
 DESCRIPTION OF CURVES BETWEEN PROVIDENCE, RI
 (MP180) AND NEW HAVEN, CT (MP73)

Curve Number	Curve Location Westend MP + Feet		Total Length Feet	Track #1		Track #2	
				West Bound		East Bound	
				Curvature Degrees	Superelevation Inches	Curvature Degrees	Superelevation Inches
142	81	287	1414	+1.00 +3.17	+2.23 +4.10	-2.58	-3.53
143	80	2266	1432	+1.17 +1.92	+4.05 +5.34	-1.42	-4.92
144	79	4923	1391	+2.67 +3.17	+6.00 +5.98	-2.92	-5.73
144A	79	580	4101	-1.83 -1.00 -1.17 -2.08	-4.65 -2.07 -2.44 -5.16	+1.17 +2.08	+2.96 +5.93
145	78	1266	1656	-2.42	-5.20	-2.08 -2.33	-5.00 -4.84
146	77	4455	1549	+3.25	+6.42	-3.00 -3.25	-5.79 -5.51
147	76	4679	3701	+1.33	+4.16	-1.25	-3.03

4-15

PHASE I SERIES 4

The fourth series of tests was designed to be a confirmation test run at a target speed slightly higher than the projected revenue speed profile. The test zone was expanded to include Providence, RI. For Phase I the speed profile for the Series 4 high speed round trip was targeted for 7 inches of cant deficiency. To assure that this speed was safe, a checkout test was run at 5 inches of cant deficiency.

4.3 PHASE II LRC TRAIN TEST

Phase II was a test of the LRC coach towed by the LRC locomotive. This phase was similar to the Phase I test and the general procedure described in the discussion of the Phase I test plans were followed for this test series as well. Table 4-3 summarizes the test runs.

PHASE II AND SERIES 1 AND 2

The Series 1 and 2 tests were performed on the same test zone as used for the Phase I tests. The Phase II tests were started at speeds which corresponded to 5 inches of cant deficiency and increased up to about 12 inches of cant deficiency on Curve 67 Track 2 (eastbound). The Series 2 test on Track 1 Curve 67 (westbound) was started at 7 inches of cant deficiency. The highest speed runs in Series 2 of Phase II were made at 15 inches of cant deficiency.

PHASE II SERIES 3 AND 4

The Phase II Series 3 and 4 tests were similar to the Amcoach tests with the exception that some of the tests were run with the LRC Coach banking system activated and some were made with the banking system inactive. The Phase II Series 3 tests were made over the same section of track.

Since the Amcoach test provided basic data at the lower speeds the Phase II Series 3 tests were started at speeds corresponding to 6 inches of cant deficiency and were repeated up to and including 11 inches of cant deficiency. As with Phase I, speed profiles were developed and the locomotive operators were asked to run the special speed profile where possible. At the higher speeds the train acceleration and braking restricted the actual speed profiles so that the ideal speed profiles were seldom achieved. The detailed analysis of the test results deal with this by considering the highest cant deficiency at each curve independent of the run history.

TABLE 4-3
PHASE II TEST SUMMARY

<u>Series</u>	<u>Date</u>	<u>Run No.</u>	<u>Max. Cant Def.</u>	<u>Route</u>	<u>Track</u>
1	8/25/80	1-8	8"	Curve 67	2 (East-wood ties)
1	8/26/80	1-7	12"	Curve 67	2
2	8/27/80	1-7	11"	Curve 67	1 (West-conc. ties)
2	8/28/80	1-7	15"	Curve 67	1
3	9/2/80	1	6"	N.H. to Groton	2
		2	7"	Groton to N.H.	1
		3	7"	N.H. to Groton	2
3	9/3/80	1	7"	N.H. to Groton	2
		2	8"	Groton to N.H.	1
		3	8"	N.H. to Groton	2
		4	9"	Groton to N.H.	1
3	9/4/80	1	9"	N.H. to Groton	2
		2	10"	Groton to N.H.	1
		3	10"	N.H. to Groton	2
		4	11"	Groton to N.H.	1
4	9/8/80	1	7"	N.H. to Prov.	2
		2	9"	Prov. to N.H.	1
4	9/9/80	1	10"	N.H. to Groton	2
		2	9"	Groton to Prov.	2
		3	3"	Prov. to Boston	2
4	9/10/80	1	9"	Prov. to Groton	1
		2	9"	Groton to Prov.	2

4.4 PHASE III AEM-7 LOCOMOTIVE TEST

The AEM-7 locomotive was equipped with a pair of instrumented wheels purchased by Amtrak from EMD. These wheelsets were developed by ASEA for the AEM-7 and were used earlier by EMD for the acceptance test of this locomotive. The basic test program for the AEM-7 electric locomotive was similar to the test on the other vehicles except the test zones were changed to the electrified territory south of New York. As part of this same test program, Amtrak performed tests on the locomotive pantograph system. These tests were supported by a photographic team from the Transportation Test Center and by technical personnel from EMD.

For the Phase III test repeated runs were made on a sequential pair of curves on the Philadelphia-Harrisburg line between Milepost 50 and 53. The pair included both a right and a left curve each at about 4° with 6 inches of superelevation. Therefore, one series of runs at this site was equivalent to Series 1 and 2 of the previous phases. The second part of the Phase III tests were continuous runs between New York and Washington and they are referred to in the Test Events Report (Ref. 23) as Series 3 because they are analogous to the Series 3 tests of the previous phases.

PHASE III SERIES 1

The repeated curving test of the AEM-7 locomotive was performed on the Harrisburg line between Milepost 50 and 53. At Milepost 51 is a 4 degree 15 minute left curve with 6-1/8 inches of cross-level and at Milepost 52 is a 4 degree 18 minute curve with 6-1/4 inches of crosslevel. The repeated tests were started at speeds corresponding to 3 inches of cant deficiency and were run up to and including 11 inches of cant deficiency. Table 4-4 lists the Phase III runs.

TABLE 4-4
PHASE III TEST SUMMARY

<u>Series</u>	<u>Date</u>	<u>No.</u>	<u>Cant Def.</u>	<u>Route</u>
1	10/31/80	1-11	11"	MP50 to 53 Phila.- Harrisburg Line
3	11/4/81	1	5"	Phila. to New York
		2	5"	New York to Phila.
		3	5"	Phila. to New York
		4	5"	Wash to Phila.
3	11/5/81	1	5"	Phila. to New York
		2	5"	New York to Phila.

PHASE III SERIES 3

The Phase III Series 3 tests were made on a test zone from Washington, DC to New York City, NY. Round trip runs were made using a speed profile corresponding to a maximum of 5 inches of cant deficiency although roughness in switches between curves frequently limited the speed. However, in addition to monitoring the forces in curves, the Phase III test included monitoring forces occurring at crosslevel interlocks and switches. The population of curves in the Phase III test zone is shown in Table 4-5.

4.5 TEST CONSISTS

GENERAL

The test was divided into three phases as described above. The consist for each phase was changed to include the particular coach or locomotive being tested but LRC train served as the basic unit. The basic consist was made up of the LRC locomotive and five coaches. The coach being tested was located directly behind the locomotive. The data acquisition system was located in the second coach (an LRC coach) for all of the tests. For the AEM-7 test in Phase III the LRC locomotive was replaced by the AEM-7 locomotive. On some of the high speed runs in Phase II the consist was reduced to the LRC locomotive plus four LRC coaches to obtain better acceleration.

PHASE I

The consist for the Phase I test was LRC locomotive No. 38 pulling Amcoach Car No. 21000 plus four LRC coaches. The Amcoach was located directly behind the LRC locomotive. The lead truck of the Amcoach was equipped with instrumented wheels, and the car was blasted with 13,000 pounds of brake shoes stacked on the floor of the car. The Amcoach was a standard car with the brakes removed on the truck equipped with instrumented wheels. The LRC coaches were all unmodified but were operated without using the banking system.

PHASE II

The consist for the Phase II test was LRC locomotive No. 38 and five LRC coaches. The lead coach being tested was No. 48. The lead truck of this car was equipped with instrumented wheels (brakes disabled) and the car instrumented as described in Section 3. 14,400 pounds of brake shoes for ballast was uniformly distributed on the floor of the car. The coach banking systems were operated except during comparison runs.

TABLE 4-5

DESCRIPTION OF CURVES BETWEEN NEW YORK (MP11)
AND WASHINGTON (MP132-FROM PHILADELPHIA)

Curve No.	Curve Location		Total Length Feet	Eastbound			3" Cant Def. Speed	Westbound			3" Cant Def. Speed
	Westend MP + Feet			Track No.	Curvature Degrees	Super-elevation Degrees		Track No.	Curvature Degrees	Super-elevation Inches	
248				TC	-1.30	0.00	57.4	TC	+1.30	0.00	57.4
249	11	2605	1527	1	+1.00	+2.75	90.6	4	-1.00	-2.85	91.4
250	13	3410	1854	1	-0.33	-0.74	127.2	2	+0.33	+1.56	140.5
251				TC	+0.10	+0.50	223.6	TC	-0.10	-0.50	223.6
252	15	3961	1128	1	+1.92	+3.71	70.7	4	-2.00	-4.01	70.8
253	15	2116	1671	1	-2.00	-4.22	71.8	4	+2.42	+3.71	62.9
254				TC	-0.17	-0.75	177.5	TC	+0.17	+0.75	177.5
255				TC	+0.13	+0.75	203.0	TC	-0.13	-0.75	203.0
256	20	3026	727	1	-0.58	-2.05	111.5	TC	+0.13	+1.50	222.4
257				TC	+0.37	+1.25	128.1	TC	-0.15	-0.75	189.0
259	21	1647	1570	1	-0.50	-2.01	119.6	3	+0.50	+2.06	120.2
260	21	1216	314	1	+0.33	+1.56	140.5	3	-0.42	-1.50	123.7
261	22	832	831	1	-0.75	-3.19	108.6	3	+0.83	+2.71	99.1
262	23	5083	704	1	+0.75	+3.27	109.3	3	-0.83	-2.96	101.3
263	23	983	1811	1	-0.75	-3.26	109.2	3	+0.75	+3.21	108.8
264	24	2466	3507	1	+0.83	+3.36	104.6	3	-0.83	-3.06	102.1
265	24	606	1241	1	-1.42	-6.40	97.2	3	+1.50	+5.87	91.8
266	25	2534	2117	1	+1.58	+6.62	93.3	3	-1.50	-6.22	93.7
267	26	2337	4441	1	-1.17	-6.41	107.2	3	+1.25	+5.77	100.1
268	27	1908	1337	1	-1.92	-6.25	83.0	3	+2.08	+6.40	80.3
269	28	4389	2120	1	+1.50	+5.95	92.3	3	-1.50	-6.23	93.8
270	28	2023	1040	1	+0.83	+3.00	TC 101.6	3	-0.92	-3.33	99.1
271	29	151	710	1	-0.50	-1.13	108.6	TC	+0.15	+1.25	201.2
272	31	1875	2048	TC	+0.38	+2.00	137.1	3	-0.50	-1.96	119.0
273	32	3570	1041	1	+0.50	+1.96	110.0	3	-0.50	-1.31	111.0
274	35	4339	2279	1	+0.50	+2.19	121.8	3	-0.50	-2.72	127.8
275	40	3694	1249	1	+0.33	+1.02	131.9	4	-0.33	-1.37	137.5
276	41	4137	4009	1	-0.58	-2.17	112.8	3	+0.50	+4.28	144.2
277	51	2727	668	1	-0.42	-1.65	125.8	4	+0.33	+2.09	148.4
278				TC	+0.25	+2.25	173.2	TC	-0.25	-2.25	173.2
279	58	3841	507	1	-1.08	-2.70	86.8	3	+0.75	+3.20	108.7
280	60	3987	5391	1	+0.58	+2.07	111.7	3	-0.83	-4.04	110.1
282	61	2385	1715	1	-0.42	-1.29	120.8	3	+0.42	+1.36	121.8
283	62	810	2697	1	-0.75	-3.45	110.8	3	+0.75	+3.43	110.7
284	65	439	1693	1	+0.67	+3.15	114.5	3	-0.67	-3.26	115.5
285	67	3754	3497	1	-0.75	-3.18	108.5	3	+0.75	+2.94	106.4
286	68	721	4871	1	-0.50	-1.47	113.0	3	+0.50	+1.33	111.2
287				TC	+0.06	0.00	267.3	TC	-0.06	0.00	267.3
288	71	2267	2787	1	+1.17	+5.47	101.7	3	-1.17	-6.16	105.8
289	73	2434	1876	1	-0.42	-1.48	123.4	3	+0.42	+1.21	119.7
290	75	2933	1897	1	+1.42	+4.40	86.3	3	-1.42	-5.22	90.9
291	76	4853	2364	1	-1.42	-5.55	92.7	3	-1.58	+6.10	90.7
292	76	3260	1411	1	+0.75	+2.96	106.5	3	-0.75	-3.46	110.9

TABLE 4-5 (Cont'd)

DESCRIPTION OF CURVES BETWEEN NEW YORK (MP11)
AND WASHINGTON (MP132-FROM PHILADELPHIA)

Curve No.	Curve Location Westend MP + Feet	Total Length Feet	Eastbound			3" Cant Def. Speed	Westbound			3" Cant Def. Speed	
			Track No.	Curvature Degrees	Super-elevation Degrees		Track No.	Curvature Degrees	Super-elevation Inches		
293	77	2785	1750	1	-0.75	-2.95	106.5	3	+0.75	+3.00	97.6
294	78	5208	1571	1	+1.00	+4.24	101.7	TC	-0.93	-5.00	110.9
295	79	2994	1373	2	-0.33	-1.65	141.9	2	-0.33	+1.72	142.9
296	80	1658	2657	1	-0.58	-1.50	105.3	3	+0.58	+1.86	109.4
297	82	3798	2072	1	+1.75	+3.03	70.2	3	-1.83	-3.13	69.2
298	82	1391	1924	1	-4.25	-6.74	57.2	3	+4.08	+5.24	53.7
299	84	950	4020	1	+2.58	+5.15	67.2	3	-2.58	-5.18	67.3
299A	85	1144	283	1	-2.17	+0.11	43.6	3	+1.83	+0.14	49.5
300	86	5111	814	1	+1.08	+1.75	79.3	3	-0.83	-1.26	85.6
301	86	4554	288	2	-1.50	-0.16	54.9	3	+2.17	+1.40	53.8
302	86	2635	778	1	+2.67	+1.93	51.4	3	-2.17	-2.90	62.3
303	87	2872	795	1	+2.08	+4.11	69.9	3	-2.00	-3.02	65.5
303A	89	354	2843	1	-3.00	-2.08	49.2	4	+3.17	+1.50	45.0
304	90	198	1236	1	-4.92	-2.81	41.1	TC	+4.33	+2.00	40.6
305	3	3496	1437	1	-2.00	-2.41	62.2	2	+2.17	+3.31	64.5
306	3	626	2284	1	+2.85	+2.85	56.9	4	-2.42	-3.07	59.9
307	4	5008	902	1	-1.17	-2.89	84.8	4	+1.25	+3.65	87.2
308	7	5211	3270	1	-1.00	-2.95	92.2	4	+1.08	+3.25	90.9
309	7	1121	4031	1	+1.08	+3.11	89.9	4	-1.00	-2.64	89.9
311	8	4159	2165	1	-1.00	-3.01	92.7	4	+1.00	+3.28	94.7
312	10	1949	1237	1	+1.17	+4.52	95.7	4	-1.00	-1.90	83.7
313	12	5165	2883	1	+1.00	+4.23	101.6	4	-0.92	-3.09	97.2
314	13	1483	4723	1	-0.83	-3.33	104.4	4	+0.92	-2.87	95.5
315	14	427	1311	1	+0.83	+2.66	98.7	4	-0.75	-2.42	101.6
316	15	214	829	1	-0.42	-2.18	132.7	4	+0.58	+2.08	111.9
317				TC	+0.17	+1.00	183.3	TC	-0.17	-1.00	183.3
318				TC	-0.07	0.00	247.4	TC	+0.07	0.00	247.4
319	19	2897	2608	1	+1.08	+5.47	105.8	4	-0.92	-5.18	112.7
320	20	750	1777	1	-1.00	-5.52	110.3	4	+1.00	+6.53	116.7
321	22	5047	2358	1	+0.83	+3.10	102.5	TC	-0.90	-2.75	95.5
322				TC	+0.17	+1.50	194.5	-	-	-	-
322A				TC	+4.67	+2.00	39.1	TC	-4.67	-2.00	39.1
322B				TC	-2.50	-1.50	50.7	TC	+2.50	+1.50	50.7
323	23	4055	1360	1	+1.08	+5.56	106.4	4	-0.92	-4.61	108.7
324	24	2482	3085	3	-1.33	-6.06	98.6	4	+1.58	+6.40	92.2
325	24	1307	1175	3	-0.92	-3.59	101.2	4	+1.08	-3.85	95.2
326	26	4341	3981	3	+0.58	+1.78	108.5	3	-0.42	-1.65	125.7
327	27	1194	3079	1	-2.08	-1.77	57.2	3	-2.33	+1.82	54.4
328	28	2583	3000	2	+3.92	+2.51	44.8	3	-3.75	-2.97	47.7
329	30	3816	3574	2	-0.83	-5.42	120.4	TC	+0.93	+5.25	112.6
330	31	3335	1699	2	-1.00	-6.39	115.8	3	+1.08	+6.32	111.0
331	31	102	1022	2	+0.58	+2.23	113.5	3	-0.50	-1.95	118.9
332	34	5139	2343	2	+1.08	+6.07	109.5	3	-0.92	-6.15	119.2

TABLE 4-5 (Cont'd)
 DESCRIPTION OF CURVES BETWEEN NEW YORK (MP11)
 AND WASHINGTON (MP132-FROM PHILADELPHIA)

Curve No.	Curve Location		Total Length Feet	Eastbound			3" Cant Def. Speed	Westbound			3" Cant Def. Speed
	Westend MP + Feet			Track No.	Curvature Degrees	Super-elevation Degrees		Track No.	Curvature Degrees	Super-elevation Inches	
333	34	1570	2137	2	-0.50	-1.46	112.9	3	+0.58	+2.42	116.1
334	35	1995	624	2	-0.50	-1.25	110.2	3	+0.50	+2.25	122.5
335				TC	+0.33	+1.00	131.6	TC	-0.33	-1.00	131.6
336	41	2778	5693	2	+0.58	+1.68	107.4	4	-0.50	-3.05	+31.5
337	42	584	686	2	-0.50	-1.56	114.1	4	+0.58	+3.83	129.7
338				TC	-0.25	-0.50	141.4	TC	+0.25	+0.50	141.4
339	46	1002	2987	2	-0.58	-2.20	113.2	4	+0.67	+2.95	112.6
340	48	4061	2883	2	-0.92	-5.47	114.7	TC	+1.00	+5.50	110.2
341	49	92	1822	2	-1.00	-5.93	112.9	4	+1.08	+6.04	109.4
342	51	1936	3849	2	+1.50	+6.16	93.4	4	-1.33	-4.96	92.5
343	52	1152	3385	2	+0.83	+3.20	103.3	TC	-0.83	-4.00	109.8
344	54	1585	2336	2	-1.08	-5.95	108.8	3	+1.17	+6.81	109.4
345	55	4652	1717	2	-0.50	-2.91	129.9	3	+0.58	+2.40	115.3
346				TC	-0.17	0.00	158.8	TC	+0.17	0.00	158.3
347	58	4605	2176	2	+1.42	+6.09	95.6	3	-1.25	-5.84	100.5
348	58	634	1530	2	-0.42	-1.47	123.3	4	+0.58	+1.60	106.4
349	62	3559	4709	2	+0.75	+1.82	95.8	4	-0.75	-1.56	93.2
350	63	1511	3552	1	-0.58	-2.38	115.1	4	+0.75	+2.88	105.8
351	66	3326	3707	3	+1.00	+3.94	99.5	4	-1.00	-6.05	113.7
352	67	1434	2709	TC	-0.68	-1.25	94.5	4	+0.58	+3.41	125.7
353				TC	-0.18	-0.75	172.5	TC	+0.18	+0.75	172.5
354				TC	-0.50	-1.50	113.4	TC	+0.50	+1.50	113.4
355				TC	-0.10	0.00	207.0	TC	+0.10	0.00	207.0
356	78	1784	556	2	+0.42	+2.44	136.0	TC	-0.50	-1.00	106.9
357	79	3250	2810	2	+1.25	+5.89	100.8	3	-1.17	-6.13	105.6
358	83	2453	10393	TC	-0.17	-0.50	171.5	4	+0.33	+1.14	133.9
359				TC	-0.82	-4.75	116.2	TC	+0.82	+4.75	116.2
360				TC	-1.00	-4.75	105.2	TC	+1.00	+4.75	105.2
361	88	3531	3636	TC	+0.75	+3.00	106.9	4	-0.75	-4.15	116.7
362	89	4333	4478	TC	+1.87	+5.75	81.8	4	-0.92	-5.73	116.4
363	90	4482	4043	1	-0.75	-1.46	92.2	TC	+0.93	+4.00	103.7
364	90	1715	2767	2	-0.42	-2.17	132.6	TC	+0.63	+2.25	109.1
365	90	534	894	2	+0.58	+2.86	120.1	4	-0.67	-1.51	98.1
369	92	4267	5095	2	-0.33	-0.72	126.9	4	-0.42	+1.05	117.4
371	92	130	596	2	+0.67	+0.33	84.3	4	-0.?	-1.9?	82?
372	93	3235	2166	1	-1.75	-2.32	65.9	4	+2.08	+2.68	62.5
373	94	4167	1927	1	+2.17	+2.33	59.2	4	-2.00	-3.90	70.2
374	95	4735	1399	1	-4.00	-2.48	44.2	4	+4.17	+3.77	48.2
375	95	2661	1360	1	+4.75	+2.84	41.9	4	-3.42	-2.33	47.2
376	96	3480	967	1	-2.25	-0.38	46.3	-	-	-	-
377	97	3563	2011	3	+7.83	+2.82	32.6	TC	-8.00	-2.50	31.3
378	98	4291	803	3	-7.42	-2.60	32.8	TC	+7.50	+2.75	33.1
379				TC	-1.00	0.00	65.5	TC	+1.00	0.00	65.5

TABLE 4-5 (Cont'd)

DESCRIPTION OF CURVES BETWEEN NEW YORK (MP11)
AND WASHINGTON (MP132-FROM PHILADELPHIA)

Curve No.	Curve Location		Total Length Feet	Track No.	Eastbound		3" Cant Def. Speed	Track No.	Westbound		3" Cant Def. Speed
	MP	+ Feet			Curva- ture Degrees	Super- elevation Degrees			Curva- ture Degrees	Super- elevation Inches	
380	99	4835	2314	2	+4.67	+3.45	44.4	TC	-3.93	-2.25	43.7
381	99	2260	1843	2	-3.83	-4.43	52.6	3	+3.75	+3.77	50.8
382	100	1285	2187	1	+2.08	+2.13	59.4	3	-2.00	-6.34	81.7
383	100	275	737	1	-1.00	-1.80	82.8	3	+1.33	+4.04	87.0
384				TC	-0.37	-0.50	116.2	TC	+0.37	+0.50	116.2
385	103	4877	3222	1	+1.08	+2.46	85.0	3	-1.00	-4.98	106.8
386	103	317	453	2	-0.33	-1.18	134.5	TC	+0.18	+1.00	178.2
387	104	1747	1082	2	-0.83	-5.21	118.9	3	+1.08	+5.21	104.2
388	105	4550	1371	2	+0.92	+5.08	112.0	3	-0.83	-4.44	113.2
389	105	1610	1500	2	-0.50	-1.92	118.6	3	-0.50	+1.59	114.5
390	106	51	3093	2	+1.00	+5.83	112.3	3	-0.92	-5.54	115.2
391	107	544	2191	2	-1.42	-5.76	93.9	3	-1.58	+6.63	93.3
392	109	2895	2066	2	+0.50	+1.92	118.6	3	-0.50	-1.60	114.6
393				TC	+0.30	+0.75	133.6	-	-	-	-
394				TC	-0.50	-1.00	106.9	-	-	-	-
395	111	3189	1200	2	+1.00	+6.60	117.1	3	-1.00	-5.59	110.8
396	112	4434	2307	2	-1.00	-5.64	111.1	3	+1.08	+6.00	109.1
397	114	2889	1376	2	-1.00	-4.27	101.9	3	+1.00	+4.51	103.6
398	115	3549	2610	2	-1.00	-5.54	110.5	3	+1.00	+6.33	115.4
399	116	2418	1966	2	+1.00	+6.05	113.7	3	-1.00	-5.47	110.0
400	117	1937	2094	2	+1.08	+7.06	115.4	3	-1.00	-5.34	109.2
401	118	3760	2511	2	-1.50	-6.10	93.1	3	+1.58	+6.74	93.8
402	118	1471	769	2	+0.83	+4.28	111.9	3	-0.83	-3.56	106.3
403	119	3742	1125	2	+0.83	+3.90	109.0	3	-1.00	-3.92	99.4
404	120	1946	3027	2	-0.50	-0.96	106.4	3	+0.50	-1.90	118.3
405	121	4196	1127	2	-0.92	-5.31	113.6	TC	+1.00	+5.50	110.2
406				TC	-0.32	-1.00	133.6	TC	+0.32	+1.00	133.6
407	126	2476	1740	1	+1.00	+3.14	93.7	TC	-1.15	-6.00	105.7
408	127	4073	1530	1	+1.00	+3.21	94.2	TC	-1.00	-5.50	110.2
409	127	295	1642	1	-0.92	-3.06	97.0	TC	+0.82	+6.00	125.2
410	128	1980	998	1	-0.50	-1.13	108.6	3	+0.58	+1.70	107.6
411	?	?	?	2	+1.00	+4.82	106.0	TC	-1.00	-4.50	103.5
412	129	1015	215	2	+0.25	+2.60	178.9	TC	-0.32	-1.25	137.7
413	131	827	8429	2	-0.83	-5.67	122.2	3	+0.75	+4.64	120.6
414	134	443	3017	2	+1.00	+4.47	103.3	3	-1.00	-4.18	101.3
415	136	5101	1178	2	+3.17	+0.94	42.1	TC	-3.00	-1.00	43.6

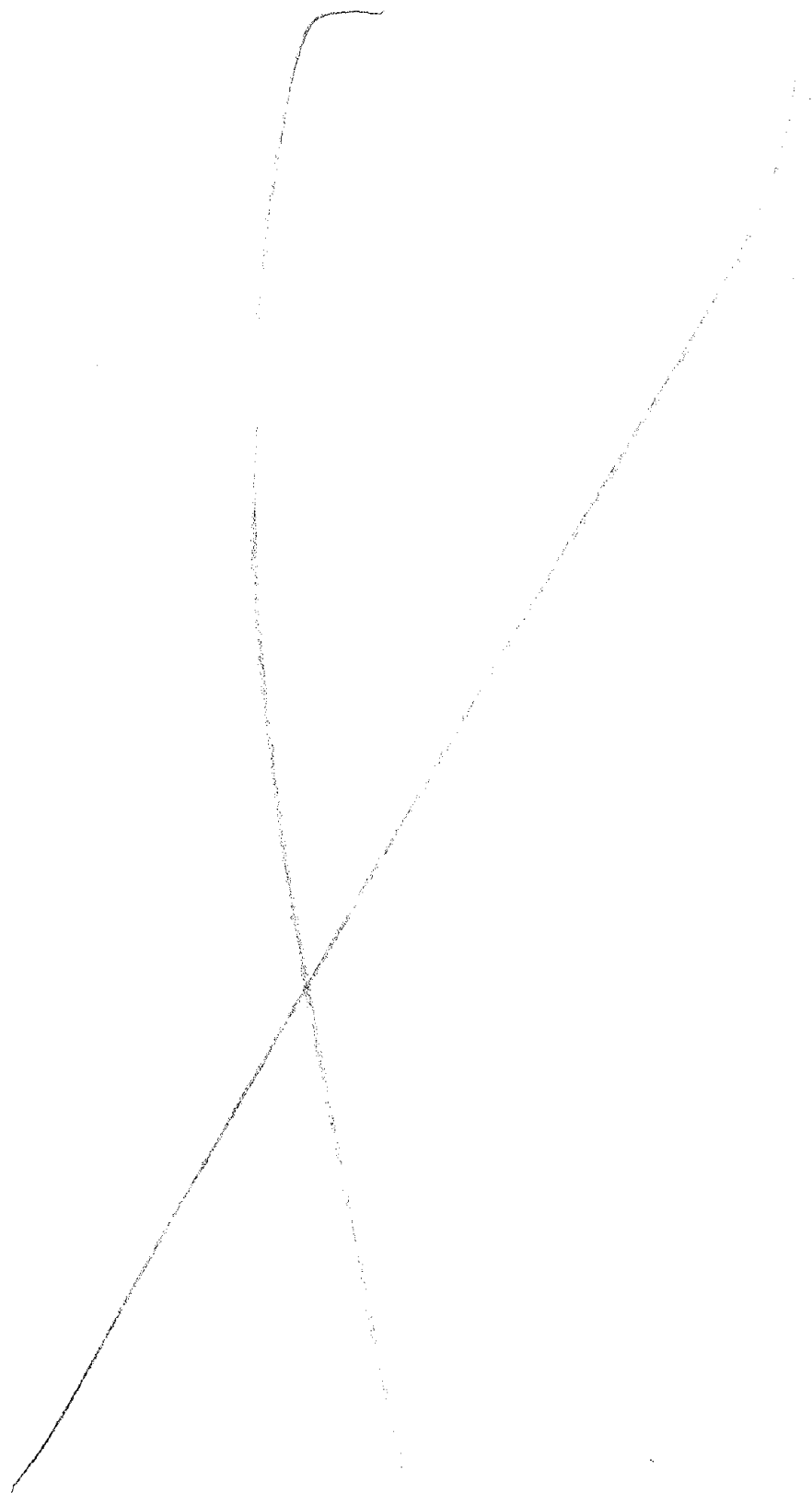
TABLE 4-5 (Cont'd)

DESCRIPTION OF CURVES BETWEEN NEW YORK (MP11)
AND WASHINGTON (MP132-FROM PHILADELPHIA)

Curve No.	Curve Location Westend MP + Feet	Total Length Feet	Track No.	Eastbound		3"	Track No.	Westbound		3"
				Curva- ture Degrees	Super- elevation Degrees	Cant Def. Speed		Curva- ture Degrees	Super- elevation Inches	Cant Def. Speed
380	99 4835	2314	2	+4.67	+3.45	44.4	TC	-3.93	-2.25	43.7
381	99 2260	1843	2	-3.83	-4.43	52.6	3	+3.75	+3.77	50.8
382	100 1285	2187	1	+2.08	+2.13	59.4	3	-2.00	-6.34	81.7
383	100 275	737	1	-1.00	-1.80	82.8	3	+1.33	+4.04	87.0
384			TC	-0.37	-0.50	116.2	TC	+0.37	+0.50	116.2
385	103 4877	3222	1	+1.08	+2.46	85.0	3	-1.00	-4.98	106.8
386	103 317	453	2	-0.33	-1.18	134.5	TC	+0.18	+1.00	178.2
387	104 1747	1082	2	-0.83	-5.21	118.9	3	+1.08	+5.21	104.2
388	105 4550	1371	2	+0.92	+5.08	112.0	3	-0.83	-4.44	113.2
389	105 1610	1500	2	-0.50	-1.92	118.6	3	-0.50	+1.59	114.5
390	106 51	3093	2	+1.00	+5.83	112.3	3	-0.92	-5.54	115.2
391	107 544	2191	2	-1.42	-5.76	93.9	3	-1.58	+6.63	93.3
392	109 2895	2066	2	+0.50	+1.92	118.6	3	-0.50	-1.60	114.6
393			TC	+0.30	+0.75	133.6	-	-	-	-
394			TC	-0.50	-1.00	106.9	-	-	-	-
395	111 3189	1200	2	+1.00	+6.60	117.1	3	-1.00	-5.59	110.8
396	112 4434	2307	2	-1.00	-5.64	111.1	3	+1.08	+6.00	109.1
397	114 2889	1376	2	-1.00	-4.27	101.9	3	+1.00	+4.51	103.6
398	115 3549	2610	2	-1.00	-5.54	110.5	3	+1.00	+6.33	115.4
399	116 2418	1966	2	+1.00	+6.05	113.7	3	-1.00	-5.47	110.0
400	117 1937	2094	2	+1.08	+7.06	115.4	3	-1.00	-5.34	109.2
401	118 3760	2511	2	-1.50	-6.10	93.1	3	+1.58	+6.74	93.8
402	118 1471	769	2	+0.83	+4.28	111.9	3	-0.83	-3.56	106.3
403	119 3742	1125	2	+0.83	+3.90	109.0	3	-1.00	-3.92	99.4
404	120 1946	3027	2	-0.50	-0.96	106.4	3	+0.50	-1.90	118.3
405	121 4196	1127	2	-0.92	-5.31	113.6	TC	+1.00	+5.50	110.2
406			TC	-0.32	-1.00	133.6	TC	+0.32	+1.00	133.6
407	126 2476	1740	1	+1.00	+3.14	93.7	TC	-1.15	-6.00	105.7
408	127 4073	1530	1	+1.00	+3.21	94.2	TC	-1.00	-5.50	110.2
409	127 295	1642	1	-0.92	-3.06	97.0	TC	+0.82	+6.00	125.2
410	128 1980	998	1	-0.50	-1.13	108.6	3	+0.58	+1.70	107.6
411	129 1230	1206	2	+1.00	+4.82	106.0	TC	-1.00	-4.50	103.5
412	129 1015	215	2	+0.25	+2.60	178.9	TC	-0.32	-1.25	137.7
413	131 827	8429	2	-0.83	-5.67	122.2	3	+0.75	+4.64	120.6
414	134 443	3017	2	+1.00	+4.47	103.3	3	-1.00	-4.18	101.3
415	136 5101	1178	2	+3.17	+0.94	42.1	TC	-3.00	-1.00	43.6

PHASE III (AEM-7 TEST)

The Phase III consist was the AEM-7 locomotive No. 901 and three LRC coaches. The lead truck of the AEM-7 locomotive and the lead truck of the first LRC coach were equipped with instrumented wheels and sensors as described in Section 3. In addition to the usual sensors, the locomotive was equipped with a video camera and roof top accelerometer to observe pantograph operation.



5.0 SAFETY AND COMFORT CRITERIA

Various criteria are used in North America, Europe and Japan for the determination of curving speed. Concern for the possibility of derailment by vehicle overturning, wheel climb, rail rollover, and lateral track panel shift and of passenger discomfort has led to a multiplicity of criteria. The curving criteria have been reviewed as part of the Improved Passenger Equipment Project by Battelle Columbus Laboratory and many of their findings published in Reference (1) are included. The original sources are referenced except for conclusions by the BTL authors. Vehicle overturning is considered in the greatest detail because it appears to be the first limiting factor for the vehicles in this study.

5.1 VEHICLE OVERTURNING CRITERIA

When the overturning moments about the high rail caused by the lateral inertial forces acting at the vehicle center of gravity and by the wind force acting at the center of pressure equal the restoring moment due to the weight, the vehicle is balanced about the high rail. Figure 5-1 demonstrates the rollover computations. All computations that follow are based on half vehicle models which have half the mass and surface area of a vehicle and only one truck. For simplicity of illustration, all vehicle mass is considered to be concentrated at the body center of gravity (c.g.) in Figure 5-1. The geometry and stiffness of the primary and secondary suspension components result in a roll center (R.C.) about which the body c.g. has rotated through the angle δ . The roll center defined in this way can be considered to translate with the body a distance ϕ due to wheel flanging and lateral deflection of the primary and secondary suspensions. At greater than balance speed the effect of suspension deflections (and passive tilt motions) is to move the c.g. closer to the high rail thereby reducing the restoring moment.

The concept of weight vector intercept is used frequently to express the risk of vehicle rollover. Momentarily neglecting the wind force, Figure 5-1 may be used to directly visualize the weight vector intercept. The lateral inertial forces and vertical gravitational force form a resultant force vector which may be projected to the plane of the railheads. The intersection of the line of action of the resultant force with the railhead plane is the point about which the vehicle, with lateral curving loads, would balance at the instant the loads were measured. The distance from the track centerline to this point is called the weight vector intercept (or vector crossing). A symmetrically loaded vehicle at rest on a level track would have zero as a weight vector intercept, and at a weight vector intercept of 30 inches (assuming 60 inches between wheel contact with left and right rails) the vertical load on the low rail wheels would be

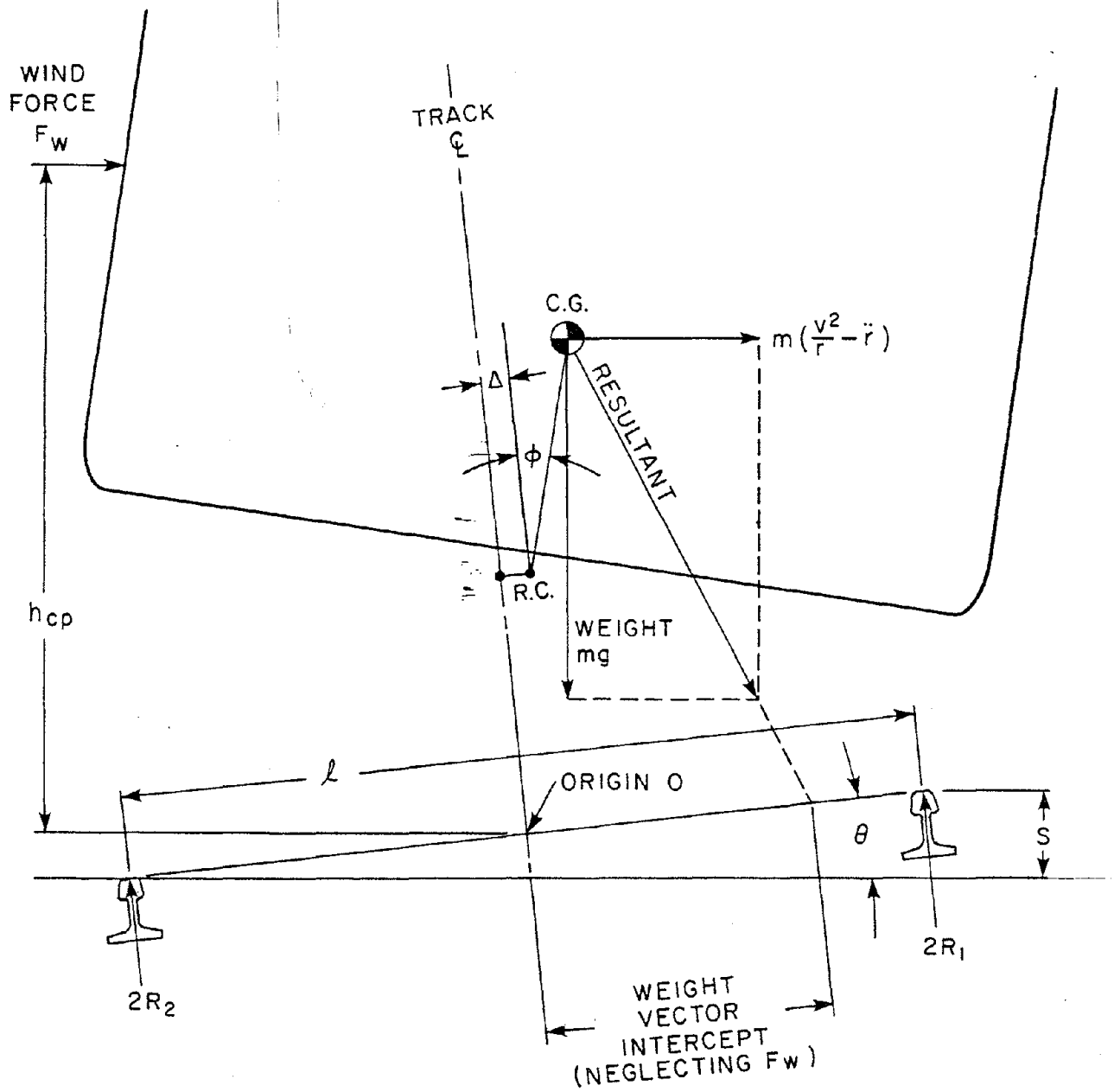


Figure 5-1. General Vehicle Overturning Model

reduced to zero. The definition of weight vector intercept as the balance point of the vehicle is also valid for a vehicle subjected to wind loads although the resultant force vector is harder to visualize because it does not pass through the c.g.

Most overturning criteria are concerned primarily with the forces acting through the c.g. The wind force is used as a modifying factor because its effect on the balance point can be computed separately and applied additively and it is not a controlled variable during testing.

The weight vector intercept measurements taken during this test program were a direct computation of the vertical balance point of the lead truck of each vehicle which was fully equipped with force measuring instrumented wheels. The computation was:

$$\text{Weight Vector Intercept} = 30 \text{ inches} \left[\frac{(R_{lf} + R_{lr}) - (R_{rf} + R_{rr})}{R_{rf} + R_{rr} + R_{lf} + R_{lr}} \right]$$

where R_{rf} , R_{rr} , R_{lf} , and R_{lr} are the vertical loads of the right front, right rear, left front and left rear wheels of the lead truck.

This measurement includes the effects of static imbalance of the vehicles, all suspension and tilt motions and typical coupler forces. It does not include the gross lateral motion of the vehicle which occurs if both outside wheels of the truck are flanged against the high rail, but this motion of the c.g. contributes very little to side load transfer. Only effects of gravitational and inertial forces contribute significantly to the test data because the wind speed was negligible.

The lateral inertial force has two components. Steady state curving criteria assume that r is constant so that only mV^2/r remains. Measurements averaged over the body of a curve approximate a steady state. Transient curving criteria also include lateral inertial forces resulting from the $-m\ddot{r}$ term. The effects of transition spirals and alignment deviations are described by \ddot{r} , the second derivative of the path radius with respect to time, which is also a function of speed. The negative sign is required because a decrease in radius results in an increase of force. In order to assess the risk of overturning using the transient weight vector intercept criteria, the time duration of the measurement must be considered. Even when the weight vector intercept as shown in Figure 5-1 is at the high rail and the low rail vertical force is zero the vehicle does not actually overturn. An even higher lateral force (implying a transient weight vector intercept greater than 30 inches) and time for this force to act

are required for actual overturning because of the c.g. must rise as it is pivoted outward and a finite amount of time is required for the net overturning moment to rotate the c.g. outside the rail.

Vehicle overturning criteria specify two essential factors: (1) the total allowable side to side weight transfer ratio and (2) the cross wind velocity whose effect on weight transfer must be allowed for in advance. The ratio of the moment of the vehicle lateral surface area to its weight determines the portion of the gross allowable weight transfer consumed by the wind allowance. The weight transfer ratio due to lateral inertial forces and lateral movement of the c.g. is compared to the net allowable weight transfer ratio. A greater net weight transfer ratio is usually allowed for locomotives than coaches under the same criteria due to their lower ratio of surface area to weight.

In order to compare various criteria stated in terms of weight vector intercept, moment safety factor, or load ratio with differing cross wind speed allowances, it is necessary to reduce them to a common basis. Weight vector intercept will be chosen as a common basis of weight transfer ratio because of its intuitive concept as the instantaneous vehicle balance point and because the data contained in Appendix A includes measurements of weight vector intercept.

5.1.1 OVERTURNING CRITERIA IN USE

1. ONE THIRD RULE - (AAR)

The "one third rule" states that the weight vector intercept computed from the vertical gravitational force and the lateral centrifugal force must remain within the center one third of the track (1). It is a common rule of thumb but it is vague and poorly documented. The description of the lateral forces as centrifugal implies that the steady state rather than transient weight vector intercept should be considered. The wind force is not considered. The middle one third of the track is usually considered to be ± 10 inches about the track centerline although it has been interpreted in one instance (2) as 20 inches from the gage side of each rail ($\pm 8\text{-}1/4$ -inch from centerline). It is believed that the one third rule is actually an earlier rule of thumb for the design of chimneys to withstand wind loads that was applied to railroad vehicles by analogy (3).

2. OVERTURNING MOMENT SAFETY FACTOR (Association of German Locomotive Manufacturers) (Ref. 4)

This factor of safety against overturning can be expressed:
 $SF = M_r/M_o \geq 1.2$ where M_o is the sum of the overturning moments

including the maximum effect of wind pressure at 12 pounds per square foot (68 mph crosswind) and M_r is the restoring moment based on the laterally shifted c.g. location. Presumably only the quasistatic lateral inertial force is included since there is no mention of time duration or transient loads.

The factor of safety criteria is translated into weight vector intercept as follows, where the free body diagram of the vehicle is Figure 5-2:

W = weight acting through the vehicle c.g.

X = lateral movement of the c.g.

F_L = resultant lateral force including wind and inertial forces

H = vertical height of the line of action of F_L . It is usually higher than the c.g. because of the wind force component

R_1 = outer rail vertical wheel force

R_2 = inner rail vertical wheel force

Considering Figure 5-2A:

$$M_O = HF_L$$

$$M_r = (30 - X)W$$

Applying the criteria limit:

$$1.2 = \frac{M_r}{M_O} \Rightarrow HF_L = \frac{(30 - X)W}{1.2}$$

Taking moments about the outer rail:

$$(30 - X)W - HF_L - 60(2R_2) = 0$$

$$120R_2 = \left(1 - \frac{1}{1.2}\right) (30 - X)W$$

Taking moments about the inner rail

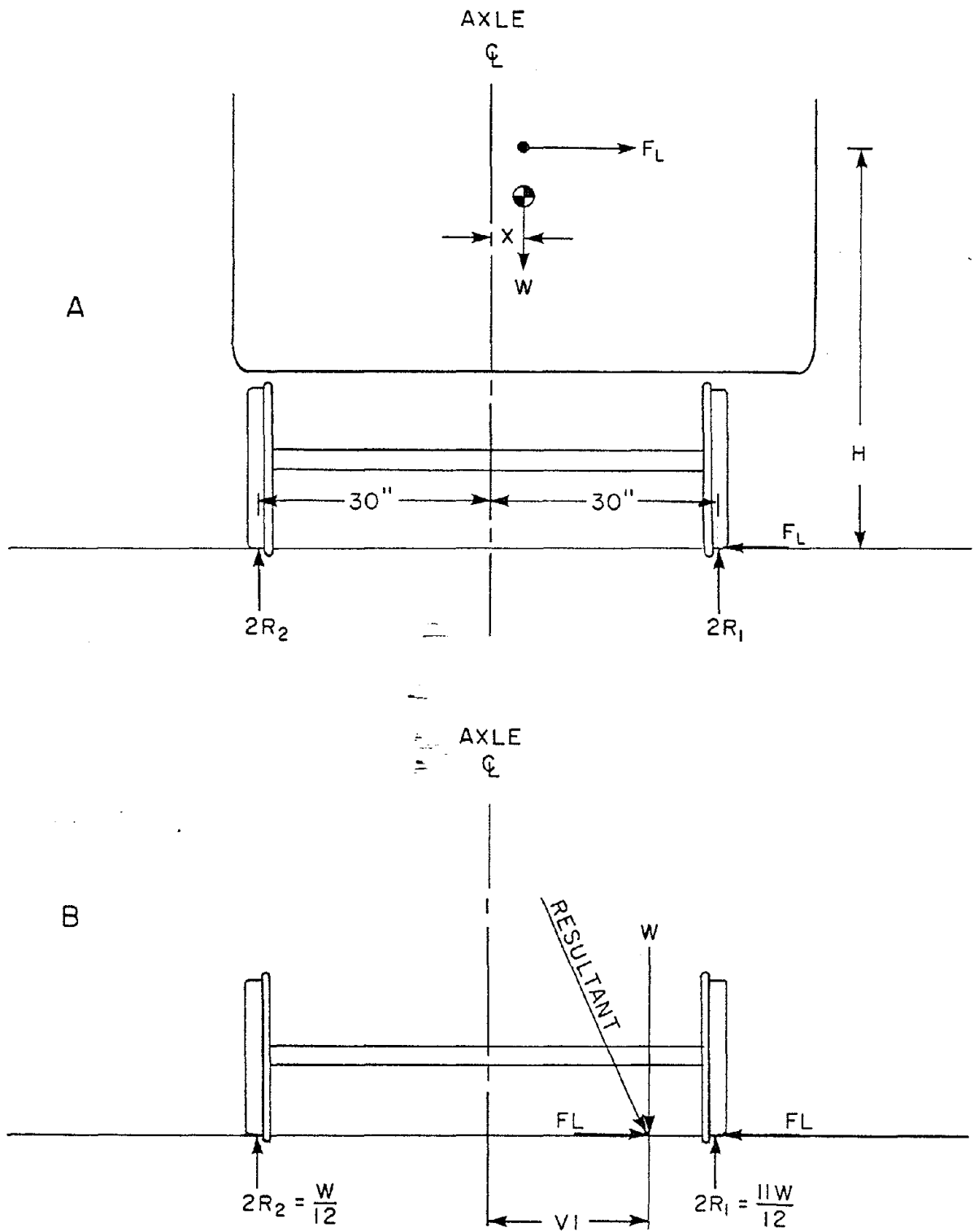


Figure 5-2. Freebody Diagram, Overturning Moment Criteria

$$-(30 - X)W - HF_L + 60(2R_1) = 0$$

$$120R_1 = (1 + \frac{1}{1.2})(30 - X)W$$

Therefore:

$$\frac{R_2}{R_1} = \frac{0.2}{2.2} = \frac{1}{11}$$

$$W = 2R_1 + 2R_2 = 24R_2$$

$$2R_2 = W/12$$

$$2R_1 = 11W/12$$

Figure 5-2B shows the resultant of W and F_L piercing the plane of the railheads at the vehicle balance point. The weight vector intercept is dimension VI. Taking moments about the balance point:

$$(30 - VI)2R_1 - (30 + VI)2R_2 = 0$$

$$(30 - VI)\frac{11W}{12} = (30 + VI)\frac{W}{12}$$

$$300 = 12VI$$

$$VI = 25"$$

The total weight transfer ratio expressed in terms of weight vector intercept for the overturning moment factor of safety criterion is 25 inches.

The amount of the 25 inch total dedicated to wind allowance will be calculated in the next section.

3. VERTICAL WHEEL LOAD REDUCTION RATIO (Japanese National Railway)

The overturning criteria used by JNR (Ref. 5) measures side to side weight transfer in terms of the percent reduction in the vertical load on the low rail wheels. The criteria specifies two levels of load transfer. A reduction in wheel load by 60% of the nominal (40% remaining) is permitted for steady state curving

which includes the effect of wind speed and centrifugal acceleration (mV^2/r term), while an 80% reduction in low rail wheel load is appropriate for comparison to transient calculations or measurements. The most recent publication (6) of the Japan Railway Technical Service emphasizes the transient criteria, and the transient calculation is performed by adding to the steady state load transfer a factor to account for the effect of only the part of the maximum lateral acceleration in excess of the centrifugal acceleration in the curve body. The transient component in the JNR calculations is essentially the $-m\ddot{r}$ term in Figure 5-1 computed for entry and exit spiral shapes. It is significant that the transient overturning computations do not include effects of alignment deviations (also manifested by the $-m\ddot{r}$ term) which can be a significant component of actual transient overturning measurements. Comparison of measured data, which included the effect of track perturbations, to the criteria is therefore more conservative than judgements based on the usual computation.

Wheel load reduction ratio may be expressed easily in terms of weight vector intercept to allow convenient comparisons to other overturning criteria and to the measurements made in this program. If R_1 is the high rail wheel load and R_2 the low rail wheel load as shown in Figure 5-1, the wheel load reduction ratio, C_r is:

$$C_r = \frac{\Delta P}{P} \times 100\% = \left[\frac{\frac{R_1 + R_2}{2} - R_2}{\frac{R_1 + R_2}{2}} \right] \times 100\% = \frac{R_1 - R_2}{R_1 + R_2} \times 100\%$$

And the weight vector intercept, VI, is:

$$VI = 30 \text{ inches} \left(\frac{2R_1 - 2R_2}{2R_1 + 2R_2} \right) = 30 \left(\frac{R_1 - R_2}{R_1 + R_2} \right)$$

$$VI = \frac{30 C_r}{100\%} \text{ inches}$$

A load reduction ratio of 80% corresponds to 24 inches of weight vector intercept.

The effect of wind force can be computed in terms of load reduction ratio or weight vector crossing to determine the portion of the load transfer allowed by either the moment factor of safety or load reduction ratio criteria due to the specified maximum wind speed.

The wind force, F_w , for half vehicle model is:

$$F_w = \frac{S}{2} \frac{\rho V^2}{2} C_d$$

where:

S = the lateral surface area of the whole vehicle, ft²

ρ = air density of .002378 slug/ft³

V = speed in ft/sec

C_d = drag coefficient

Under the usual assumption that C_d = 1

$$F_w = 1.28 \times 10^{-3} S V^2 \text{ for } V \text{ in mph}$$

The change in side to side load transfer that results from an overturning moment, M_o about the origin in Figure 5-3 can be computed in general terms. Considering only M_o and summing moments about the origin.

$$0 = 2R_1 \left(\frac{\ell}{2}\right) - 2R_2 \left(\frac{\ell}{2}\right) - M_o$$

$$R_1 - R_2 = \frac{M_o}{\ell}$$

however the half vehicle weight W = 2(R₁ + R₂)

$$\frac{\Delta P}{P} = \frac{R_1 - R_2}{R_1 + R_2} = \frac{2M_o}{\ell W}$$

and

$$VI = \frac{60M_o}{\ell W}$$

The overturning moment due to the wind load is

$$M_o = F_w (h_{cp}) \cos \theta$$

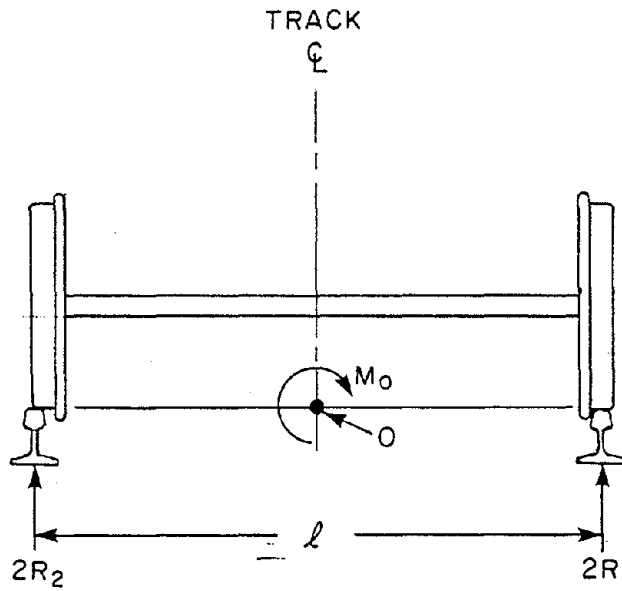


Figure 5-3. Freebody Diagram for Weight Transfer Due to General Overturning Moment

where h_{cp} is the height of the center of wind pressure in feet and θ is the crosslevel angle.

Since $\cos \theta \approx 1$ and $\ell = 5$ feet, the effect of wind in terms of load reduction ratio is:

$$Cr = \frac{2F_w(h_{cp})}{5W} = (0.51 \times 10^{-3} V^2 S(h_{cp})/W) \times 100\%$$

and in terms of weight vector intercept

$$VI = 0.0153 V^2 S(h_{cp})/W \text{ with } V \text{ in mph}$$

3a. Steady State Criteria

Reference 6 identifies the two sources of steady state load transfer as "excessive centrifugal force" and wind force. It gives the formula for "excessive centrifugal force", F_B as:

$$F_B = W_B \frac{V^2}{127r} - \frac{s}{\ell}$$

where:

W_B = weight of half carbody

V = velocity of vehicle, KM/h

r = radius of curve, meters

s = superelevation

ℓ = effective tread gage

The JNR criteria apparently neglects the mass of the truck in the computation of the net steady state lateral force parallel to the railhead plane (centrifugal minus gravitational component). Although it is not stated explicitly in Reference 6, F_B causes a wheel load reduction by setting up two moments about the origin as in Figure 5-4.

The direct lateral force moment is $F_B h_{GB}$, where h_{GB} is the height of the body c.g. above the railhead. The second moment, due to

the lateral shift of the body c.g., is $X = W_B$, where X is the lateral shift. Reference 6 uses a term C_y as the suspension lateral compliance in units of displacement per force. Presumably C_y accounts for lateral movement by both translation and rotation. Therefore, $X = C_y F_B$.

The wheel load reduction ratio, $\Delta P_1/P$, due to "excessive centrifugal force is:

$$\frac{\Delta P_1}{P} = \frac{2M_o}{\ell W} = \frac{2F_B(h_{GB} + C_y W_B)}{\ell W} = \frac{0.4F_B(h_{GB} + C_y W_B)}{W}$$

As derived previously the wheel load reduction ratio, $\Delta P_2/P$, due to a lateral wind of velocity, V :

$$\frac{\Delta P_2}{P} = 0.51 \times 10^{-3} V^2 S h_{cp} / W$$

The JNR steady state overturning safety criteria may be summarized:

$$.6 > \frac{\Delta P_1 + \Delta P_2}{P} = .4F_B(h_{GB} + C_y W_B) + .51 \times 10^{-3} V^2 S h_{cp} / W$$

where

F_B = net lateral centrifugal and gravitational force, lbs

h_{GB} = height of body c.g., ft

C_y = overall lateral compliance ft/lb

W_B = weight of half body, lbs

V = allowed wind velocity, mph

S = side area of whole carbody, ft²

h_{cp} = height of center of wind pressure, ft

W = weight of half vehicle, lbs

It may be stated in terms of weight vector intercept as

$$18 \text{ inches} \geq [12F_B(h_{GB} + C_Y W_B) + .0153V^2 Sh_{cp}/W]$$

3b. Transient Criteria

Reference (6) adds a third source of load transfer to the steady state low rail wheel load reduction for an analytic model of transient wheel load reduction. The resulting wheel load reduction ratio is compared to the criteria maximum of 80% to assess operating safety regarding overturning.

The transient component of load transfer is attributed to "vibration of the carbody." The term apparently refers to the difference between the instantaneous maximum lateral acceleration in a spiral ($mV^2/r_s - m\ddot{r}_s - \sin\theta_s$) and the steady state lateral acceleration in the curve body ($mV^2/r_c - \sin\theta_c$). It is purely a function of spiral length, curve body radii, superelevation and speed under the assumption of perfect track geometry. The formula

$$\Delta P_3 = \frac{(h_{GB} + C_Y W_B) W_B a_Y}{2l}$$

is given for the absolute load transfer in units of force.

This expression can be derived considering a_Y as lateral acceleration in excess of the steady state value and superimposing its effects on the steady state equilibrium condition in Figure 5-4.

Summing moments about 0 for the transient effects

$$0 = 2\Delta R_1(l/2) - 2\Delta R_2(l/2) - W_B a_Y h_{GB} - y W_B$$

but

$$\Delta R_1 = \Delta P_3 \text{ and } \Delta R_2 = -\Delta P_3$$

and

$$y = C_Y W_B a_Y$$

$$0 = \Delta P_3 l - (-\Delta P_3) l - W_B a_Y h_{GB} - (C_Y W_B a_Y) W_B$$

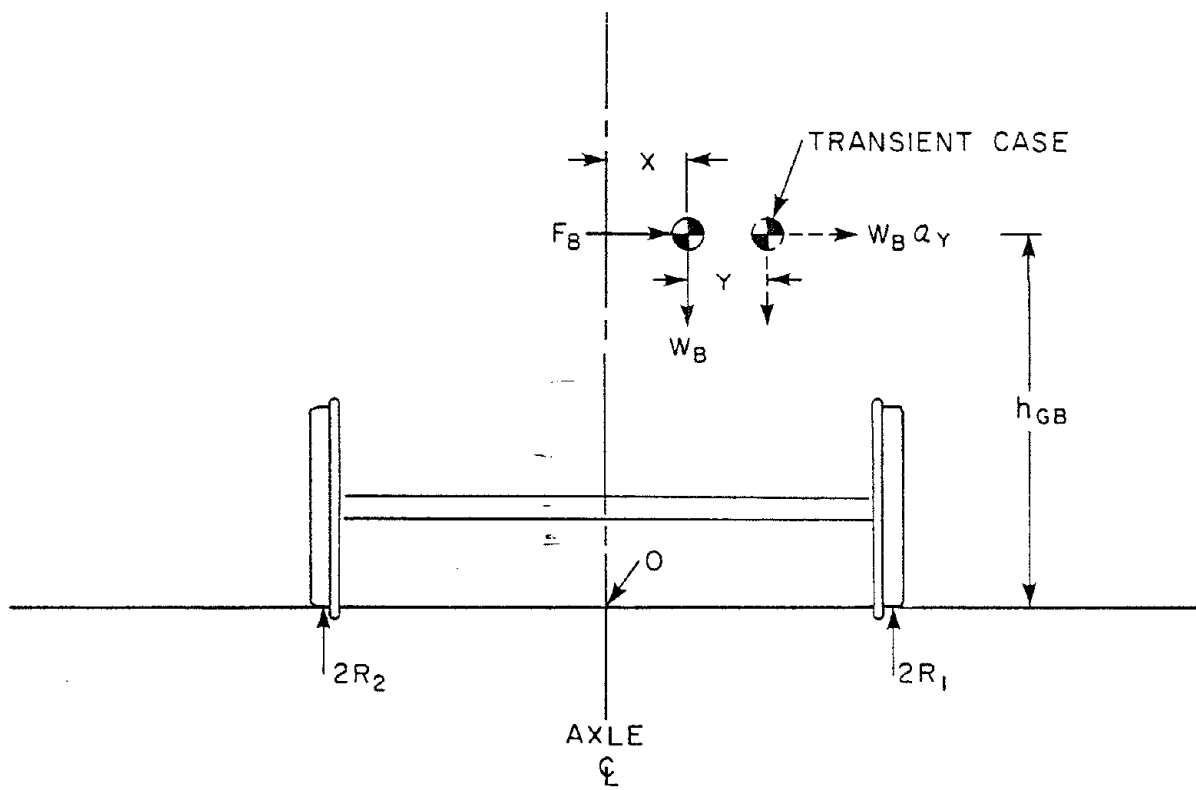


Figure 5-4. Free Body Diagram, Vertical Load Reduction Ratio Criteria

and

$$\Delta P_3 = \frac{(h_{GB} + C_Y W_B) W_B a_Y}{2\ell}$$

The additional load reduction ratio term in decimal form is:

$$\frac{\Delta P_3}{P} = \frac{\Delta P_3}{W/4} = \frac{2(h_{GB} + C_Y W_B) W_B a_Y}{\ell W}$$

since $\ell = 5$ feet

$$\frac{\Delta P_3}{P} = \frac{.4(h_{GB} + C_Y W_B) W_B a_Y}{W}$$

The JNR transient overturning safety criteria may be summarized in vertical wheel load reduction ratio:

$$.8 \geq \frac{\Delta P_1 + \Delta P_2 + \Delta P_3}{P} = [.4(F_B + W_B a_Y)(h_{GB} + C_Y W_B) + .51 \times 10^{-3} V^2 S(hcp)]/W$$

or in terms of weight vector intercept:

$$24 \text{ inches} \geq [12(F_B + W_B a_Y)(h_{GB} + C_Y W_B) + .0153 V^2 S(hcp)]/W$$

5.1.2 COMPARISON OF OVERTURNING CRITERIA

The net weight vector intercept specified by each criteria for a particular lateral wind speed may be obtained by subtracting $.0153 V^2 S h_{cp}/W$ from the maximum weight vector intercept. The net weight vector intercept includes the effects of inertial and gravitational forces and is appropriate for comparison to test data or the results of mathematical modeling. Figures 5-5 and 5-6 compare the various overturning criteria as applied to the LRC coach and locomotive by plotting the net weight vector intercept as a function of lateral wind speed allowance. The characteristics of the vehicles effecting the wind speed allowance are shown below.

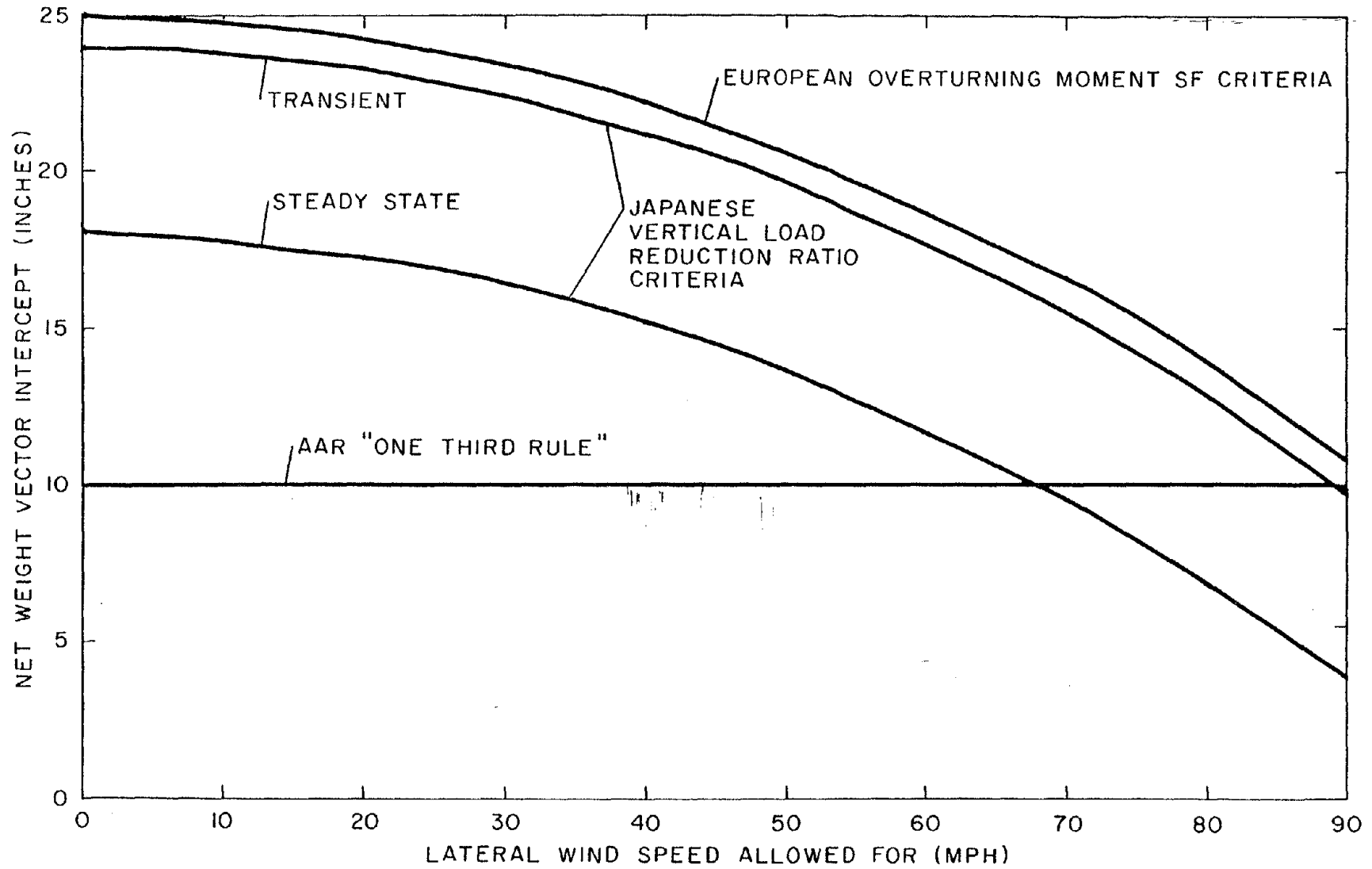


Figure 5-5. Comparison of Various Overturning Safety Criteria for LRC Coach

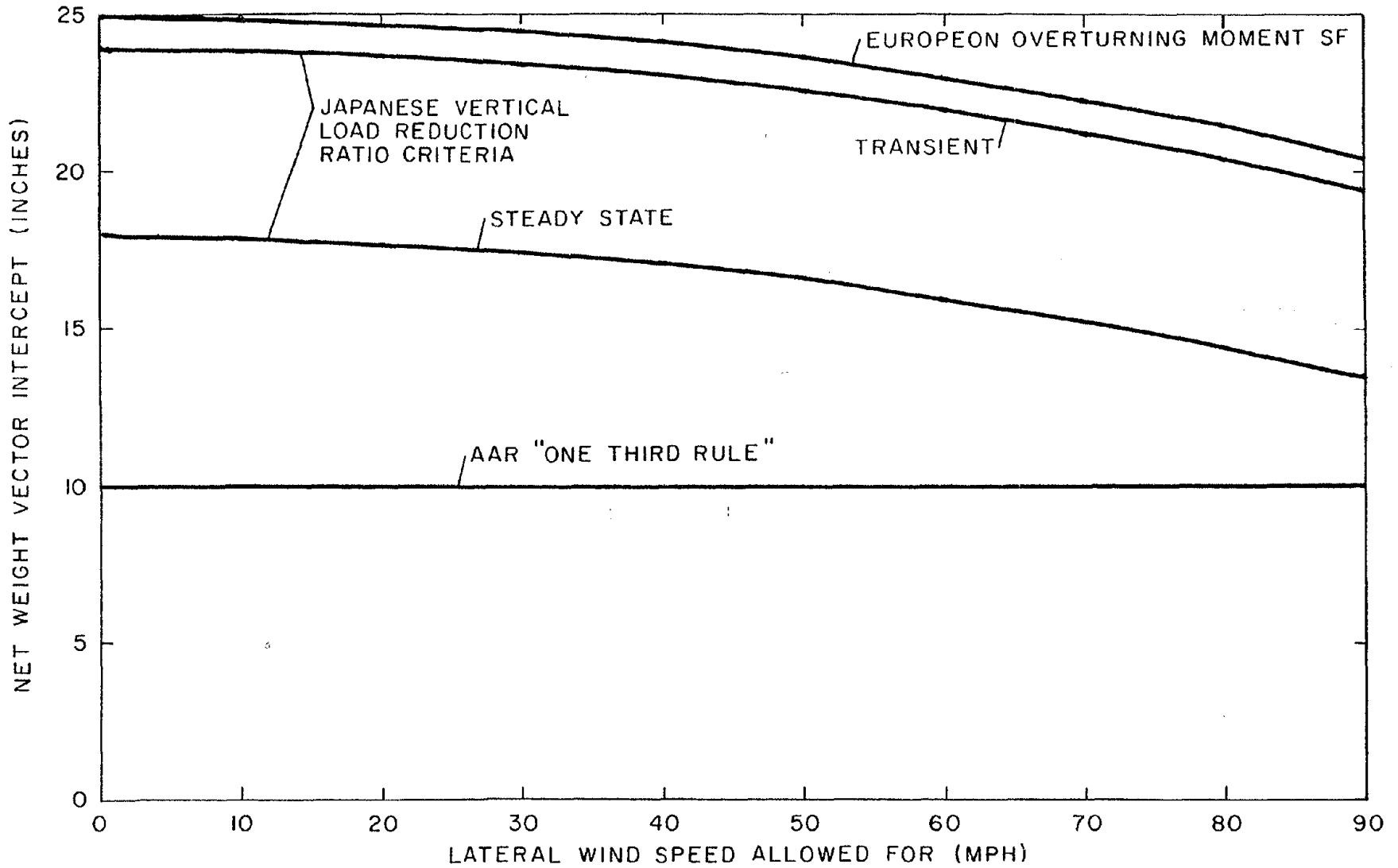


Figure 5-6. Comparison of Various Overturning Safety Criteria for LRC Locomotive

	<u>LRC Coach</u>	<u>LRC Locomotive</u>
Body Length	85 ft	62 ft
Height of Body Side	11 ft	11 ft
Lateral Area, S	935 ft ²	682 ft ²
Height of Center of Pressure, h _{cp}	6-1/2 ft	6-1/2 ft
One-Half Vehicle Weight, W	52,750 lb	125,400 lb

Comparing Figures 5-5 and 5-6 reveals that the wind speed allowance can restrict the net weight vector intercept significantly for coaches without greatly limiting locomotives. A prudent choice of the allowance for wind speed is required because an overly conservative wind speed assumption wastefully reduces the normal operating criteria since other factors such as visibility and debris on the track limit track speed in high wind. Maximum operating wind speeds of 68 mph and 76 mph are assumed by German and British railroads, respectively whereas the Japanese compute the transient wheel load reduction ratio based on a 45 mph lateral wind. The maximum ten year mean recurrent wind speed at less than 15 feet altitude is 56 mph for cities along the Northeast Corridor. The assumption of normal operation in winds of 68 to 76 mph appears overly conservative.

The European overturning moment safety factor criteria is by far the least restrictive if it is interpreted as pertaining to quasistatic moments. It is slightly greater than the JNR transient criteria. The one third rule is much more restrictive than even the JNR steady state criteria for the LRC locomotive and for the LRC coach at wind speeds less than 67 mph. The one third rule would be more comparable to other criteria under moderate winds if unloaded box cars were under consideration.

5.2 WHEEL CLIMB CRITERIA

The classic characterization of wheel climb by Nadal in 1896 predicts that the critical ratio of lateral to vertical force for a single wheel is $L/V = (\tan \alpha \pm \mu) / (1 \pm \mu \tan \alpha)$ where α is angle

of the wheel flange with respect to the horizontal at the point of contact with the side of the rail, and μ is the coefficient of friction between wheel and rail. Nadal's formula does not directly address several first order wheel climb factors including wheel/rail angle of attack critical time duration of the derailment quotient nor any of the reported second order factors such as absolute vertical load, vertical and lateral velocity at impact, wheelset mass, rail head contour or torsional and lateral track stiffness. The choice of μ is also controversial.

Many of the second order factors such as wheelset mass, lateral velocity and track stiffness should manifest themselves as components in the instantaneous L/V measurement. Railhead contour can be viewed as a modifier to the flange angle and forward velocity would seem to be related to the allowed time duration of the derailment quotient. Criteria which specify the critical L/V ratio as a function of time duration appear to address implicitly all the factors except absolute vertical load.

Yokose (Ref. 7) offers an interpretation of Nadal's formula as follows:

For positive angles of attack:

$$\text{Critical L/V} = \frac{\tan \alpha - \mu_e}{1 + \mu_e \tan \alpha}$$

For negative angles of attack:

$$\text{Critical L/V} = \frac{\tan \alpha + \mu_e}{1 - \mu_e \tan \alpha}$$

and for zero angle of attack:

$$\text{Critical L/V} = \tan \alpha$$

where μ_e is the effective coefficient of friction which converges to the static coefficient of friction μ as the angle of attack increases. This interpretation corresponds with the intuitive notion that flange friction promotes wheel climb at positive angles of attack and hinders it at negative angles. Reference 7 also presents laboratory test data obtained with scale model

wheelsets which converge to the Nadal predictions ($\alpha = 61^\circ$, $\mu = .4$) for large angles of attack. In accordance with this study, the Japanese National Railway limits L/V to .8 for durations of 50 ms or greater. Another JNR researcher (Matsudaira, Ref. 8) recommends an L/V limit of 4 at 10 ms duration decreasing to .8 at 50 ms. JNR also recommends (Ref. 5) a maximum lateral impact speed of 1.6 ms at 6-ton static wheel loads in cases of hunting or severe alignment deviations.

Kaffman recommends (Ref. 9) a maximum L/V of 1.2 for British four-wheel "wagons" where the effect of track twist on long wheel base vehicles generates high L/V ratios by vertical force reduction as well as lateral force application. The recommendation apparently results from Nadal's formula also but with $\alpha = 68^\circ$ and $\mu = .33$. He cites test data in reference 10 of four-wheel cars sustaining L/V = 1.6 and bogie vehicles at L/V = 2.35 without wheel climb. The time duration is referred to as instantaneous without quantitative definition.

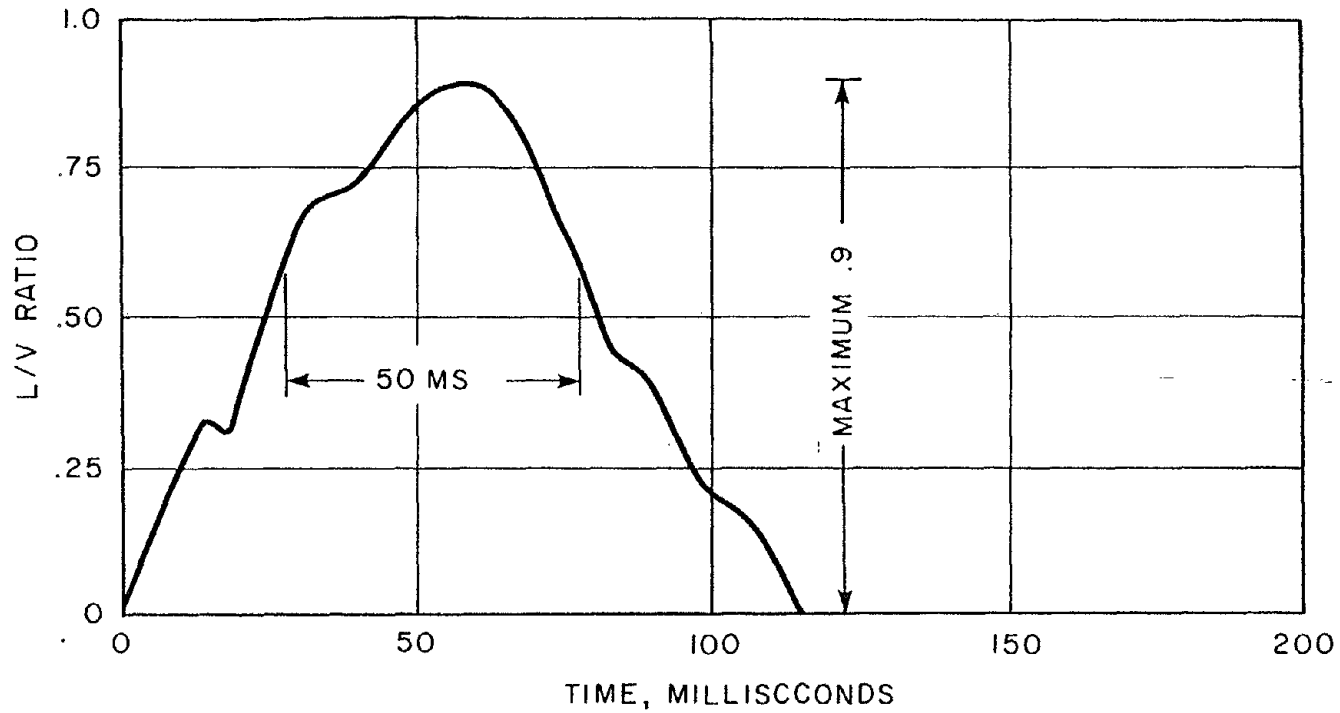
Amtrak has included in its specifications for the AEM-7 locomotive (AAR flange angle $66^\circ - 68^\circ$, increasing further with wear) an L/V criteria which clearly relates its permissible magnitude to pulse duration. The method of defining pulse duration in this specification has been described by EMD (Ref. 11). EMD interprets the pulse width as the time that L/V exceeds the criteria threshold rather than the time L/V exceed zero during a pulse peaking at the criteria. Figure 5-7 illustrates the difference between the EMD and JNR interpretation of an L/V spike. The EMD definition is easier to apply to the usual test data pattern in which short duration spikes are superimposed over a steady state curving level. The maximum L/V ratio recommended by EMD is:

$$(L/V) \text{ max} < 0.056T^{-0.927}$$

with $(L/V) \text{ max} \leq .90$ at $T > 50$ ms

Dean and Ahlbeck (Ref. 12) recommend a maximum L/V of 1.0 for durations greater than 50 ms as a conservative limit supported by the results of tests by the European ORE Committee B55.

Figure 5-8 compares the various recommended criteria. The JNR criteria is the most restrictive because of its interpretation of L/V measurements. All of the criteria represent judgements based in part on Nadal's formula. The judgement of μ greatly influences the predicted critical L/V. Rule of thumb estimates of μ have usually placed it between .2 and .3, but ORE Committee B10 has reported (Ref. 10) measurements of much higher wheel/rail friction coefficients. The effective lateral coefficient of friction μ_e converges on μ as the angle of attack becomes very



THE ABOVE L/V PULSE WOULD BE CLASSIFIED BY JNR AS A PULSE OF .9 FOR 115MS EXCEEDING THEIR CRITERIA. HOWEVER THE SAME PULSE WOULD BY CLASSIFIED BY EMD AS A PULSE EXCEEDING .6 FOR 50MS WELL WITHIN THEIR CRITERIA.

Figure 5-7. Interpretation of Instantaneous L/V Measurements

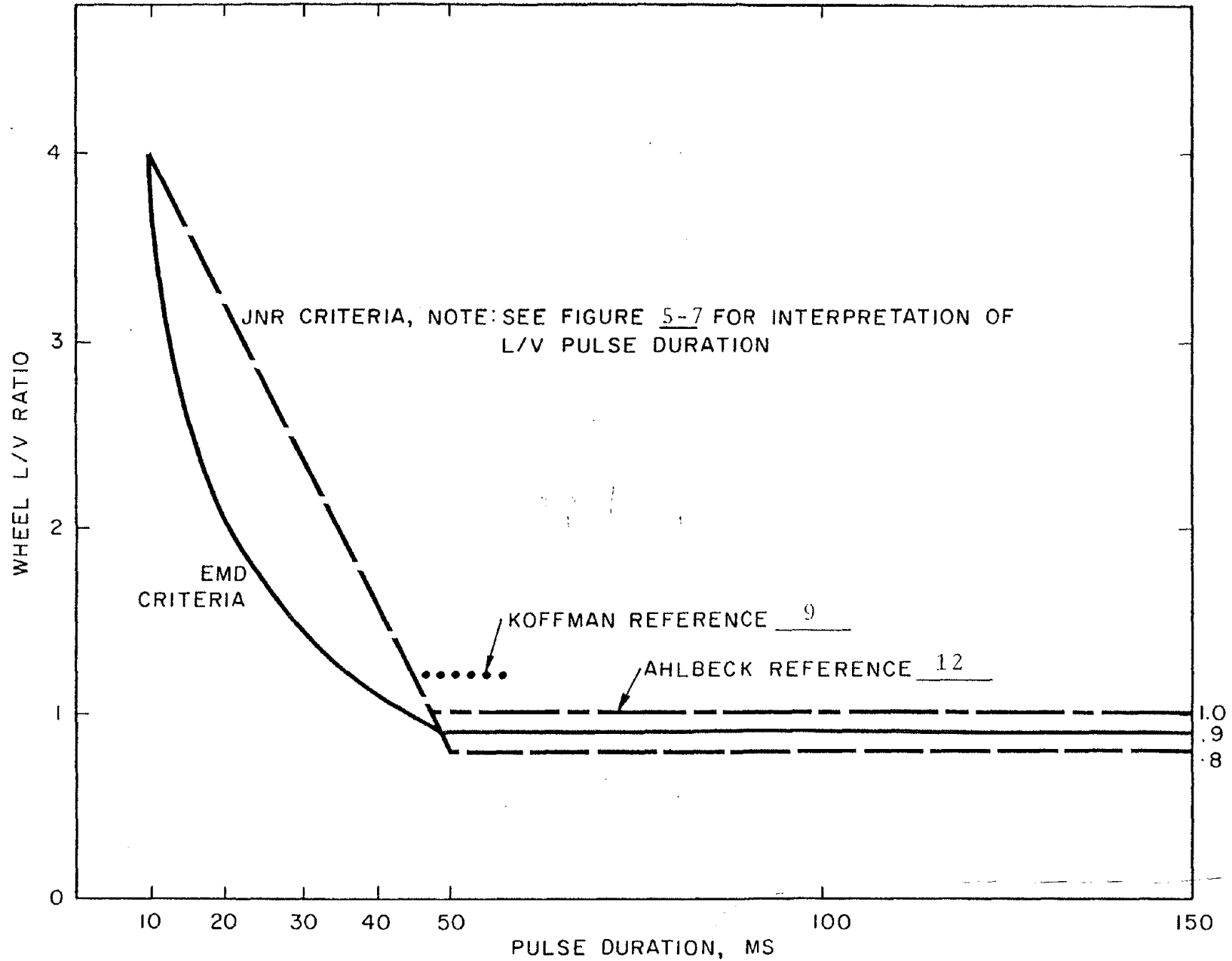


Figure 5-8. Comparison of Various Wheel Climb Criteria

large and the speed becomes very low but it should remain considerably less than the maximum reported values of μ of .55 for any conceivable high cant deficiency conditions. It also is in agreement with Nadal's formula that the most conservative L/V criteria was proposed by a railroad (JNR) using wheels with the lowest flange angle ($\alpha = 61^\circ$).

Experiments by BR using an instrumented full scale wheelset on a mobile test bed with controlled loads and angles of attack (Ref. 14) had indicated much higher L/V ratios at derailment than commonly expected. It has been hypothesized that very high longitudinal creep forces under derailment conditions reduce the lateral friction forces because the vector sum of longitudinal and lateral frictional forces is limited by μP . The concept of μ_e was an inexact way of describing the same phenomenon. Further evidence that the JNR criteria is overly conservative is recent testing of a low c.g. subway vehicle involving this author that indicates routine curving with peak L/V ratios exceeding 0.8. However, the time durations associated with critical L/V pulses have not been determined empirically at this time and even very specific transient L/V criteria such as that used by Amtrak is a product of judgement rather than testing.

5.3 RAIL ROLLOVER CRITERIA

Derailment is likely to occur more rapidly by rail rollover than by other hazards because the inertia of the rail opposing rotation is so slight. The knowledge of instantaneous conditions favoring rail rollover is especially important in assessing risk. Japanese and European papers covering other safety considerations (Ref. 5 and 14) appropriate to high speed curving do not offer rail rollover criteria, but a series of criteria based on various degrees of track structural integrity has been developed from AAR studies (Ref. 15 and 16). The instantaneous ratio of the sum of lateral forces to the sum of vertical forces of the wheels on the high rail side of a truck is used to quantify the likelihood of rail rollover. It is known as the truck L/V ratio and is referred to in the data appendix by the more descriptive term of high rail side truck L/V ratio.

A totally unrestrained rail can sustain lateral forces without rollover as long as the resultant of the lateral and vertical wheel forces intersects a point within the base of the rail. The limit of the purely geometrical resistance to rollover as shown in Figure 5-9 has been stated conservatively as $L/V = 0.5$. However even if the truck side L/V is less than 0.5, the lead wheel must be scrutinized separately if no fastener resistance is to be assumed. If the rail is held flat at the trailing wheel and the torsional rigidity of the rail is considered as rollover resistance at the front wheel, the front wheel lateral force cannot be greater by more than about 2,300 pounds over that permitted by

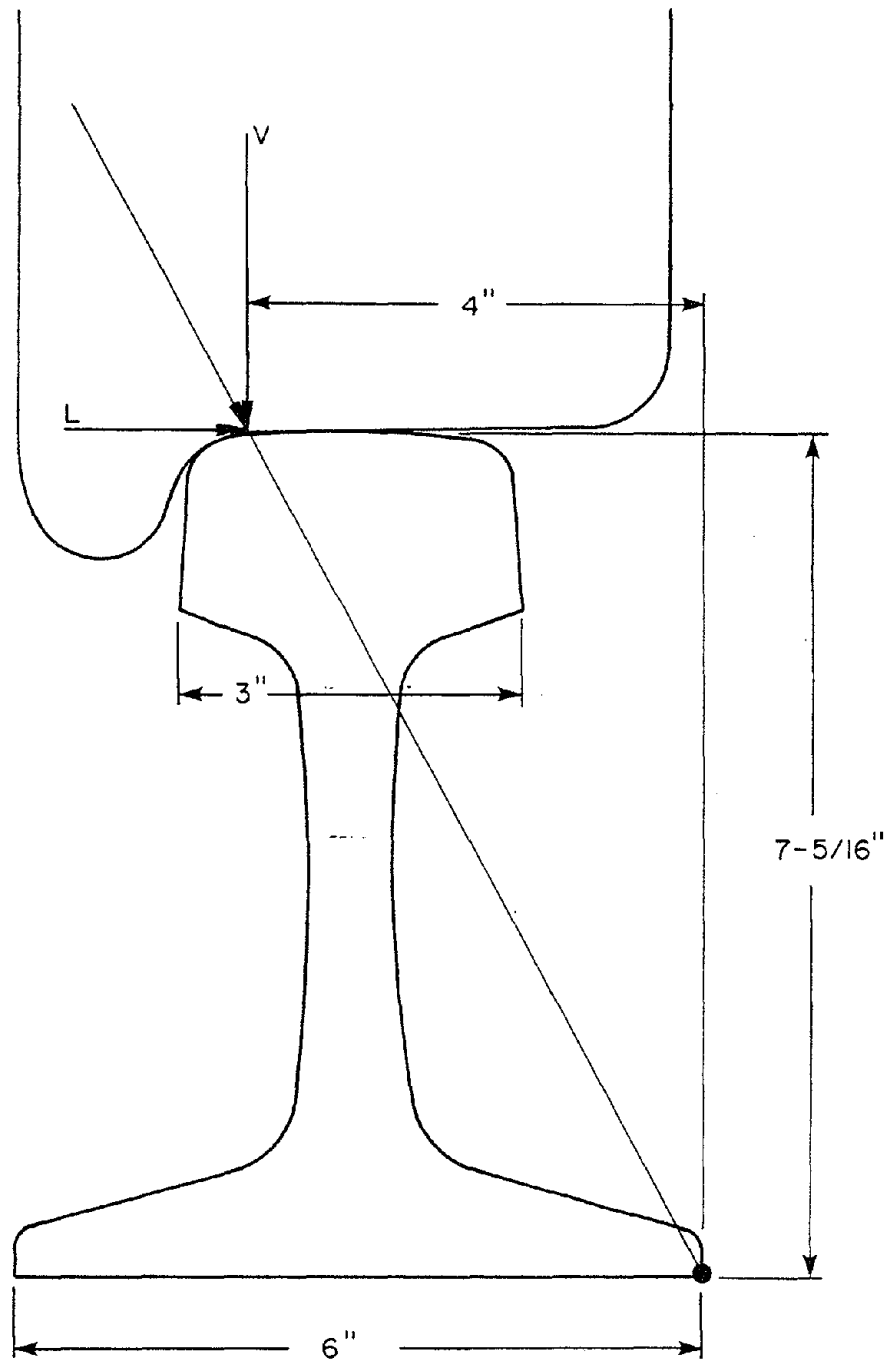


Figure 5-9. Cross Section Geometric Resistance to Rail Rollover

the rail cross section geometry alone without gage widening in excess of 1/4-inch (Ref. 16).

AAR reports that newly spiked wood tie fasteners can sustain a lateral force of 3,600 pounds and 8,000 pounds can be sustained at the railhead with concrete tie fasteners. This has been translated into a truck L/V limit of $0.5 + 3,600 \text{ lb/Pw}$ (Ref. 1). Such a truck L/V limit appears to be erroneous because the instantaneous truck L/V will be calculated using a V greater than Pw because of load transfer while 3,600 pounds is actually an absolute number independent of the vertical load.

The torsional rigidity of the rail allows fasteners other than those at the wheels to contribute resistance to rail rollover. An additional 20,000 pounds of lateral force over the geometric limit can be sustained by newly spiked fasteners in a vicinity of up to seven ties with less than 1/4-inch of gage widening. This has been expressed as a truck L/V limit of $0.5 + 20,000 \text{ lb/Pw}$ which also appears to overstate the value of the absolute lateral force.

The rail rollover criteria has several deficiencies. The geometric resistance to rollover appears to be overly conservative. Examination of the wheel and rail contact pattern during calibration of the instrumented wheelsets even at low lateral forces suggests the geometry pictured in Figure 5-9 which results in an allowable L/V of 0.55. Flange contact would result in even more favorable geometry. Dean and Ahlbeck (Ref. 12) recommend 0.55 assuming no excessive wear.

It is well known that the spikes loosen quickly, and one is hesitant to base the rail rollover criteria on the additional lateral force sustainable by newly installed spikes (in addition to the inconsistent translation of lateral force to truck L/V between references). However, simulated revenue service test runs (Ref. 1) commonly exceed the truck L/V limited by cross section geometry and torsion alone. A realistic assessment of the rollover resistance to be expected from loosened fasteners as well as a clear definition of the time duration is necessary for a comprehensive rail rollover criteria. Empirical information concerning the critical pulse durations of truck L/V measurements and rollover resistance of loose fasteners were not found in the rail research literature.

A recent AEM-7 locomotive specification describes a rail rollover criteria which is specific in regard to pulse time duration and appears to be consistent with typical experience. The basis for its selection is experienced judgement rather than new data. Figure 5-10 plots the criterion which may be stated:

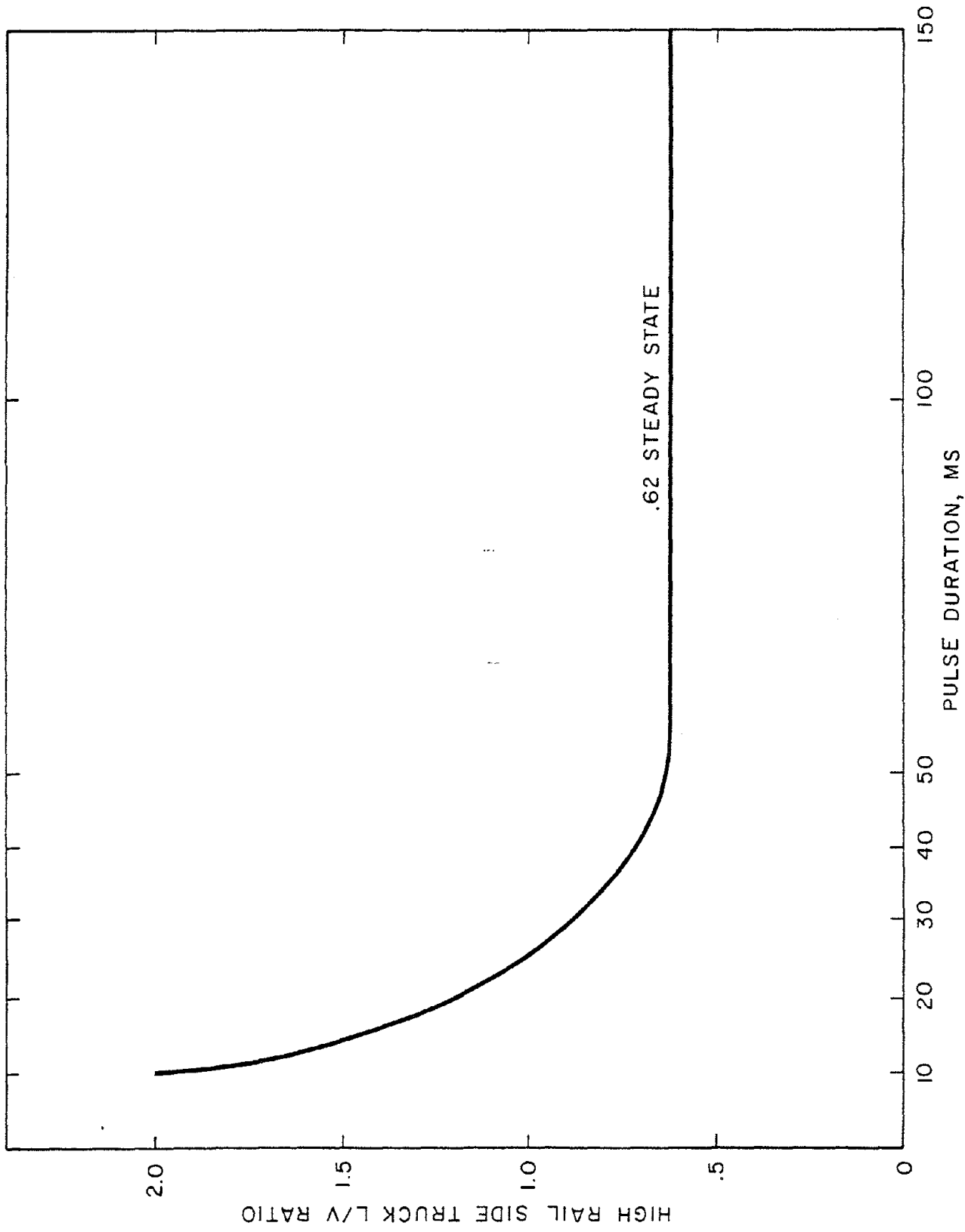


Figure 5-10. Rail Rollover Criteria, AEM-7 Specifications

$$\text{Truck (L/V)} < .070 T^{-0.728}$$

where T equals time duration exceeding limit, and $\text{Truck (L/V)} \leq .62$ for $T = 50$ ms or greater

5.4 LATERAL TRACK SHIFT CRITERIA

The steady state and transient inertial forces and the wind force acting on rail vehicles are transmitted to the ground through the track structure. Criteria have been proposed for limits on the lateral axle load to prevent the permanent lateral movement of the ties relative to the ground. The lateral translation of the rails relative to the ties is assumed to be prevented by friction and by the fasteners, and rail rotation has been considered in the previous set of criteria.

The restraint of the tie by the ballast and the number of ties sharing the burden determine the strength against lateral shift of the track. The interlocking ability of the ballast aggregate, its compaction, depth, width and gradation, the shape, weight and material of the tie and its vertical load determine the ultimate lateral tie resistance. Reference 16 lists test data from various sources that show a range 400 pounds to 1,550 pounds lateral resistance for various unloaded ties in uncompacted ballast and 1,170 pounds to 2,500 pounds in ballast compacted by two million gross tons of traffic. The differences due to the size, shape, and material of the ties appears to be of the same magnitude as the effect of compaction, although differences in the test methodology and ballasting may produce a deceptively great range. Compaction causes a great increase in the lateral resistance of the unloaded ties and perhaps an even greater increase in the lateral resistance of loaded ties. Reference 16 cites a doubling of the lateral resistance of loaded ties after 100,000 gross tons (metric) of traffic and eventual stabilization at nearly three times the uncompacted resistance after about 1.5 million gross tons.

The distribution of the vehicle lateral forces among the ties depends on the tie spacing and the stiffness of the rail and fasteners. Experiments by SNCF suggest that about seven ties bear the load of a single wheelset with 40 to 60 percent taken by the tie under the wheelset. The advantage of stiff rails and fasteners in tie load distribution is outweighed by the internal track forces which result from tie restraint of continuous welded rails subjected to changes in temperature. These internal forces reduce the tie resistance available to oppose the vehicle forces. Reference 16 presents a reduction factor, r , to account

for the maximum change in temperature from rail installation ($\Delta\theta$, F°), the rail cross section area (A , in²) and the curvature (D°):

$$\Gamma = 1 - \frac{A\Delta\theta}{22320} (1 + .458D)$$

The lateral track shift criteria suggested by both Ahlbeck (1) and Lawson (16) are derived from measurements on French track using the "Wagon Derailleur" car (17). This tester features a third axle centrally located which is capable of applying various combinations of vertical and lateral loads while the car is in motion. Lateral loads causing actual permanent track shift were measured under realistic conditions and expressed as a function of vertical axle load for several track conditions. Although the following results were obtained with rail of about 92 lb/yard and tie spacing of 24 inches they apparently represent the most exact findings in the literature.

$$F_C = .33P + 2,245 \text{ pounds for uncompacted wood tie track}$$

$$F_C = .33P + 4,400 \text{ pounds for uncompacted concrete tie track}$$

$$F_C = .61P + 5,520 \text{ pounds for wood tie track compacted by nine million gross tons of traffic}$$

where F_C is the net lateral axle load causing permanent deformation and P is the vertical axle load.

Ahlbeck (1) has estimated for the more common 20-inch tie spacing:

$$F_C = .4P + 2,700 \text{ pounds for uncompacted ballast with wood ties}$$

and

$$F_C = .7P + 6,600 \text{ pounds for compacted ballast with wood ties}$$

similarly Lawson (Ref. 16) estimated:

$$F_C = .66P + 4,490 \text{ pounds for compacted ballast with wood ties}$$

$F_c = .66P + 8,800$ pounds for compacted ballast with concrete ties

When these lateral axle forces are compared to zero wind measurements and applied to traffic on continuous welded rail, a wind force allowance and a reduction factor for thermally induced rail forces must be applied. Assuming temporary speed restrictions on new or newly worked track, measurements should be compared to the maximum axle lateral force for compacted ballast as calculated below, following Alhbeck's recommendation for wood ties:

$$F_{max} = \left[1 - \frac{A\Delta\theta}{22320} (1 + .458D) \right] \left[.7P + 6,600 \right] - (1.28 \times 10^{-3}SV^2)$$

where:

A = rail cross section area, in²

$\Delta\theta$ = max temperature change after rail installation, °F

D = track curvature, degrees

P = vertical axle load, pounds

S = lateral surface area of vehicle, ft²

V = lateral wind speed, mph

and it is assumed that a single axle bears half the entire wind load. For typical NEC conditions of 140-pound rail (A = 13.8 in²), $\Delta\theta$ max of 70°F and D max of 4°.

$$F_{max} = .61P + 5,800 - 1.28 \times 10^{-3}SV^2$$

Figure 5-11 shows the maximum lateral axle forces following Albeck's interpretation of the SNCF criteria for the LRC locomotive and LRC coach as a function of the wind speed allowance. The SNCF criteria for uncompacted ballast computed for the AEM-7 locomotive is also compared to the Amtrak procurement specification which assumes uncompacted ballast. Comparison with the high rail lateral wheel force is a conservative practice because a positive angle of attack results in a lateral creep force on the lower rail wheel which opposes the high rail flange force reducing the net lateral axle force.

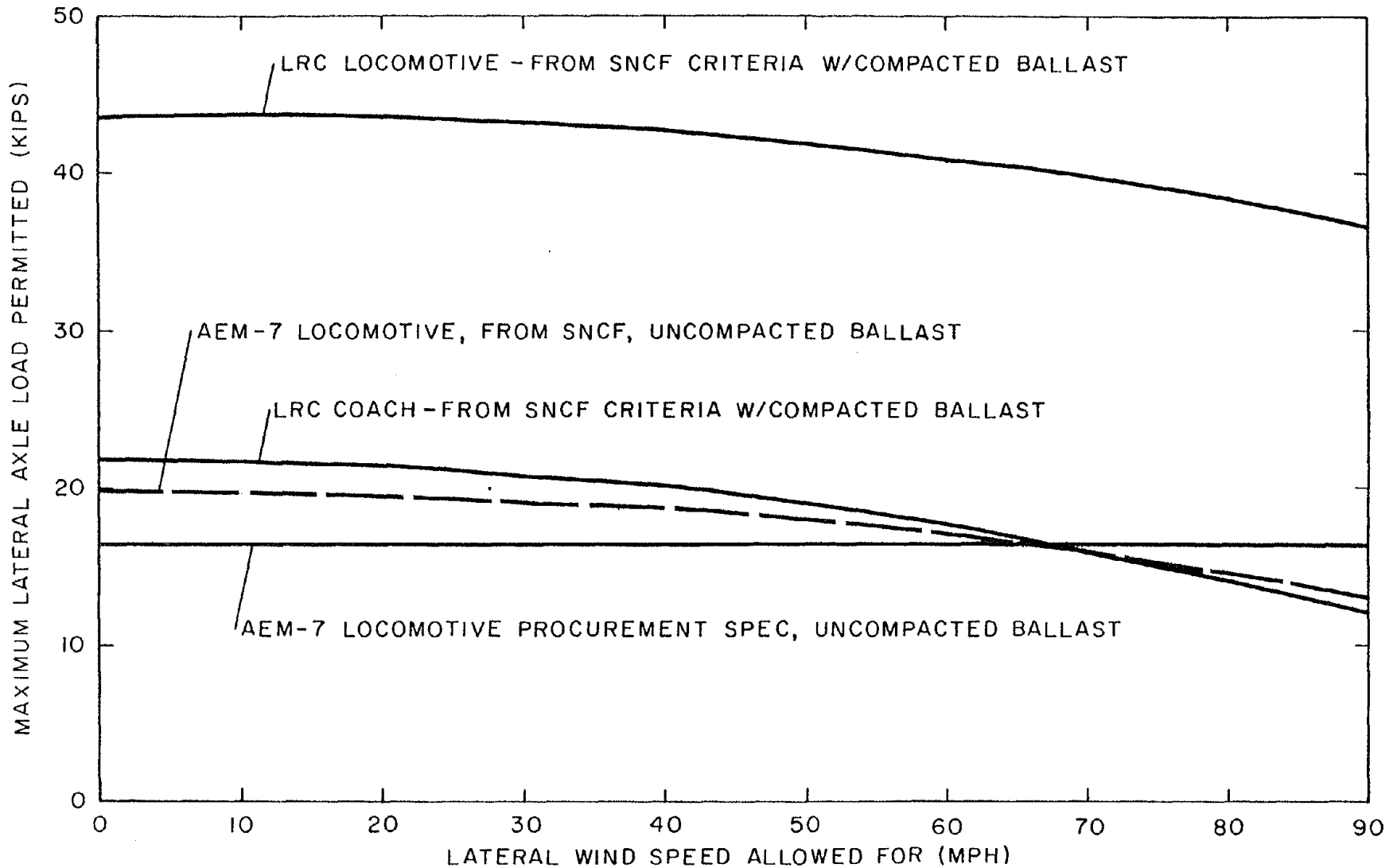


Figure 5-11. Comparison of Various Lateral Track Shift Criteria

All of the track resistance measurements quoted were obtained from steady state experiments and presumably the resulting criteria should be compared to steady state rather than transient measurements. The only criteria, however, to specifically address the time duration of the measurement has been Amtrak's AEM-7 procurement specification which requires $F_{max} \leq .85 (.33P + 2,200)$ for $T \leq 50ms$ or $X \leq 6$ feet and includes CWR rail on uncompacted ballast. This criteria allows higher lateral axle loads for very short durations in recognition that considerable energy is required to deform the track permanently. However, 50 ms may be overly conservative in this respect because it is more typical of the time duration of a well filtered peak measurement rather than a steady state. This criteria would be more useful if it were defined for running on compacted ballast because high speed curving is normally prohibited on newly worked track.

Recommendations have been made by Battelle for considering the combined effect of several axles of one truck on shifting the track laterally. It has been proposed that: $F_{max} (truck) = .7nF_{max} (axle)$ where n equals the number of axles per truck. Reducing the axle force summation is reasonable because the seven tie influence zones of several axles will overlap.

The specific criteria proposed for U.S. service appears to be judgements by various investigators based mainly on the French experiments. Differences between the French test sites and typical NEC track are not known nor is the variation between places on the NEC. The relationship between time duration and amplitude of destructive lateral axle force pulses was not defined by the French experiments thus the topic has been treated conservatively or not at all.

5.5 RIDE QUALITY CRITERIA

The most obvious factor affecting passenger comfort in high cant deficiency curving is the steady state level of lateral acceleration. It can be determined mathematically by

$$A_y = \frac{v^2}{r} + g \left(\sin \phi - \frac{s}{l} \right)$$

and expressing A_y in g's with ϕ a small angle:

$$A_y = \left(\frac{v^2}{rg} - \frac{s}{l} \right) + \phi = \frac{\text{cant deficiency}}{l} + \phi$$

where

V = running speed (ft/sec)

r = curve radius (ft)

g = gravitational acceleration (32.2 ft/sec²)

s = crosslevel (inches)

ℓ = effective tread gage (60 in)

φ = body roll angle, radians

In the case of active or passive tilt body coaches, φ can be such that the acceleration of gravity cancels the effect of cant deficiency. The effectiveness of reducing the lateral acceleration by controlling the body roll angle depends on the range and control characteristics of the tilt system.

Figure 5-12 presents the results of an often quoted AAR Study (Ref. 20) which related subjective assessment of comfort by observers to objective measurements. The observers were asked to disregard accelerations due to track irregularities and spiral transitions and to concentrate solely on steady state curving. A maximum steady state level of 0.1 g including the effect of body roll angle was recommended as a result of the test program. Lateral accelerations in successive opposite curves have been mentioned as especially harmful to ride comfort (Ref. 5). Table 5-1 summarizes the lateral acceleration recommendations by several organizations (many of them quoted in Reference 21) for steady state lateral acceleration and other criteria.

Figure 5-13 illustrates the characteristics of the lateral acceleration measured at the car floor during a typical curve negotiation. The average slope of lateral acceleration with respect to time in the spirals is known as "jerk" and it is a prime consideration in the design of transition spirals. AAR (Ref. 20) recommends that spiral lengths be set according to the formula $L_{min} = 4.88 V$ which allows a minimum of 3.3 seconds travel time between tangent track and circular curve. This has been interpreted as a maximum "jerk" specification of .03 g/sec (to .1 g) but the actual rate could be higher due to body roll overshoot. The body roll overshoot is the subject of a comfort criteria used by JNR (Ref. 9). "Transient response diagrams" of "carbody vibration" are included in Reference 6 for ease in applying the ±.08 g maximum specification. These diagrams (Figure 5-14 as an example) are essentially plots modeled throughout a curve of A_y (transient) = $(V^2/rg - s/\ell) + \phi - r/g$ where φ is assumed to reach a steady state value sufficient to cancel $(V^2/rg - s/\ell)$. The response time of φ is important to apparent "carbody vibration" under this application of the criteria. The concept of "carbody vibration" was applied to a tilt body coach in Reference 6, and

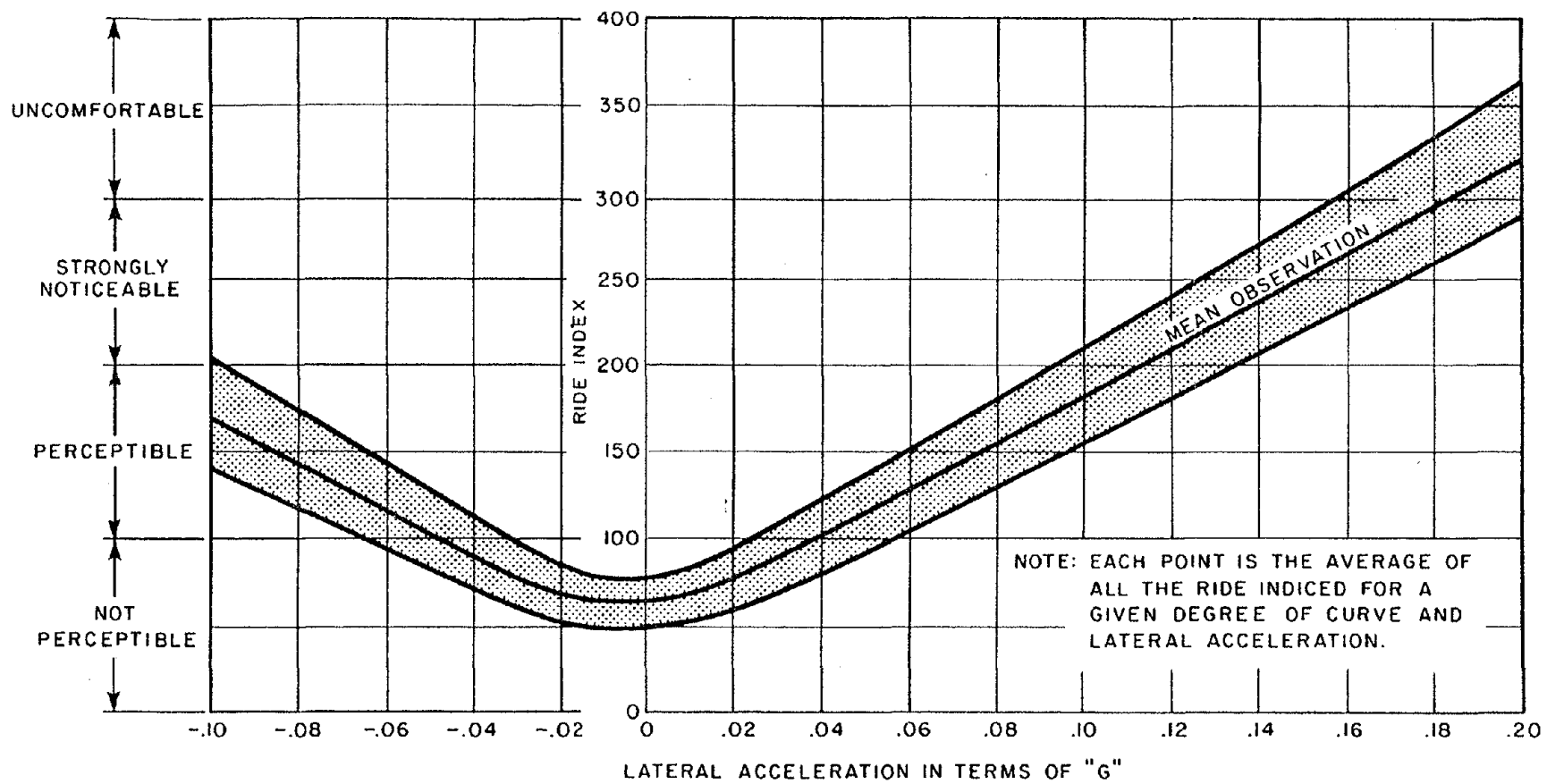


Figure 5-12. Relation of Subjective Comfort Rating to Carbody Lateral Acceleration for AAR Experiment

TABLE 5-1

LATERAL ACCELERATION RIDE COMFORT CRITERIA

Source	Maximum Steady State, g	Maximum "Jerk", g/sec	Maximum Carbody Vibration, g
BR	0.074	0.042	-
Koffman (ref 14)	General European practice	0.066 + body roll	-
	Newer European limits	0.087 + body roll	-
	Recommended max for locomotives	0.160 + body roll	-
AAR (ref 20)	0.1	0.03	
JNR (ref 5)	0.08	0.03	±.08
OHSGT	0.08	0.03	-
SNCF	0.15	0.1	-
DB	.066 (< 124 mph)	-	-
	.031 (< 186 mph)	-	-

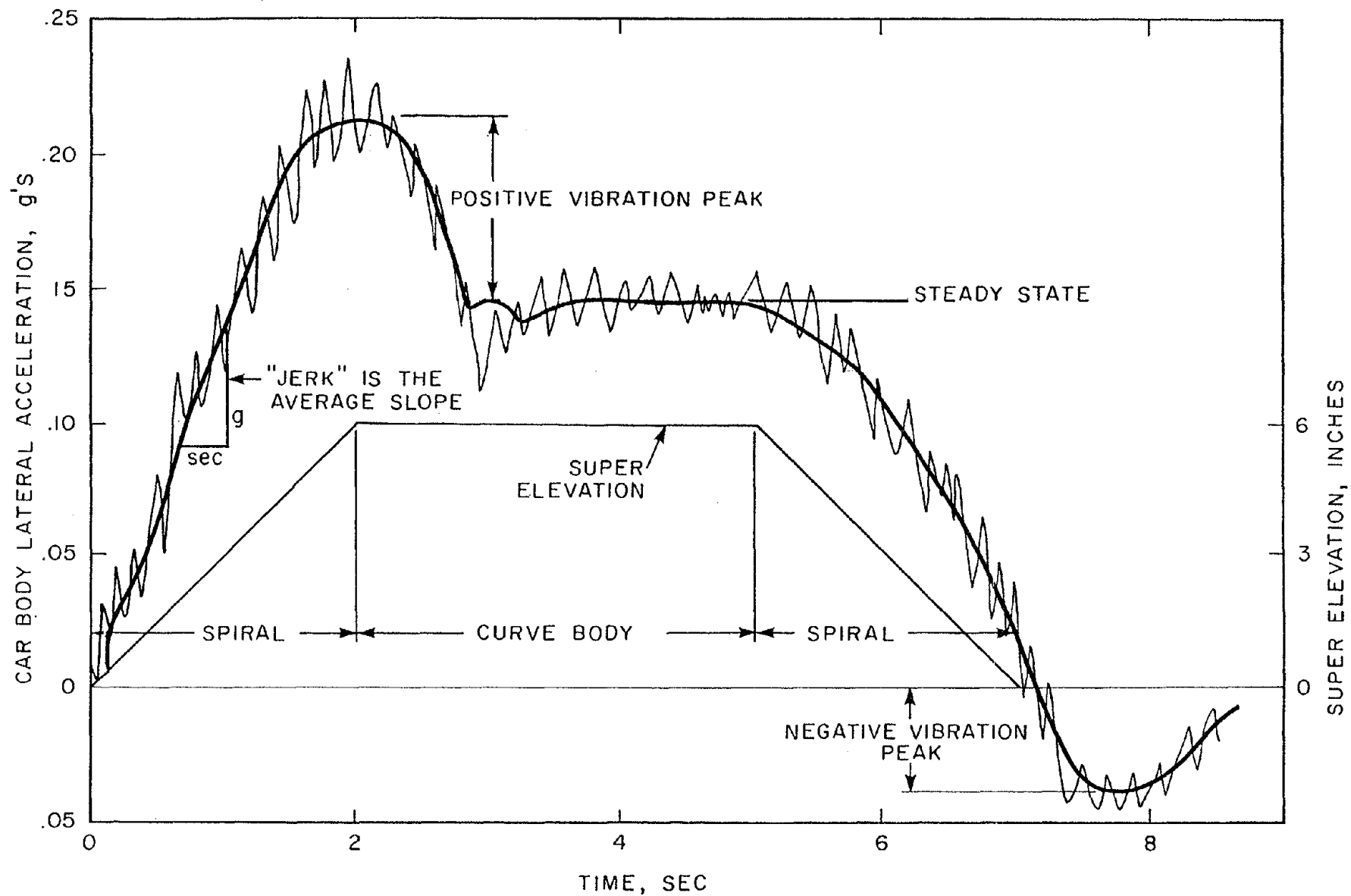


Figure 5-13. Features of Carbody Lateral Acceleration Referenced to Location on Curve

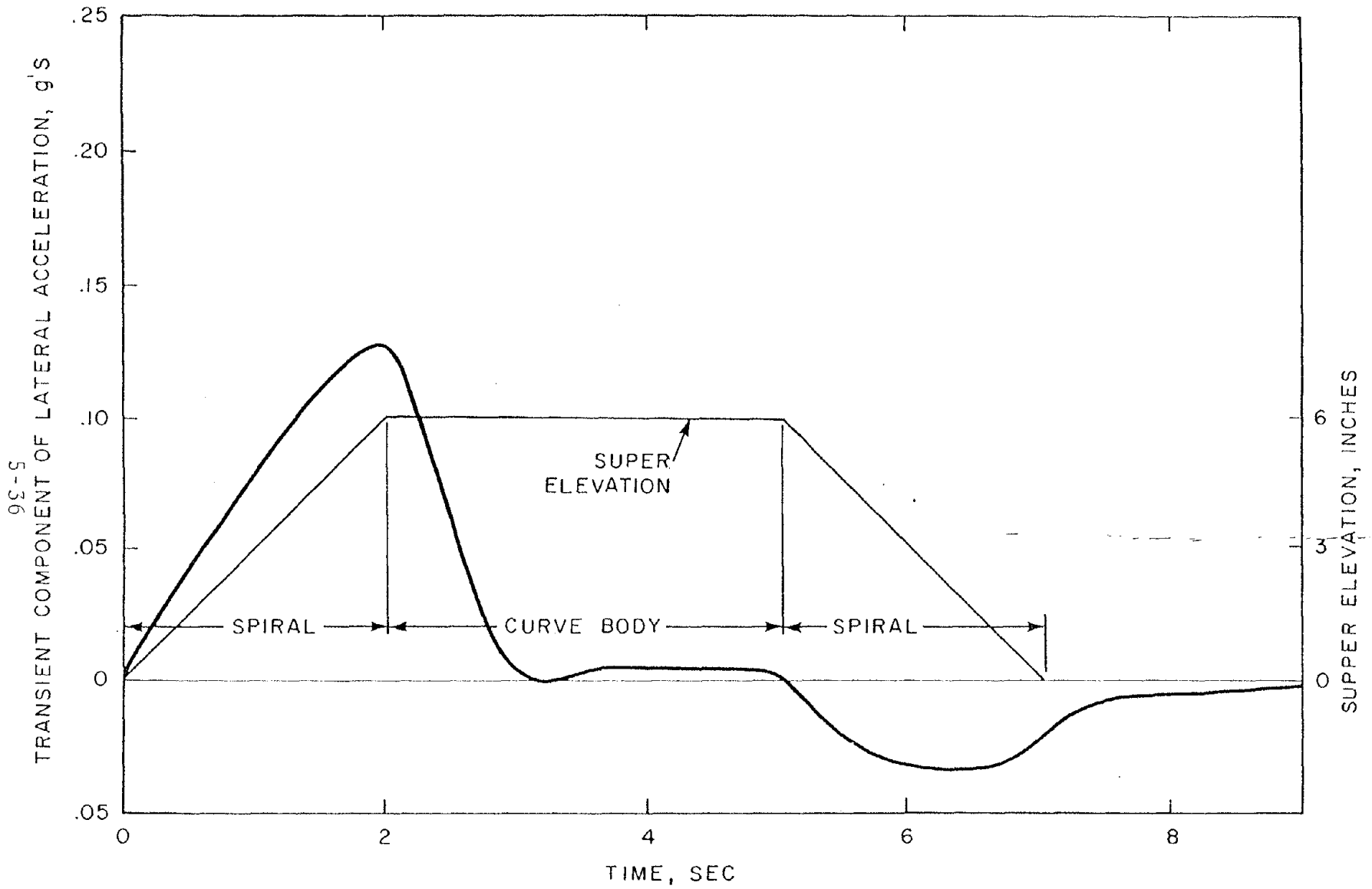


Figure 5-14. Typical "Transient Response Diagram" of "Carbody Vibration"

it may be more valuable than the other more common criteria of "jerk" and steady state lateral acceleration in assessing the effect on ride comfort of the extra lateral acceleration pulses that are a consequence of tilting motions. Steady state lateral acceleration, "jerk" and "carbody vibration" are all measured at 1 Hz or less. The higher frequency components are usually ignored in curving comfort criteria except for Reference 6 which uses Figure 5-15 to judge the natural frequency response of proposed suspension systems to mathematically model steady sinusoidal track perturbations.

5.6 RECOMMENDED SAFETY AND RIDE COMFORT CRITERIA

VEHICLE OVERTURNING

A criterion based on the JNR load ratio standards is useful for comparison to steady state models and measurements and to peak measurements, and it offers a convenient method to handle the safety implications of high crosswinds. Peak measurements of about 50 ms duration should be used, and the lower of the two limits derived from steady state and peak comparisons should be taken when both measurements are available. The criterion may be stated by the following two conditions expressed in terms of weight vector intercept.

$$\begin{array}{l} \text{Steady State} \\ \text{Vector Intercept} \end{array} \leq 18 - (.0153V^2Sh_{cp}/W) \text{ inches}$$

and

$$\begin{array}{l} \text{Peak Vector} \\ \text{Intercept} \end{array} \leq 24 - (.0153V^2Sh_{cp}/W) \text{ inches}$$

where:

V = the lateral wind speed in mph

S = the lateral surface area of the vehicle in ft²

h_{cp} = the height of the center of wind pressure in ft

W = one-half of the unloaded weight of the vehicle
in pounds

WHEEL CLIMB

The criterion of safety against wheel climb used by Amtrak and EMD is recommended because it clearly specifies the maximum

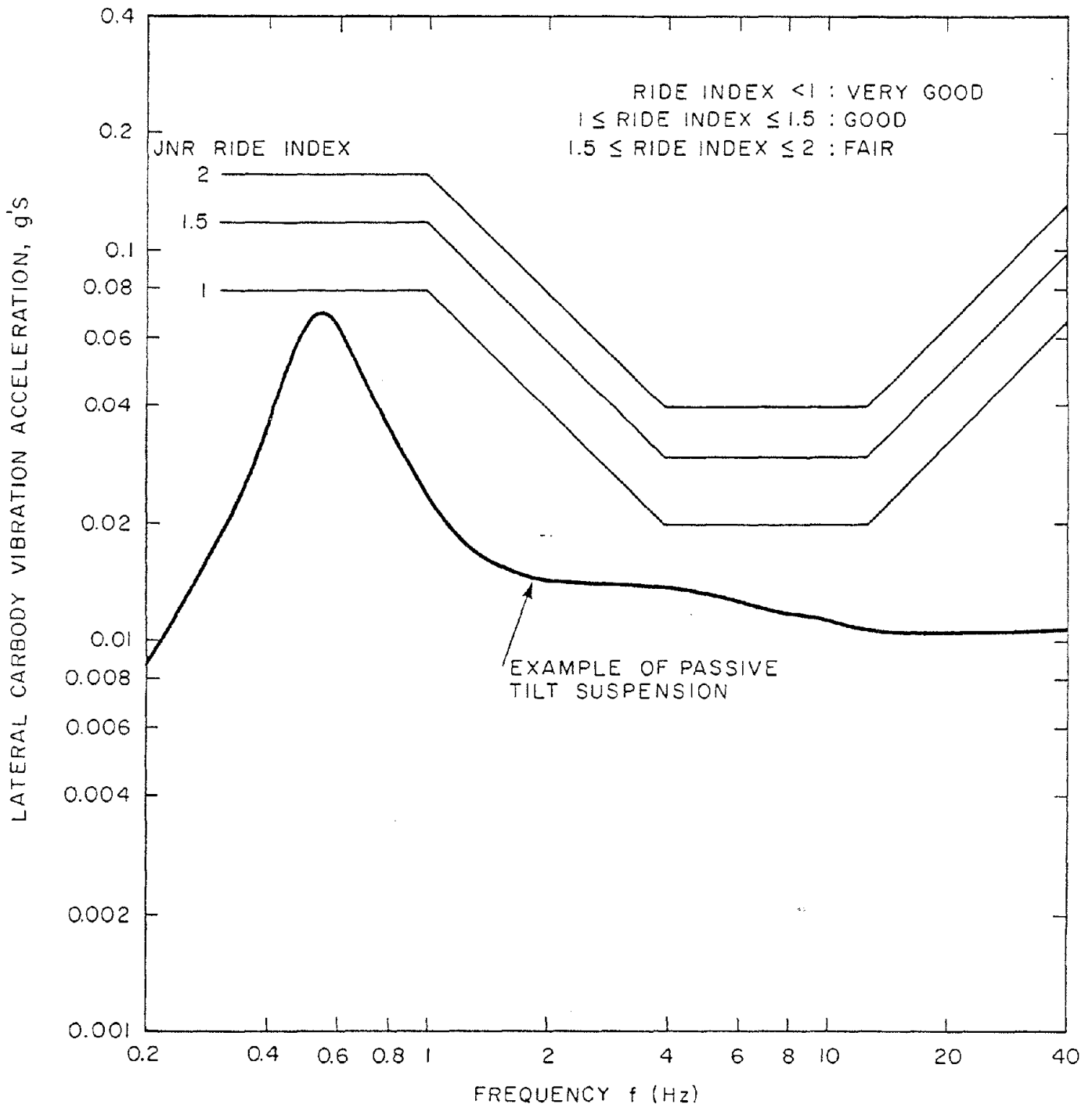


Figure 5-15. Suspension Frequency Response to Steady Sinusoidal Lateral Perturbation

permissible measurement as a function of time duration and it considers the AAR flange angle. It may be expressed as:

$$\text{Peak Wheel (L/V)} < 0.056T^{-0.927} \quad \text{for } T < 50 \text{ ms}$$

and

$$\text{Peak Wheel (L/V)} \leq 0.90 \quad \text{for } T \geq 50 \text{ ms}$$

The peak measurement for a particular time duration is the maximum level that was exceeded for that time duration. Because of a lack of full scale measurements, this criterion is based on Nadal's formula with conservative judgements of friction coefficient and angle of attack.

RAIL ROLLOVER

The rail rollover criterion based on rail section geometry and AAR measurements of the torsional support of the surrounding rail but which assumes zero pull out strength of the fasteners has been expressed:

$$\text{Peak truck (L/V)} \leq 0.5 + 2,300/P_w$$

for peaks of 50 ms or greater duration where P_w is the nominal wheel load. For peaks of less than 50 ms duration greater levels can be endured safely as given by the rule:

$$\text{Peak truck (L/V)} \leq .113 (0.5 + 2300/P_w) T^{-0.728}$$

for $T < 50 \text{ ms}$

TRACK PANEL SHIFT

A criteria for determining the maximum lateral axle force on wood tie track with compacted ballast which takes into account the internal forces in CWR due to temperature changes and the lateral carbody forces caused by unfavorable high crosswinds is:

$$F_{\text{max}} = \left[1 - \frac{A\Delta\theta}{22320} (1 + .458D) \right] \left[.7P + 6600 \right] - (1.28 \times 10^{-3} S V^2)$$

where

A = rail section area, in²
 $\Delta\theta$ = max temperature change after rail installation, °F
 D = track curvature, degrees
 P = vertical axle load, lbs
 S = lateral surface area of vehicle, ft²
 V = lateral wind speed, mph

and it is assumed that a single axle bears half the entire wind load. For typical NEC conditions of 140-pound rail (A = 13.8 in²), $\Delta\theta$ max of 70°F and D max of 4°.

$$F_{\max} = .61P + 5800 - 1.28 \times 10^{-3} SV^2$$

A maximum truck force criteria for the CWR example can be expressed:

$$F_{\max} (\text{truck}) = .7N \left[.61P + 5800 - (1.28/.7N)10^{-3}SV^2 \right]$$

where N is the number of axles per truck and one truck supports half the total wind load. Peak measurements of high rail wheel and high rail truck side lateral forces having durations of about 50 ms are suitably conservative measures of maximum axle and truck lateral loads, respectively. This conservativeness is warranted because the only track shift measurements in the literature were taken on French 92 lb/yd rail and even the best criteria in use is an extrapolation from the French experiment.

RIDE QUALITY

Current AAR standards limit steady state lateral acceleration to 0.1 g and "jerk" to 0.03 g/sec. The JNR criteria of $\pm .08$ g maximum additional transient component upon entering and existing curves should be considered, especially for tilt body cars. Low frequency measurements filtered at about 1 Hz are appropriate for comparison to these comfort standards.

6.0 RESULTS OF TESTING THE LRC TRAIN AT HIGH CANT DEFICIENCY

The LRC locomotive and active tilt coach were tested in two modes. In the first mode, many repetitive runs at various speeds were made over two specific test curves, one left and one right. The steady state performance of the vehicles was determined on these test curves. The second mode of testing was a series of runs over hundreds of miles of NEC track. The peak level measurements which depend on actual track irregularities were taken from these tests as well as from the repetitive curving tests. The safety criteria are discussed in detail in Section 5.0 and the data reduction techniques are covered in Section 3.5

6.1 VEHICLE OVERTURNING

The vehicle overturning criteria used by the Japanese National Railway is the most comprehensive in the literature. It is appropriately conservative and it includes separate criteria for peak and steady state measurements. It may be summarized, in terms of vector intercept, by the following two equations:

$$\begin{array}{l} \text{Steady State} \\ \text{Vector Intercept} \end{array} \leq 18 - (.0153V^2Sh_{cp}/W) \text{ inches}$$

and

$$\begin{array}{l} \text{Peak Vector} \\ \text{Intercept} \end{array} \leq 24 - (.0153V^2Sh_{cp}/W) \text{ inches}$$

where:

V is the lateral wind speed in mph

S is the lateral surface area of the vehicle in ft²

h_{cp} is the height of the center of wind pressure in ft

W is one half of the unloaded weight of the vehicle in pounds.

For the LRC vehicles:

<u>Locomotive</u>	<u>Coach (unloaded)</u>
S ≈ 682 ft ²	S ≈ 935 ft ²
h _{cp} ≈ 6.5 ft	h _{cp} ≈ 6.5 ft
W = 125,400 lb	W = 52,750 lb

The second term in the above equations is an allowance for the maximum detrimental effect of wind speed. The weight vector intercept specified by each criterion represents the maximum still air test measurement permitted for operation at the given wind speed. The above two equations are graphed on Figure 6-1 which expresses the separate criteria appropriate for peak and steady state measurements as functions of the allowed wind speed.

6.1.1 WIND SPEED EFFECT

The overturning criteria are extremely sensitive to wind speed especially over 50 mph for the coach although smaller heavier vehicles such as the locomotive are less susceptible. The operational cant deficiency should be chosen to allow for sudden unexpected lateral winds, but train speed need not be limited by overturning considerations to include heedless operation in gales and hurricanes because train speeds must be reduced under these circumstances to meet other conditions such as reduced visibility or the danger of debris on the track. The operational cant deficiency chosen will provide safe operation for the maximum wind speed corresponding to the 10 year mean recurrence interval. This cant deficiency is sufficiently conservative to provide for safety during unexpected winds. The level of wind speed for locations along the NEC is greatest in Boston where it is 70 mph measured 30 ft above the ground (ref 24). Reference (24) also provides a factor to adjust wind speed measurement for other distances above ground level. At 15 feet above the ground the 10 year mean recurrence interval wind speed is $0.8 \times 70 \text{ mph} = 56 \text{ mph}$. As indicated on Figure 6-1, the cant deficiency at which weight vector intercept measurements are less than 12.5 inches steady state and 18.5 inches peak provides for safe operation of the LRC Coach at up to 56 mph crosswinds. The critical vector intercept measurements for the LRC locomotive are 16.3 inches steady state and 22.3 inches peak for the same crosswind allowance.

6.1.2 STEADY STATE MEASUREMENTS

Figures 6-2 and 6-3 give the steady state test results with respect to weight vector intercept of the LRC coach and locomotive relative to cant deficiency. The differences in right and left hand curves result from slight static imbalances of the weight carried by the lead trucks. These are typical of production differences in mass distribution, spring installation and, in the case of a banking coach, tilt sensor null position between

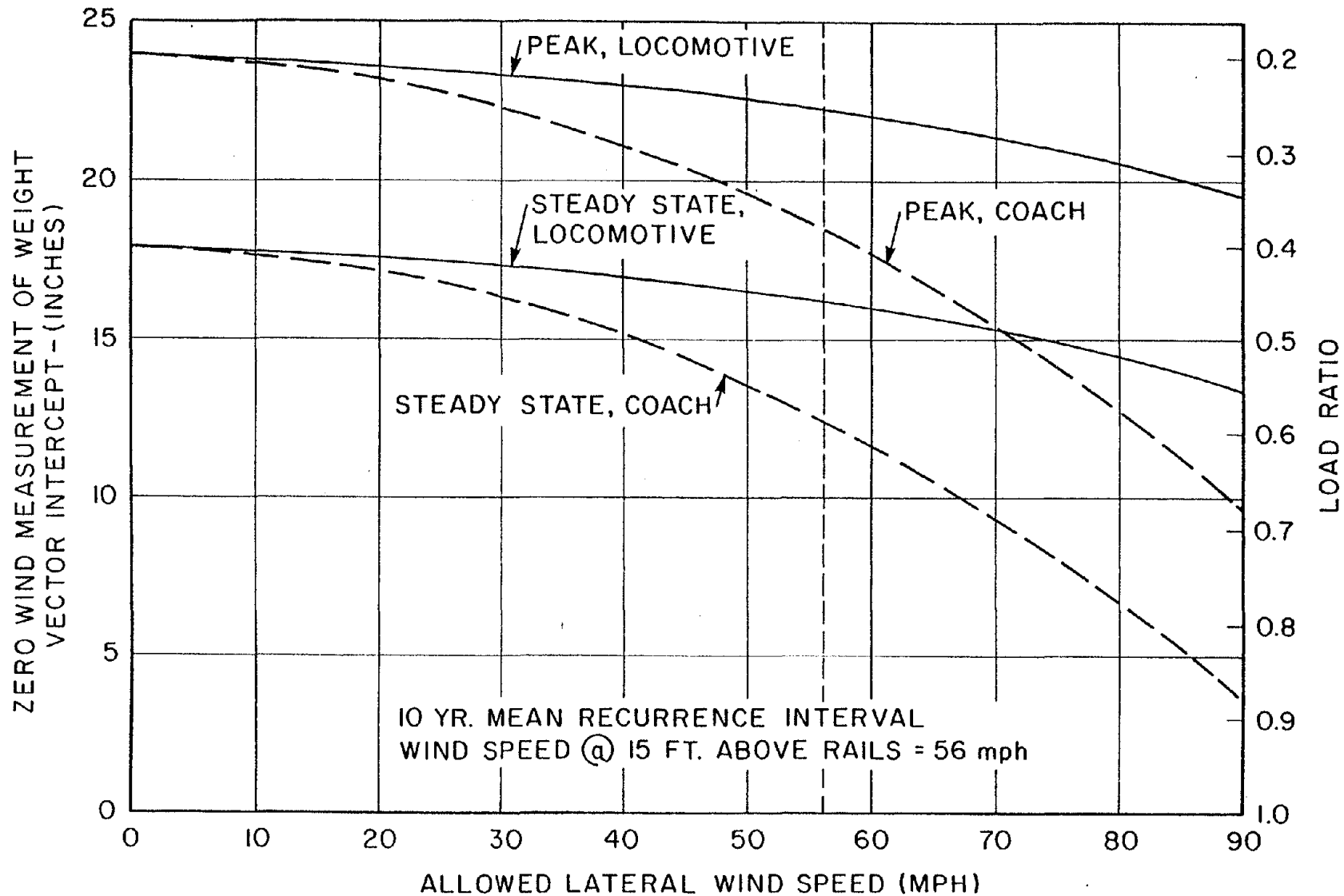


FIGURE 6-1

WEIGHT VECTOR INTERCEPT MEASUREMENT (ZERO WIND) V.S.
ALLOWED LATERAL WIND SPEED FOR LRC LOCOMOTIVE AND
COACH BASED ON JNR RECOMMENDED LOAD RATIOS

lead and trailing trucks. The unfavorable curving direction is used for a conservative comparison to the overturning safety criteria. Although the weight transfer characteristics of the coach and locomotive are very similar, the coach reaches the vector intercept limit at about 9 inches of cant deficiency and the locomotive at over 12 inches because the allowance for a 56 mph crosswind is more restrictive for the coach. The measurements in Figure 6-2 were made with banking but measurements taken the same day without banking confirm that steady state weight transfer of the LRC coach is substantially independent of banking because of the proximity of the banking center of rotation to the body c.g.

6.1.3 TRANSIENT (PEAK) MEASUREMENTS

The overturning safety criteria for both steady state and peak measurements must be satisfied for safe operation. Steady state measurements are similar for all constant radius curves negotiated at a particular cant deficiency. Peak measurements, however, will vary greatly due to geometry deviations and spiral design. Peak measurements of weight vector intercept were taken at the spirals and bodies of the test curves which were used for the steady state measurements in Figures 6-2 and 6-3. The highest measurements of the coach occurred at the entry spiral of the right curve and are plotted in Figure 6-4 as a function of cant deficiency. The highest measurements of the locomotive, shown in Figure 6-5, occurred in the body of the same curve. The peak measurements of both vehicles are quite linear with cant deficiency at the test curves where runs were repeated at several speeds. Thus the locomotive measurements may be extrapolated to the critical value of 22.3 inches specified by the transient criteria. Coach measurements were made above the critical value of 18.5 inches vector intercept. Since the peak vector intercept limit occurs at over 13 inches of cant deficiency, the locomotive would be limited first, in these curves, by the steady state overturning criteria at about 12 inches of cant deficiency. Likewise the steady state criteria poses the lower limit of about 9 inches for the coach on these curves. Many of the curves in the New Haven to Providence NEC test zone are typical of the worst track irregularities that the LRC train encounters in service. The results of the single pass over-the-road tests must be used to predict whether the transient overturning criteria poses a lower limit than the steady state criteria under these harsh service conditions.

Figures 6-4 and 6-5 also illustrate a method of determining, from a peak measurement at lower cant deficiency, whether the maximum cant deficiency with regard to overturning safety is first limited by the steady state or by the transient criteria. The projection of the transient criteria to low cant deficiencies is an estimate of the maximum peak vector intercept in a curve in which the steady state overturning criteria still limits cant

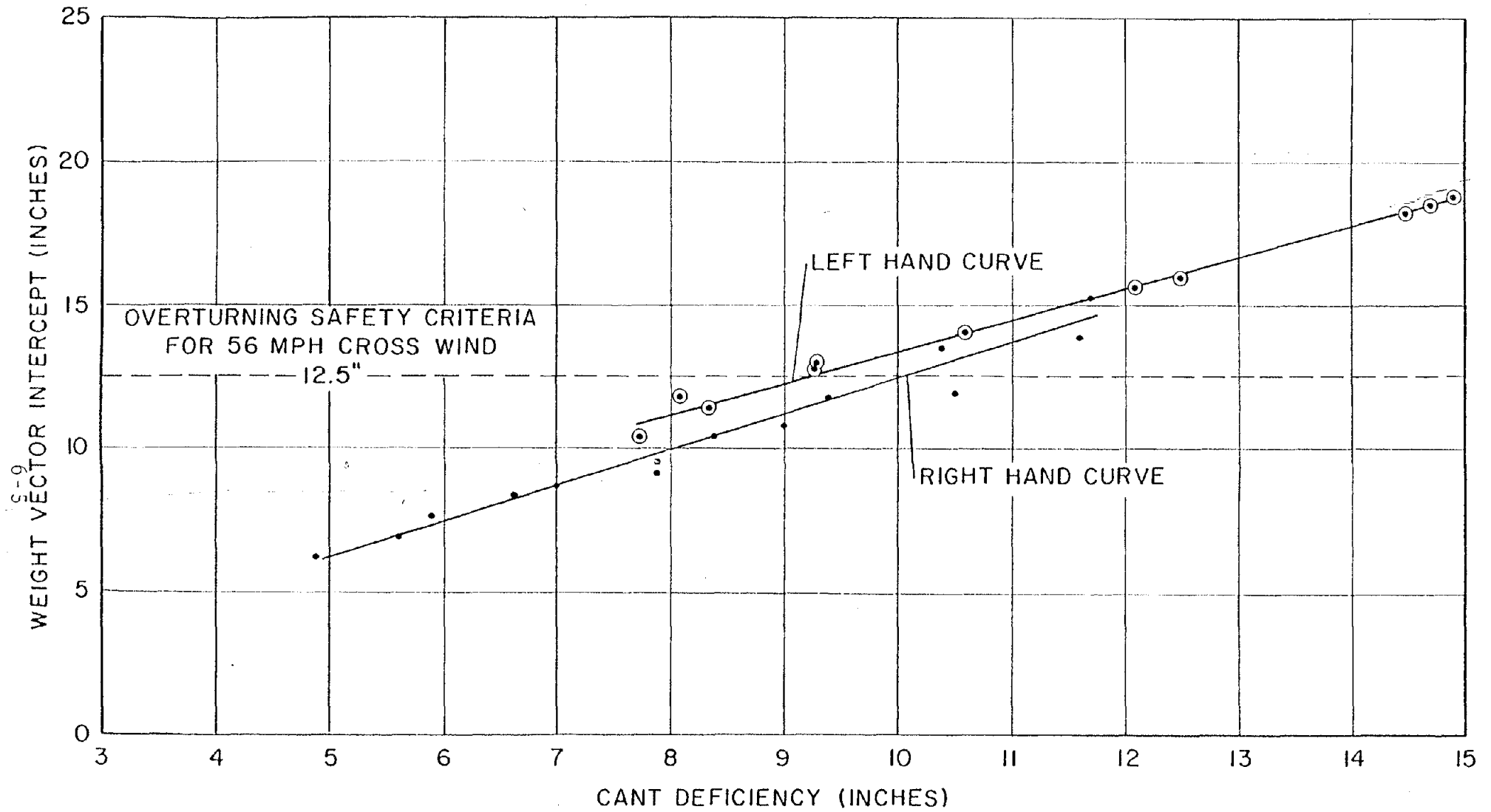


FIGURE 6-2

STEADY STATE MEASUREMENT OF LRC COACH OVERTURNING SAFETY

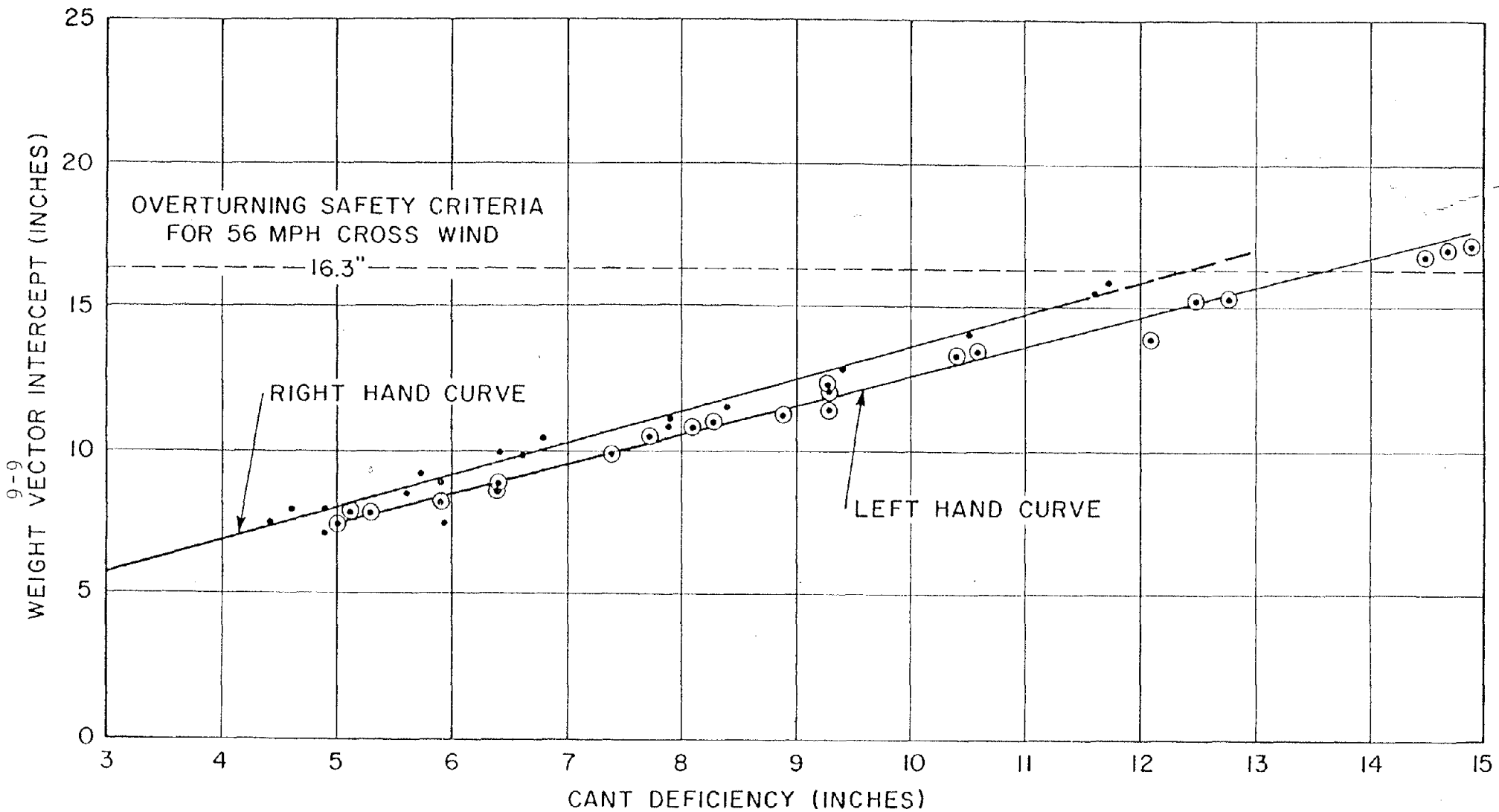


FIGURE 6-3

STEADY STATE MEASUREMENT OF LRC LOCOMOTIVE OVERTURNING SAFETY

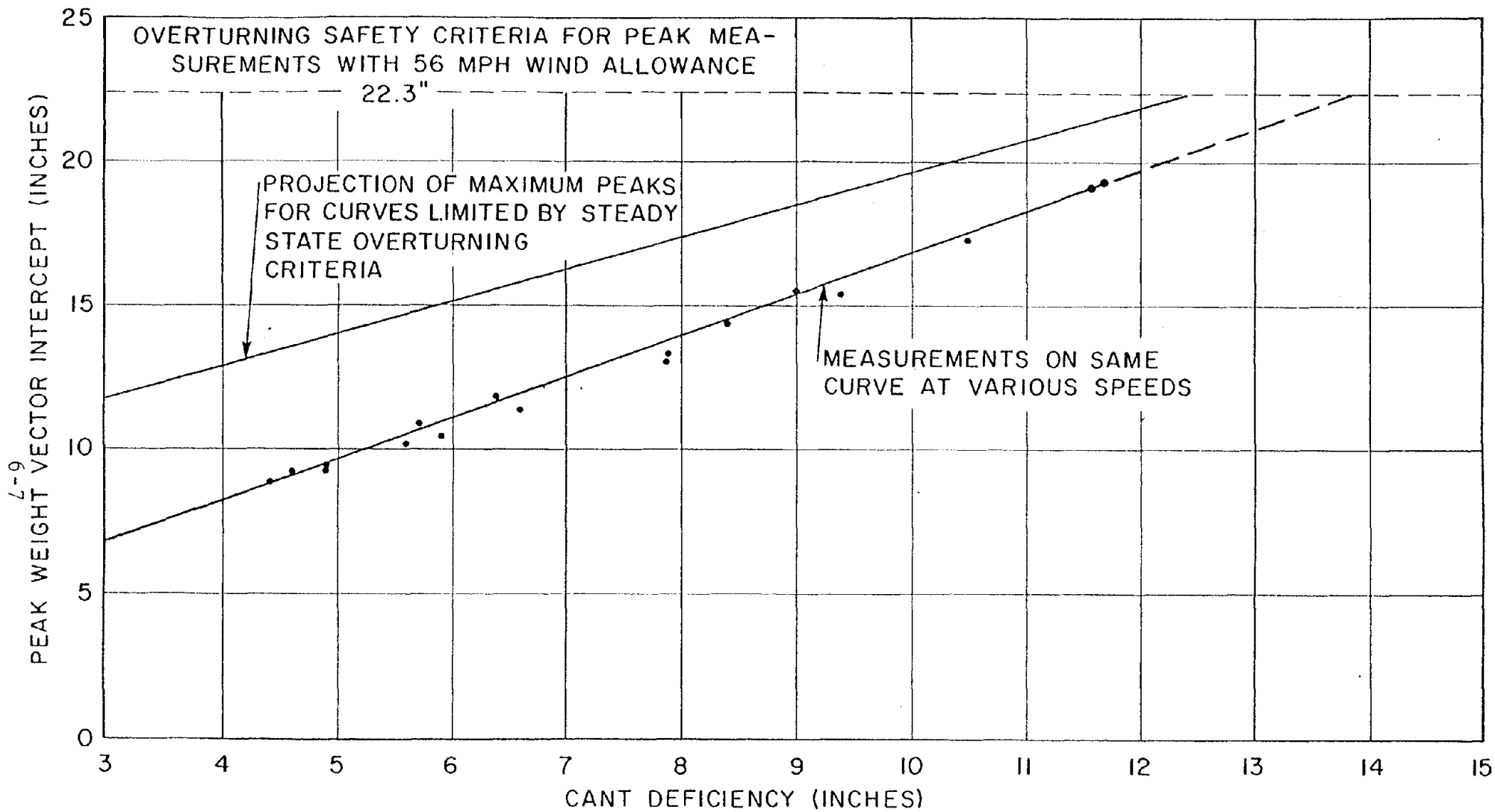


FIGURE 6-4

COMPARISON OF PEAK WEIGHT VECTOR INTERCEPT OF LOCOMOTIVE AT RIGHT HAND CURVE TO OVERTURNING SAFETY CRITERIA

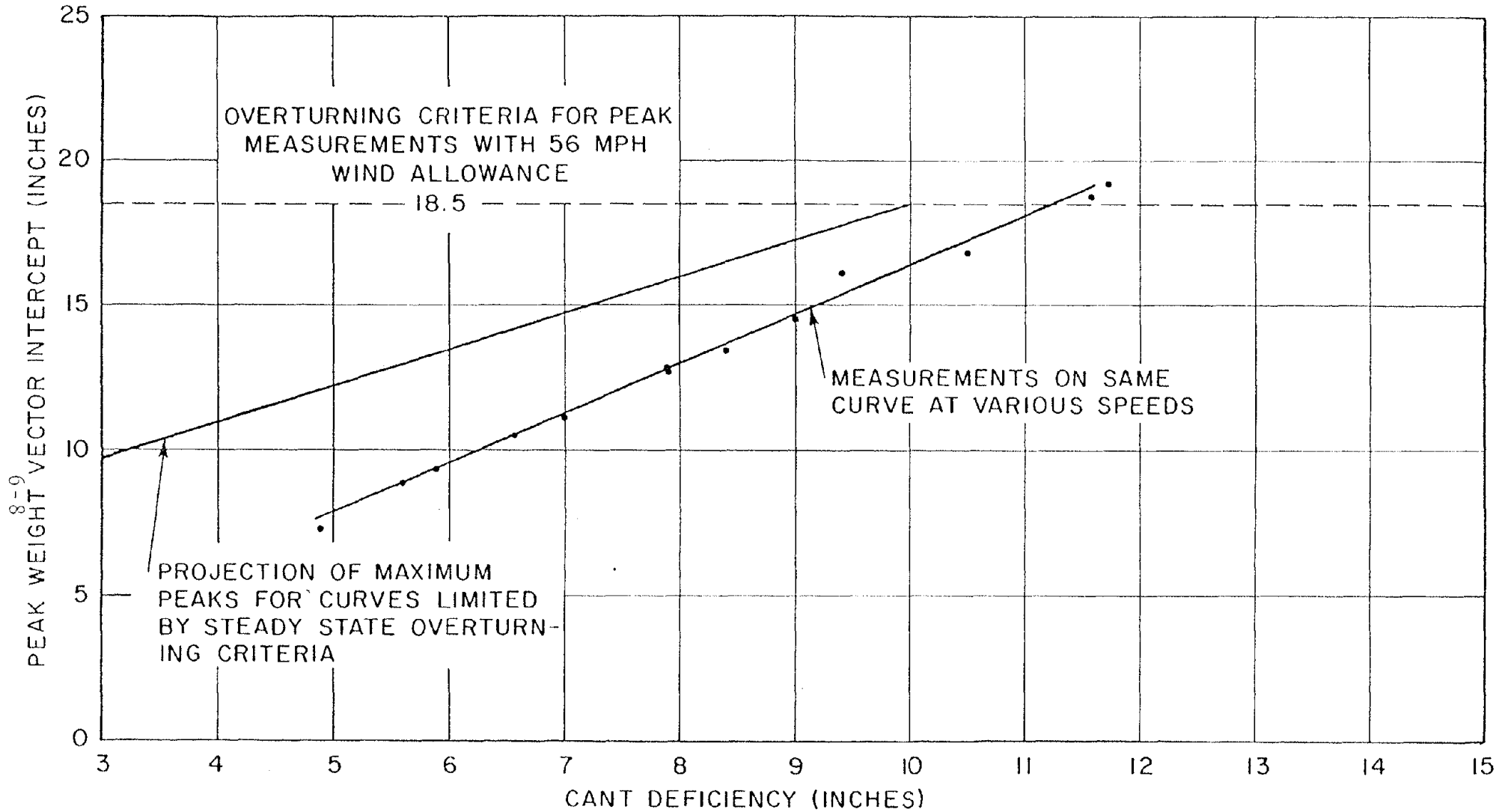


FIGURE 6-5

COMPARISON OF PEAK WEIGHT VECTOR INTERCEPT OF LRC COACH (BANKING) AT RIGHT HAND TEST CURVE TO OVERTURNING SAFETY CRITERIA

deficiency. If a peak measurement at any cant deficiency falls below the projection line, the steady state criteria will limit cant deficiency (at about 9 1/4 and 12 inches for the coach and locomotive, respectively). If the peak measurement exceeds the projection, the transient criteria will limit the cant deficiency at less than these values. The projection line was constructed by subtracting from the transient weight vector intercept limit the difference between the steady state limit and the steady state measurement (Figures 6-2 and 6-3) at each cant deficiency. The method avoids biasing for curve direction and it allows consideration of all types of track irregularities even if the particular test curve was speed limited by other factors.

For example, the peak measurements for the coach in Figure 6-5 were made at over 9 inches cant deficiency without exceeding the transient overturning criteria. However, if only one peak measurement at low cant deficiency were available at this curve, comparison with the projection line would correctly predict that the steady state criteria sets the lower cant deficiency limit. Figure 6-6 is a collection of single peak measurements at many curves. At curve 137 the peak measurement lies on the projection line. If the cant deficiency were increased, the peak vector intercept would be expected to increase along the projection line. It would reach the critical value of 18.5 inches at 9 1/4 inches cant deficiency which is also the limit set by the steady state criteria. If the cant deficiency were increased at curve 129, where the measurement exceeds the projection line, the peak vector intercept would be estimated to follow the dashed line parallel to the projection line. At this curve, the critical level would be reached at less than 3-1/2 inches cant deficiency. Curves at which peak vector intercept measurements exceed the projection line are not necessarily being negotiated unsafely at the test cant deficiency, but the cant deficiency at which the transient overturning safety criteria is achieved is lower than the limit set by the steady state criteria.

Figures 6-6 through 6-13 compare coach and locomotive peak measurements at groups of curves in the NEC between New Haven and Providence to the projection of the transient overturning criteria which indicates curves potentially limited to lower cant deficiency by this criteria. The projection line was exceeded at some curves, and at these, the absolute transient overturning criteria would be expected to limit the coach to less than 9 1/4 inches cant deficiency or the locomotive to less than 12 in the absence of any other speed restrictions. Tables 6-1 and 6-2 list the curves which fall on or above the projection line. The measurement of peak weight vector intercept, the test speed and cant deficiency, the estimated maximum safe cant deficiency and limiting factor, and the presence of unusual features are identified for each curve.

01-9

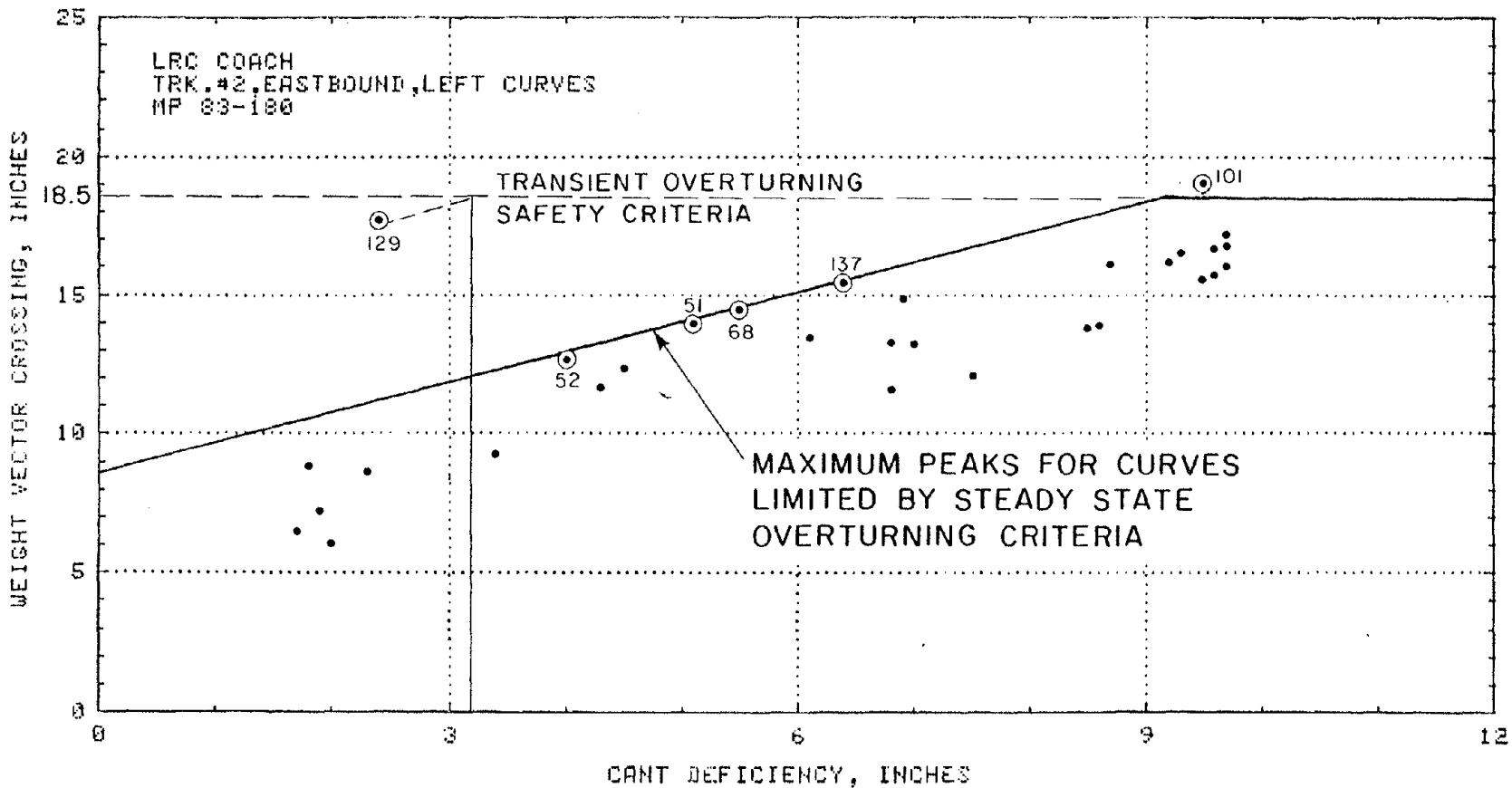


FIGURE 6-6

COMPARISON OF PEAK MEASUREMENTS OF WEIGHT VECTOR INTERCEPT FOR CURVES IN NEC TEST ZONE TO MAXIMUM PEAKS FOR CURVES LIMITED BY STEADY STATE OVERTURNING CRITERIA.

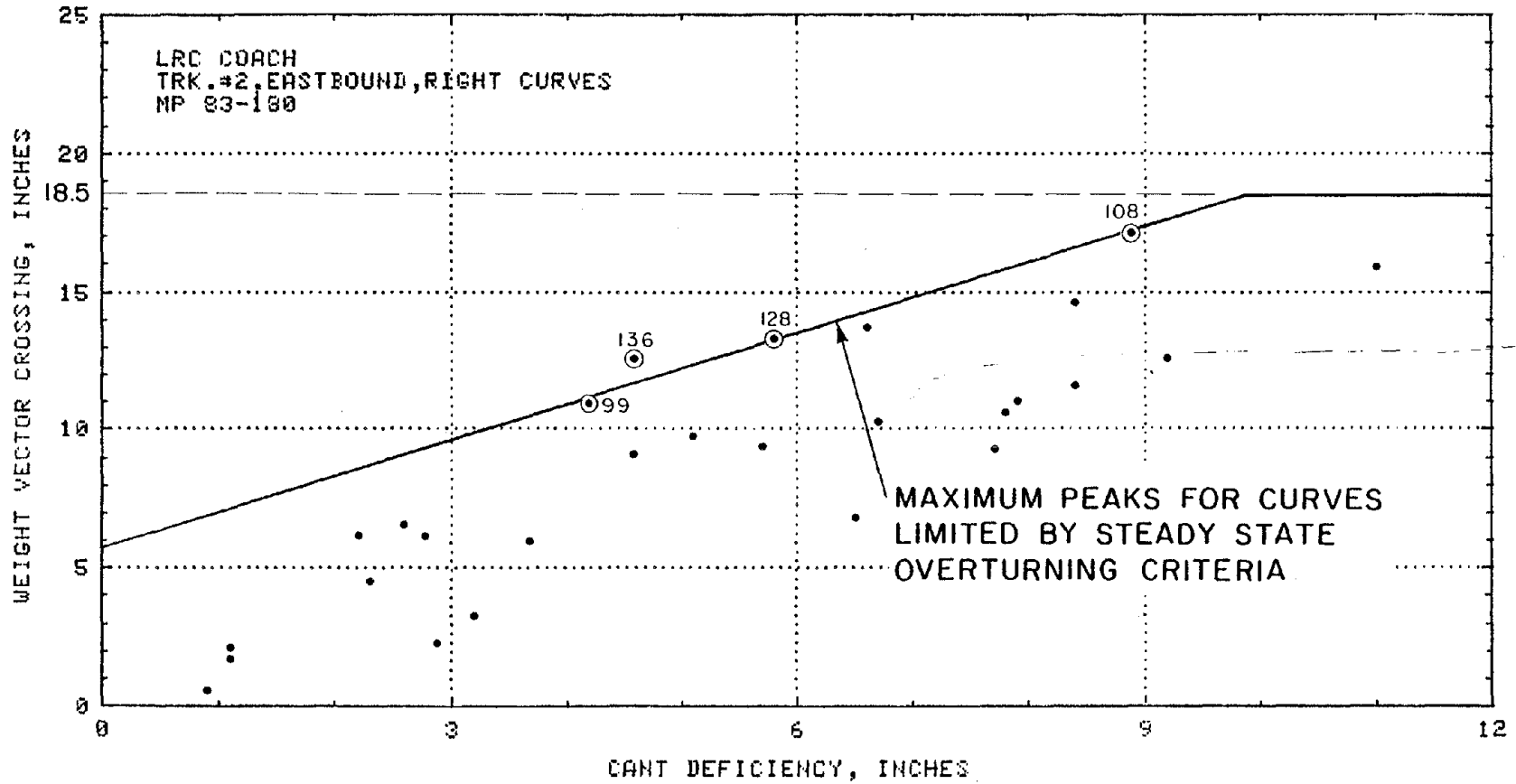


FIGURE 6-7

COMPARISON OF PEAK MEASUREMENTS OF WEIGHT VECTOR INTERCEPT FOR CURVES IN NEC TEST ZONE TO MAXIMUM PEAKS FOR CURVES LIMITED BY STEADY STATE OVERTURNING CRITERIA.

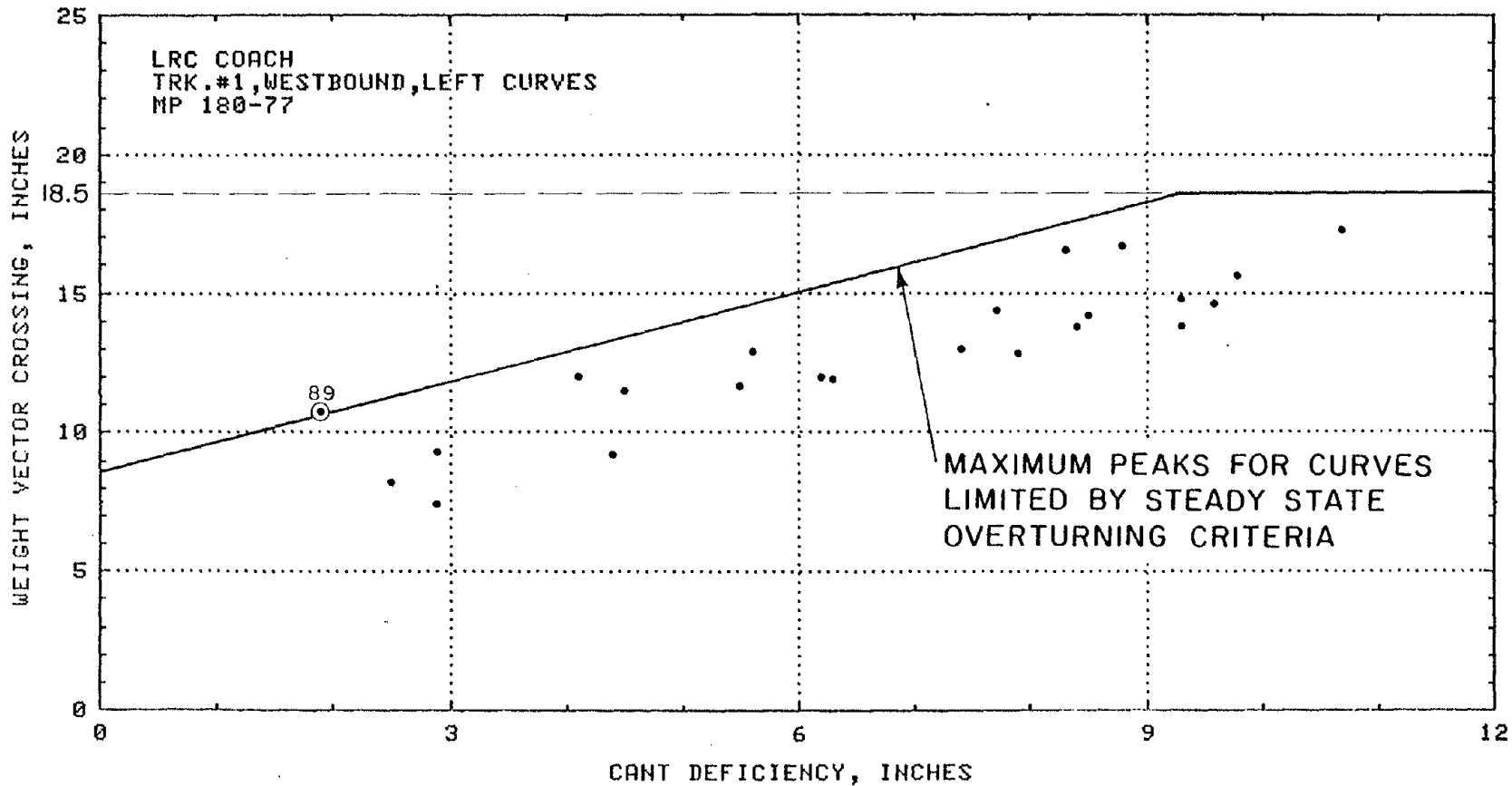


FIGURE 6-8

COMPARISON OF PEAK MEASUREMENTS OF WEIGHT VECTOR INTERCEPT FOR CURVES IN NEC TEST ZONE TO MAXIMUM PEAKS FOR CURVES LIMITED BY STEADY STATE OVERTURNING CRITERIA.

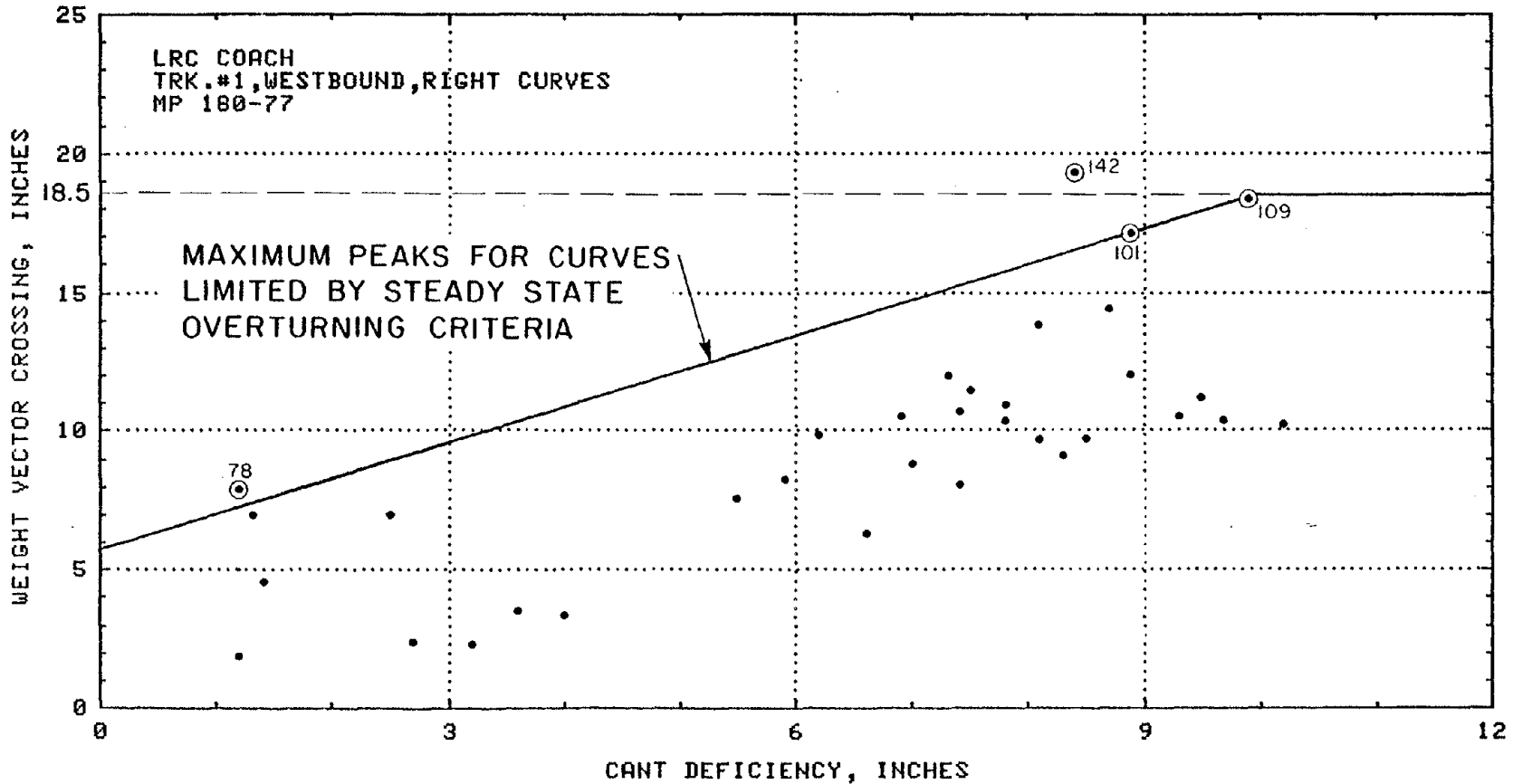


FIGURE 6-9

COMPARISON OF PEAK MEASUREMENTS OF WEIGHT VECTOR INTERCEPT FOR CURVES IN NEC TEST ZONE TO MAXIMUM PEAKS FOR CURVES LIMITED BY STEADY STATE OVERTURNING CRITERIA.

6-14

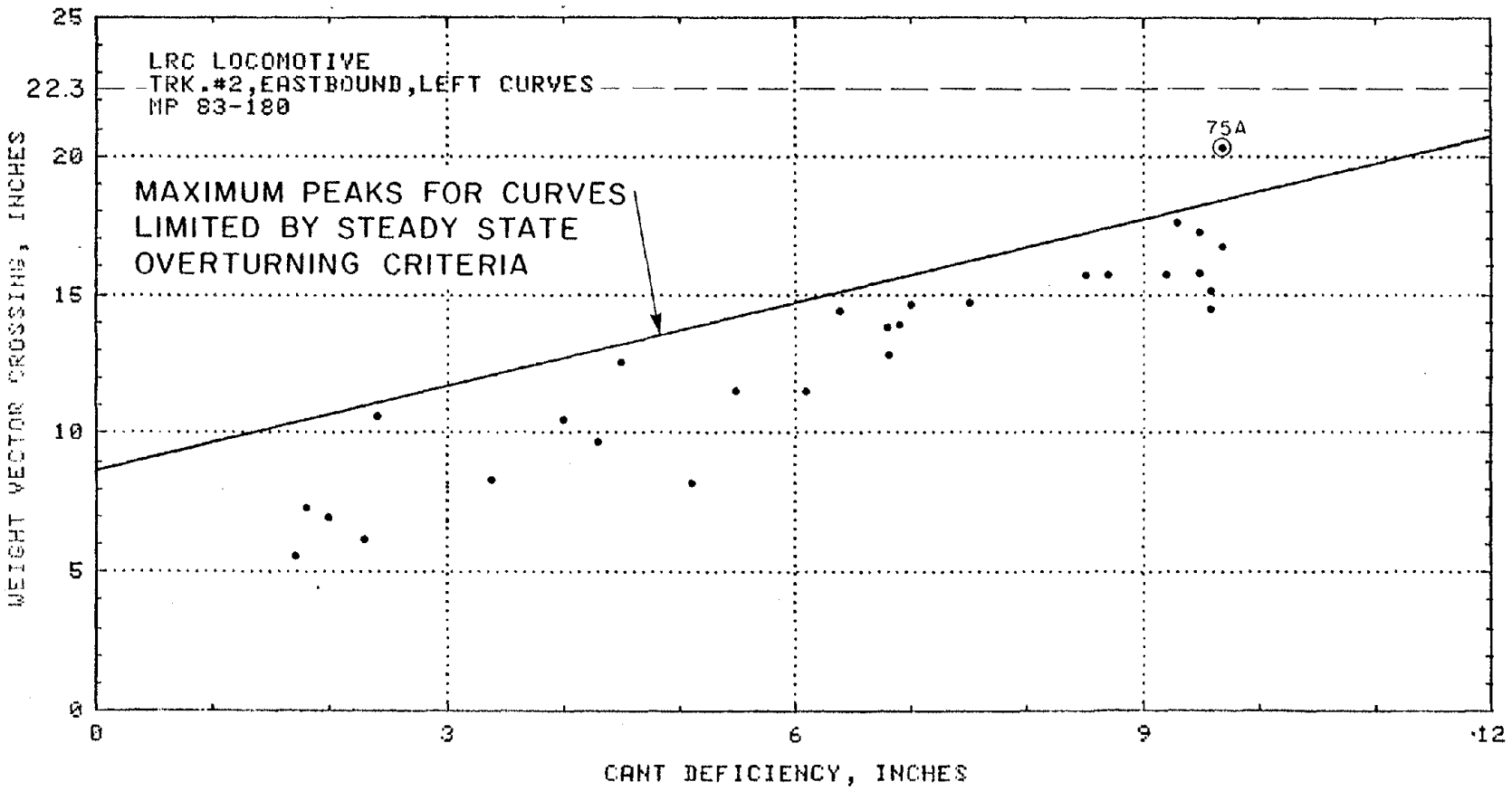


FIGURE 6-10

COMPARISON OF PEAK MEASUREMENTS OF WEIGHT VECTOR INTERCEPT FOR CURVES IN NEC TEST ZONE TO MAXIMUM PEAKS FOR CURVES LIMITED BY STEADY STATE OVERTURNING CRITERIA.

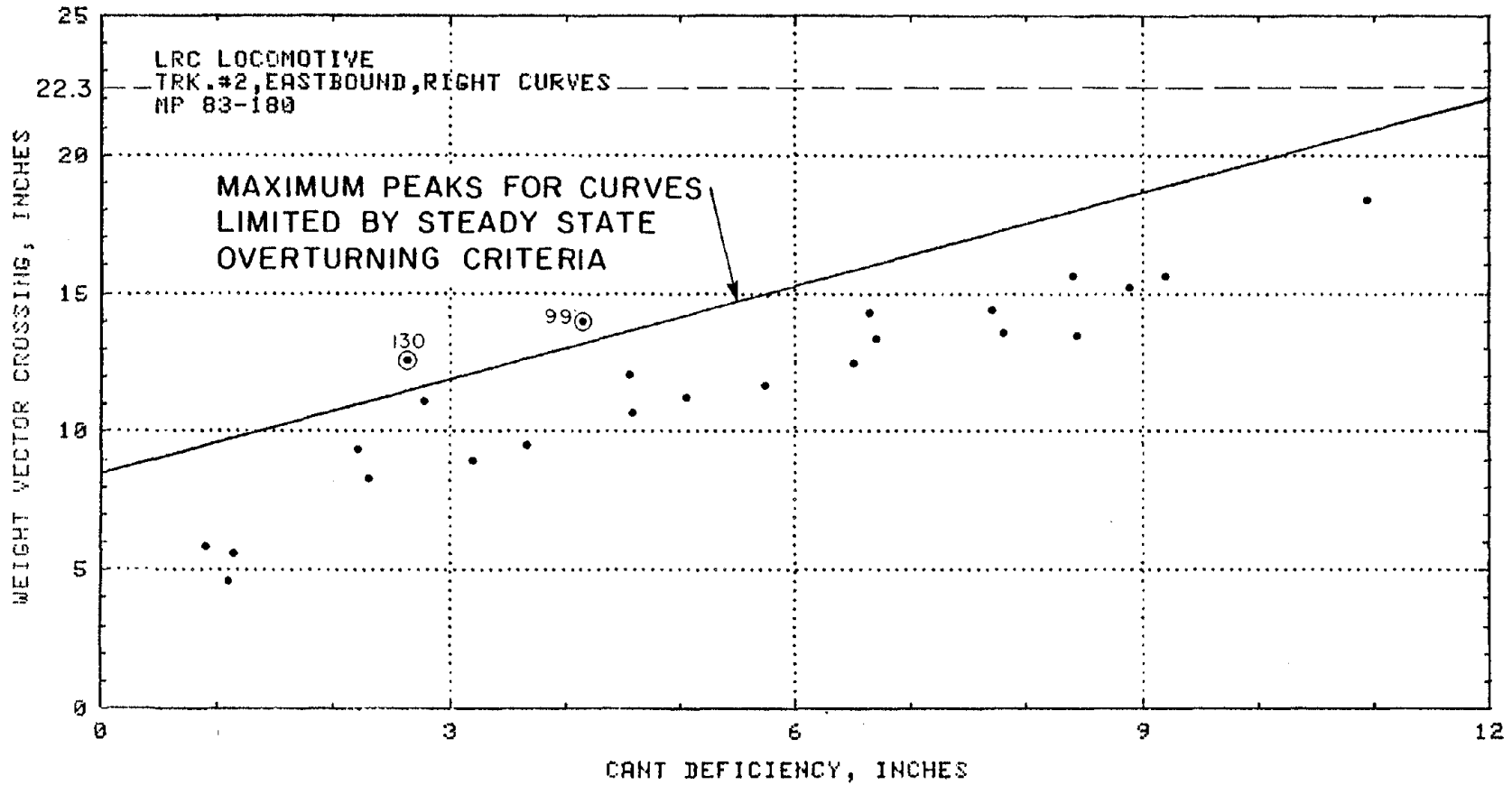


FIGURE 6-II

COMPARISON OF PEAK MEASUREMENTS OF WEIGHT VECTOR INTERCEPT FOR CURVES IN NEC TEST ZONE TO MAXIMUM PEAKS FOR CURVES LIMITED BY STEADY STATE OVERTURNING CRITERIA.

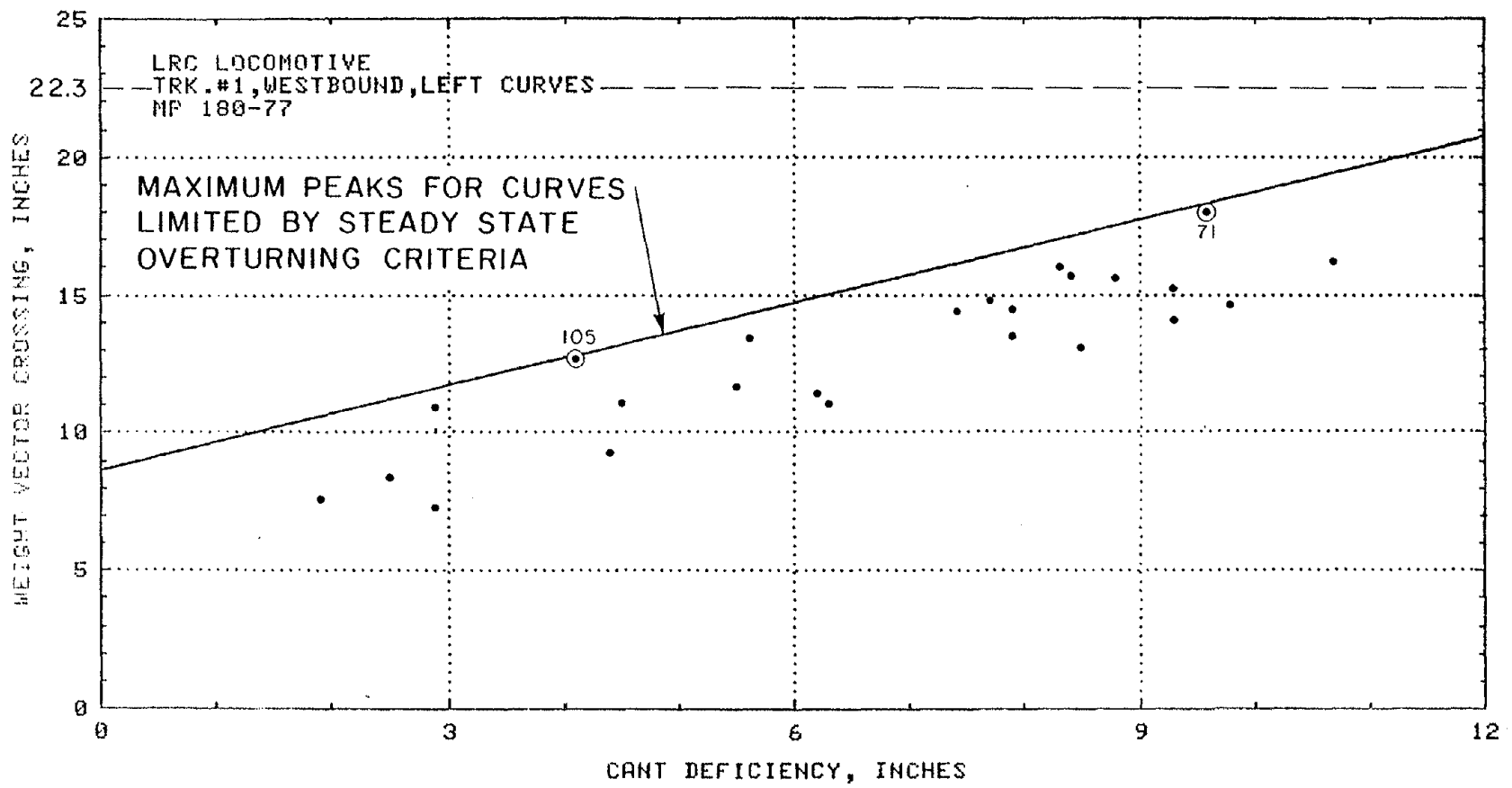


FIGURE 6-12

COMPARISON OF PEAK MEASUREMENTS OF WEIGHT VECTOR INTERCEPT FOR CURVES IN NEC TEST ZONE TO MAXIMUM PEAKS FOR CURVES LIMITED BY STEADY STATE OVERTURNING CRITERIA.

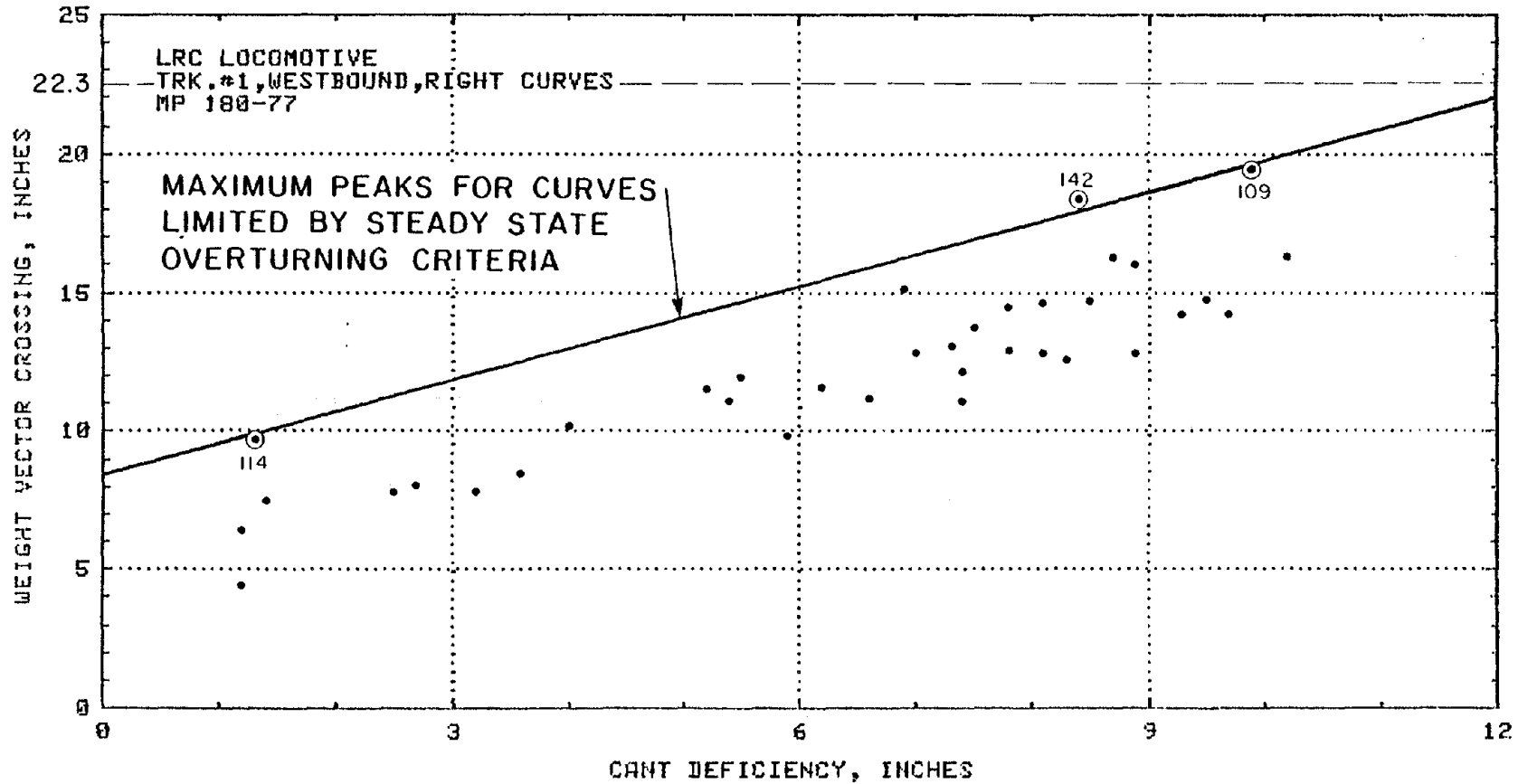


FIGURE 6-13

COMPARISON OF PEAK MEASUREMENTS OF WEIGHT VECTOR INTERCEPT FOR CURVES IN NEC TEST ZONE TO MAXIMUM PEAKS FOR CURVES LIMITED BY STEADY STATE OVERTURNING CRITERIA.

There are three categories of curves listed in Tables 6-1 and 6-2. Curves in the first category were tested at very high speed relative to a low cant deficiency because of their low curvature. Considerable side to side dynamic weight transfer occurs at moderate track geometry deviations because of the speed. However the 110 mph speed limit prevents operation at cant deficiencies high enough to produce critical weight vector intercept peaks. Although the coach vector intercept limit is not reached below 110 mph at curve 129E, it causes an extraordinary amount of transient weight transfer at a mere 2.4 inches cant deficiency. The curve does not appear to have geometry perturbations, but rather it is the first of a pair of mild "S" curves taken at full speed. The effect is much more pronounced on the servo-tilting coach than on the conventional locomotive. Many of the curves in all categories may be limited in speed by braking and accelerating rates from stations and slow curves, but only the overturning criteria and the maximum NEC track speed are considered for a worst case evaluation of the effect of track condition on overturning safety.

Curves of the second category have switches or undergrade bridges as specific unusual features in their immediate vicinity. The discontinuity in track stiffness may promote perturbations and hinder maintenance of such sites. Switches are associated with particularly severe disturbances in the AEM-7 test zone south of New York (Section 8.0), and the most severe curve for the LRC Coach was 142 which included a switch. The transient overturning criteria limits the coach to less than 7 inches cant deficiency in this curve. Curve 101 which includes an undergrade bridge also causes the coach to exceed the transient criteria slightly but nearly nine inches of cant deficiency is still permitted. The locomotive is also limited by the transient overturning criteria in curve 142 and in curve 99 containing another switch. The exceedances are so slight, however, that over 11 inches of cant deficiency is still permitted.

Curves of the third category are those which have no unusual features identified on the track chart but at which the curving speed of a vehicle would be limited by transient side to side weight transfer. The peak weight vector intercept measurements of the coach and the locomotive were disproportionately high at curves 78 and 75A respectively, but cant deficiencies of over 8 inches for the coach and over 10 inches for the locomotive were still permitted. Other curves limited by steady state overturning but having relatively high peaks are also listed in the tables. The list indicates that the banking coach and the conventional locomotive respond adversely to different types of perturbations.

The steady state overturning criteria are more restrictive than the transient criteria for the LRC coach and locomotive in all

TABLE 6-1
 CURVES AT WHICH THE LRC COACH PEAK VECTOR WEIGHT
 INTERCEPT WAS HIGH IN RELATION TO CANT DEFICIENCY

Curve Number	Peak Vector Intercept (inches)	Test Conditions		Estimated Maximum Cant Defi- ciency (in)	Limiting* Factor	Unusual* Features
		Speed (mph)	Cant Deficiency (inches)			
Category I - Curves (w/o unusual features) limited by maximum track speed.						
128E	13.3	110.2	5.8	5.8	110 mph	-
129E	17.7	110.2	2.4	2.4	110 mph	-
136E	12.6	96.9	4.6	6.6	110 mph	-
Category II - Curves with unusual features						
101E	19.1	80.3	9.5	8.8	TOC	UGB
101W	17.1	80.8	8.9	9.3	SSOC	UGB
109W	18.3	83.3	9.9	9.3	SSOC	UGB
137E	15.5	95.7	6.4	9.3	SSOC	UGB
142W	19.3	75.2	8.4	6.8	TOC	SC
Category III - Curves (w/o unusual features) limited by vehicle overturning safety						
78W	7.9	79.5	1.2	8.7	TOC	-
89W	10.8	67.6	1.9	9.3	SSOC	-
108E	17.1	82.4	8.9	9.3	SSOC	-

*Legend: UGB - Undergrade Bridge
 SC - Switch in Curve
 TOC - Transient Vehicle Overturning Criteria
 SSOC - Steady State Vehicle Overturning Criteria

TABLE 6-2
 CURVES AT WHICH THE LRC LOCOMOTIVE PEAK WEIGHT VECTOR
 INTERCEPT WAS HIGH IN RELATION TO CANT DEFICIENCY

<u>Curve Number</u>	<u>Peak Vector Intercept (inches)</u>	<u>Test Conditions</u>		<u>Estimated Maximum Cant Deficiency (in)</u>	<u>Limiting* Factor</u>	<u>Unusual* Features</u>
		<u>Speed (mph)</u>	<u>Cant Deficiency (inches)</u>			
Category I - Curves (w/o unusual features) limited by maximum track speed.						
130E	12.6	110.2	2.6	2.6	110 mph	-
Category II - Curves with unusual features.						
99E	14.0	73.8	4.2	11.7	TOC	SC
105W	12.7	81.8	4.2	12.2	SSOC	UGB
142W	18.4	75.2	8.4	11.9	TOC	SC
Category III - Curves (w/o unusual features) limited by vehicle overturning safety						
75AE	20.3	76.8	9.7	10.6	TOC	-

*Legend: UGB - Undergrade Bridge
 SC - Switch in Curve
 TOC - Transient Vehicle Overturning Criteria
 SSOC - Steady State Vehicle Overturning Criteria

but a few unusually harsh curves. Of the curves first limited by overturning safety, the coach would be limited to less than 8 inches cant deficiency at only one, and it had an alignment perturbation near a switch. The rate of change of alignment appears to be quite severe at about 2 inches per 30 feet of travel but the deviation of alignment from uniformity satisfies the class four track safety standards. In this curve, the transient overturning criteria would limit the coach to 70 mph while the track classification would permit 80 mph. The steady state overturning criteria permits about 12 inches of cant deficiency for the locomotive, and the transient criteria did not limit it below 10 1/2 inches at any test curve. The coach performance clearly sets the limits for the LRC train with respect to overturning safety.

6.2 RAIL ROLLOVER

Rail rollover is related to peak truck side L/V ratio. The peak rather than steady-state should be considered because this mode of derailment may be rapid and pulses of relatively low energy are capable of turning the rail whereas a very great amount of energy is required to overturn a vehicle with its great inertia.

A conservative rail rollover criteria should assume zero pull out resistance of the fasteners. Only the geometry of the rail section and the torsional stiffness of the surrounding rail should be considered for a general safety criteria.

Section 5.0 describes rail rollover criteria based on the above two factors. It can be expressed as: $\max \text{ truck side } L/V = 0.5 + 2300/P_w$, where P_w is the single wheel nominal vertical load. This criteria may underestimate the effect of rail section geometry and overestimate the effect of torsional stiffness of the surrounding rail but it appears to be based on the best available information. It should be interpreted as a restriction based on measurements having time duration of more than 50 milliseconds. Higher measurements are permitted for lesser time durations.

For the LRC Locomotive, $P_w \approx 31,000$ lb and a limiting value of 0.57 should be compared to the peak measurements of truck side L/V ratio. It should be limited to 0.65 for a loaded coach with $P_w \approx 15,000$ lb. Figure 6-14 compares the measurements taken at the right and left test curves to the criteria. At these relatively smooth curves, the measurements were far below the critical levels. Truck L/V ratio measured at the high rail side of the vehicles did not increase rapidly with cant deficiency due to the moderating influence of the vertical load transfer, and the performance was virtually identical for right and left curving.

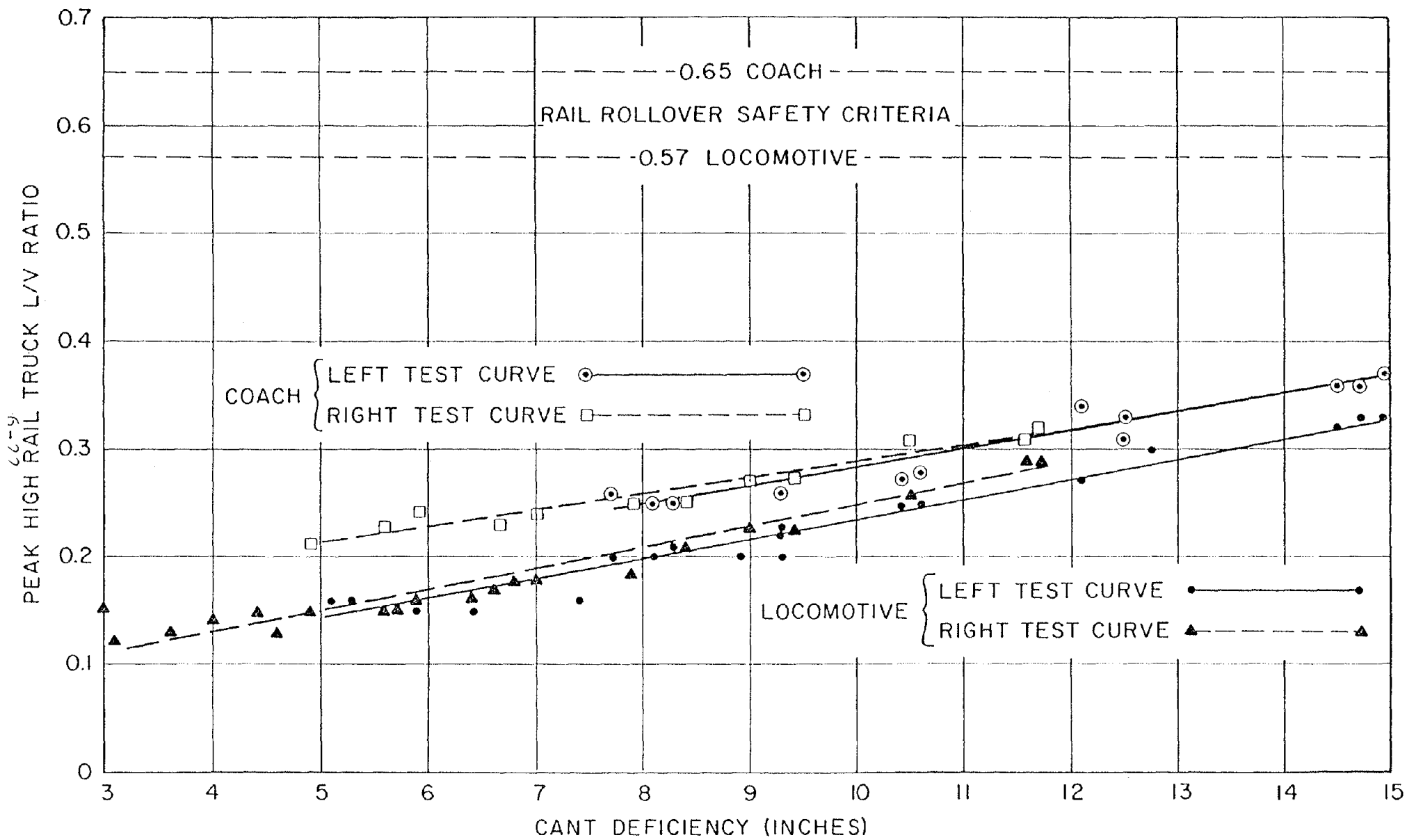


FIGURE 6-14

PEAK TRUCK L/V RATIOS OF THE LRC VEHICLES AS FUNCTIONS OF CANT DEFICIENCY MEASURED AT RIGHT AND LEFT TEST CURVES

Truck side L/V ratio observed at over one hundred curves in the NEC test zones remained low relative to the critical levels. The locomotive measurements were less than 0.35 and the coach measurements were less than 0.40 at all the curves. Cant deficiencies up to 11 inches were achieved in the test zone.

6.3 LATERAL TRACK SHIFT

Although the inertia and pulse energy requirement to move the track structure laterally is much greater than that required for rail rotation, the peak force levels of about 50ms duration provide a conservative measure of safety. The use of a single wheel force rather than axle force introduces another estimate on the conservative side. The net axle force which moves the track is usually less than a single wheel peak force because the wheel forces on the same axle tend to oppose one another.

The safety criteria discussed in Section 5.0 assumes compacted ballast for full operational cant deficiency, and it allows for the force of crosswinds encountered in service. For the conservative assumption of wood ties, the criteria can be expressed as follows:

$$F_{\max} = 1 - \frac{A\Delta\theta}{22320} (1 + .458D) \quad .7P + 6600 - (1.28 \times 10^{-3}SV^2)$$

A = rail cross section area, in²

$\Delta\theta$ = Max temperature change after rail installation, °F

D = track curvature, degrees

P = vertical axle load, lbs

S = lateral surface area of vehicle, ft²

V = lateral wind speed, mph

and it is assumed that a single axle bears half the entire wind load. For typical NEC conditions of 140 lb rail (A = 13.8 in²), $\Delta\theta$ max of 70°F and D max of 4°.

$$F_{\max} = .61P + 5800 - 1.28 \times 10^{-3}SV^2$$

For the LRC locomotive axle load of 62,700 lb and an allowance for 56 mph crosswinds the maximum permissible lateral axle force is 41,300 lb. The maximum truck lateral force for a two axle

truck should be limited to only 1.4 times the single axle maximum lateral force because fewer than twice the number of ties support the lateral force. The lateral track shift criteria permits a maximum truck lateral force of 58,900 lb allowing for one half of the 56 mph crosswind body side load at each truck. For the unloaded coach, axle load 26,400 lb, the maximum permissible lateral axle force is 18,200 lb, and the maximum truck lateral force is 26,900 lb.

Figure 6-15 compares the high rail lead wheel and truck side peak lateral force measurements of the LRC vehicles on the left test curve to the rail rollover criteria. Both measurements remain at little more than half the critical levels at 15 inches of cant deficiency on the relatively smooth test curve. The peak measurements of truck side lateral force taken in the NEC test zone, including rougher curves, were always well below the safety criteria for both vehicles. The highest peak measurements at over 120 curves between New Haven and Boston were 31,100 lb for the locomotive and 16,700 for the coach. Both were recorded on curve 126 eastbound at 11 inches of cant deficiency and 104 mph. These measurements also were little more than half the critical levels, indicating that safety against lateral track shift does not limit the cant deficiency of the LRC train.

6.4 WHEEL CLIMB

The most appropriate criteria of safety concerning wheel climb for comparison to the test results of the LRC vehicles is that used by Amtrak in its AEM-7 acceptance specification. This criteria takes into account the AAR flange angle and it appears to have been based on conservative judgments. It states that the wheel (L/V) ratio must be less than $0.056/T^{-0.927}$ where T is the duration of the peak level in seconds, and that the maximum wheel L/V ratio for peaks of duration greater than 50 milliseconds is 0.90.

Figure 6-16 shows that the peak wheel L/V ratios of both the coach and locomotive are very low with respect to the wheel climb safety criteria on unperturbed curves. It also shows that wheel L/V ratio is slightly less sensitive than truck L/V to increases in cant deficiency indicating that the rear wheel bears a greater portion of the high rail lateral force as cant deficiency increases. The greater rear wheel lateral force suggests the possible benefit of a reduction in angle of attack at higher cant deficiencies.

Truck side L/V was recorded at over one hundred curves in the NEC test zone. The highest absolute measurements were 0.34 for the locomotive and 0.40 for the coach. Both measurements were taken at 11 inches cant deficiency on curve 126 eastbound. The highest

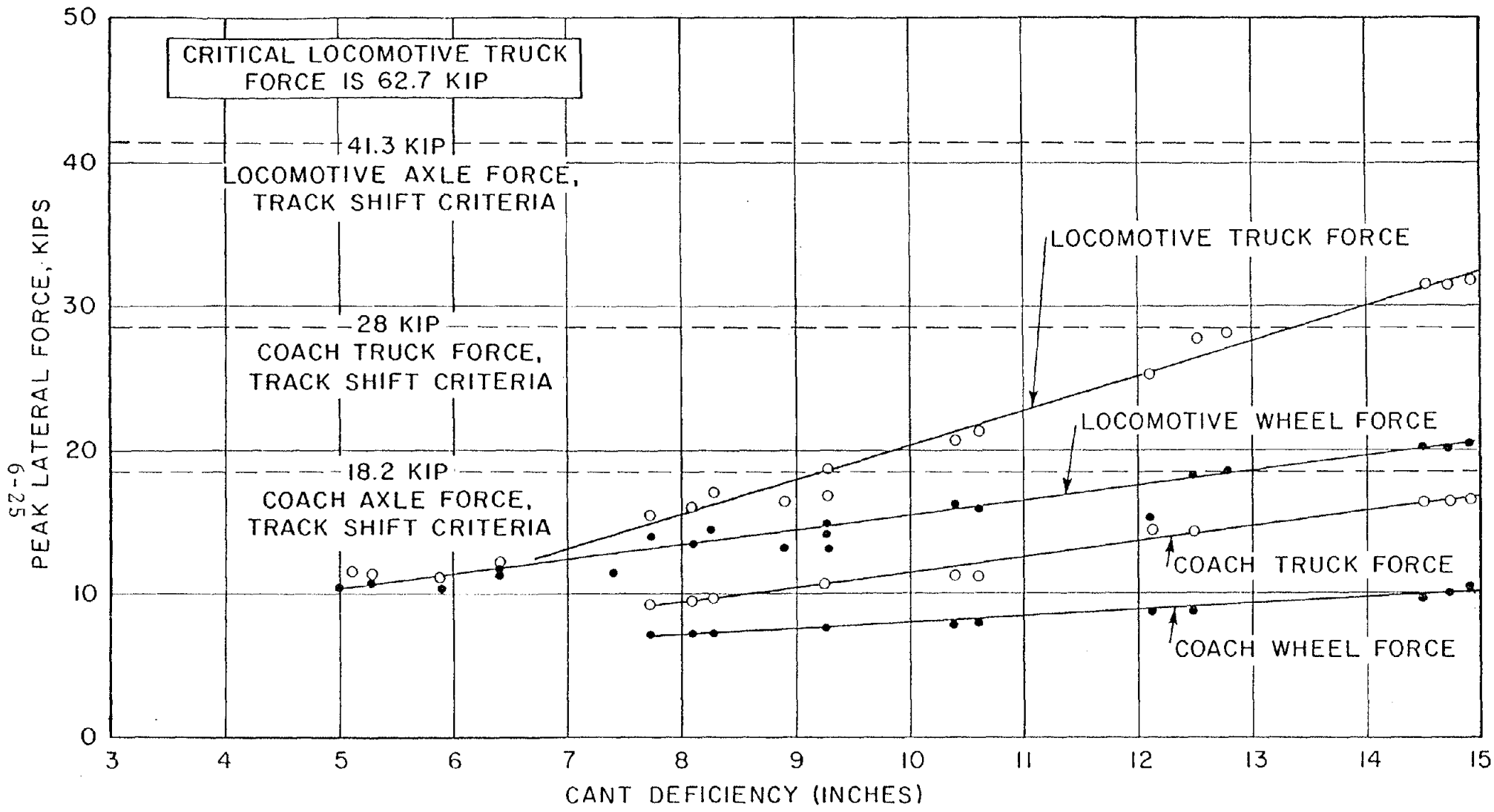


FIGURE 6-15

COMPARISON OF PEAK LATERAL FORCE MEASUREMENTS OF LEAD WHEEL AND TRUCK SIDE OF LRC VEHICLES TO TRACK SHIFT CRITERIA

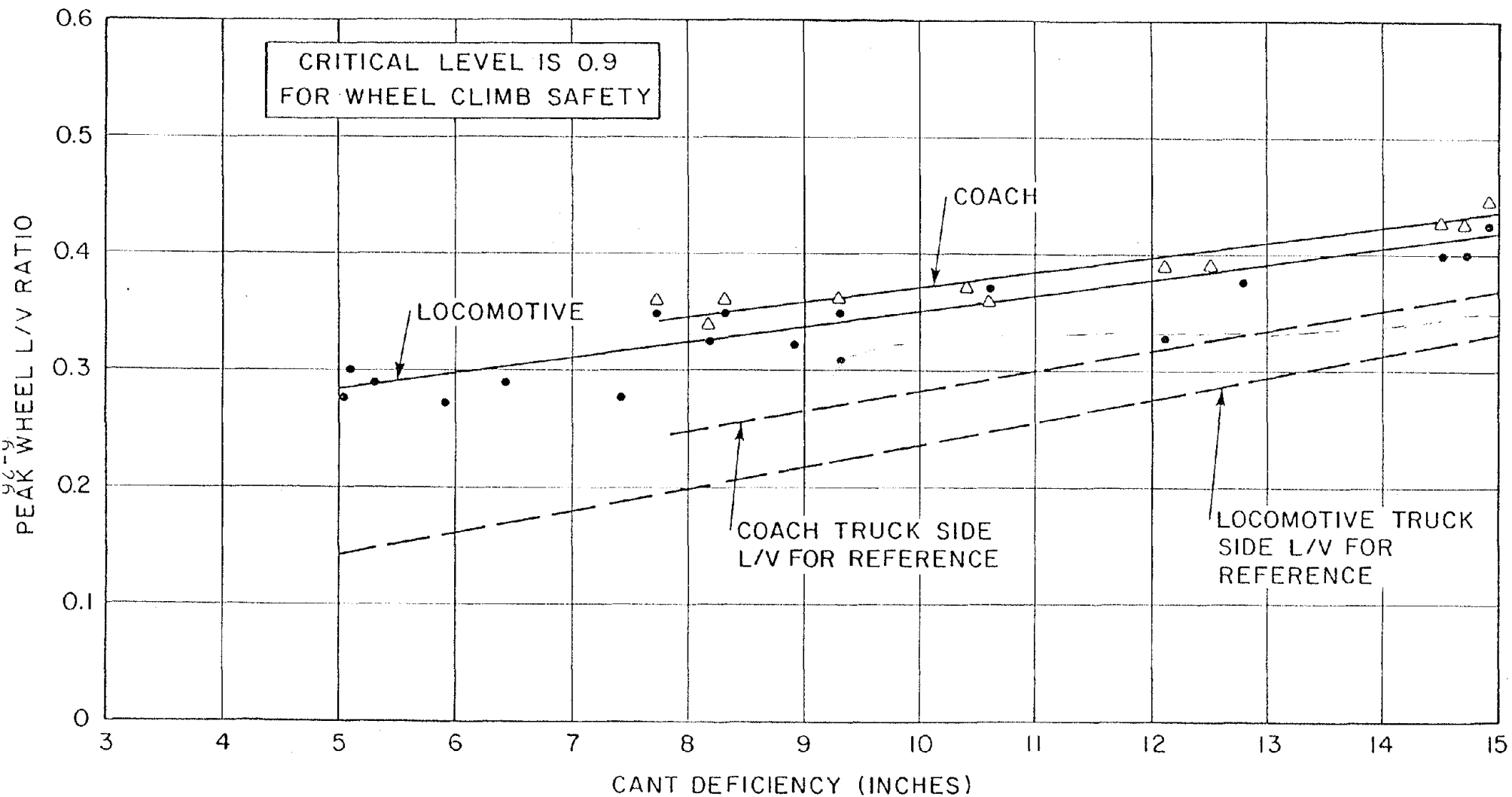


FIGURE 6-16

PEAK WHEEL L/V RATIO OF LRC VEHICLES AS A FUNCTION OF CANT DEFICIENCY AT THE MORE SEVERE OF RIGHT AND LEFT TEST CURVES

measurements relative to cant deficiency were on curve 90 west-bound at 5 1/2 inches cant deficiency. The truck side L/V ratios were 0.32 for the locomotive and 0.39 for the coach. Even under the assumption that the lead wheel bears the entire lateral load (which is unrealistically conservative at high cant deficiency) critical wheel L/V ratios can not be projected at less than 13 inches cant deficiency on the most severe curve tested. The LRC train is not limited by wheel climb safety criteria.

6.5 RIDE COMFORT

Section 5.0 includes a variety of criteria for lateral acceleration used by organizations throughout the world as indices for ride comfort evaluation. The most commonly recognized standards in the U.S. are the AAR recommendations of 0.1g maximum steady state and 0.03g/sec maximum "jerk". The least restrictive standards are those of SNCF which permit 0.15g and 0.10g/sec respectively. The JNR has an additional standard of $\pm 0.08g$ maximum carbody "vibration" which pertains to the transient response of a carbody tilt system upon entering and exiting a curve.

When the AAR study was undertaken in the early 1950's, coach suspensions were designed such that large body roll angles occurred in curving. The component of gravitational acceleration in the plane of the coach floor added substantially to the centrifugal acceleration as the coach body rolled toward the outside of the curve. At three inches of cant deficiency, the body roll of contemporary coaches was usually sufficient to cause a total of 0.1g lateral acceleration in the plane of the floor.

Figure 6-17 compares the banking coach and conventional locomotive to a hypothetical rigid suspension vehicle with zero body roll. The data for the left and right test curves is given, and the bold lines estimate the mean characteristics of the vehicles removing the effect of asymmetry. The LRC locomotive reaches the AAR coach ride comfort criteria at about 4 1/2 inches of cant deficiency while a vehicle with zero roll would reach it at 6 inches cant deficiency. About 2 1/2 degrees of body roll is indicated at 9 inches cant deficiency. In contrast, the banking system of the coach provides "negative" body roll to maintain lateral acceleration at about one half the AAR comfort limit until the banking stops are reached at around 7 1/2 inches cant deficiency. The steady state lateral acceleration then increases to the AAR limit at about 9 1/2 inch cant deficiency and to the zero roll equivalent at over 15 inches cant deficiency.

6.6 MAXIMUM OPERATIONAL CANT DEFICIENCY

The operational cant deficiency of the LRC train is first limited by the coach overturning safety criteria. The critical level dictated by the steady state overturning safety criteria is

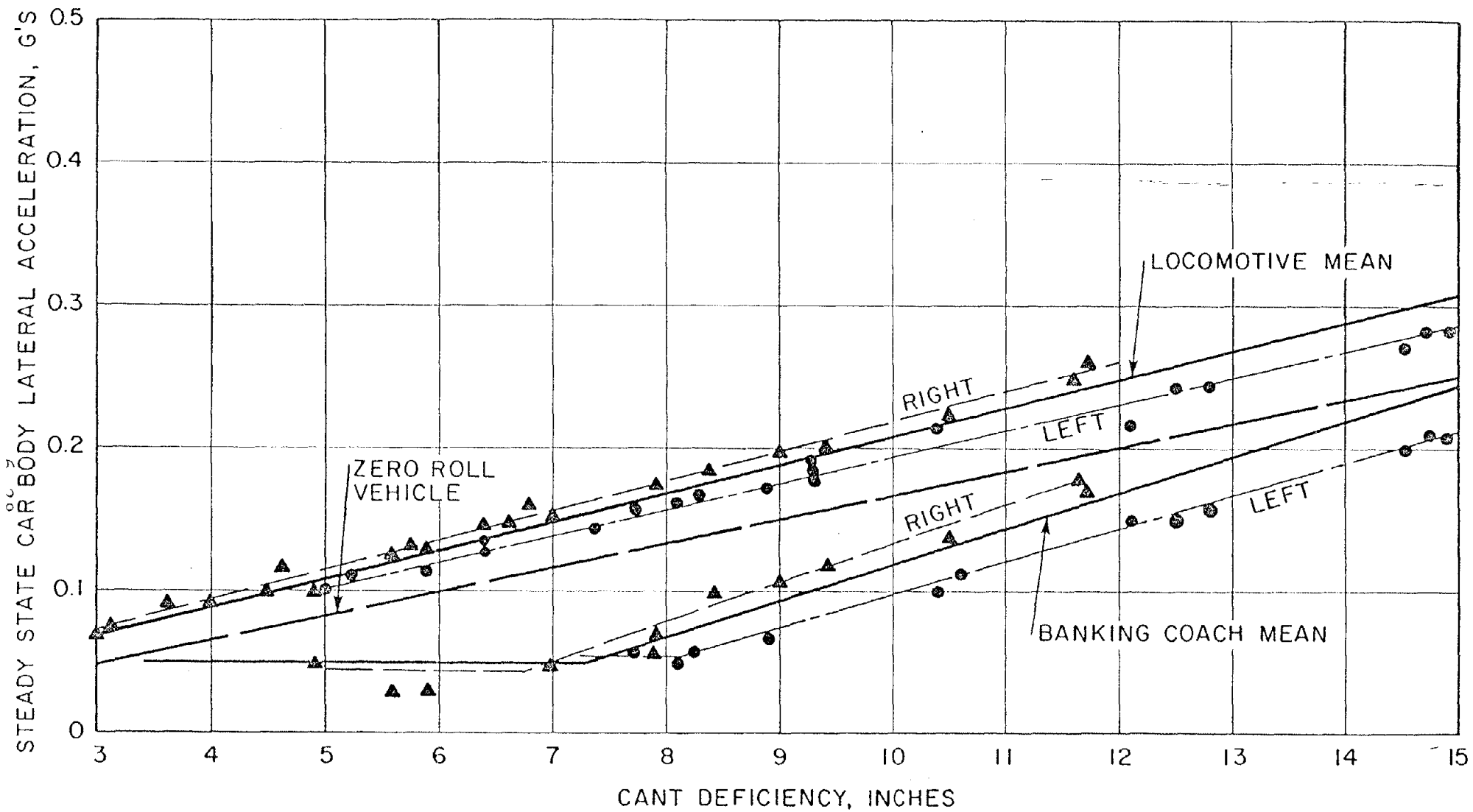


FIGURE 6-17

STEADY STATE LATERAL ACCELERATION OF LRC VEHICLES COMPARED TO A VEHICLE WITH ZERO ROLL ANGLE

reached at 9 1/4 inches of cant deficiency allowing for a simultaneous lateral wind of 56 mph. The measurements indicating safety against rail rollover, lateral track shift and wheel climb are well below critical levels for both vehicles at this cant deficiency. However, the safety criteria against vehicle overturning based on transient measurements sets a lower limit of cant deficiency at a few perturbed curves in the New Haven - Providence test zone. Most of the exceptionable curves identified by the test data include an unusual feature such as a switch or undergrade bridge. At the worst curve, limited by overturning safety rather than by the maximum track speed, the safety limit would be exceeded above about 6 1/2 inches of cant deficiency. One curve without special track work was also limited at about 8 1/2 inches of cant deficiency by the transient vehicle overturning safety criteria.

It is not feasible to limit the LRC train by the worst perturbation in the test zone. Steady state overturning safety provided the first limit at about 9 inches cant deficiency for "normal" curves. The abnormal curves, which may include others not measured in this test, should be identified individually. Many may be limited by other factors such as acceleration and braking distances or proximity to stations. The remaining curves should either be repaired if practical or be given special speed restrictions. The measurements indicate safe operation at up to eight inches of cant deficiency at all curves without special track work. The identification and repair of a few problem curves could increase the safe cant deficiency to 9 inches. The banking system enables the LRC coach to operate below the AAR ride comfort criteria for steady state lateral acceleration at the maximum safe cant deficiency.

6.7 COMPARISON OF TEST RESULTS TO SIMPLE QUASISTATIC PREDICTIONS

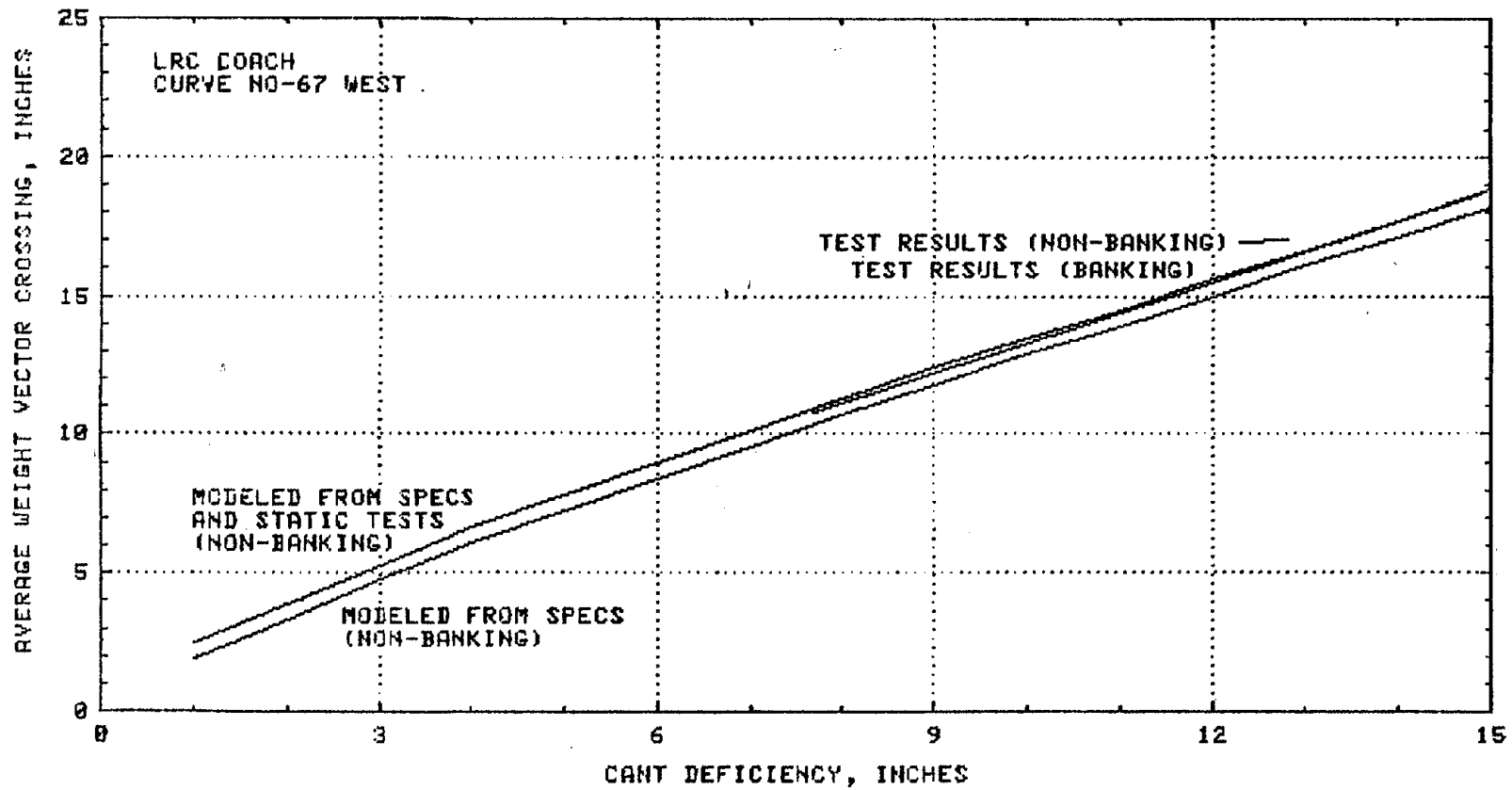
A simple quasistatic model described in Appendix B was formulated to predict several steady state measurements. The published specifications of the vehicles and the results of static tests to estimate weight distribution and suspension spring rates as installed, which were used in these calculations, are listed in Appendix C. Such predictions can be useful in estimating the performance potential of vehicles which are limited by steady state criteria of overturning safety and lateral acceleration ride quality. Safety and ride quality considerations which depend on knowledge of peak values and of transient distributions of wheel forces are not likely to be satisfied by modeling because of the range of complex, interactive, and non-obvious track influences in service, which were sampled experimentally in the large test zone. Although steady state overturning limits the LRC train speed in most curves, lower limits were indicated for some curves based on transient measurements.

The coach was modeled without considering the banking system since the c.g. was located close to the center of rotation. Figures 6-18 and 6-19 show very close agreements between the predicted weight vector intercepts and the test data with banking. Figure 6-18 also shows the results of two runs without banking which confirm that body tilt does not alter weight distribution. Figures 6-20 and 6-21 illustrate the benefit of banking in reducing steady state lateral acceleration from the non-banking predictions. The non-banking tests in Figure 6-20 validate the predictions. The high rail side truck lateral force measurements in Figures 6-22 and 6-23 are slightly lower than the predictions for the whole truck but show good general agreement.

The weight vector intercept measurements of the locomotive are also in excellent agreement with the predictions in Figures 6-24 and 6-25. The lateral accelerations shown in Figures 6-26 and 6-27 are slightly below the prediction, suggesting lower body roll. The truck side lateral force measurements are considerably below the prediction for the whole truck shown in Figures 6-28 and 6-29.

FIGURE 6-18

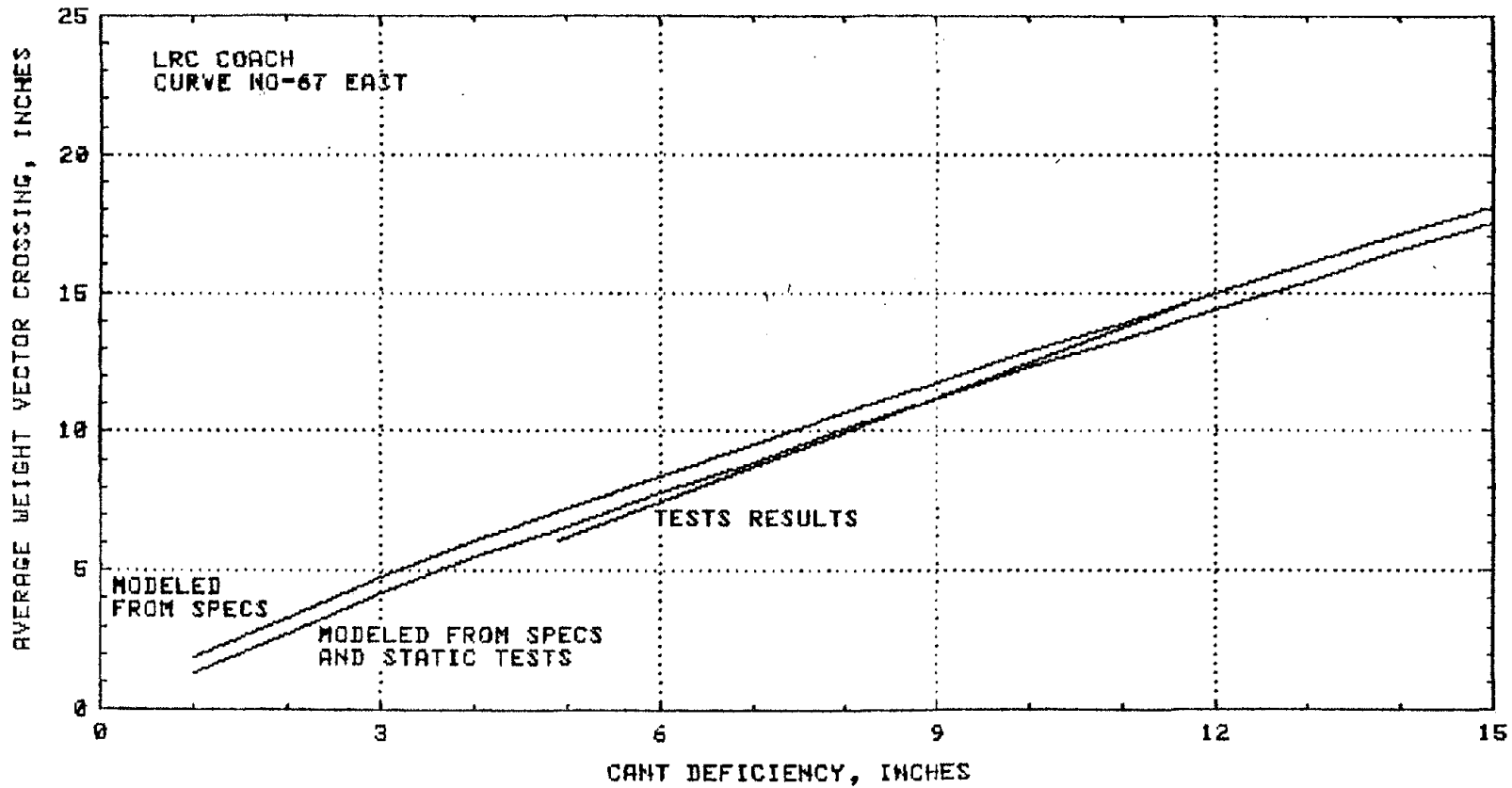
COMPARISON OF STEADY STATE WEIGHT VECTOR INTERCEPT PREDICTIONS TO TEST RESULTS FOR LRC COACH IN LEFT HAND CURVE



6-31

FIGURE 6-19

COMPARISON OF STEADY STATE WEIGHT VECTOR INTERCEPT PREDICTIONS TO TEST RESULTS FOR LRC COACH IN RIGHT HAND CURVE



6-32

FIGURE 6-20

COMPARISON OF STEADY STATE CAR BODY LATERAL ACCELERATION PREDICTIONS TO TEST RESULTS FOR LRC COACH IN LEFT HAND CURVE

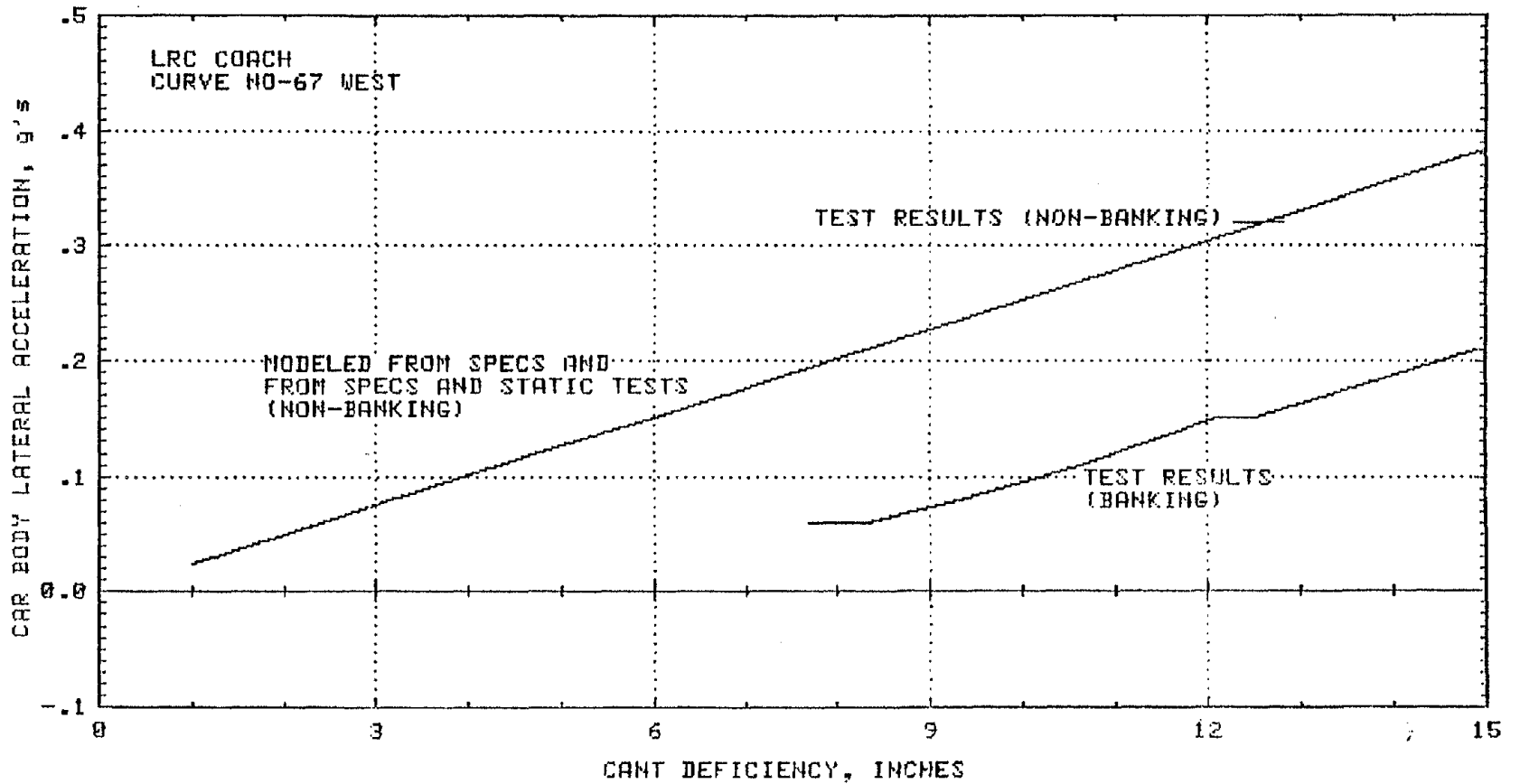


FIGURE 6-21

COMPARISON OF STEADY STATE CAR BODY LATERAL ACCELERATION PREDICTIONS TO TEST RESULTS FOR LRC COACH IN RIGHT HAND CURVE

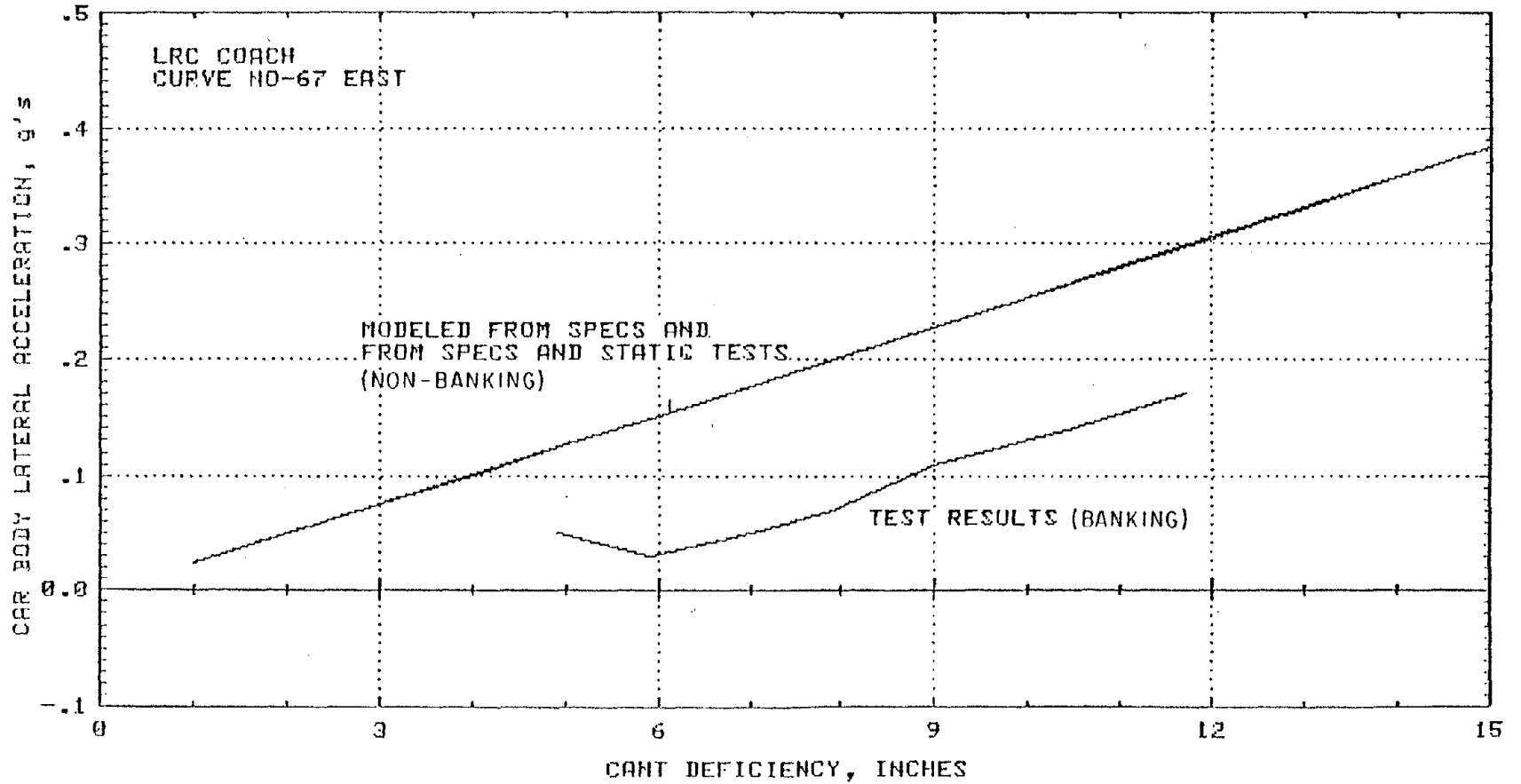


FIGURE 6-22

COMPARISON OF STEADY STATE NET TRUCK LATERAL FORCE PREDICTIONS TO TEST MEASUREMENTS OF HIGH RAIL SIDE TRUCK LATERAL FORCE FOR LRC COACH IN LEFT HAND CURVE

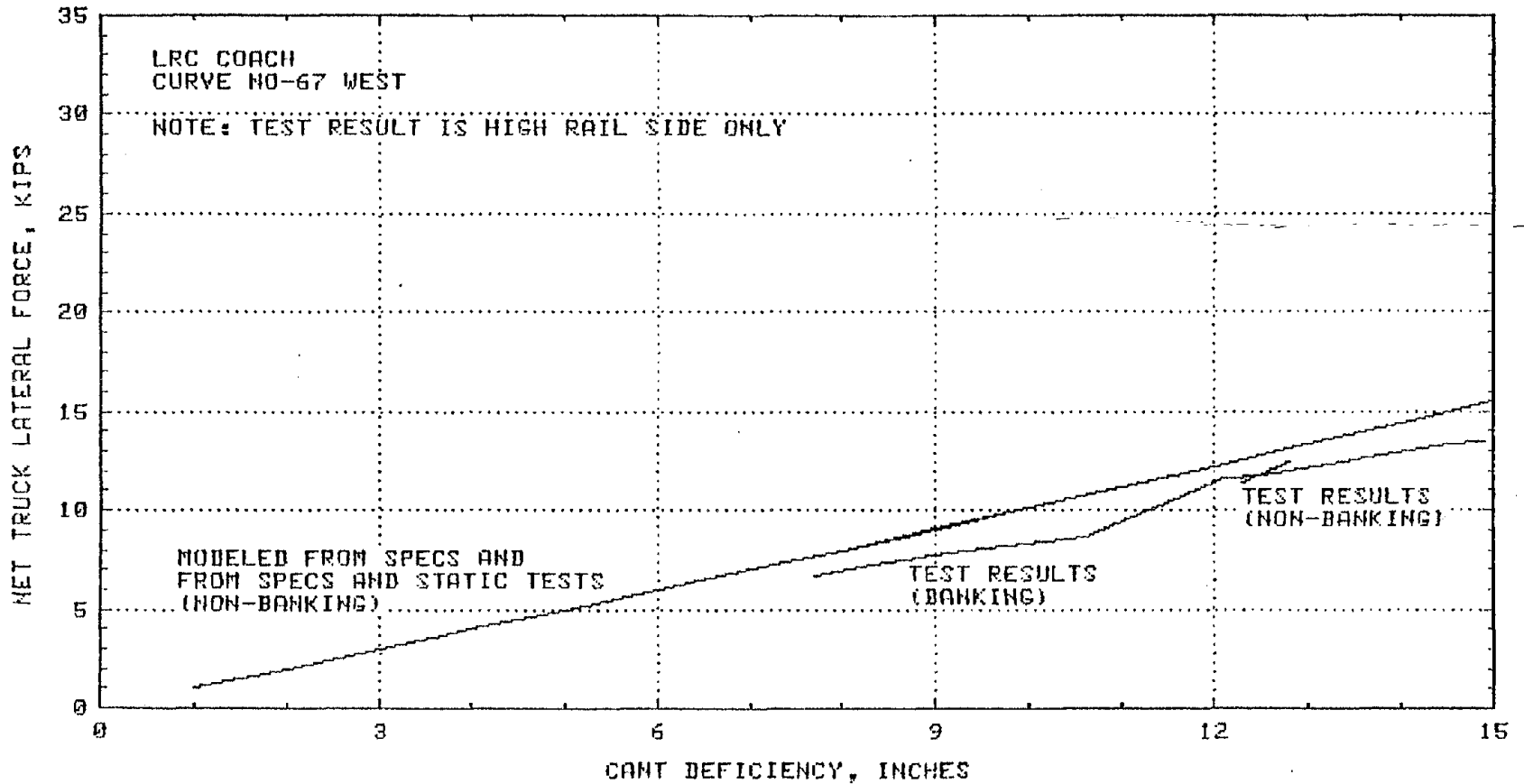
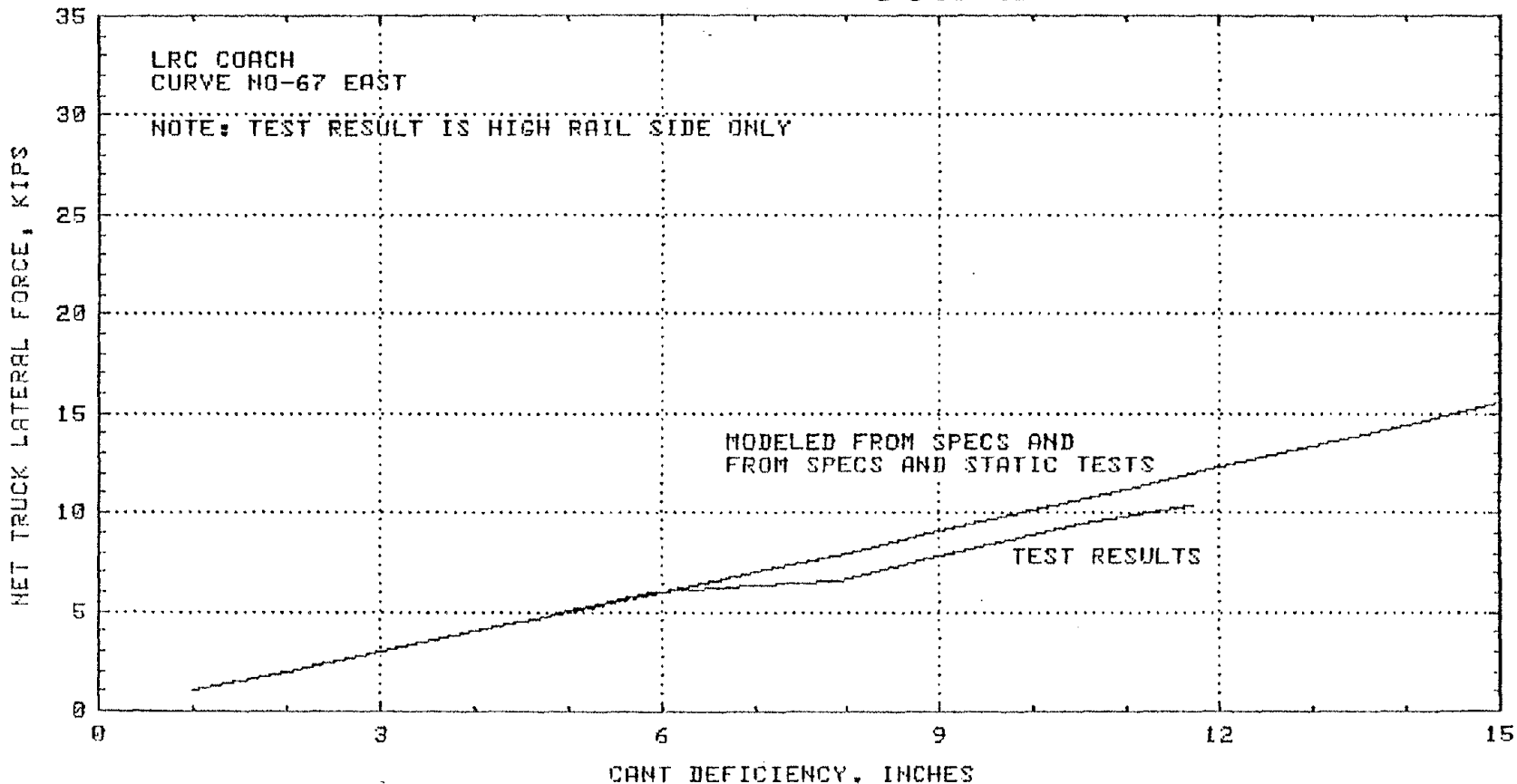


FIGURE 6-23

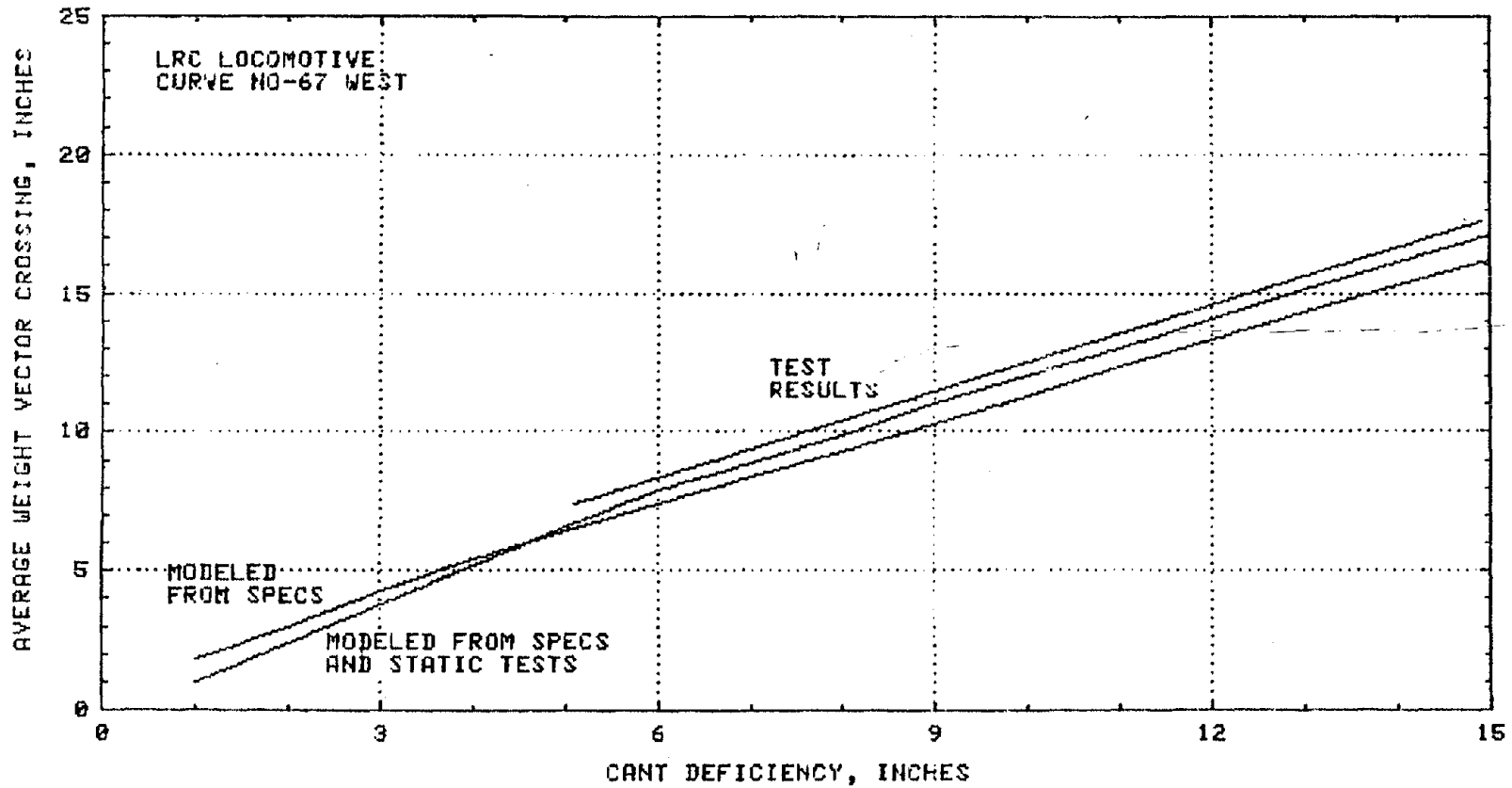
COMPARISON OF STEADY STATE NET TRUCK LATERAL FORCE PREDICTIONS TO TEST MEASUREMENTS OF HIGH RAIL SIDE TRUCK LATERAL FORCE FOR LRC COACH IN RIGHT HAND CURVE



6-36

FIGURE 6-24

COMPARISON OF STEADY STATE WEIGHT VECTOR INTERCEPT PREDICTIONS TO TEST RESULTS FOR LRC LOCOMOTIVE IN LEFT HAND CURVE



6-37

FIGURE 6-25

COMPARISON OF STEADY STATE WEIGHT VECTOR INTERCEPT PREDICTIONS TO TEST RESULTS FOR LRC LOCOMOTIVE IN RIGHT HAND CURVE

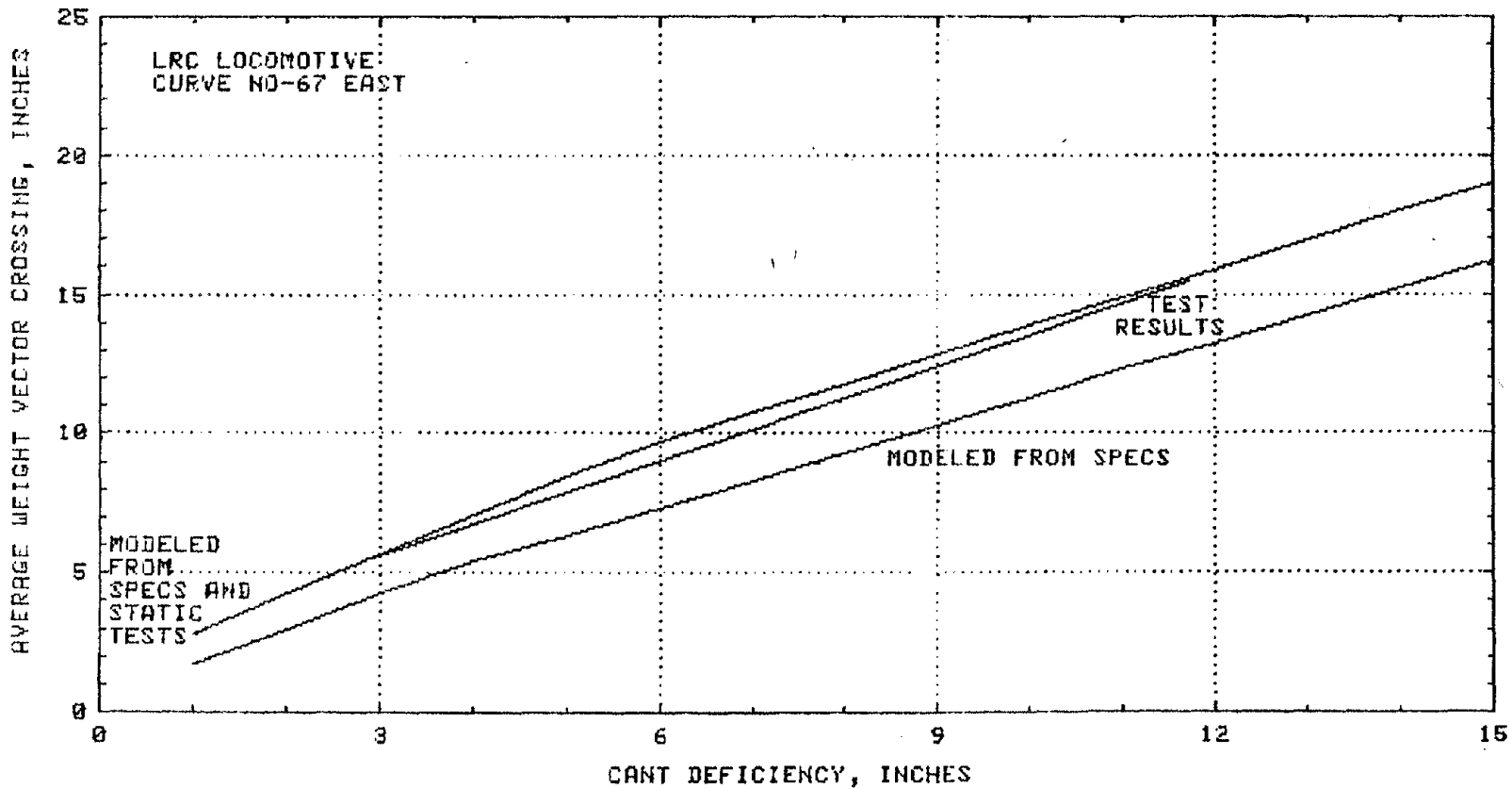


FIGURE 6-26

COMPARISON OF STEADY STATE CAR BODY LATERAL ACCELERATION PREDICTIONS TO TEST RESULTS FOR LRC LOCOMOTIVE IN LEFT HAND CURVE

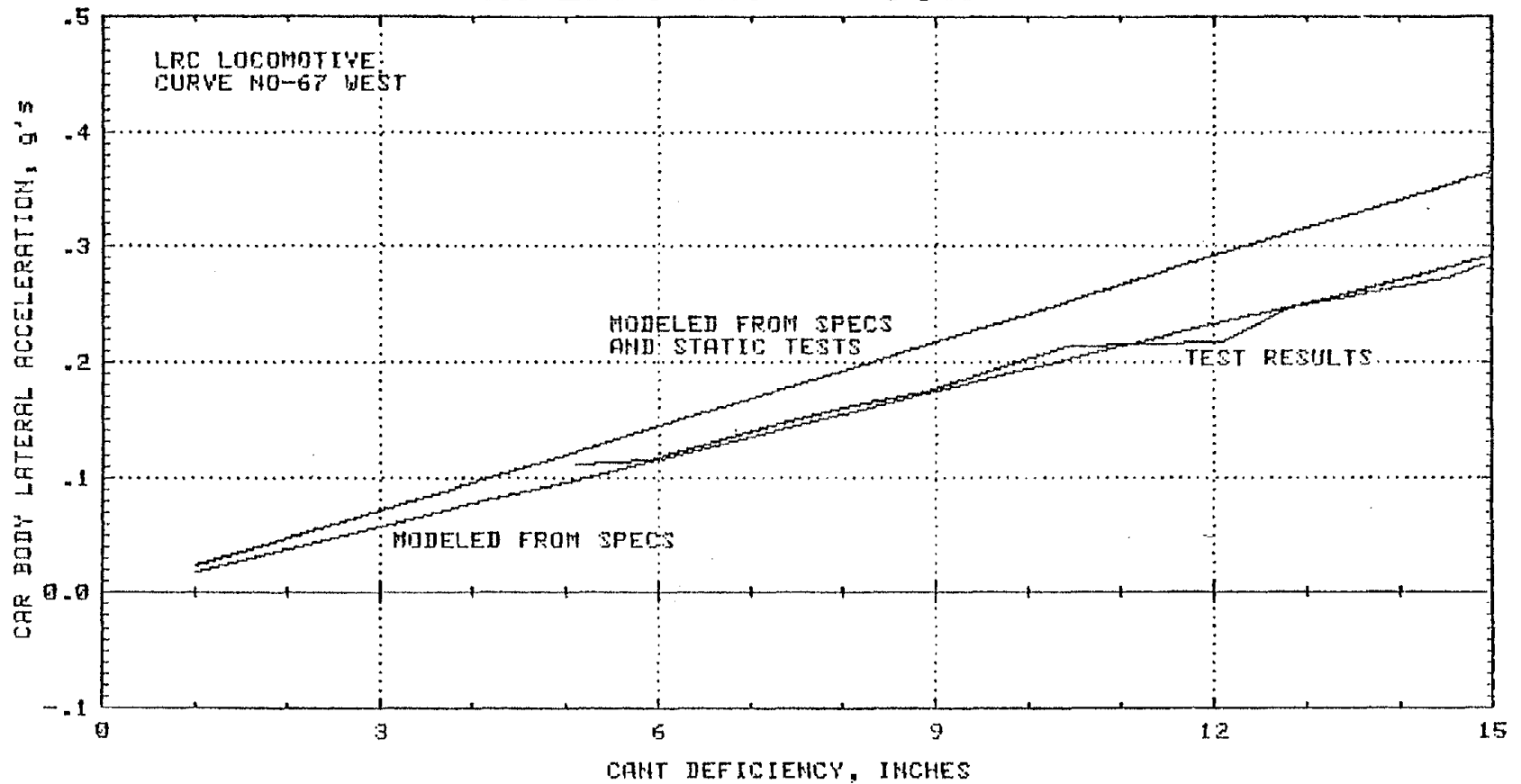


FIGURE 6-27

COMPARISON OF STEADY STATE CAR BODY LATERAL ACCELERATION PREDICTIONS TO TEST RESULTS FOR LRC LOCOMOTIVE IN RIGHT HAND CURVE

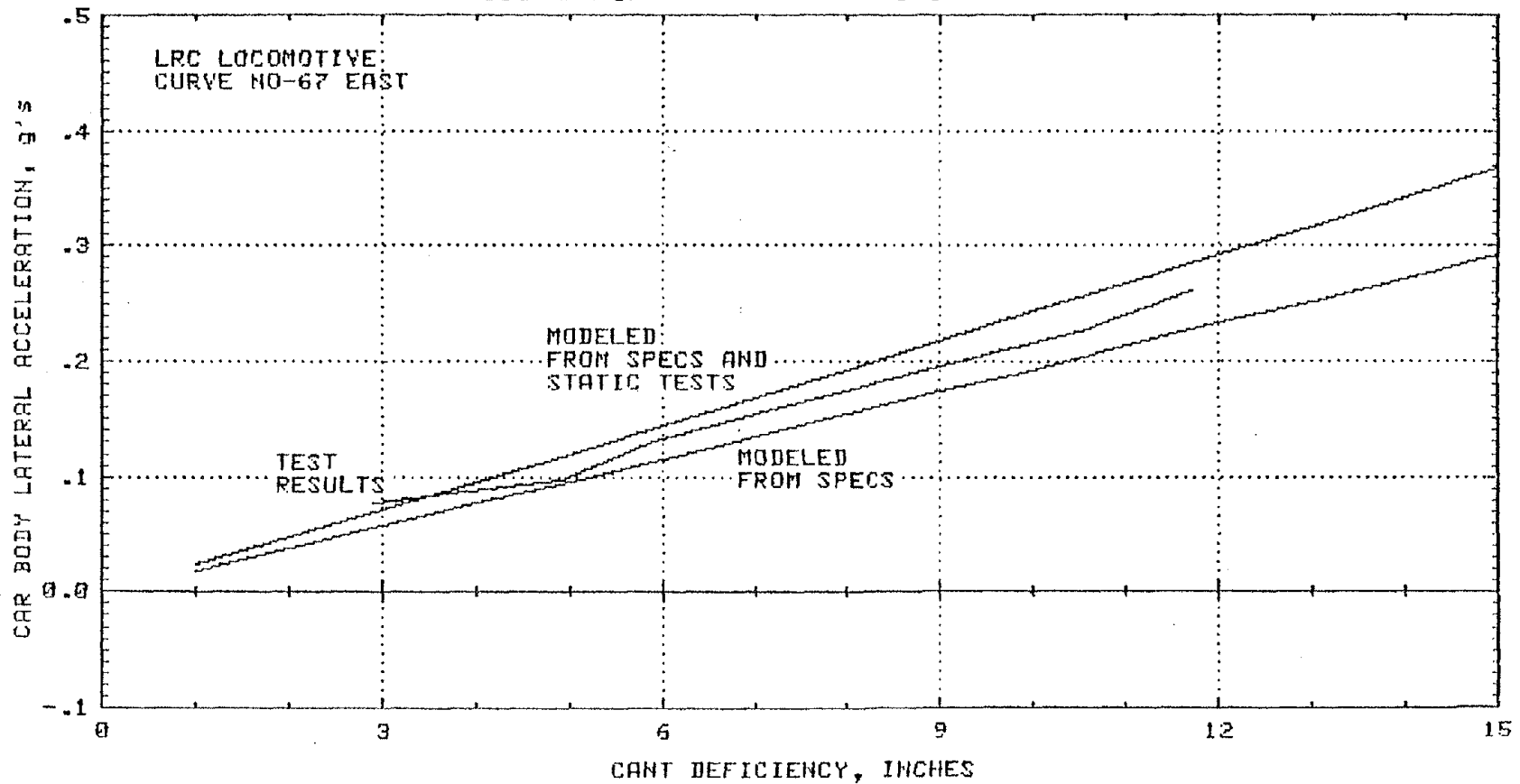
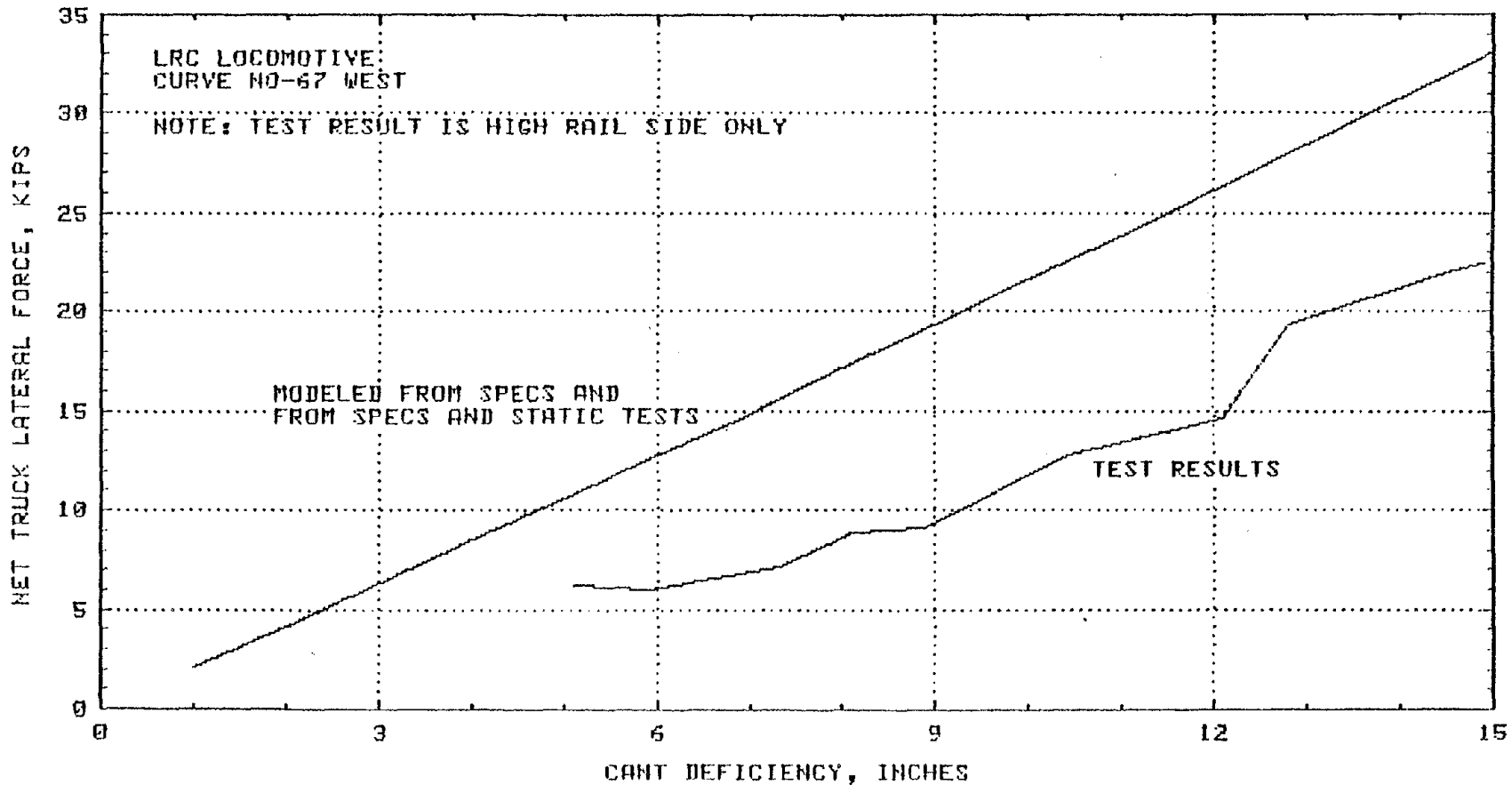


FIGURE 6-28

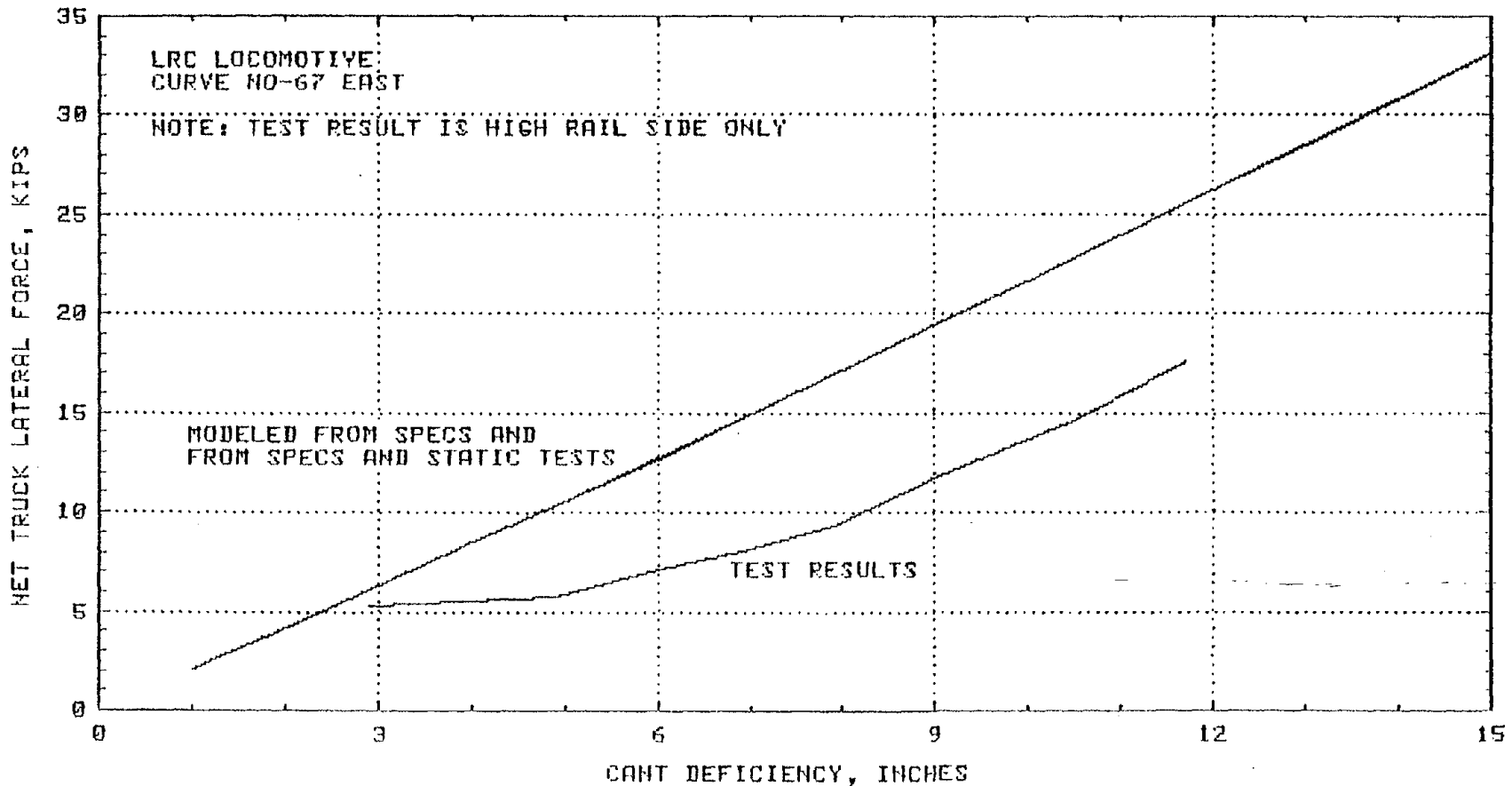
COMPARISON OF STEADY STATE NET TRUCK LATERAL FORCE PREDICTIONS TO TEST MEASUREMENTS OF HIGH RAIL SIDE TRUCK LATERAL FORCE FOR LRC LOCOMOTIVE IN LEFT HAND CURVE



6-41

FIGURE 6-29

COMPARISON OF STEADY STATE NET TRUCK LATERAL FORCE PREDICTIONS TO TEST MEASUREMENTS OF HIGH RAIL SIDE TRUCK LATERAL FORCE FOR LRC LOCOMOTIVE IN RIGHT HAND CURVE



6-42

7.0 RESULTS OF TESTING THE AMCOACH AT HIGH CANT DEFICIENCY

The Amcoach was tested in two modes. Repetitive runs at various speeds were made over two specific test curves, one left and one right. The steady state performance of the vehicle was determined on these carefully measured test curves. The second mode of testing was a series of runs over hundreds of miles of NEC track. The peak level measurements which depend on actual track irregularities were taken from these tests as well as from the repetitive curving tests. The safety criteria are discussed in detail in Section 5.0 and the data reduction techniques are covered in Section 3.5.

7.1 VEHICLE OVERTURNING

The vehicle overturning criteria used by the Japanese National Railway is the most comprehensive in the literature. It is appropriately conservative and includes separate criteria for peak and steady state measurements. It may be summarized, in terms of vector intercept, by the following two equations:

$$\begin{array}{l} \text{Steady State} \\ \text{Vector Intercept} \end{array} \leq 18 - (.0153V^2Sh_{cp}/W) \text{ inches}$$

and

$$\begin{array}{l} \text{Peak Vector} \\ \text{Intercept} \end{array} \leq 24 - (.0153V^2Sh_{cp}/w) \text{ inches}$$

where:

V is the lateral wind speed in mph

S is the lateral surface area of the vehicle in ft²

h_{cp} is the height of the center of wind pressure in ft

W is one half of the unloaded weight of the vehicle in pounds.

For the Amcoach:

$$S \approx 765 \text{ ft}^2$$

$$h_{cp} \approx 7.5 \text{ ft}$$

$$W = 52,200 \text{ lb}$$

The second term in the above equations is an allowance for the maximum detrimental effect of wind speed. The weight vector intercept specified by each criterion represents the maximum still air test measurement permitted for operating at the given wind speed. The above equations are graphed on Figure 7-1 which expresses the separate criteria appropriate for peak and steady state measurements as functions of the allowed wind speed.

7.1.1 WIND SPEED EFFECT

The overturning criteria are extremely sensitive to wind speed especially over 50 mph, and the operational cant deficiency should be chosen to allow for sudden unexpected lateral winds. However, the operational cant deficiency need not be limited by overturning considerations to include heedless operation in actual gales and hurricanes because the speed must be reduced to meet other special conditions such as reduced visibility or the danger of debris on the track. The operational cant deficiency chosen provides safe operation at the maximum wind speed corresponding to the 10 year mean recurrence intervals. This cant deficiency is sufficiently conservative to provide for safety during unexpected winds. The level of wind speed for locations along the NEC is greatest in Boston where it is 70 mph measured 30 ft above the ground (ref 24). Reference (24) also provides a factor to adjust wind speed measurement for other distances above ground level. At 15 feet above the ground the 10 year mean recurrence interval wind speed is $0.8 \times 70 \text{ mph} = 56 \text{ mph}$. The safe cant deficiency for crosswinds up to 56 mph must be chosen to limit weight vector intercept of the Amcoach to 12.8 inches steady and 18.8 inches peak when measured in still air as indicated in Figure 7-1. No more than 12.8 inches must be measured in a still air test so that vector intercept will remain less than 18 inches steady state (JNR criteria) in a 56 mph wind. Likewise, still air peaks less than 18.8 inches prevent peaks greater than 24 inches (JNR criteria) with maximum wind forces.

7.1.2 STEADY STATE MEASUREMENTS

Figure 7-2 gives steady state test results which relate weight vector intercept to cant deficiency. The weight distribution on the instrumented truck was offset from the geometric centerline about one inch to the left. Consequently, the weight vector intercept was expected to be greater for right hand curving as was confirmed. The test results for a right hand curve represent the worst case and should be used for comparison to safety criteria. The test data did not exceed the overturning safety criteria of 12.8 inches weight vector intercept; however, extrapolation is justified by the high degree of linearity measured between vector intercept and cant deficiency. The worst case test data indicate that operation at 8 inches of cant deficiency

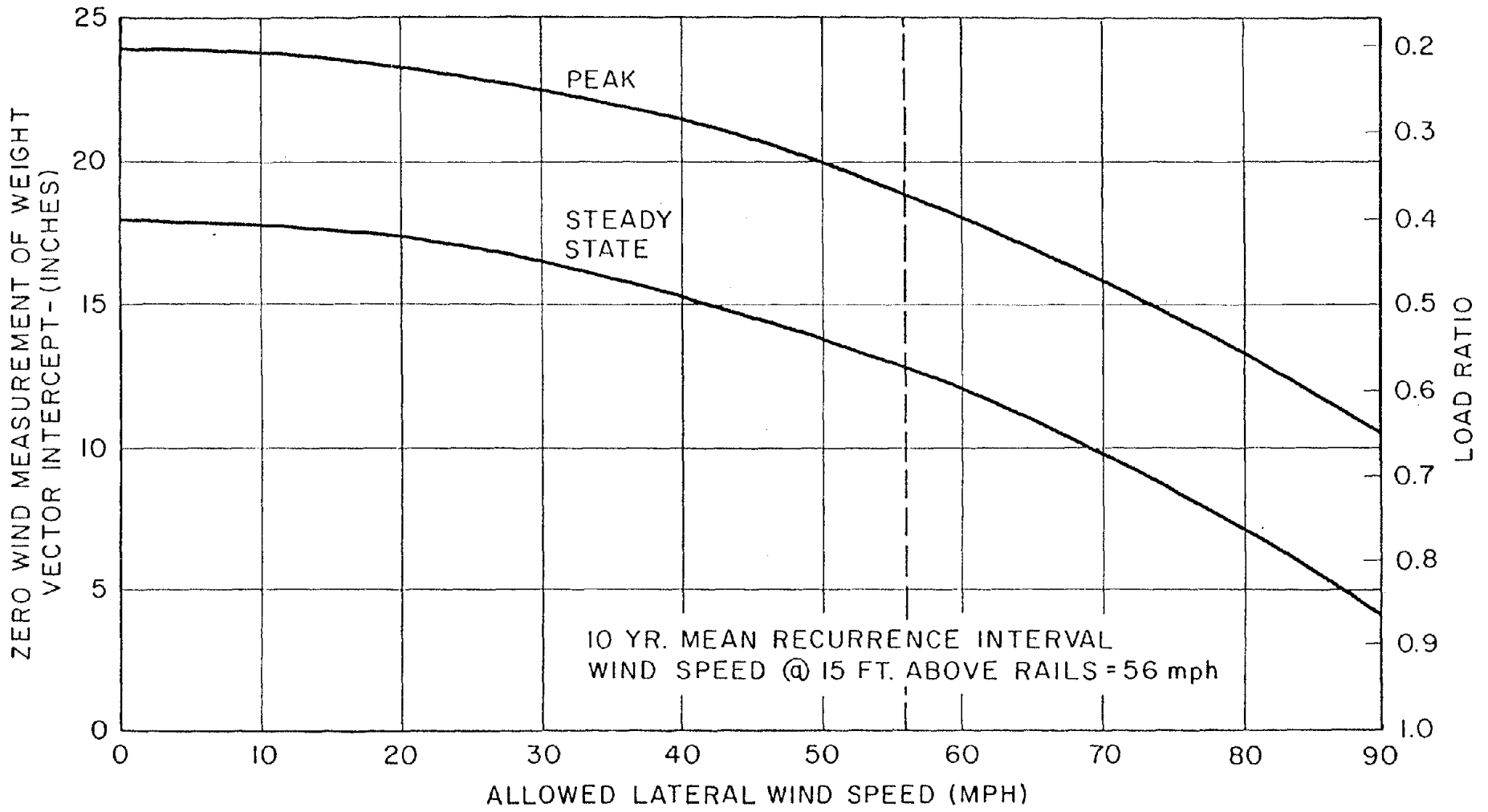


FIGURE 7-1

WEIGHT VECTOR INTERCEPT MEASUREMENT (ZERO WIND) V.S.
ALLOWED LATERAL WIND SPEED FOR UNLOADED AMCOACH
BASED ON JNR RECOMMENDED LOAD RATIOS

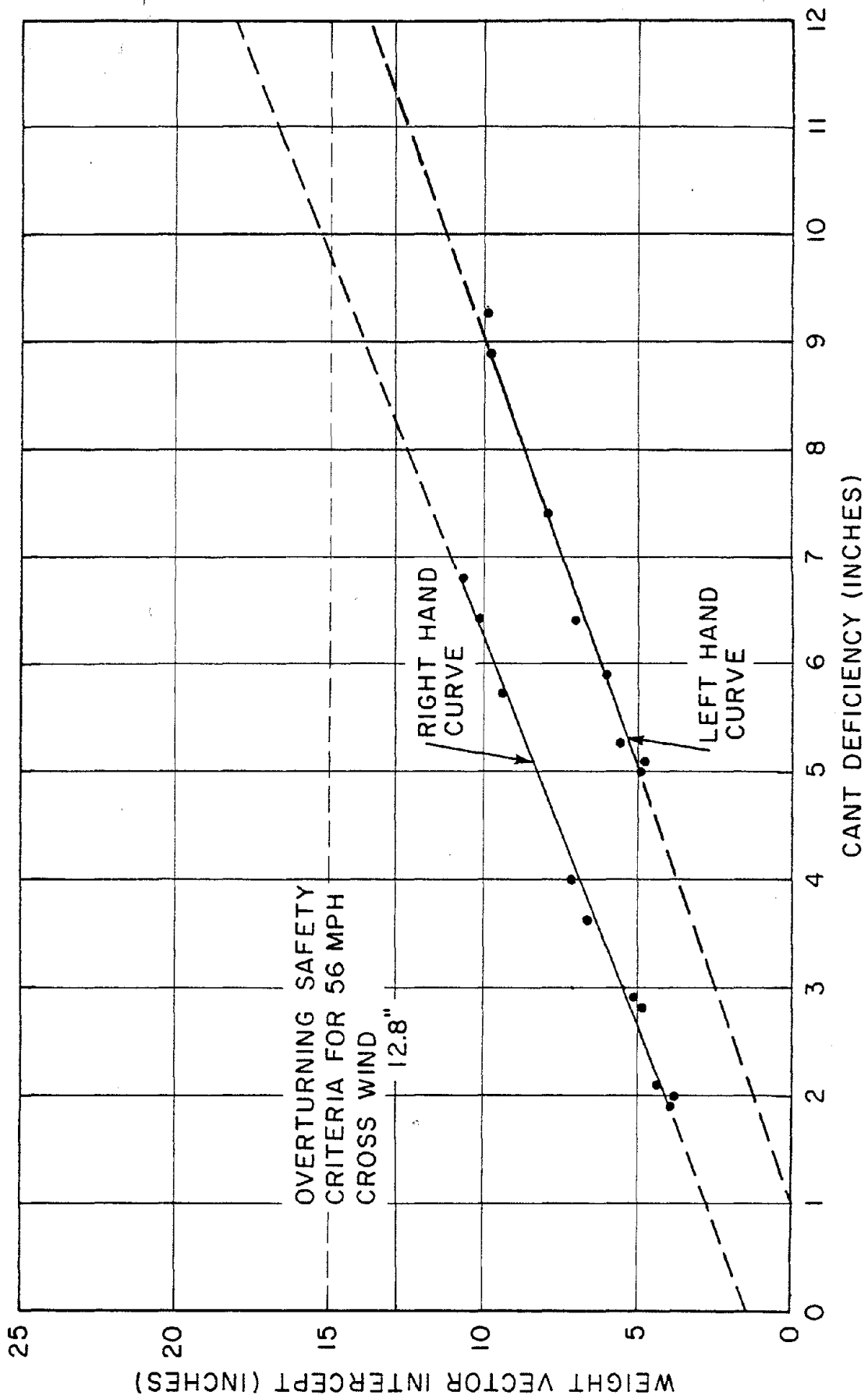


FIGURE 7-2
 STEADY STATE MEASUREMENT OF AMCOACH OVERTURNING SAFETY

can be achieved without exceeding the steady state overturning safety criteria of 12.8 inches vector intercept for curving with up to 56 mph crosswinds.

7.1.3 TRANSIENT MEASUREMENTS

Steady state measurements are similar for all constant radius curves negotiated at a particular cant deficiency. Peak measurements, however, will vary greatly due to geometry deviations and spiral design. A test zone of over one hundred miles in the section of the NEC having the greatest curve density was selected in order to measure peak weight vector intercepts over the full range of curve anomalies which can excite dynamic response. The overturning criteria for peak measurements of the Amcoach which allows for operation with up to 56 mph crosswinds is 18.8 inches weight vector intercept. If a curve is tested at the cant deficiency producing the maximum steady state weight vector intercept, a direct comparison of the peak measurement to the peak criteria will reveal whether it is dynamic or steady state performance that limits safe operation. However, the over-the-road testing resulted in peak measurements of single passes over a multitude of curves, many at low cant deficiency. Comparison of the peak measurement at the test cant deficiency to the maximum peak expected at the same cant deficiency of a curve, limited by steady state overturning, can be used to indicate whether the transient overturning criteria poses a lower limit for the Amcoach at any curve in the test zone. The maximum peaks for a curve limited by steady state overturning was determined by subtracting from the transient weight vector intercept limit, the difference between the steady state limit and the steady state measurement at the same cant deficiency. This method has been used in Figures 7-3 to 7-6 which display the peak measurements of weight vector intercept for groups of curves in the test zone. Points which fall below the line of projected maximum peaks for steady state limited curves represent curves over which the Amcoach would experience a peak vector intercept below 18.8 inches at 8 inches cant deficiency where it reaches the steady state criteria of 12.8 inches. The Amcoach is limited in overturning safety by steady state performance in curves represented by points below the line and by dynamic performance in curves represented by points above the line. The projection method avoids biasing in favor of left hand curves, and it allows consideration of all types of track irregularities in the test zone even though some curves are speed limited for various other reasons.

All of the measurements in Figures 7-3 to 7-6 fall below the projection lines, therefore, the Amcoach is limited by the steady state rather than transient vehicle overturning at the curves encountered on the NEC test zone. It is satisfactory in regard to overturning safety for operation at up to 8 inches of cant deficiency with allowance for 56 mph crosswinds. Curves having

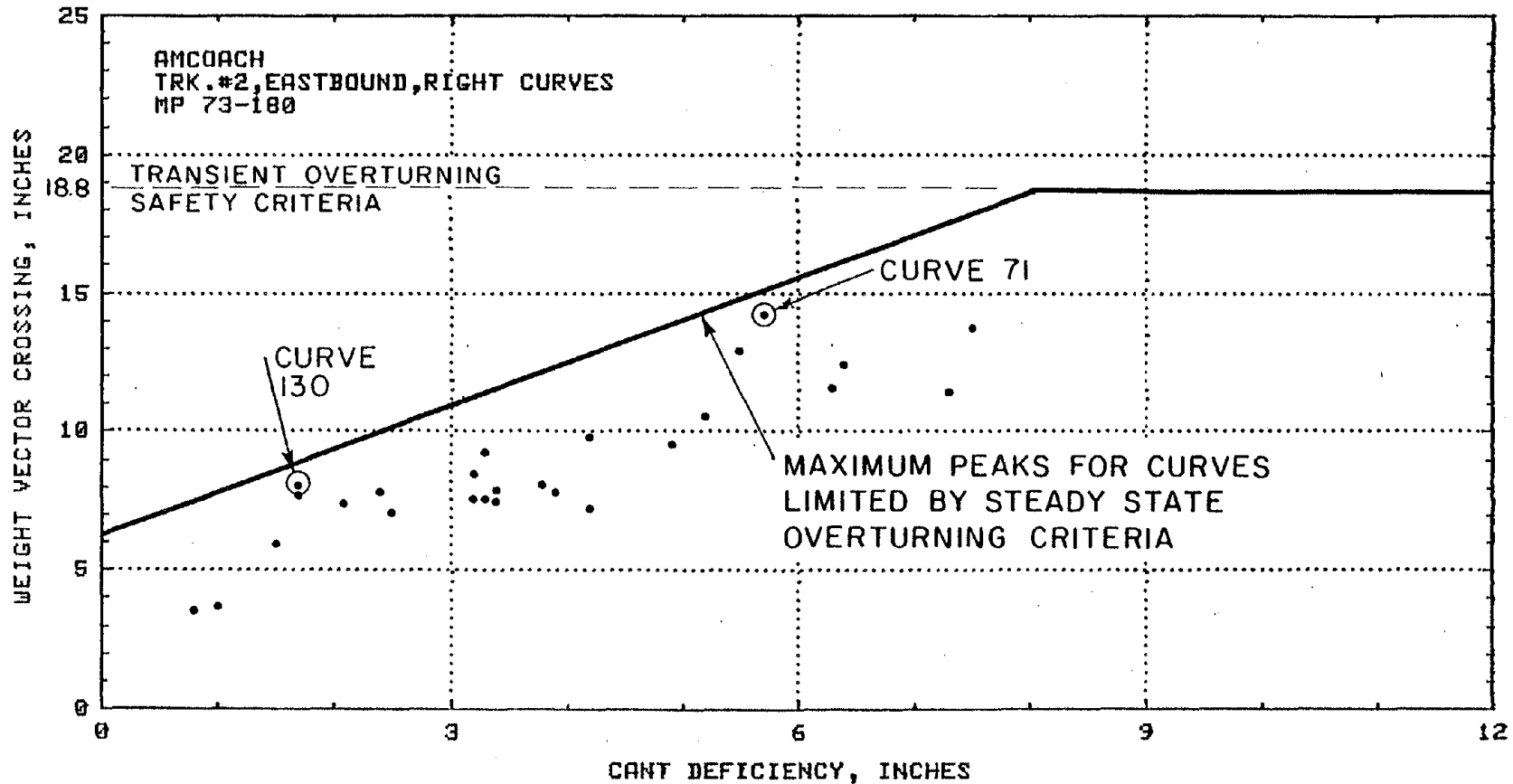


FIGURE 7-3

COMPARISON OF PEAK MEASUREMENTS OF WEIGHT VECTOR INTERCEPT FOR CURVES IN NEC TEST ZONE TO MAXIMUM PEAKS FOR CURVES LIMITED BY STEADY STATE OVERTURNING CRITERIA.

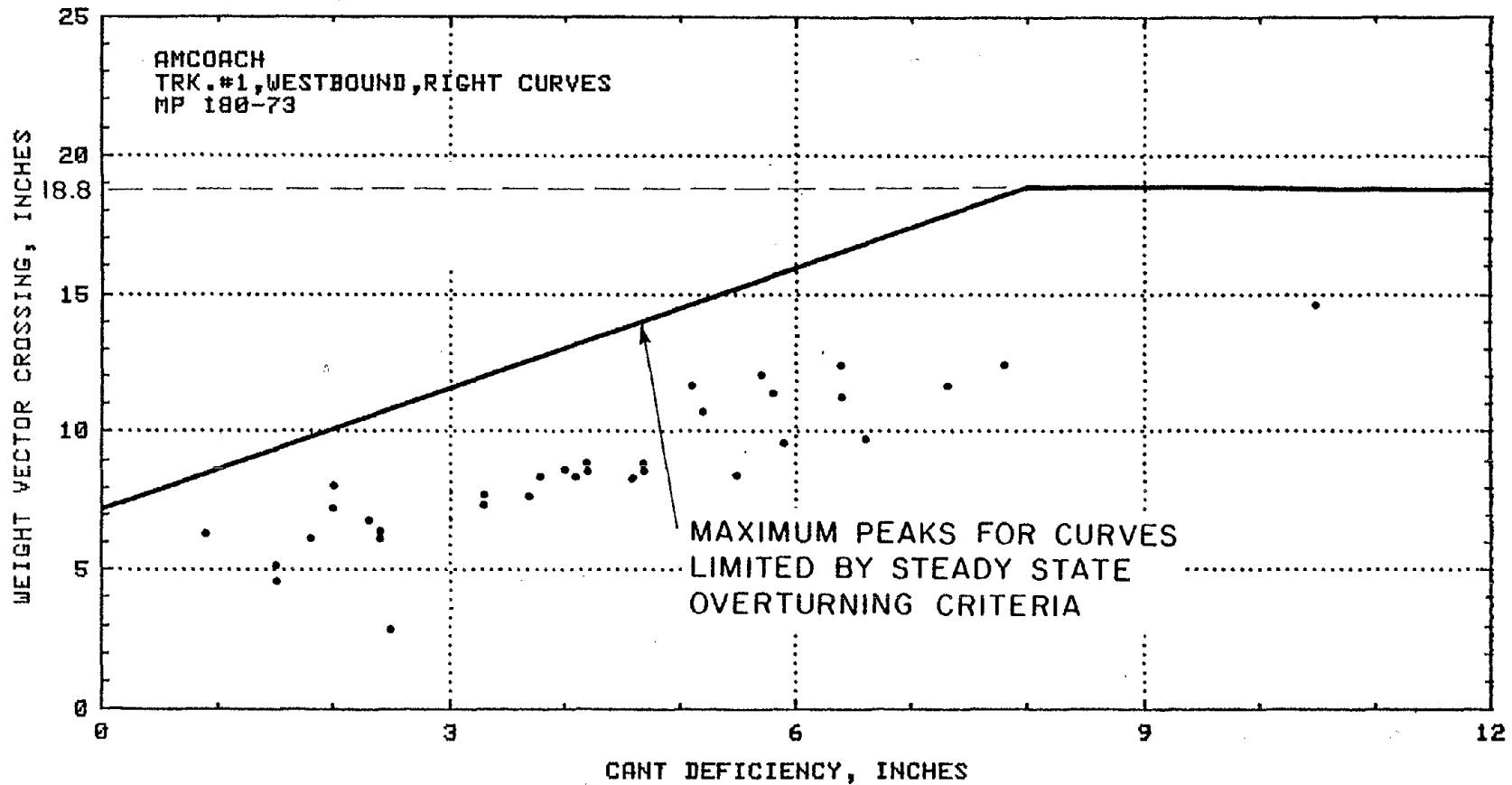


FIGURE 7-4

COMPARISON OF PEAK MEASUREMENTS OF WEIGHT VECTOR INTERCEPT FOR CURVES IN NEC TEST ZONE TO MAXIMUM PEAKS FOR CURVES LIMITED BY STEADY STATE OVERTURNING CRITERIA.

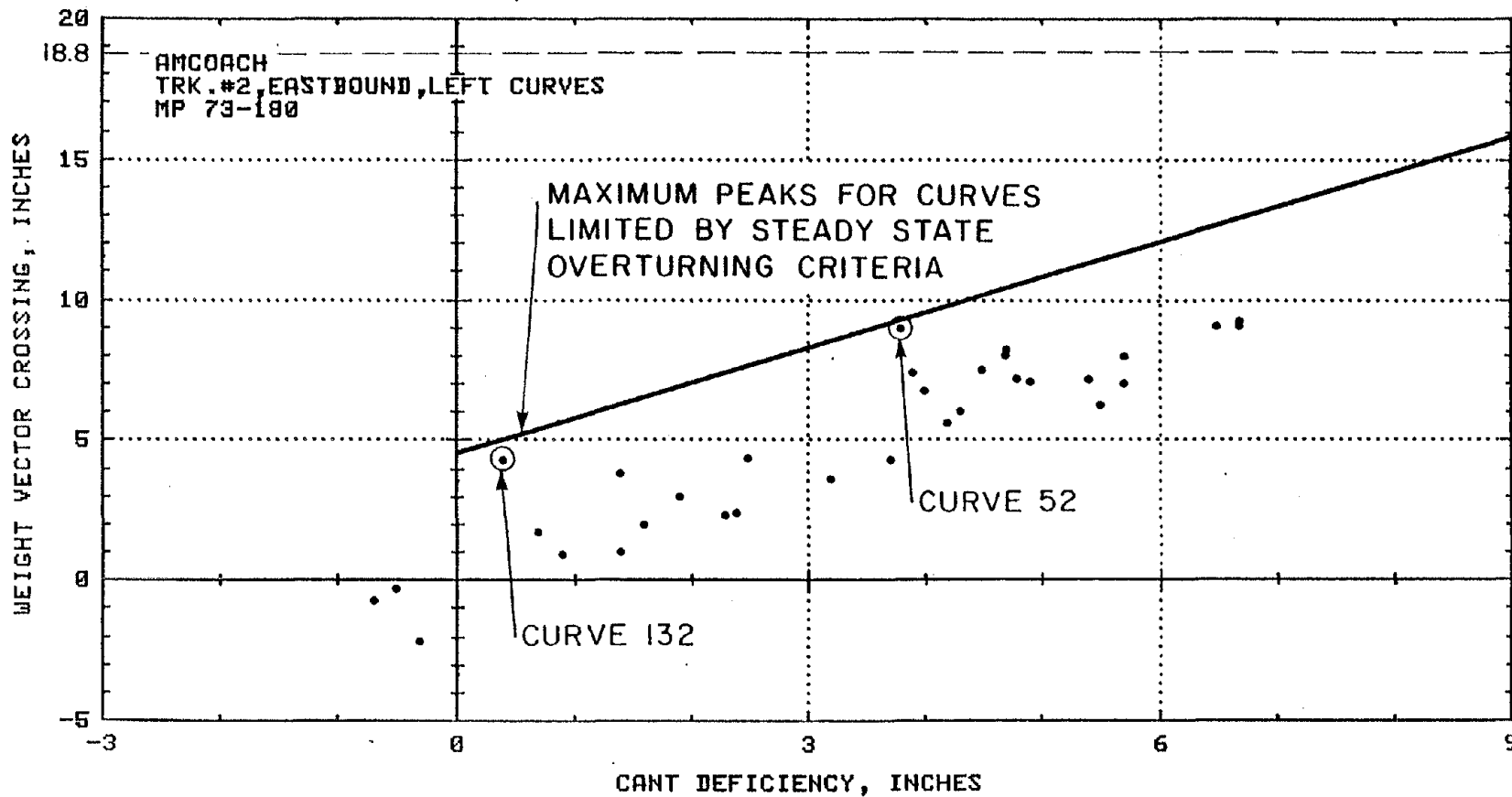


FIGURE 7-5

COMPARISON OF PEAK MEASUREMENTS OF WEIGHT VECTOR INTERCEPT FOR CURVES IN NEC TEST ZONE TO MAXIMUM PEAKS FOR CURVES LIMITED BY STEADY STATE OVERTURNING CRITERIA.

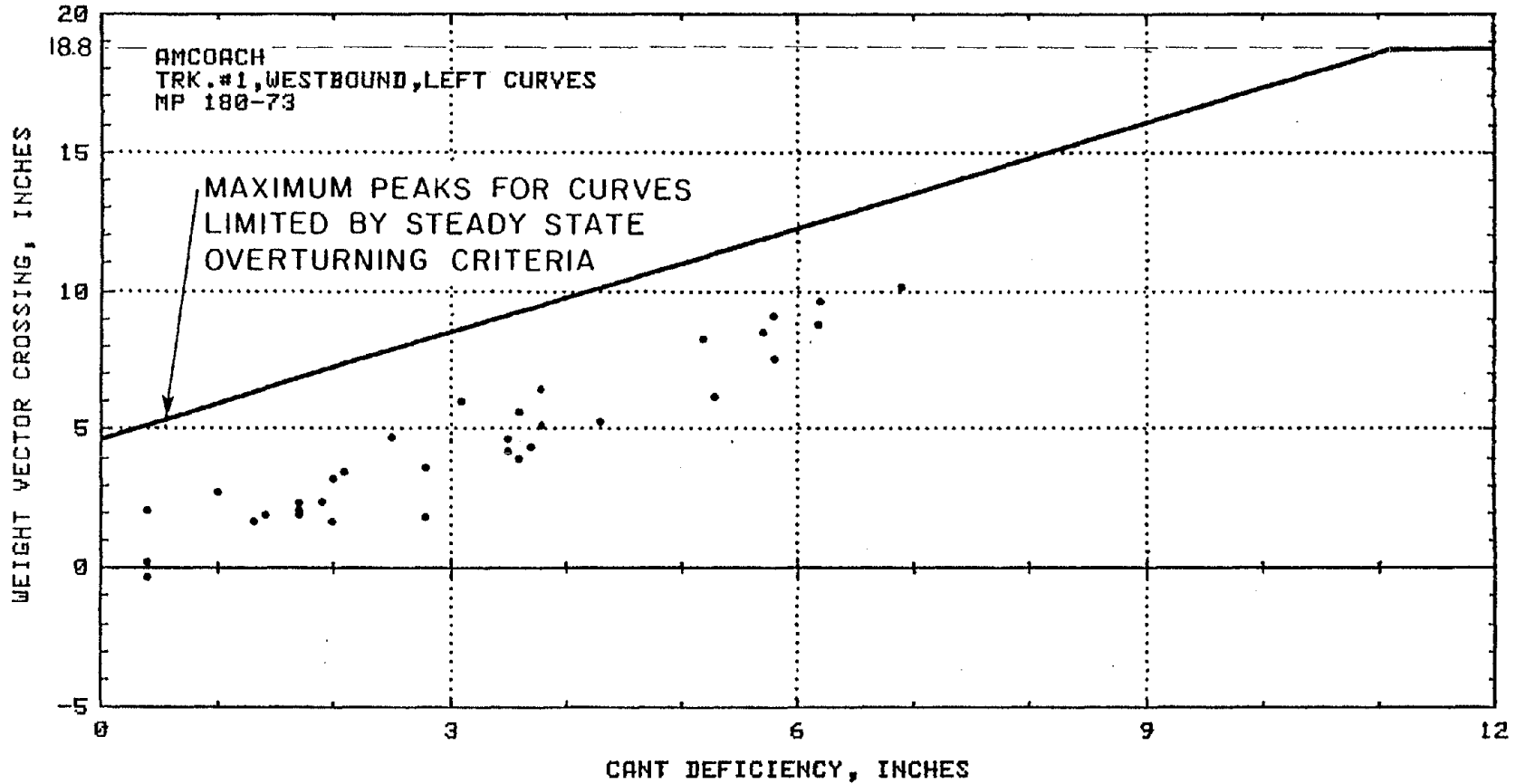


FIGURE 7-6

COMPARISON OF PEAK MEASUREMENTS OF WEIGHT VECTOR INTERCEPT FOR CURVES IN NEC TEST ZONE TO MAXIMUM PEAKS FOR CURVES LIMITED BY STEADY STATE OVERTURNING CRITERIA.

the perturbation characteristics of curves 52, 71, 87, 130 and 132 in the New Haven to Providence test zone cause the greatest dynamic response of the Amcoach although curve 71 is the only one of these examples which would be limited by even steady state overturning rather than by the 110 mph track speed.

7.2 RAIL ROLLOVER

Rail rollover is related to peak truck side L/V ratio. The peak rather than steady-state should be considered because this mode of derailment may be rapid and pulses of relatively low energy are capable of turning the rail whereas a very great amount of energy is required to overturn a vehicle with its great inertia.

A conservative rail rollover criteria should assume zero pull out resistance of the fasteners. Only the geometry of the rail section and the torsional stiffness of the surrounding rail should be considered for a general safety criteria.

Section 5.0 describes rail rollover criteria based on the above two factors. It can be expressed as $\max \text{ truck side } L/V = 0.5 + 2300/P_w$, where P_w is the single wheel nominal vertical load. This criteria may underestimate the effect of rail section geometry and overestimate the effect of torsional stiffness of the surrounding rail, but it appears to be based on the best available information. It should be interpreted as a restriction based on measurements having time duration of more than 50 milliseconds. Higher measurements are permitted for lesser time durations.

For a loaded Amcoach, $P_w \approx 15,000$ lb, and a limiting value of 0.65 should be compared to the peak measurements of truck side L/V ratio. Examination of the peak measurements at over one hundred curves on the NEC, indicates that the rail rollover criteria does not limit the operational cant deficiency of the Amcoach. The highest measurement of truck side L/V ratio was only 0.38 at 7.3 inches cant deficiency with the next highest 0.37 at 10.5 and at 3.8 inches of cant deficiency. The truck side L/V ratio of the Amcoach is not very sensitive to high cant deficiency because the vertical load increases with cant deficiency almost as greatly as does the lateral load.

7.3 LATERAL TRACK SHIFT

Although the inertia and pulse energy requirement to move the track structure laterally is much greater than that required for rail rotation the peak force levels of about 50ms duration provide a conservative measure of safety. The use of a single wheel force rather than axle force introduces another estimate on the

conservative side because the net axle force which moves the track is usually less than a single wheel peak force because the wheel forces on the same axle tend to oppose one another.

The safety criteria discussed in Section 5.0 assumes compacted ballast for full operational cant deficiency, and it allows for the force of crosswinds encountered in service. For the conservative assumption of wood ties, the criteria can be expressed as follows:

$$F_{\max} = \left[1 - \frac{A\Delta\theta}{22320} (1 + .458D)\right] [.7P + 6600] - (1.28 \times 10^{-3} SV^2)$$

A = rail cross section area, in²

$\Delta\theta$ = max temperature change after rail installation, °F

D = track curvature, degrees

P = vertical axle load, lbs.

S = lateral surface area of vehicle, ft²

V = lateral wind speed, mph

and it is assumed that a single axle bears half the entire wind load. For typical NEC conditions of 140 lb rail (A = 13.8 in², $\Delta\theta$ max of 70°F and D max of 4°):

$$F_{\max} = .61P + 5800 - 1.28 \times 10^{-3} SV^2$$

For the unloaded Amcoach axle load of 26,100 lb and an allowance for 56 mph crosswinds the maximum permissible lateral axle force is 18,600 lb. The maximum truck lateral force for a two axle truck should be limited to only 1.4 times the single axle maximum lateral force since fewer than twice the number of ties support the lateral force. The lateral track shift criteria permits a maximum truck lateral force of 27,300 lb allowing for one half of the 56 mph crosswind body side load at each truck.

The peak truck side lateral forces measured for the Amcoach on over one hundred curves were very low in comparison to the lateral track shift safety criteria. The highest measurement for the truck side was 17,300 lb at 10.5 inches of cant deficiency which is lower than the lateral force permitted for a single axle. The next highest measurement was 17,000 lb at 7.3 inches

of cant deficiency, and the highest truck side lateral force in relation to cant deficiency was 14,700 lb at 3.8 inches on curve 103 westbound. Curves 102 and 103 are severe relative to the other curves in the test zone. However, the lateral track shift safety criteria does not limit the safe curving speeds of the Amcoach because the truck lateral force measurements were well below the limiting force.

7.4 WHEEL CLIMB

The most appropriate criteria of safety concerning wheel climb for comparison to the Amcoach test results is that used by Amtrak as an acceptance specification for the AEM-7 locomotive. This criteria takes into account the AAR flange angle and it appears to have been based on conservative judgements. It states that the wheel (L/V) ratio must be less than $0.056T^{-0.927}$ where T is the duration of the peak level in seconds and that the maximum wheel (L/V) ratio for peaks of duration greater than 50 milliseconds is 0.90.

The static vertical load imbalance and side to side vertical load transfer in curving that produce weight vector intercepts, which limit safe operating cant deficiency act to reduce the high rail wheel and truck L/V ratios. The right hand test curve where safe cant deficiency was limited by the steady state vehicle overturning criteria produced wheel L/V ratios of only 0.22 steady state and 0.31 peak at about seven inches of cant deficiency. The left hand test curve produced slightly higher wheel L/V ratios of 0.28 steady state and 0.40 peak at up to nine inches of cant deficiency because the vertical load was reduced by the slight static vertical load imbalance. Several curves with greater perturbations were analyzed for wheel L/V ratio along with the instrumented test curves. The highest peak wheel L/V ratio encountered was 0.53 at 7.3 inches cant deficiency on curve 110 eastbound and the next highest was 0.49 at 6.5 inches cant deficiency on curve 109 eastbound. Wheel L/V ratio did not increase rapidly with cant deficiency after reaching the threshold of flange contact because the vertical force increase due to load transfer, kept pace with the increase in lateral force caused by higher curving speed.

Truck L/V ratio rather than wheel L/V ratio was recorded during tests in the zone containing over one hundred curves. However, even under the unlikely assumption that only one axle supported the entire lateral truck force the maximum measured peak truck L/V ratio of 0.38 could not result in a wheel L/V ratio of more than 0.76. The Amcoach will not develop wheel L/V ratios greater than those permitted by the wheel climb safety criteria at cant deficiencies permitted by other safety criteria.

7.5 RIDE COMFORT

Section 5.0 included a variety of criteria for lateral acceleration used by organizations throughout the world as indices for ride comfort evaluation. The most commonly recognized standards in the U.S. are the AAR recommendations of 0.1g maximum steady state and 0.03g/sec maximum "jerk". The least restrictive standards are those of SNCF which permit 0.15g and 0.10g/sec, respectively. The JNR has an additional standard of $\pm 0.08g$ maximum carbody "vibration" which pertains to the transient response of a carbody tilt system upon entering and exiting a curve.

When the AAR study was undertaken in the early 1950's, coach suspensions were designed such that large body roll angles occurred in curving. The component of gravitational acceleration in the plane of the coach floor added substantially to the centrifugal acceleration as the coach body rolled toward the outside of the curve. At three inches of cant deficiency, the body roll of contemporary coaches was usually sufficient to cause a total of 0.1g lateral acceleration in the plane of the floor.

Figure 7-7 shows that the Amcoach suspension controls body roll much better than the earlier designs. The Amcoach reaches the AAR steady state lateral acceleration criteria of 0.1g at about 5 inches of cant deficiency. A coach with zero body roll, subject only to centrifugal acceleration, would reach the AAR criteria at 6 inches of cant deficiency. The value of tilt body coaches such as the LRC (as shown in Figure 7-7) is that they achieve negative roll angles and can use the component of gravity in the plane of the floor to counteract centrifugal acceleration.

7.6 MAXIMUM OPERATIONAL CANT DEFICIENCY

The operational cant deficiency of the Amcoach is limited by the steady state vehicle overturning safety criteria. The maximum low rail to high rail weight transfer (expressed in terms of weight vector intercept) may exceed the steady state safety criterion if it is operated above eight inches of cant deficiency with a 56 mph unfavorable crosswind. Under these conditions, the transient weight transfer is below the safety criteria level on the most severely perturbed of typical NEC curves. Measurements of safety related to wheel climb, rail rollover and track panel shift are well below critical levels at the cant deficiency limited by overturning safety.

The safety criteria are based on the law of physics governing modes of derailment, and comparisons of measurements to them yield objective conclusions. Steady state ride comfort criteria are based on subjective evaluations of something impossible to measure in absolute terms. Comfort, unlike derailment, exists as

7-14

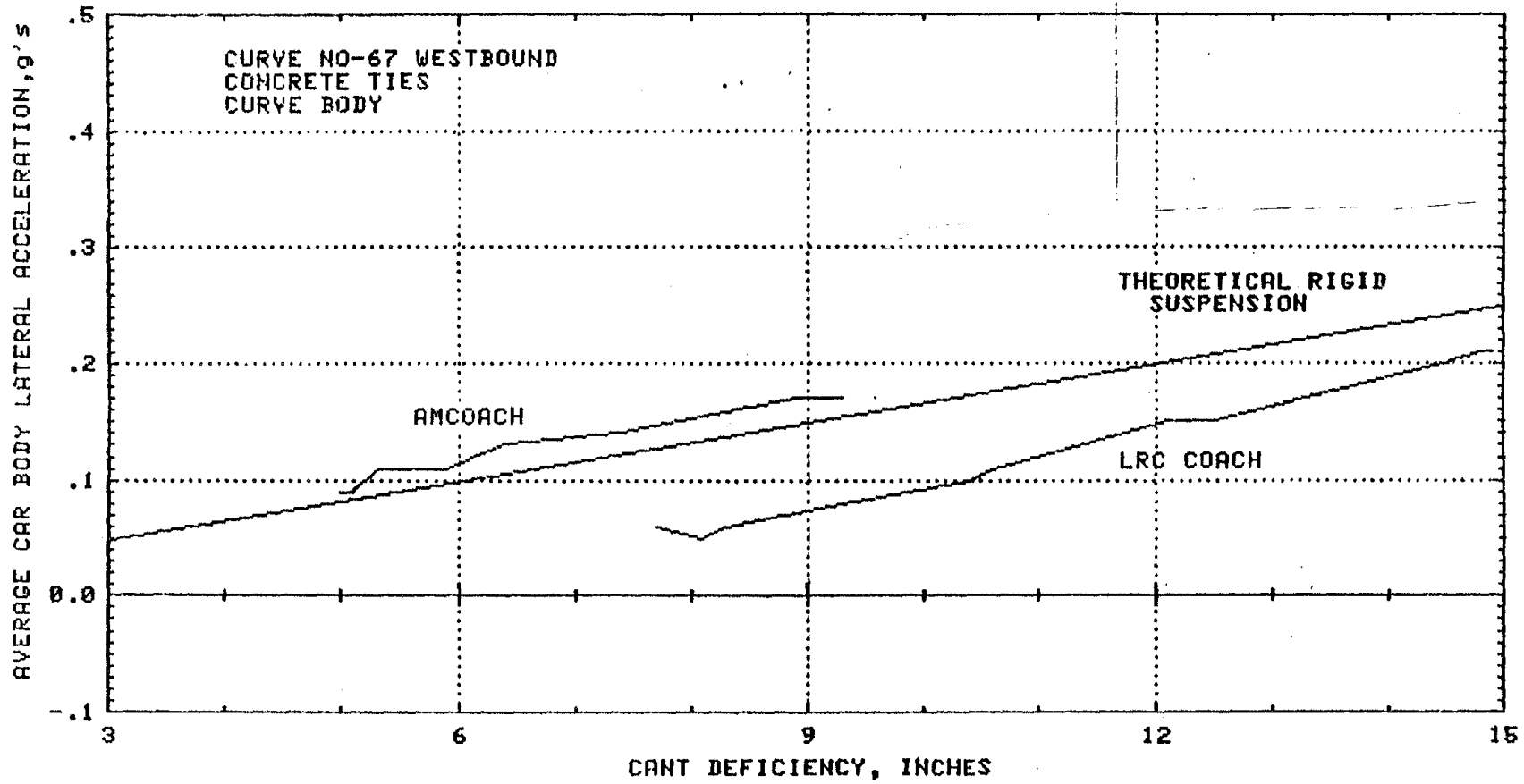


FIGURE 7-7

STEADY STATE LATERAL ACCELERATION OF AN AMCOACH COMPARED TO A VEHICLE WITH ZERO ROLL AND TO A TILTING COACH

a continuum. The safety considerations can be satisfied by the Amcoach at high cant deficiency, but the lateral acceleration felt by the passengers will be greater. An AAR committee was comfortable at up to 0.10g while their French counterpart was comfortable at up to 0.15g. The steady state lateral acceleration at the floor of the Amcoach was 0.15g at eight inches of cant deficiency. The AAR judged this level of lateral acceleration as "strongly noticeable." The increase of operating cant deficiency of the Amcoach to eight inches reduces ride quality without compromising safety.

7.7 COMPARISON OF TEST RESULTS TO SIMPLE QUASISTATIC PREDICTIONS

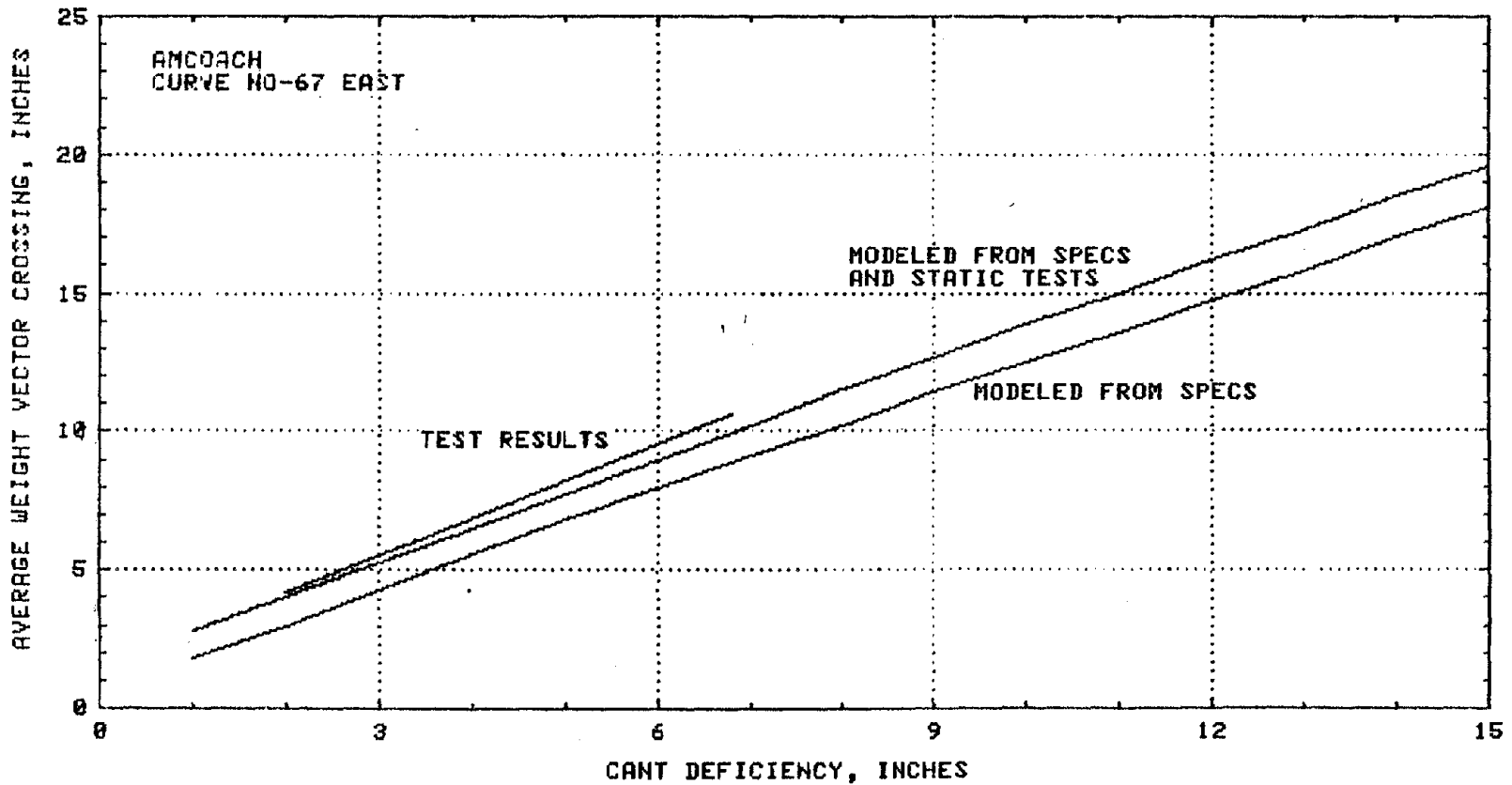
A simple quasistatic model described in Appendix B was formulated to predict several steady state measurements. The published specifications of the vehicles and the results of static tests to estimate weight distribution and suspension spring rates as installed, which were used in these calculations, are listed in Appendix C. Such predictions can be useful in estimating the performance potential of vehicles like the Amcoach which are actually limited by steady state criteria of overturning safety and lateral acceleration ride quality. Safety and ride quality considerations which depend on knowledge of peak values and of transient distributions of wheel forces are not likely to be satisfied by modeling. This is due to the range of complex, interactive, and non-obvious in service track influences, which could be sampled experimentally in a test zone of over one hundred curves.

Figure 7-8 and 7-9 show the measurements of weight vector intercept (from Figure 7-2) compared with the predictions. They agree within about one inch of vector intercept at a given cant deficiency when the "as installed" estimates of vehicle properties are considered. Similarly, the measurements of steady state lateral acceleration are compared to prediction in Figure 7-10 and 7-11. The variability between right and left hand curves is greater than expected, but the average between them agrees with the predictions.

The prediction of the net lateral force summation of all four wheels of a truck was compared to the measurements of the summation of only the two high rail wheels in order to test the order of magnitude of the measurements against basic physical laws. Figures 7-12 and 7-13 indicate that the magnitude of the test data is reasonable. The high rail side lateral force measurement is greater than the predicted net truck lateral force for the right hand curve tested at lower cant deficiencies while it is lower than the prediction for the truck for the left curve tested at higher cant deficiencies. It is not clear whether the truck is sensitive to curve direction or whether the low rail wheels contribute differently at higher cant deficiency.

FIGURE 7--8

COMPARISON OF STEADY STATE WEIGHT VECTOR INTERCEPT PREDICTIONS TO TEST RESULTS FOR AMCOACH IN RIGHT HAND CURVE



7-16

FIGURE 7-9

COMPARISON OF STEADY STATE WEIGHT VECTOR INTERCEPT PREDICTIONS TO TEST RESULTS FOR AMCOACH IN LEFT HAND CURVE

7-17

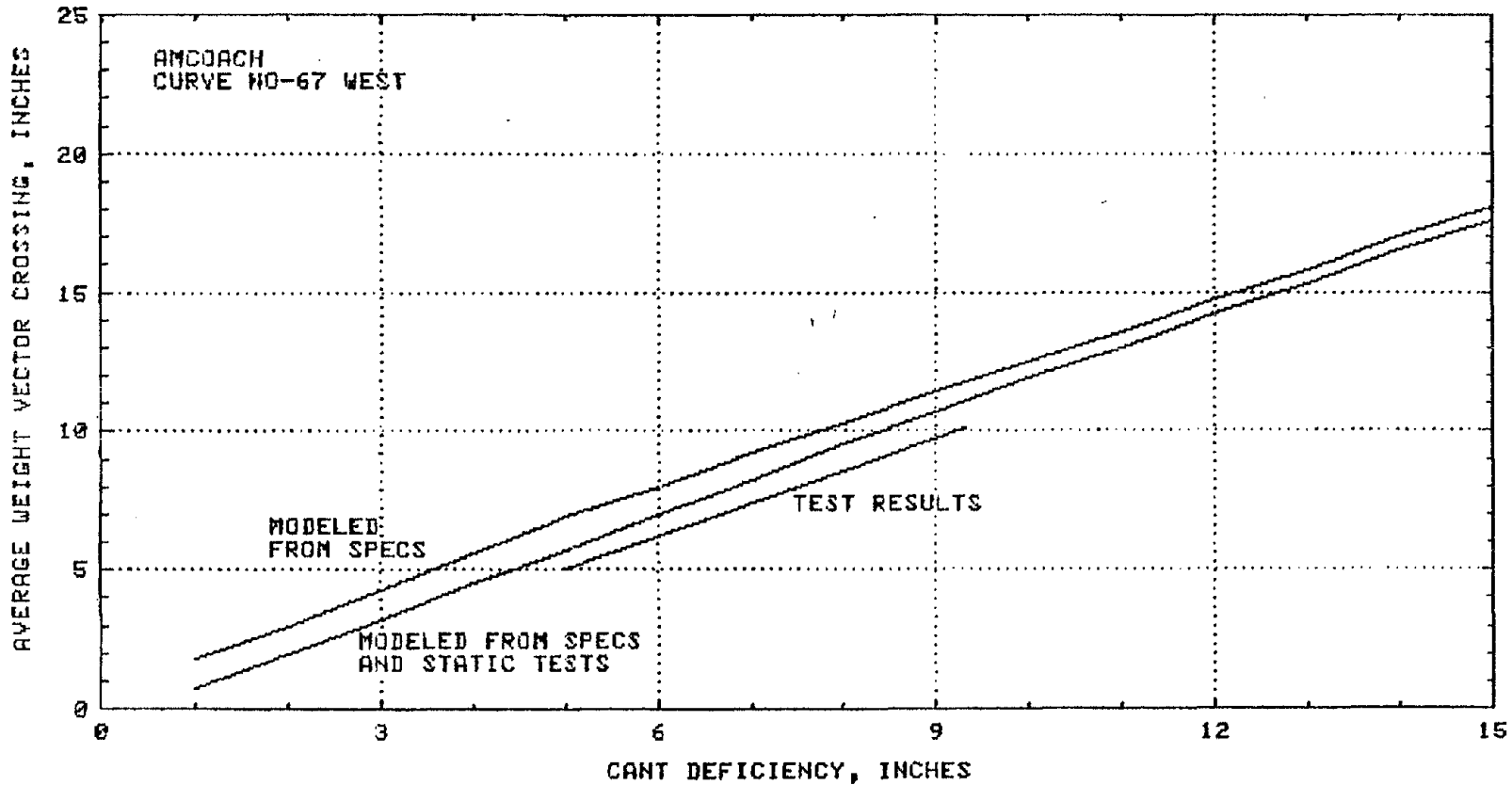


FIGURE 7-10

COMPARISON OF STEADY STATE CAR BODY LATERAL ACCELERATION PREDICTIONS TO TEST RESULTS FOR AMCOACH IN RIGHT HAND CURVE

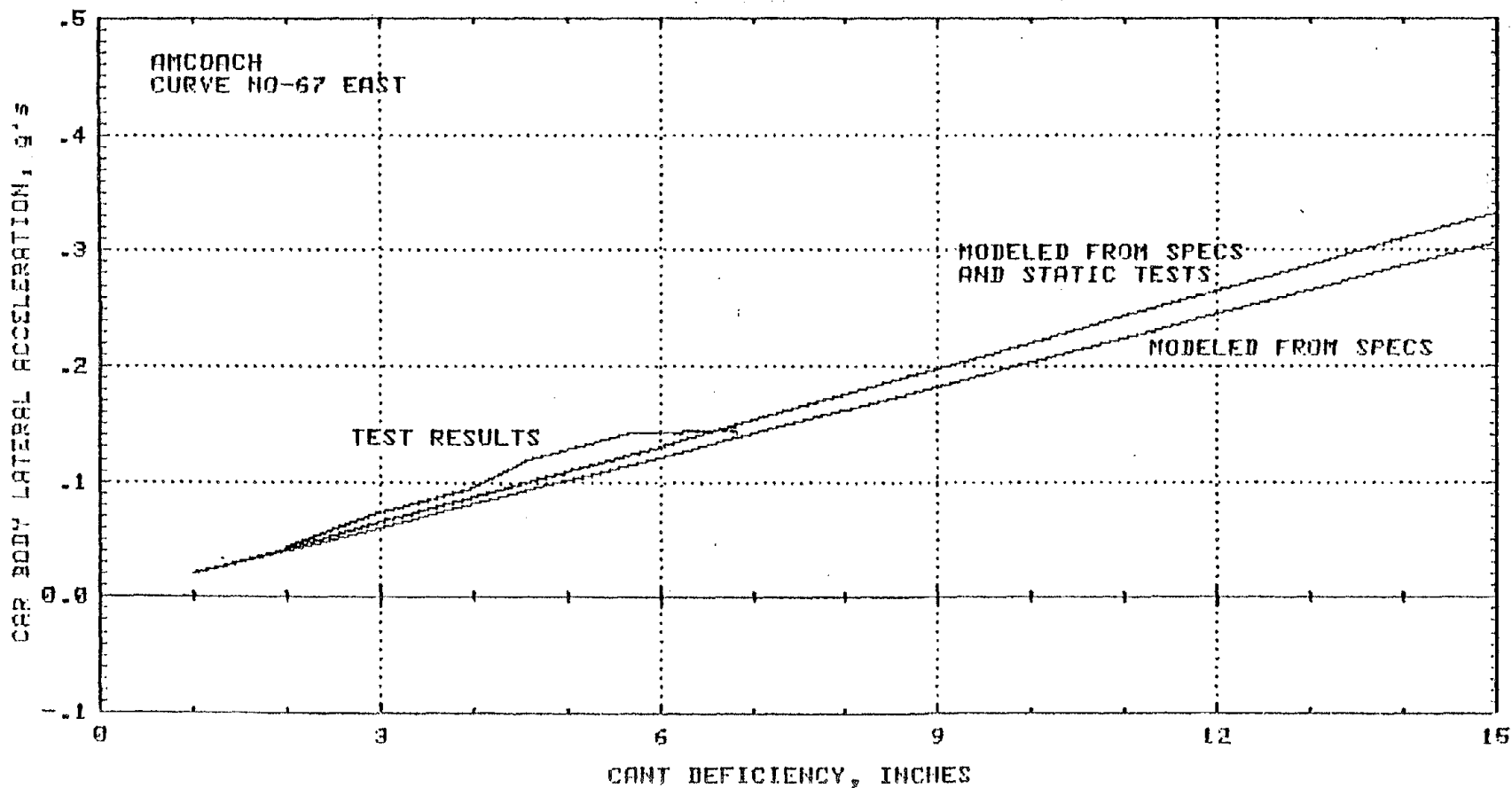


FIGURE 7-11

COMPARISON OF STEADY STATE CAR BODY LATERAL ACCELERATION PREDICTIONS TO TEST RESULTS FOR AMCOACH IN LEFT HAND CURVE

7-7

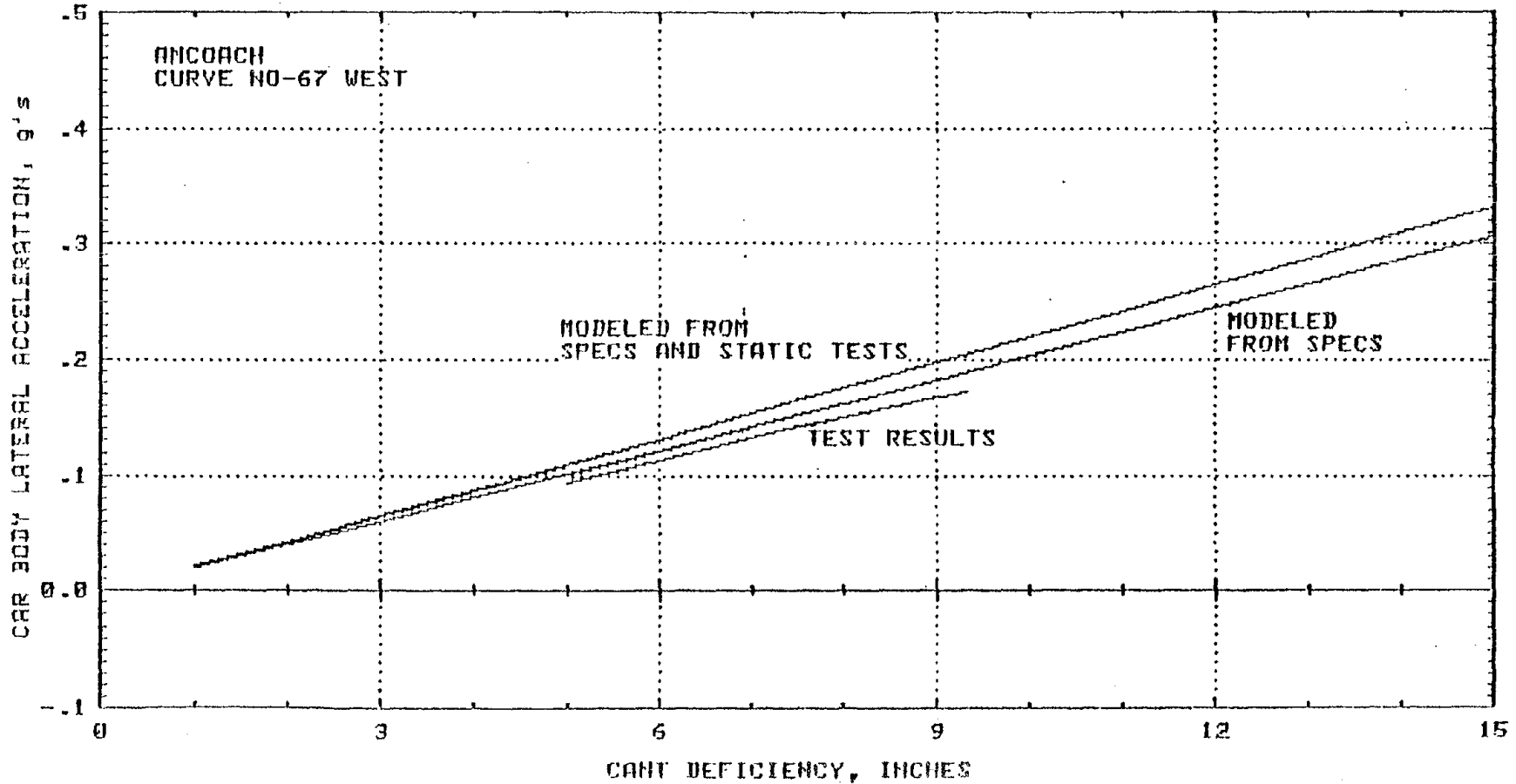
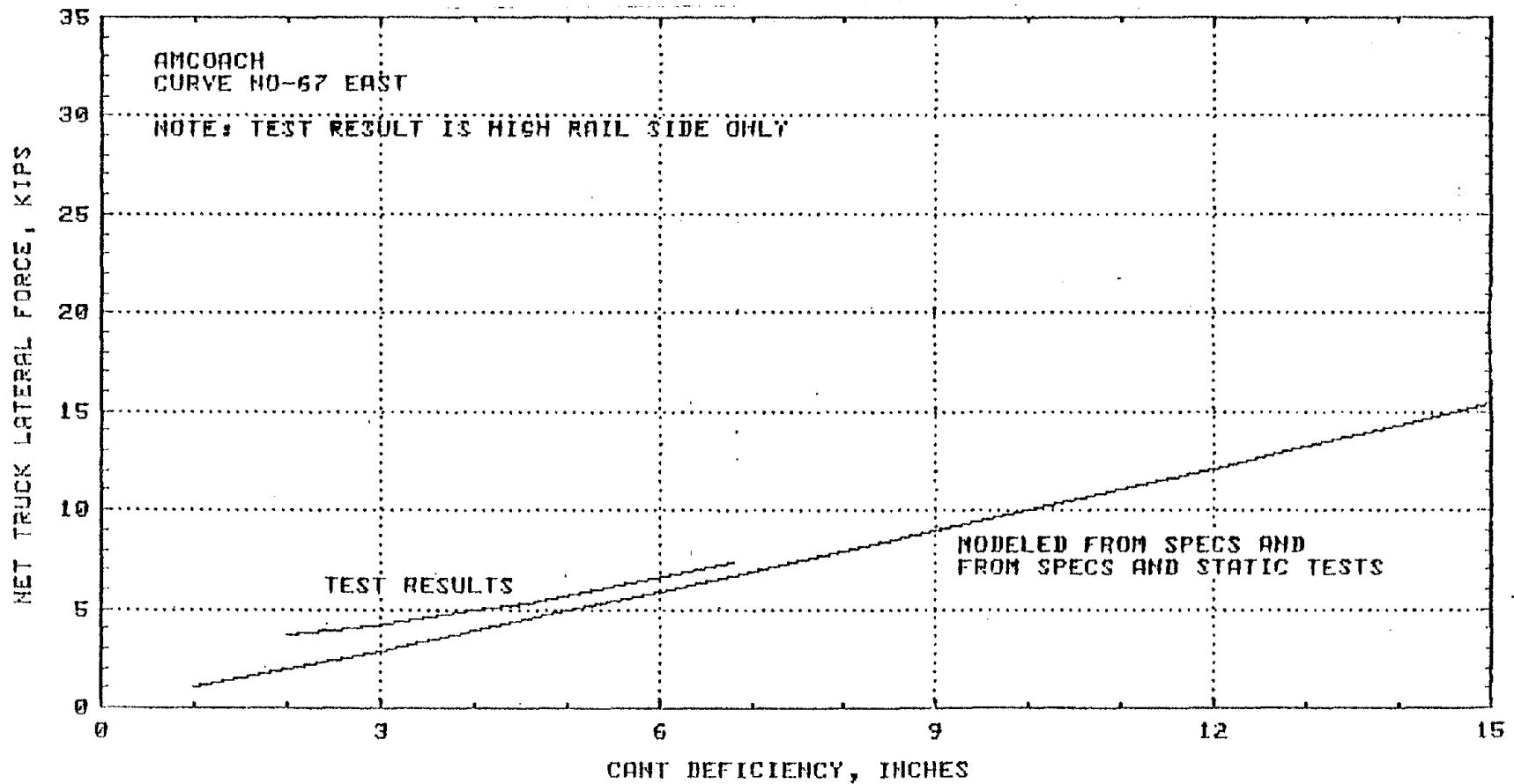


FIGURE 7-12

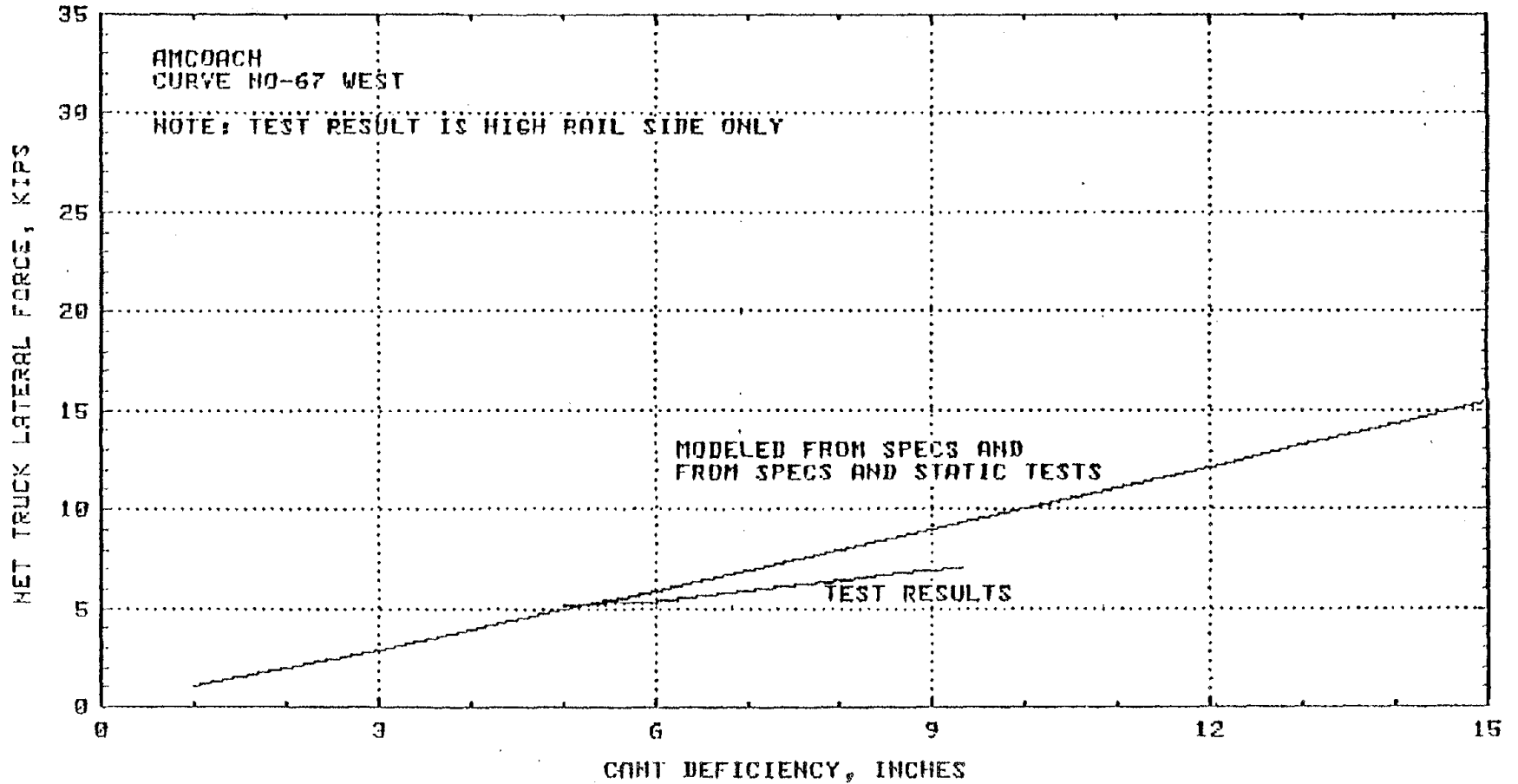
COMPARISON OF STEADY STATE NET TRUCK LATERAL FORCE PREDICTIONS TO TEST MEASUREMENTS OF HIGH RAIL SIDE TRUCK LATERAL FORCE FOR AMCOACH IN RIGHT HAND CURVE

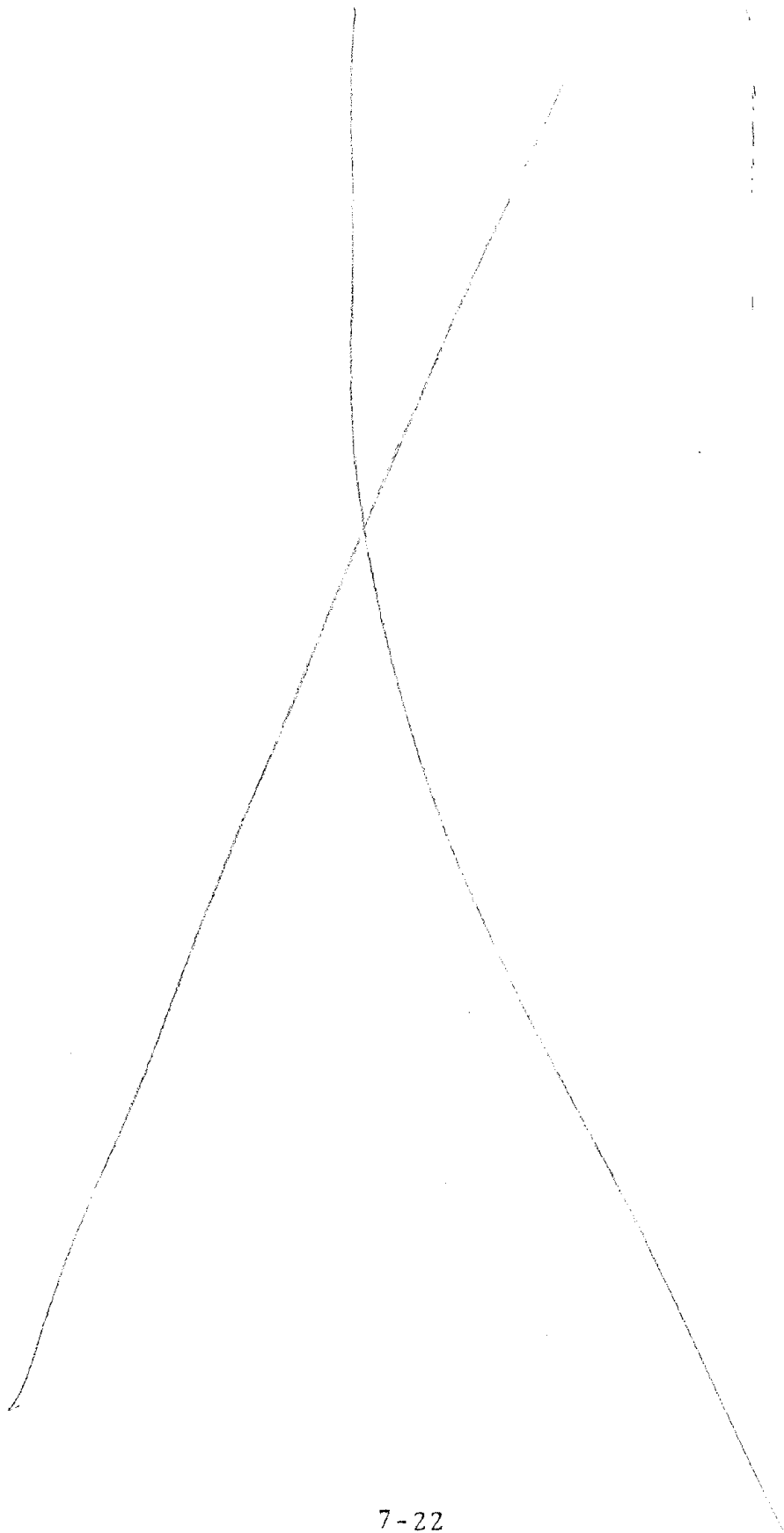


7-20

FIGURE 7-13

COMPARISON OF STEADY STATE NET TRUCK LATERAL FORCE PREDICTIONS TO TEST MEASUREMENTS OF HIGH RAIL SIDE TRUCK LATERAL FORCE FOR AMCOACH IN LEFT HAND CURVE





8.0 RESULTS OF TESTING THE AEM-7 LOCOMOTIVE AT HIGH CANT DEFICIENCY

The AEM-7 was tested in two modes. In the first mode, repetitive runs at various speeds were made over two specific test curves, one left and one right. The steady state performance of the vehicle was determined on these test curves. The second mode of testing was a series of runs over hundreds of miles of NEC track. The peak level measurements which depend on actual track irregularities were taken from these tests as well as from the repetitive curving tests. The safety criteria are discussed in detail in Section 5.0 and the data reduction techniques are covered in Section 3.5.

8.1 VEHICLE OVERTURNING

The vehicle overturning criteria used by the Japanese National Railway is the most comprehensive in the literature. It is appropriately conservative and it includes separate criteria for peak and steady state measurements. It may be summarized, in terms of vector intercept, by the following two equations:

$$\text{Steady State Vector Intercept} \leq 18 - (.0153V^2Sh_{cp}/W) \text{ inches}$$

and

$$\text{Peak Vector Intercept} \leq 24 - (.0153V^2Sh_{cp}/W) \text{ inches}$$

where:

V is the lateral wind speed in mph

S is the lateral surface area of the vehicle in ft²

h_{cp} is the height of the center of wind pressure in ft

W is one half of the unloaded weight of the vehicle in pounds.

For the AEM-7 Locomotive:

$$S \approx 500 \text{ ft}^2$$

$$h_{cp} \approx 7.5 \text{ ft}$$

$$W = 99,000 \text{ lb.}$$

The second term in the above equations is an allowance for the maximum detrimental effect of wind speed. The weight vector intercept specified by each criterion represents the maximum still air test measurement permitted for operation at the given wind speed. The above equations are graphed on Figure 8-1 which expresses the separate criteria appropriate for peak and steady state measurements as functions of the allowed wind speed.

8.1.1 WIND SPEED EFFECT

The overturning criteria are extremely sensitive to wind speed especially over 50 mph. However, small heavy vehicles such as the AEM-7 locomotive are the least susceptible. The operational cant deficiency should be chosen to allow for sudden unexpected lateral winds, but train speed need not be limited by overturning considerations to include heedless operation in gales and hurricanes. Train speeds must be reduced under those circumstances to meet other conditions such as reduced visibility or the danger of debris on the track. The operational cant deficiency chosen will provide safe operation at the maximum wind speed corresponding to the 10 year mean recurrence interval. This cant deficiency is sufficiently conservative to provide for safety during unexpected winds. The level of wind speed for locations along the NEC is greatest in Boston where it is 70 mph measured 30 ft. above the ground (ref 24). Reference (24) also provides a factor to adjust wind speed measurements for other distances above ground level. At 15 feet above the ground the 10 year mean recurrence interval wind speed is $0.8 \times 70 \text{ mph} = 56 \text{ mph}$. The cant deficiency safe for crosswinds up to 56 mph must be chosen to limit the weight vector intercept of the AEM-7 locomotive to 16.2 inches steady state and 22.2 inches peak when measured in still air as indicated in Figure 8-1.

8.1.2 STEADY STATE CURVING MEASUREMENTS

Figure 8-2 gives steady state test results which relate weight vector intercept to cant deficiency. The weight distribution on the instrumented truck was offset from the geometric centerline about one inch to the right. Consequently, the vector intercept was expected to be greater for left hand curving, and this was confirmed. The test results for the left hand curve represent the worst case and should be used for comparison to safety criteria. The worst case test data indicate that operation at 10-1/2 inches of cant deficiency can be achieved without exceeding the steady state overturning safety criteria of 16.2 inches vector intercept for curving with up to 56 mph crosswinds.

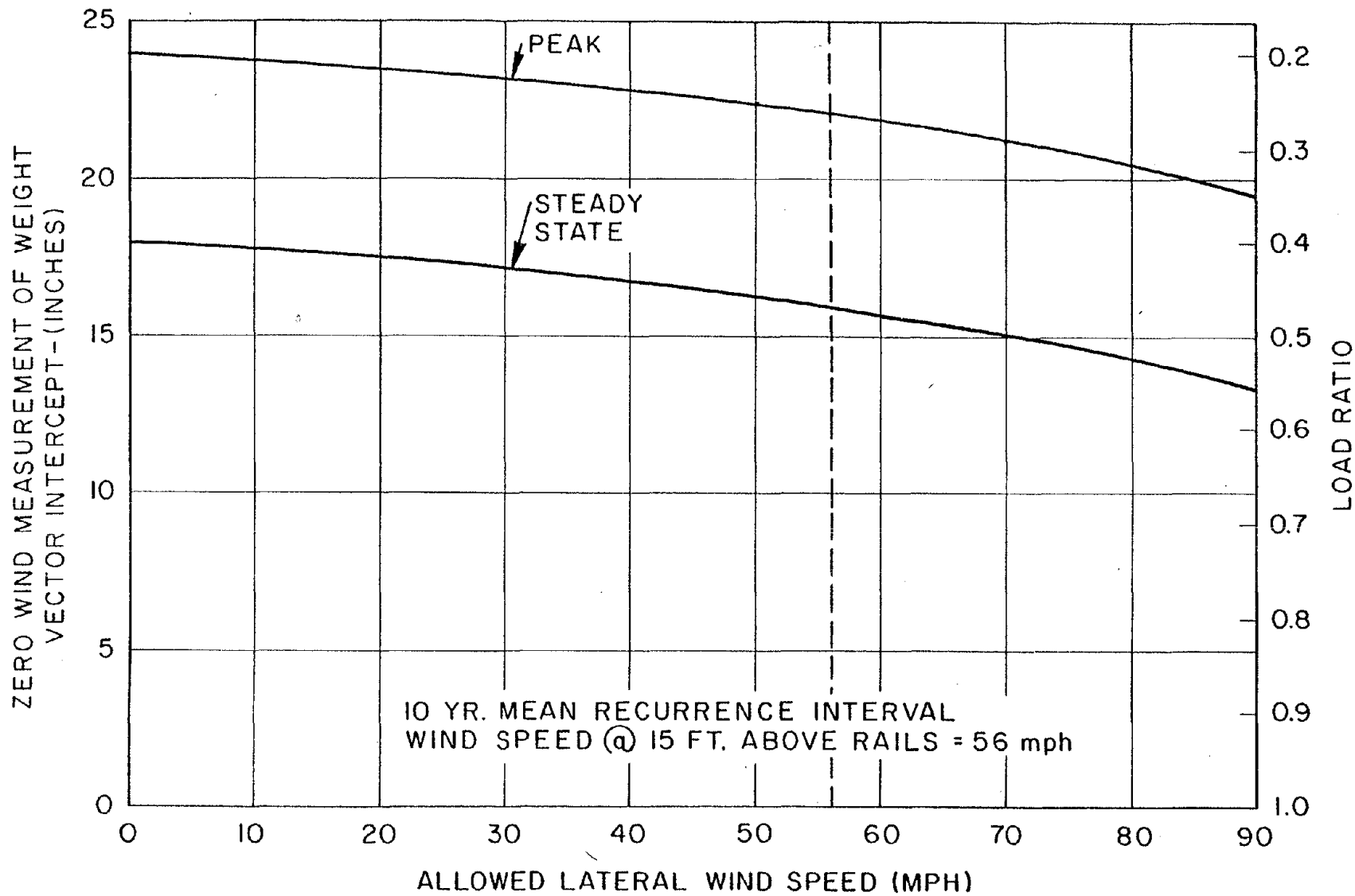


FIGURE 8-1

WEIGHT VECTOR INTERCEPT MEASUREMENT (ZERO WIND) V.S.
ALLOWED LATERAL WIND SPEED FOR AEM-7 LOCOMOTIVE
BASED ON JNR RECOMMENDED LOAD RATIOS

8.1.3 TRANSIENT CURVING MEASUREMENTS

The overturning safety criteria for both steady state and peak measurements must be satisfied for safe operation. Steady state measurements are similar for all constant radius curves negotiated at a particular cant deficiency. Transient (peak) measurements, however, will vary greatly due to geometry deviations and spiral design. Peak measurements of weight vector intercept were taken at the spirals and curve bodies of the test curves which were used for the steady state measurements in Figure 8-2. The highest measurements occurred at the entry spiral of the left curve and are plotted in Figure 8-3 as a function of cant deficiency. The peak measurements were quite linear with cant deficiency at the test curves where runs were repeated at several speeds. Thus the measurements may be extrapolated to the critical value of 22.2 inches specified by the transient criteria. Since the peak vector intercept limit occurs at over 12 inches of cant deficiency, the locomotive would be limited first, in these curves, by the steady state overturning criteria at 10-1/2 inches of cant deficiency. However, many of the curves in the New York to Washington NEC test zone are typical of the worst track irregularities that the AEM-7 locomotive encounters in service, and the results of these single pass tests must be used to predict whether the transient overturning criteria poses a lower limit than the steady state criteria in harsh service conditions.

Figure 8-3 also illustrates a method of determining, from a peak measurement at lower cant deficiency, whether the maximum cant deficiency with regard to overturning safety is limited by the steady state or by the transient criteria. The projection of the transient criteria to low cant deficiencies is an estimate of the maximum peak vector intercept in a curve in which the steady state overturning criteria still limits cant deficiency. If a peak measurement at any cant deficiency falls below the projection line, the steady state criteria will limit cant deficiency to 10-1/2 inches. If the peak measurement exceeds the projection, the transient criteria will limit the cant deficiency to less than 10-1/2 inches. The projection line was constructed by subtracting from the transient weight vector intercept limit the difference between the steady state limit and the steady state measurement (Figure 8-2) at each cant deficiency. The method avoids biasing in favor of right curves and it allows for consideration of all types of track irregularities even if the particular test curve was speed limited by other factors.

The peak measurements in Figure 8-3 were made at over 10-1/2 inches cant deficiency without exceeding the transient overturning criteria. However, if only one peak measurement at low cant deficiency were available at this curve, comparison with the projection line would correctly predict that the steady state criteria sets the lower cant deficiency limit. Figure 8-4 is an example of single peak measurements at many curves. At curve 403

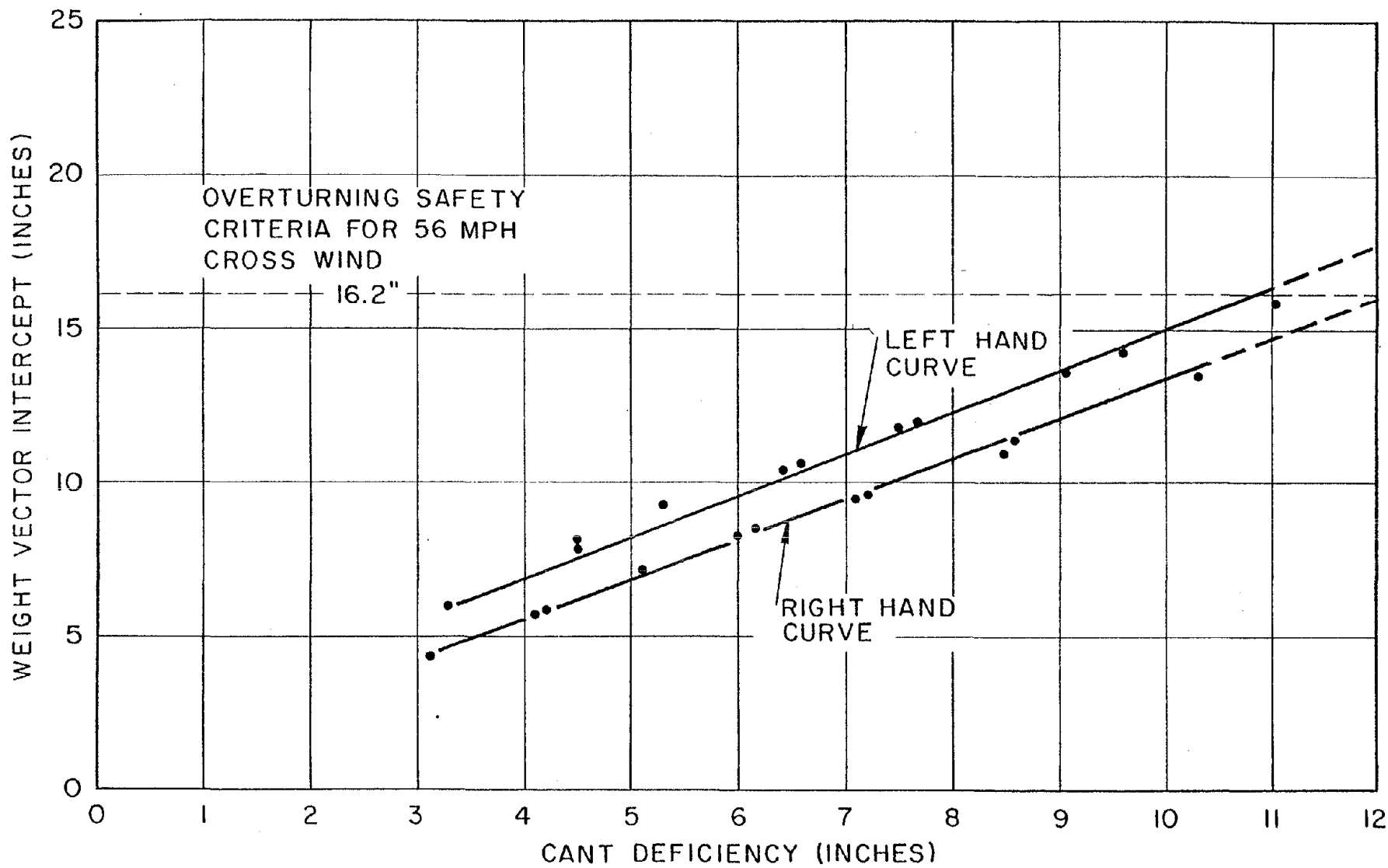


FIGURE 8-2

STEADY STATE MEASUREMENT OF AEM-7 LOCOMOTIVE OVERTURNING SAFETY

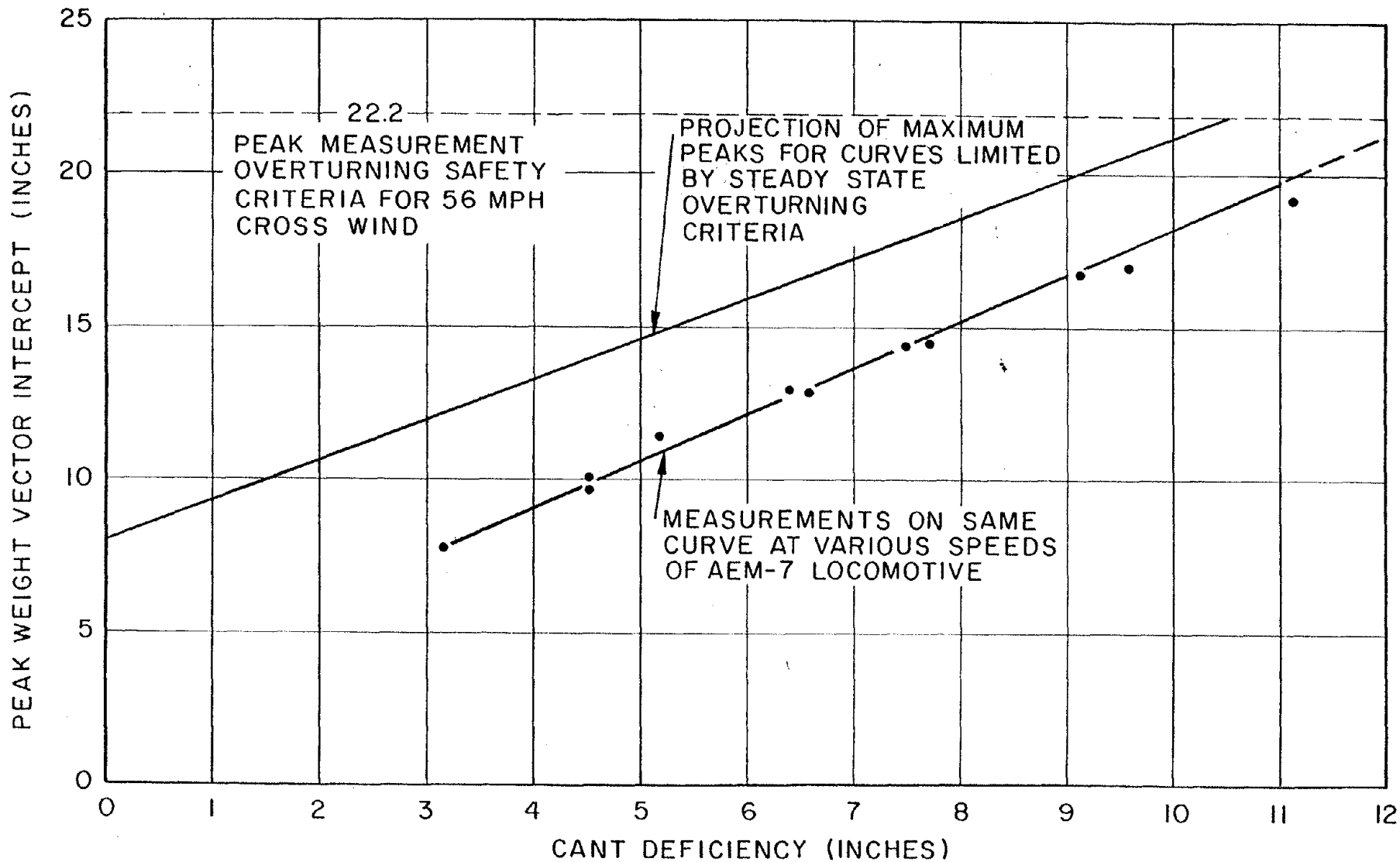


FIGURE 8-3

COMPARISON OF PEAK WEIGHT VECTOR INTERCEPT MEASURED ON ENTRY SPIRAL OF LEFT HAND TEST CURVE TO PROJECTED MAXIMUM PEAKS FOR CURVES LIMITED BY STEADY STATE OVERTURNING CRITERIA

the peak measurement lies on the projection line. If the cant deficiency were increased, the peak vector intercept would be expected to increase along the projection line. It would reach the critical value of 22.2 inches at 10-1/2 inches cant deficiency which is also the cant deficiency limit set by the steady state criteria. If the cant deficiency were increased at curve 373, where the measurement exceeds the projection line, the peak vector intercept would be estimated to follow the dashed line parallel to the projection line. At this perturbed curve, the critical level would be reached at only 4-1/2 inches cant deficiency. Curves at which peak vector intercept measurements exceed the projection line are not being negotiated unsafely at the test cant deficiency, but the cant deficiency at which the transient overturning safety criteria is achieved is lower than the limit set by the steady state criteria.

Figure 8-4 through 8-7 compare groups of curves on the NEC between New York and Washington to the projection of the transient overturning criteria which indicates curves potentially limited to lower cant deficiency by this criteria. The projection line was exceeded at many curves at which the absolute transient overturning criteria would be expected to limit the AEM-7 to less than 10-1/2 inches cant deficiency in the absence of any other speed restrictions. Table 8-1 lists the curves which fall on or above the projection line. The measurement of peak weight vector intercept, the test speed and cant deficiency, the estimated maximum safe cant deficiency and limiting factor, and the presence of unusual features are identified for each curve.

There are three categories of curves listed in Table 8-1. Curves in the first category were tested at a very high speed relative to a low cant deficiency because of their low curvature. Considerable side to side dynamic weight transfer occurs at moderate track geometry deviations because of the speed. However the 110 mph speed limit prevents operations at cant deficiencies high enough to produce critical weight vector intercept peaks. Many of the curves in all categories may be limited in speed by braking and accelerating rates from stations and slow curves, but only the overturning criteria and the maximum NEC track speed are considered for a worst case evaluation of the effect of track condition on overturning safety.

Curves of the second category have specific unusual features such as switches, grade crossings or undergrade bridges. Many have curvature so slight that the cant deficiency remains low at 110 mph, but the transient overturning safety criteria limits the safe operation of the AEM-7 on others. Curves 248, 373, 374, and 381 westbound and curves 253, 297, 374, and 375 eastbound cause dynamic side to side weight transfer in the AEM-7 great enough to

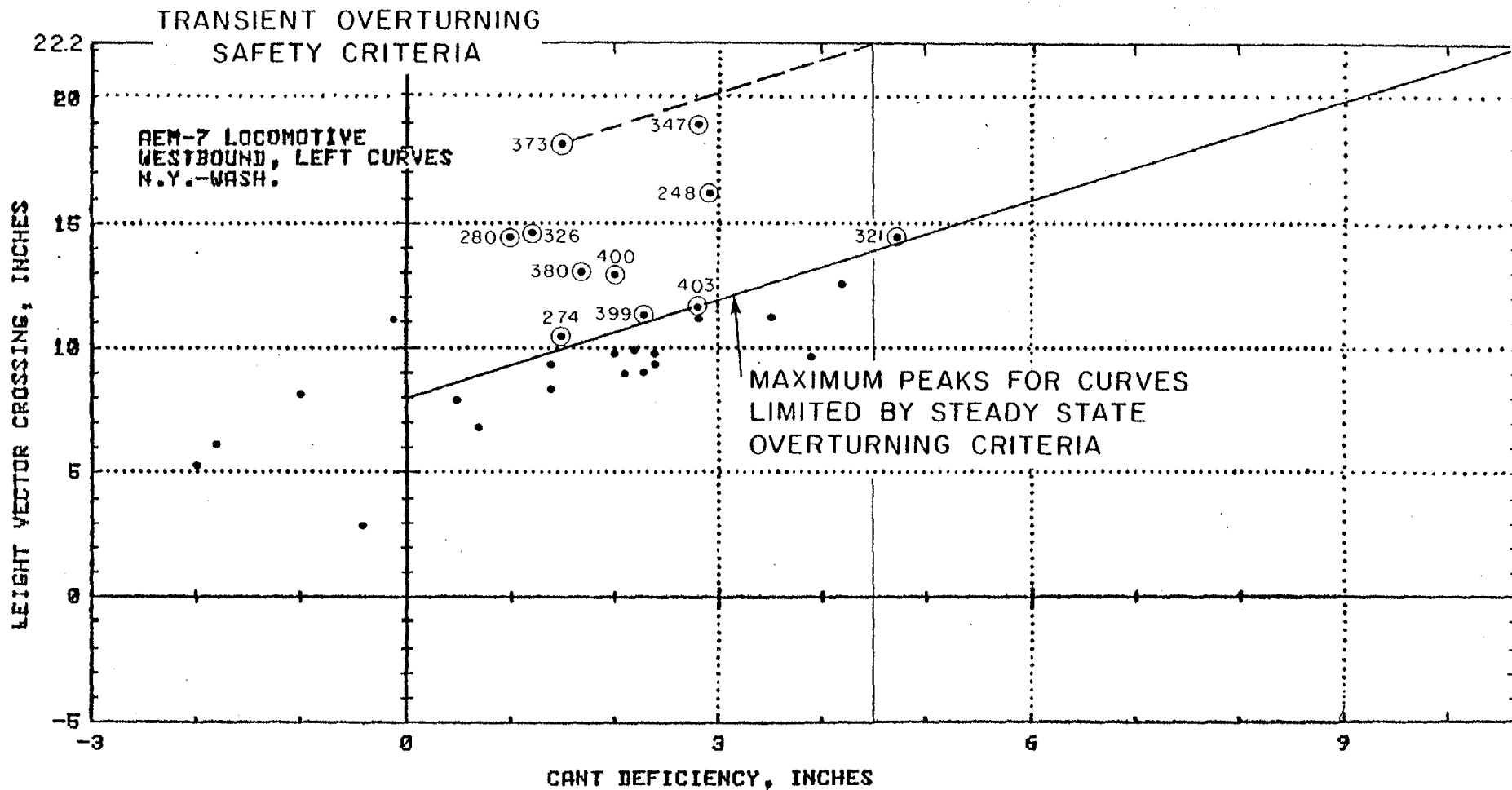


FIGURE 8-4

COMPARISON OF PEAK MEASUREMENTS OF WEIGHT VECTOR INTERCEPT FOR CURVES IN NEC TEST ZONE TO MAXIMUM PEAKS FOR CURVES LIMITED BY STEADY STATE OVERTURNING CRITERIA.

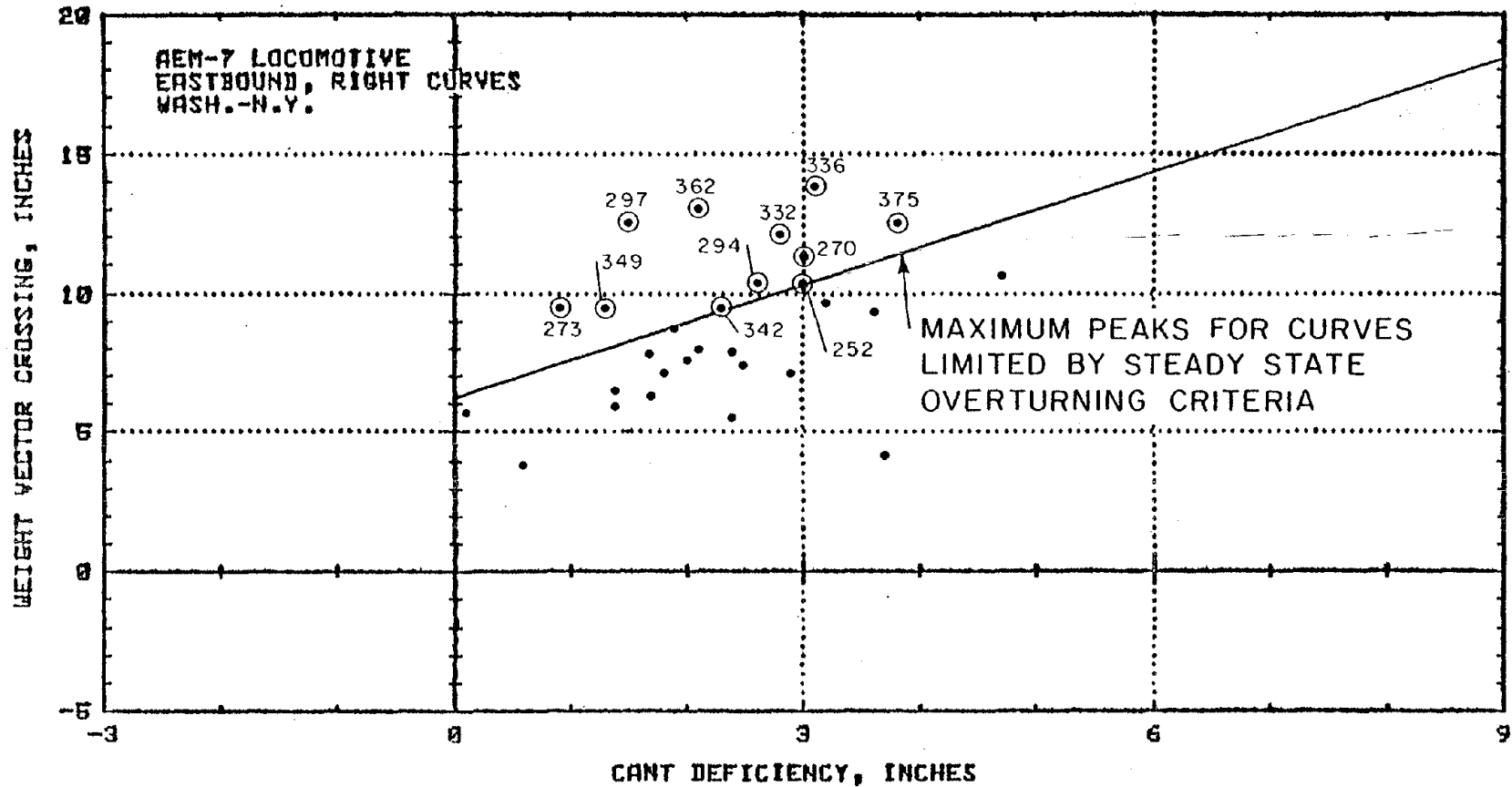


FIGURE 8-5

COMPARISON OF PEAK MEASUREMENTS OF WEIGHT VECTOR INTERCEPT FOR CURVES IN NEC TEST ZONE TO MAXIMUM PEAKS FOR CURVES LIMITED BY STEADY STATE OVERTURNING CRITERIA.

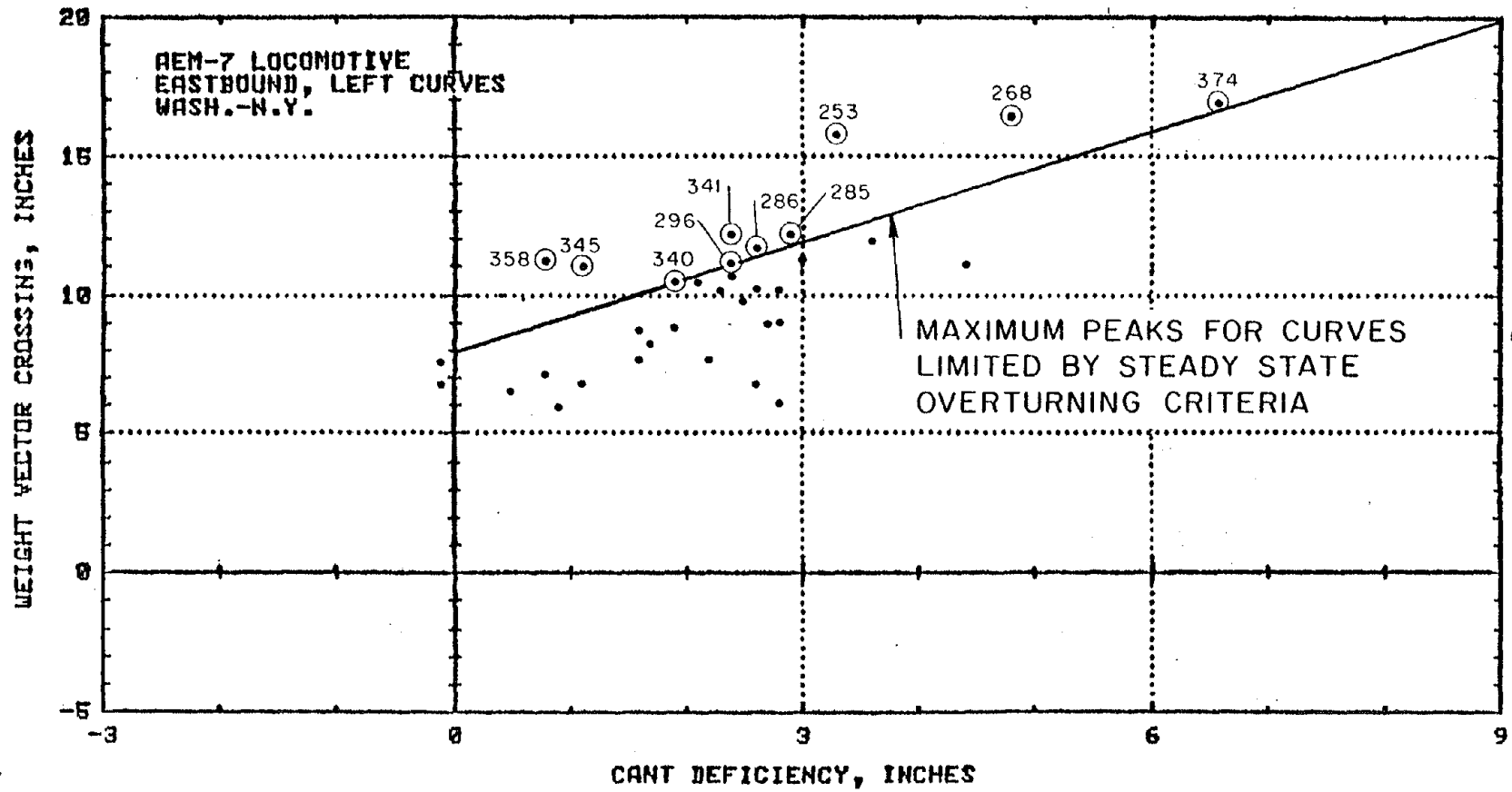


FIGURE 8-6

COMPARISON OF PEAK MEASUREMENTS OF WEIGHT VECTOR INTERCEPT FOR CURVES IN NEC TEST ZONE TO MAXIMUM PEAKS FOR CURVES LIMITED BY STEADY STATE OVERTURNING CRITERIA.

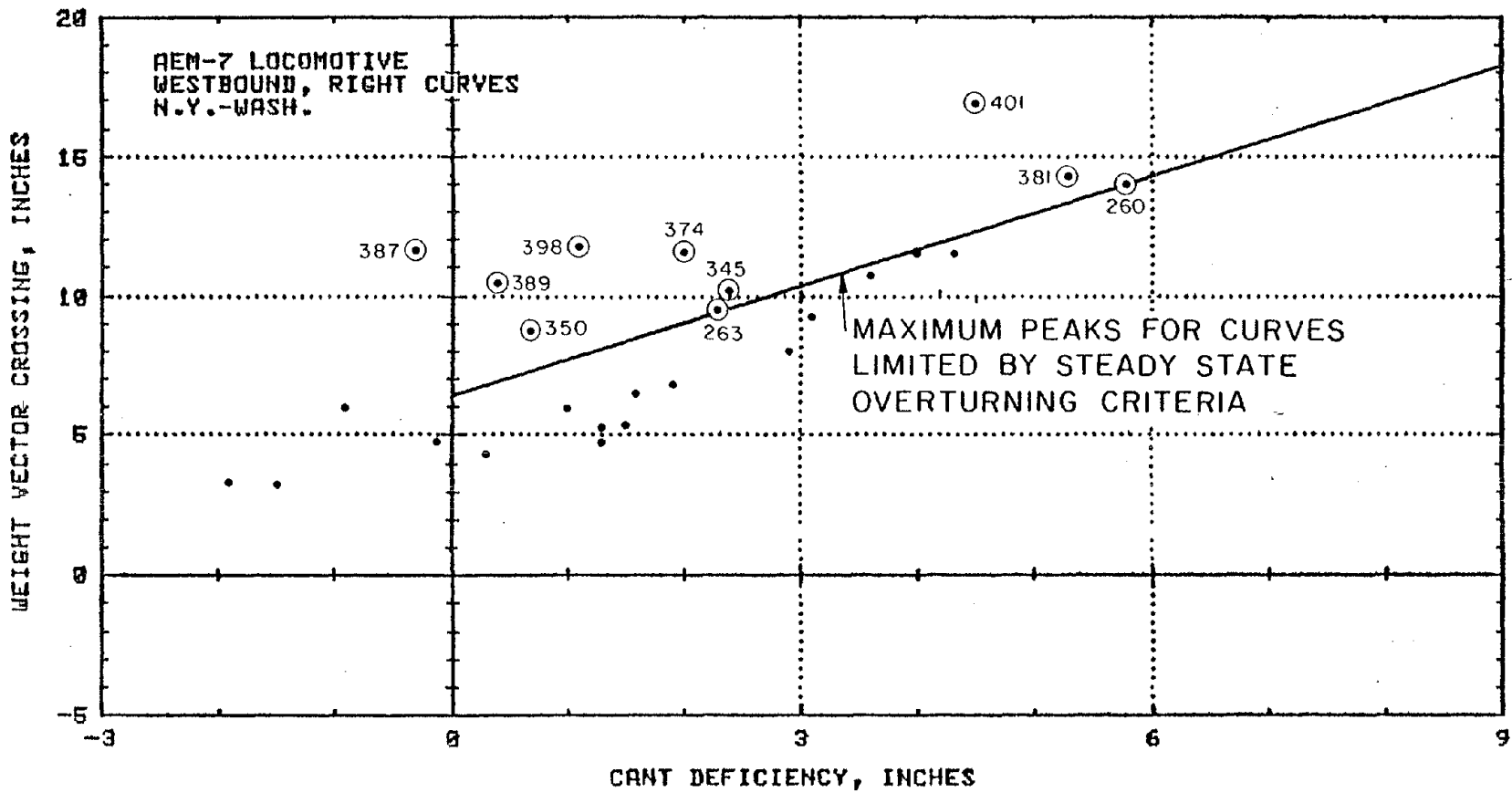


FIGURE 8-7

COMPARISON OF PEAK MEASUREMENTS OF WEIGHT VECTOR INTERCEPT FOR CURVES IN NEC TEST ZONE TO MAXIMUM PEAKS FOR CURVES LIMITED BY STEADY STATE OVERTURNING CRITERIA.

TABLE 8-1

CURVES AT WHICH THE PEAK WEIGHT VECTOR INTERCEPT
WAS HIGH IN RELATION TO CANT DEFICIENCY

Curve Number	Peak Vector Intercept (inches)	Test Conditions		Estimated Maximum Cant Defi- ciency (in)	Limiting* Factor	Unusual* Features
		Speed (mph)	Cant Deficiency (inches)			
Category I - Curves (w/o unusual features) limited by maximum track speed.						
263W	9.5	102.0	2.3	3.1	110 mph	-
274W	10.5	109.2	1.5	1.5	110 mph	-
280W	14.4	93.2	1.5	3.0	110 mph	-
294E	10.4	98.6	2.6	4.2	110 mph	-
296E	11.1	97.6	2.4	3.4	110 mph	-
340E	10.5	107.3	1.9	2.3	110 mph	-
341E	12.2	109.1	2.4	2.5	110 mph	-
342E	9.5	69.7	2.3	6.5	110 mph	-
345W	10.1	108.7	2.4	2.5	110 mph	-
362E	13.0	110.1	2.1	2.1	110 mph	-
389W	10.5	79.7	0.4	2.6	110 mph	-
398W	11.8	103.2	1.1	2.1	110 mph	-
399W	11.3	105.5	2.3	3.0	110 mph	-
401W	16.9	100.8	4.5	6.6	110 mph	-
403W	11.1	98.0	2.8	4.6	110 mph	-
Category II - Curves with unusual features.						
248W	16.1	56.5	2.9	7.4	TOC	SC
252E	10.3	70.5	3.0	10.5	SSOC	UGB
253E	15.7	73.5	3.3	8.1	TOC	UGB
270E	11.3	101.2	3.3	4.0	110 mph	UGB
273E	9.5	90.9	0.9	2.3	110 mph	UGB
285E	12.2	107.3	2.9	3.2	110 mph	UGB
286E	11.7	107.4	2.6	2.8	110 mph	UGB
297E	12.5	60.6	1.5	7.6	TOC	SC
321W	14.4	107.8	4.7	4.9	110 mph	UGB
326W	14.6	98.0	1.2	1.9	110 mph	UGB
332E	12.1	108.2	2.8	3.1	110 mph	UGB
336E	13.8	108.1	3.1	3.2	110 mph	UGB
347W	18.9	99.4	2.8	4.7	110 mph	UGB
349E	9.5	77.6	1.3	4.5	110 mph	UGB
350W	8.7	82.5	0.7	3.5	110 mph	UGB
358E	11.2	106.0	0.8	0.9	110 mph	GC
373W	18.1	62.0	1.5	4.7	TOC	SC
374E	16.9	56.9	6.6	10.3	TOC	UGB
374W	11.5	44.3	2.0	8.8	TOC	UGB

TABLE 8-1 (Cont'd)

CURVES AT WHICH THE PEAK WEIGHT VECTOR INTERCEPT
WAS HIGH IN RELATION TO CANT DEFICIENCY

<u>Curve Number</u>	<u>Peak Vector Intercept (inches)</u>	<u>Test Conditions</u>		<u>Estimated Maximum Cant Defi- ciency (in)</u>	<u>Limiting* Factor</u>	<u>Unusual* Features</u>
		<u>Speed (mph)</u>	<u>Cant Deficiency (inches)</u>			
Category II - Curves with unusual features (cont'd)						
375E	12.5	44.8	3.8	9.6	TOC	UGB
381W	14.3	58.9	5.3	9.8	TOC	UGB
387W	11.6	80.5	-0.3	3.9	110 mph	UGB
400W	12.9	102.4	2.0	3.1	110 mph	UGB

Category III - Curves (w/o unusual features) limited by vehicle overturning safety

268E	16.5	90.8	4.8	8.9	TOC	-
268W	14.0	91.6	5.8	10.5	SSOC	-
380W	13.0	38.0	1.7	8.5	TOC	-

*Legend: SC - Switch in Curves
 UGB - Undergrade Bridge
 GC - Grade Crossing
 TOC - Transient Vehicle Overturning Criteria
 SSOC - Steady State Vehicle Overturning Criteria

limit its safe speed below that imposed by the steady state overturning criteria or the maximum track speed. The most severe curve is 373 westbound which includes a switch, and operation over about 4-1/2 inches of cant deficiency would violate the transient overturning safety criteria.

Curves of the third category are those which have no unusual features identified on the track chart, but at which the curving speed of a vehicle would be limited by transient side to side weight transfer. The peak weight vector intercept measurements of the AEM-7 locomotives were disproportionately high at curves 268 eastbound and 380 westbound in the third category. The transient overturning safety criteria would limit the AEM-7 to operation at between 8 and 9 inches of cant deficiency rather than 10-1/2 as indicated by the steady state criteria.

A significant number of curves in the test zone have geometry perturbations which limit the safe cant deficiency of the AEM-7 by dynamic load transfer before the steady state limits are reached. Particularly severe disturbances are associated with switches in curves, but other less obvious features of the test curves should be identified for comparison to the curves which were not included in the test.

8.1.4 TRANSIENT MEASUREMENTS AT TANGENT SWITCHES

The tendency for switches in curves to excite pronounced dynamic responses raises interest in switches on tangent track. Peak weight vector intercept was monitored at each switch for a two-way pass over the test zone between New York and Washington. Figures 8-8 and 8-9 show plots of the test results against speed. The most obvious way of judging whether switches tested at low speed would cause dynamic load transfer in excess of the transient overturning criteria at maximum track speed is to compare their measurements to a linear projection of the overturning criteria, from 22.2 inches peak weight vector intercept at 110 mph to zero at rest. The trend of the data, however, is that most switches produced peak weight vector intercepts falling in a band between 6 and 11 inches even though some switches were traversed at much higher speeds than others. As a result the low speed measurements exceed the projected overturning criteria while those at higher speeds are below it. This observation implies either that the dynamic weight transfer at switches is not very sensitive to speed or that the train engineer adjusted the speed at each switch for a relatively uniform level of roll impulse. The latter case appears likely because for most of the switches below 40 mph the test speed was well below the track chart speed.

Particularly high measurements were made at the South St. and Canton interlocks, shown in Figure 8-8, but these switches occur

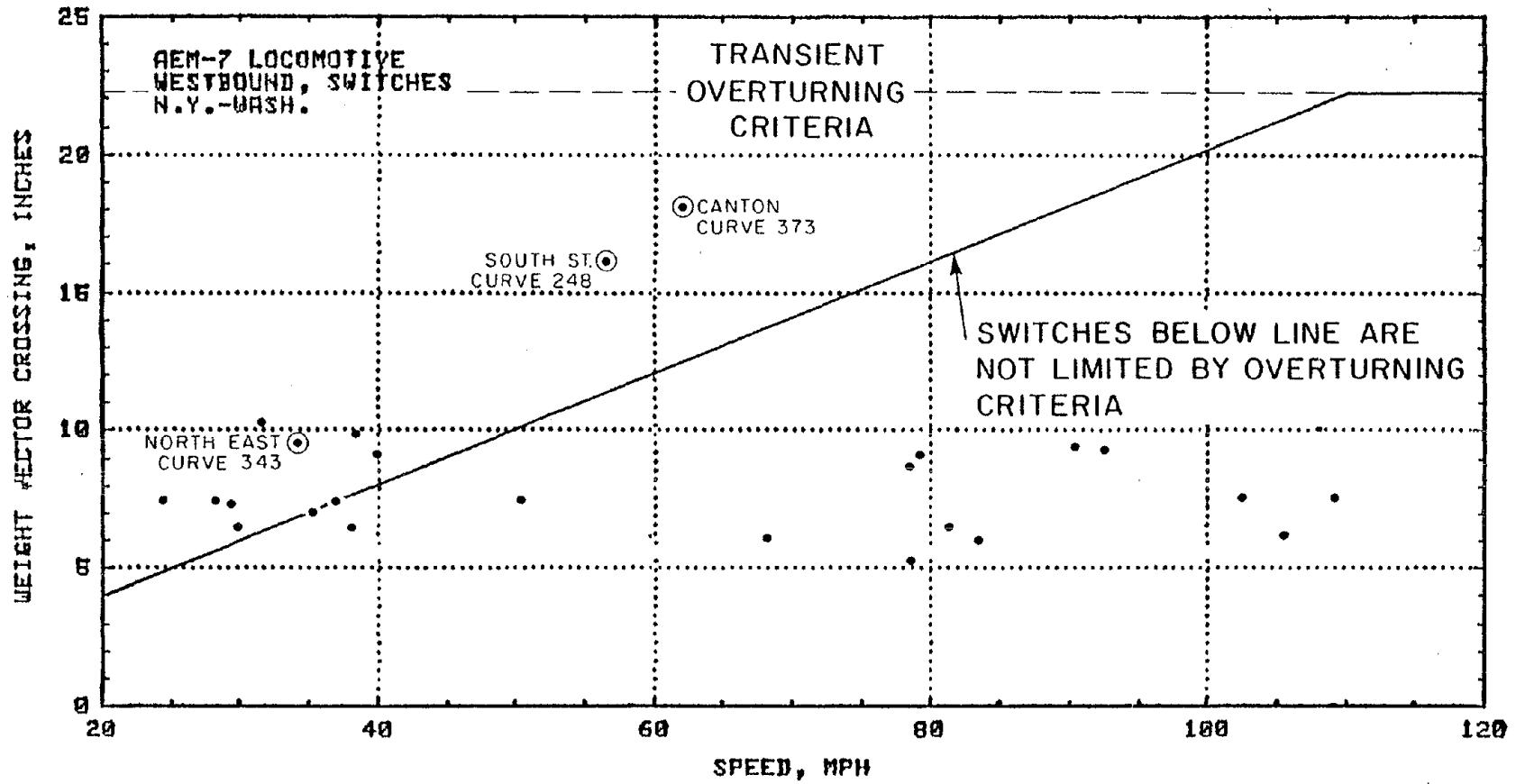


FIGURE 8-8

COMPARISON OF PEAK MEASUREMENTS OF WEIGHT VECTOR INTERCEPT AT SWITCHES IN THE NEC TEST ZONE TO THE VEHICLE OVERTURNING SAFETY CRITERIA

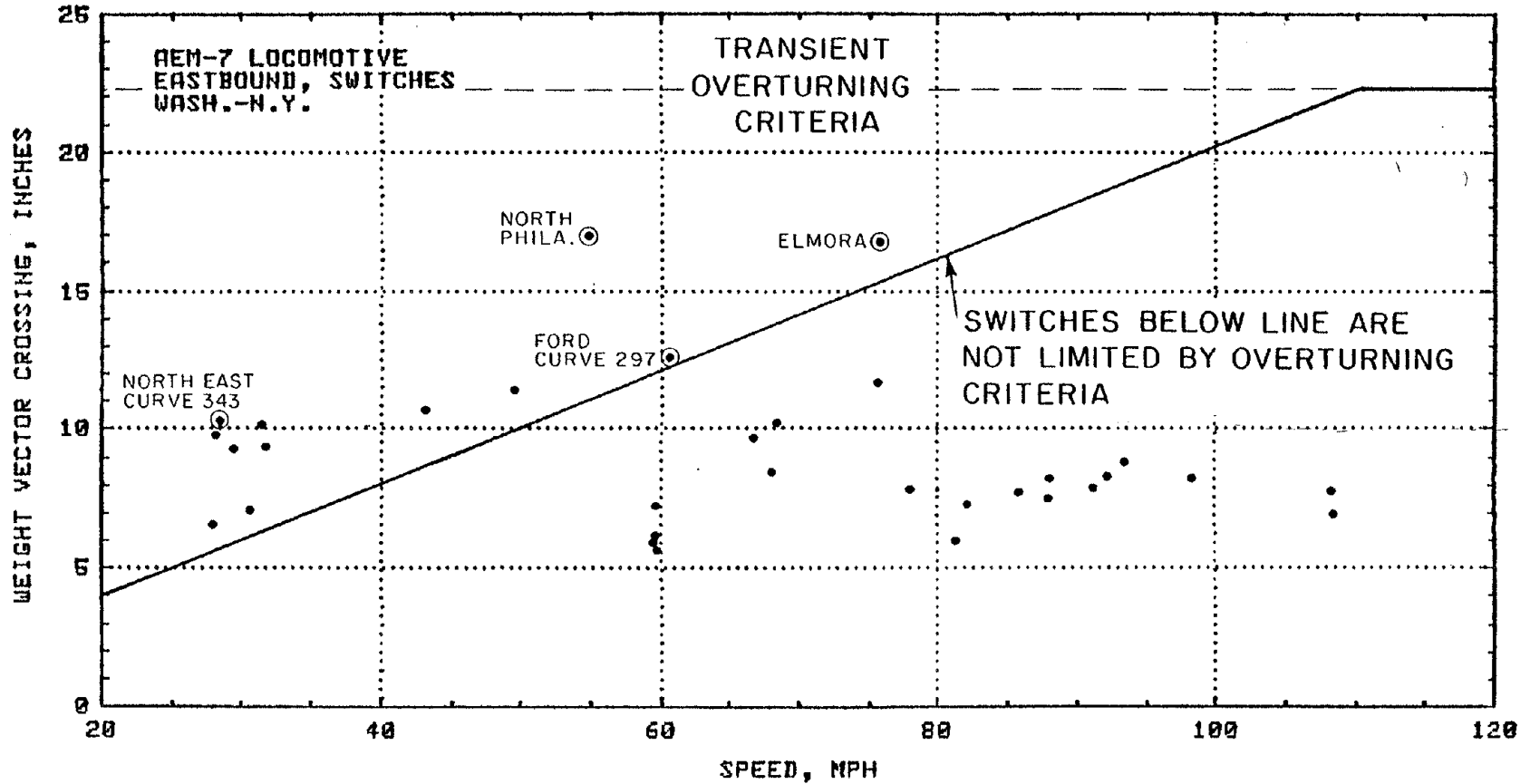


FIGURE 8-9

COMPARISON OF PEAK MEASUREMENTS OF WEIGHT VECTOR INTERCEPT AT SWITCHES IN THE NEC TEST ZONE TO THE VEHICLE OVERTURNING SAFETY CRITERIA

in curves. However, the interlocks at North Philadelphia and Elmora at which the highest measurements shown in Figure 8-9 occur are on tangent track. Speed restrictions or track work at many switches may be required especially for operation of the AEM-7 at higher cant deficiency.

8.2 RAIL ROLLOVER

Rail rollover is related to peak truck side L/V ratios. The peak rather than steady-state should be considered because this mode of derailment may be rapid and pulses of relatively low energy are capable of turning the rail whereas a great amount of energy is required to overturn a vehicle with its great inertia.

A suitably conservative rail rollover criteria should assume zero pull out resistance of the fasteners. Only the geometry of the rail section and the torsional stiffness of the surrounding rail should be considered for a general safety criteria.

Section 5.0 describes a rail rollover criteria based on the above two factors. It can be expressed as maximum truck side $L/V = 0.5 + 2300/P_w$, where P_w is the single wheel nominal vertical load. This criteria may underestimate the effect of rail section geometry and overestimate the effect of torsional stiffness of the surrounding rail but it appears to be based on the best available information. It should be interpreted as a restriction based on measurements having time duration of more than 50 milliseconds. Higher measurements are permitted for lesser time durations.

For the AEM-7 Locomotive, $P_w \approx 25,000$ lb, and a limiting value of 0.59 should be compared to the peak measurements of truck side L/V ratio. Figure 8-10 compares the measurements taken at the right and left test curves to the criteria. At these relatively smooth curves, the measurements were far below the critical level. Truck L/V ratio measured at the high rail side of the AEM-7 locomotive did not increase rapidly with cant deficiency because of the moderating influence of the vertical load transfer, and the performance was virtually identical for right and left curving.

Higher measurements occurred in the NEC test zone between New York and Washington. The highest measurement was 0.39 at 1.5 inches of cant deficiency on curve 297. Assuming the relationship between truck L/V ratio and cant deficiency, as shown in Figure 8-10, a ratio of about 0.51 would be projected at 10-1/2 inches of cant deficiency. Therefore, despite the presence of a rough switch (which may brace the rail against rollover) critical levels of truck L/V ratio would not be expected. The most severe measurement in a curve without a switch was 0.32 on curve 280 at

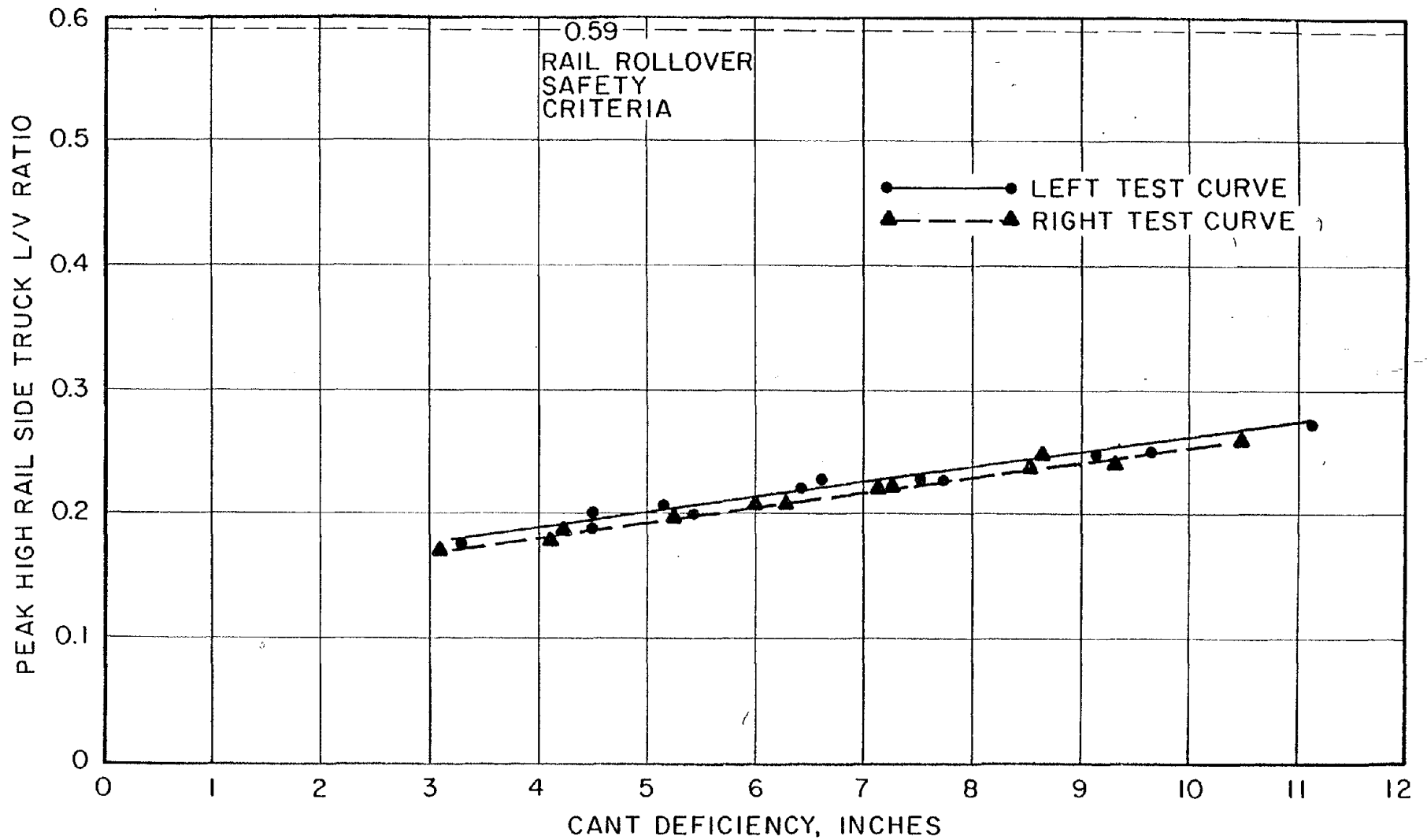


FIGURE 8-10

PEAK TRUCK L/V RATIO OF THE AEM-7 LOCOMOTIVE, AS A FUNCTION OF CANT DEFICIENCY MEASURED AT RIGHT AND LEFT TEST CURVES

1 inch cant deficiency, and a ratio of less than 0.45 is projected at 10-1/2 inches of cant deficiency. The rail rollover criteria does not limit the operational cant deficiency of the AEM-7 locomotive.

8.3 LATERAL TRACK SHIFT

Although the inertia and pulse energy requirement to move the track structure laterally is much greater than that required for rail rotation, the peak force levels of about 50ms duration provide a conservative measure of safety. Using a single wheel force rather than axle force introduces another estimate on the conservative side because the net axle force which moves the track is usually less than a single wheel peak force as the wheel forces on the same axle tend to oppose one another.

The safety criteria discussed in Section 5.0 assumes compacted ballast for full operational cant deficiency, and it allows for the force of crosswinds encountered in service. For the conservative assumption of wood ties, the criteria can be expressed as follows:

$$F_{\max} = 1 - \frac{A\Delta\theta}{22320} (1 + .458D) [.7P + 6600] - (1.28 \times 10^{-3}SV^2)$$

A = rail cross section area, in²

$\Delta\theta$ = max temperature change after rail installation, °F

D = track curvature, degrees

P = vertical axle load, lbs.

S = lateral surface area of vehicle, ft²

V = lateral wind speed, mph

and it is assumed that a single axle bears half the entire wind load. For typical NEC conditions of 140 lb rail (A = 13.8 in², $\Delta\theta$ max of 70°F and D max of 4°.

$$F_{\max} = .61P + 5800 - 1.28 \times 10^{-3} SV^2$$

For the AEM-7 locomotive axle load of 49,500 lb and an allowance for 56 mph crosswinds the maximum permissible lateral axle force is 34,000 lb. The maximum truck lateral force for a two axle

truck should be limited to only 1.4 times the single axle maximum lateral force since fewer than twice the number of ties support the lateral force. The lateral track shift criteria permits a maximum truck lateral force of 48,400 lb allowing for one half of the 56 mph crosswind body side load at each truck.

Figure 8-11 compares the high rail lead wheel and truck side peak lateral force measurements on the right and left test curves to the rail rollover criteria. Both measurements remain at less than half the critical levels at 11 inches of cant deficiency on the relatively smooth test curves.

The peak measurements of truck side lateral force taken on the NEC test zone, including many rough curves, was well below the safety criteria, even when projected to estimate the effect of perturbations at the maximum cant deficiency limited by other criteria. The highest measurement of truck side lateral force was 19.4 kips on curve 297 at 1.5 inches cant deficiency. Less than 33 kips was projected at 10-1/2 cant deficiency on this severe curve which includes a switch. The most severe curve, without a switch, was curve 280 at which 17.2 kips was measured at 1 inch of cant deficiency. If a curve with this degree of perturbation could be traversed at 10-1/2 inches of cant deficiency, less than 31 kips lateral force would be expected at the lead truck. Since the measurements and projections of truck lateral force are well below the critical level of 49 kips, the rail rollover safety criteria does not limit the safe cant deficiency of the AEM-7 locomotive.

8.4 WHEEL CLIMB

The most appropriate criteria of safety concerning wheel climb for comparison to the test results of the AEM-7 locomotive is that used by Amtrak in its acceptance specification. This criteria takes into account the AAR flange angle and it appears to have been based on conservative judgements. It states that the wheel (L/V) ratio must be less than $0.056/T^{-0.927}$ where T is the duration of the peak level in seconds and that the maximum wheel (L/V) ratio for peaks of duration greater than 50 milliseconds is 0.90.

Figure 8-12 shows that the wheel L/V ratio of the AEM-7 is very low with respect to the wheel climb safety criteria on unperturbed curves. It also shows that wheel L/V ratio is less sensitive than truck L/V to increases in cant deficiency indicating that the rear wheel bears a greater portion of the high rail lateral force as cant deficiency increases. The greater rear wheel lateral force suggests the possible benefit of a reduction in angle of attack at higher cant deficiencies.

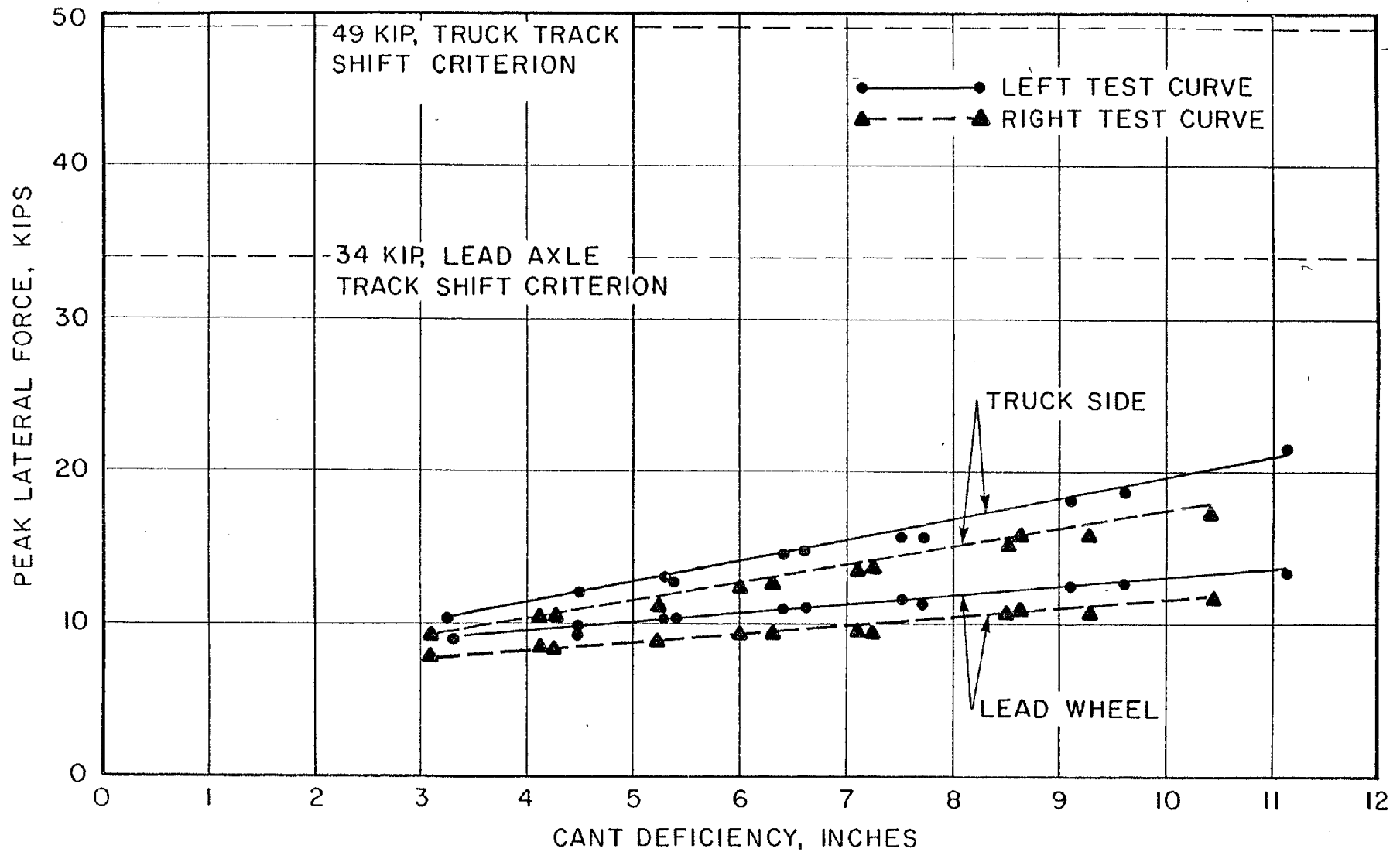


FIGURE 8-II

COMPARISON OF PEAK LATERAL FORCE MEASUREMENTS OF LEAD WHEEL AND TRUCK SIDE OF THE AEM-7 LOCOMOTIVE TO TRACK SHIFT CRITERIA.

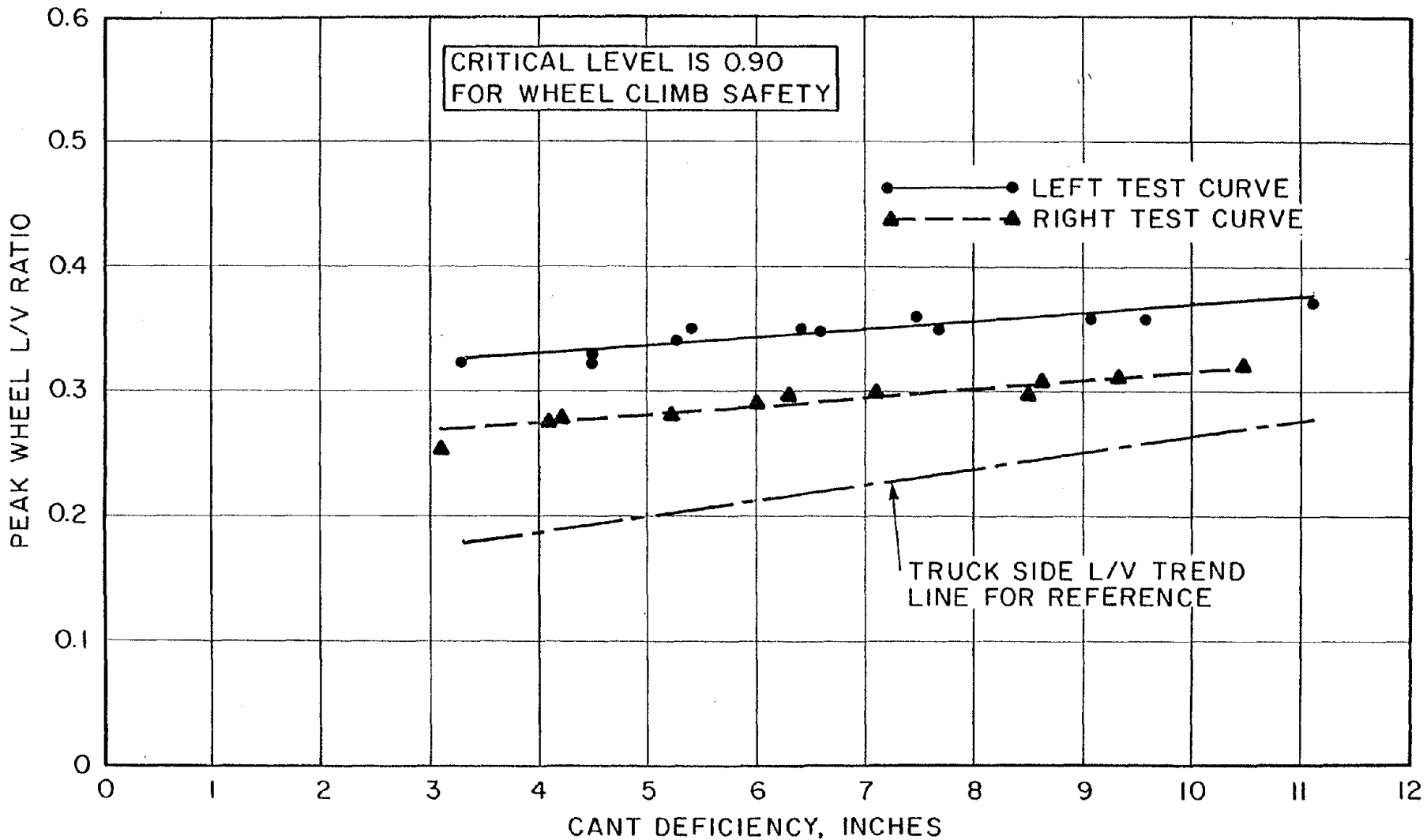


FIGURE 8-12

PEAK WHEEL L/V RATIO OF THE AEM-7 LOCOMOTIVE AS A FUNCTION OF CANT DEFICIENCY MEASURED AT RIGHT AND LEFT TEST CURVES

The curves in the test zone between New York and Washington which produced the greatest truck side L/V ratios were curves 280 westbound and 297 eastbound (which included a switch). Under the conservative assumption that the wheel L/V is twice the truck side L/V (no rear wheel lateral force) and projecting to 10-1/2 inches of cant deficiency, even these unusually harsh curves would not be expected to cause the AEM-7 to exceed the wheel climb criteria.

The peak wheel L/V ratio was also measured at switches because a lateral impact force without the benefit of simultaneous vertical load transfer may be the worst case for wheel climb of the AEM-7. Wheel L/V measurements westbound at the Fulton interlock and eastbound at the North Philadelphia interlock were disproportionately high with respect to train speed. A wheel L/V of 0.44 at 24.4 mph was measured at Fulton and 0.53 at 54.8 mph was measured at North Philadelphia. If the lateral force is approximately proportional to speed, the wheel climb criteria could be violated at rough switches at less than maximum tangent track speed. The test measurements, however, are not sufficient to establish a relationship between speed and switch forces since the engineer apparently adjusted his speed to compensate for roughness of the switches in the test zone. Limiting values of wheel L/V ratio are not predicted for the AEM-7 even in rough curves, but high speed tangent running through rough switches may exceed the wheel climb criteria.

8.5 RIDE COMFORT

Section 5.0 includes a variety of criteria for lateral acceleration used by organizations throughout the world as indices for ride comfort evaluation. The most commonly recognized standards in the U.S. are the AAR recommendations of 0.1g maximum steady state and 0.03g/sec maximum "jerk". The least restrictive standards are those of SNCF which permit 0.15g and 0.10g/sec respectively. The JNR has an additional standard of $\pm 0.08g$ maximum carbody "vibration" which pertains to the transient response of a carbody tilt system upon entering and exiting a curve.

When the AAR study was undertaken in the early 1950's, coach suspensions were designed such that large body roll angles occurred in curves. The component of gravitational acceleration in the plane of the coach floor added substantially to the centrifugal acceleration as the coach body rolled toward the outside of the curve. At three inches of cant deficiency, the body roll of contemporary coaches was usually sufficient to cause a total of 0.1g lateral acceleration in the plane of the floor.

Figure 8-13 shows that the AEM-7 locomotive suspension controls steady state body roll well. The AAR coach ride comfort criteria

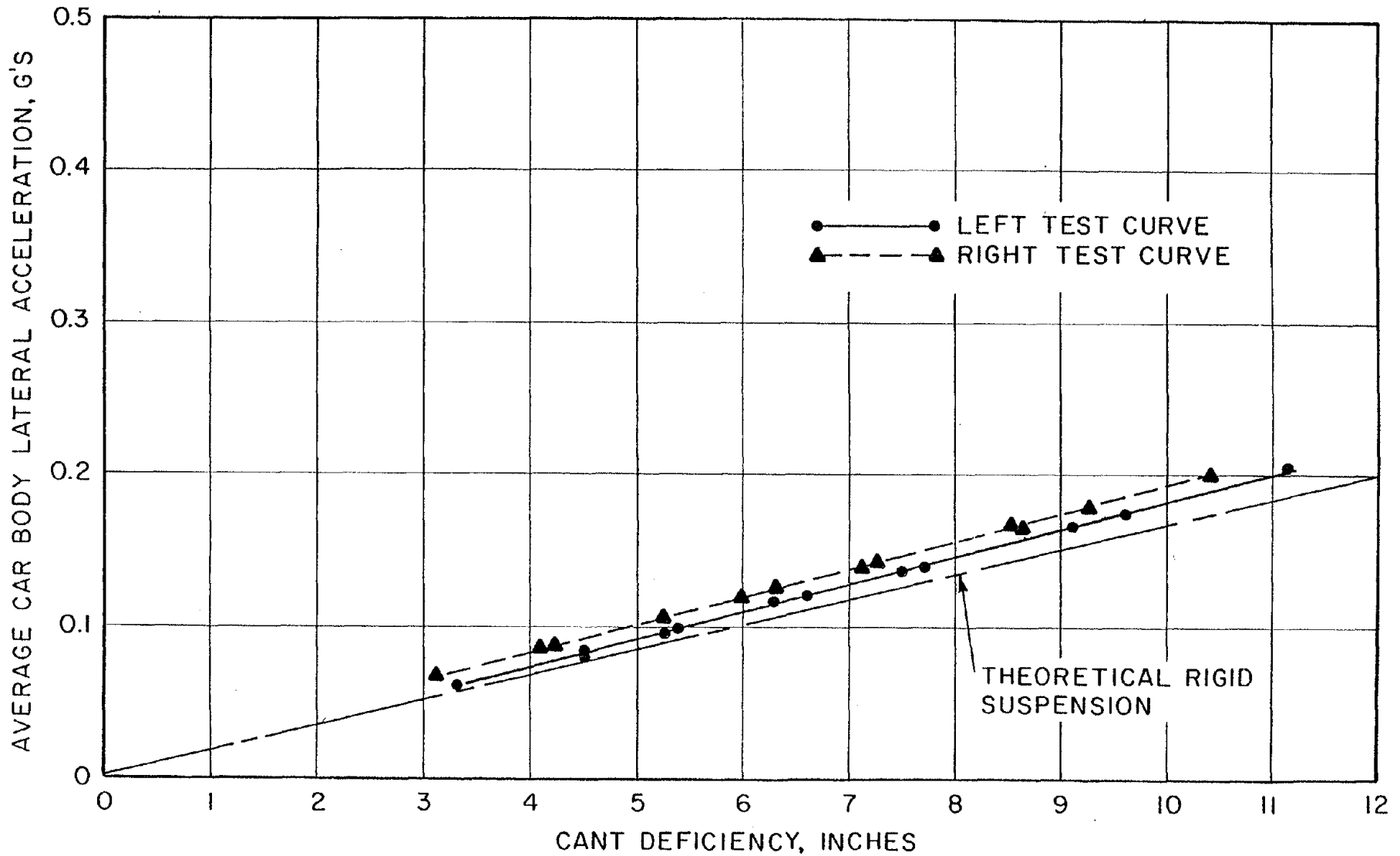


FIGURE 8-13
STEADY STATE LATERAL ACCELERATION OF THE AEM-7 LOCOMOTIVE
COMPARED TO A VEHICLE WITH ZERO ROLL ANGLE

is reached at between 5 and 5-1/2 inches of cant deficiency. A vehicle with zero body roll would reach this criteria at 6 inches of cant deficiency. The slight difference in lateral acceleration between right and left curving is probably due to an initial slant of the floor panel to which the accelerometer was attached.

8.6 MAXIMUM OPERATIONAL CANT DEFICIENCY

The operational cant deficiency of the AEM-7 locomotive is first limited by the vehicle overturning safety criteria. The critical level dictated by the steady state overturning safety criteria is reached at 10-1/2 inches of cant deficiency allowing for a simultaneous lateral wind of 56 mph. The measurements indicating safety against rail rollover, lateral track shift and wheel climb are well below critical levels at 10-1/2 inches of cant deficiency. However, the safety criteria against vehicle overturning based on transient measurements sets a lower limit of cant deficiency at some highly perturbed curves in the New York-Washington test zone. Most of the objectionable curves identified by the test data include an unusual feature such as a switch or undergrade bridge. At the worst curve, the safety limit probably would be exceeded at only 4-1/2 inches of cant deficiency. Two curves without special track work were also limited to as low as 8 inches of cant deficiency by the transient vehicle overturning safety criteria.

It is not feasible to limit the AEM-7 locomotive by the worst perturbation in the test zone. Steady state overturning safety provided the first limit at 10-1/2 inches of cant deficiency for "normal" curves. The abnormal curves, which may include others not measured in this test should be identified individually. Many may be limited by factors such as acceleration and braking distances or proximity to stations. The remainder should be either repaired if practical or given special speed restrictions. The measurements indicate safe operation at up to eight inches of cant deficiency at all curves without special trackwork. The identification and repair of problem curves could increase the safe cant deficiency to over 10 inches, but the coaches may well limit the train cant deficiency to a lower level due to of the more restrictive wind force factor on vehicles of lighter weight and greater surface area.

8.7 COMPARISON OF TEST RESULTS TO SIMPLE QUASISTATIC PREDICTIONS

A simple quasistatic model described in Appendix B was formulated to predict several steady state measurements. The published specifications of the vehicles and the results of statis tests to estimate weight distribution and suspension spring rates as installed, which were used in these calculations, are listed in Appendix C. Such predictions can be useful in estimating the

performance potential of vehicles limited by steady state criteria of overturning safety and lateral acceleration ride quality. Safety and ride quality considerations which depend on knowledge of peak values and of transient distributions of wheel forces are not likely to be satisfied by modeling because of the range of complex, interactive, and non-obvious track influences in service, which were sampled experimentally in the large test zone. Although steady state performance limits the AEM-7 curving speed in most curves, lower limits were indicated for some curves based on transient measurements.

Figures 8-14 and 8-15 show the measurements of weight vector intercept (from Figure 8-2) compared with the predictions. The agreement with predictions based on suspension constants deduced from spring deflection measurements of a locomotive stopped on superelevated track was excellent. The measurements of lateral acceleration (Figures 8-16 and 8-17), however, agreed more closely with predictions based on the published specifications of spring constants rather than on those based on the "as installed" spring constants.

In steady state curving with cant deficiency, the high rail lead wheel and both wheels of the trailing axle of the AEM-7 develop lateral forces in the direction of the curve, while the lateral creep force of the low rail lead wheel is in the opposite direction. The lateral component of the coefficient of friction on the low rail of the test curves was about 0.2. With an increase in cant deficiency, the lateral force of lead wheel on the high rail increases moderately and that of the trailing wheel considerably. The lateral creep force of the lead wheel on the low rail decreases due to vertical load transfer, and that of the trailing wheel increases until it saturates.

Figures 8-18 and 8-19 show truck lateral force, the high rail side lateral force, and the predicted truck lateral force as a function of cant deficiency. The high rail side lateral force is greater than the net truck lateral force below approximately 11 inches of cant deficiency, and the measured truck lateral force is within 20% of the predicted.

FIGURE 8-14

COMPARISON OF STEADY STATE WEIGHT VECTOR INTERCEPT PREDICTIONS TO TEST RESULTS FOR AEM-7 LOCOMOTIVE IN LEFT HAND CURVE

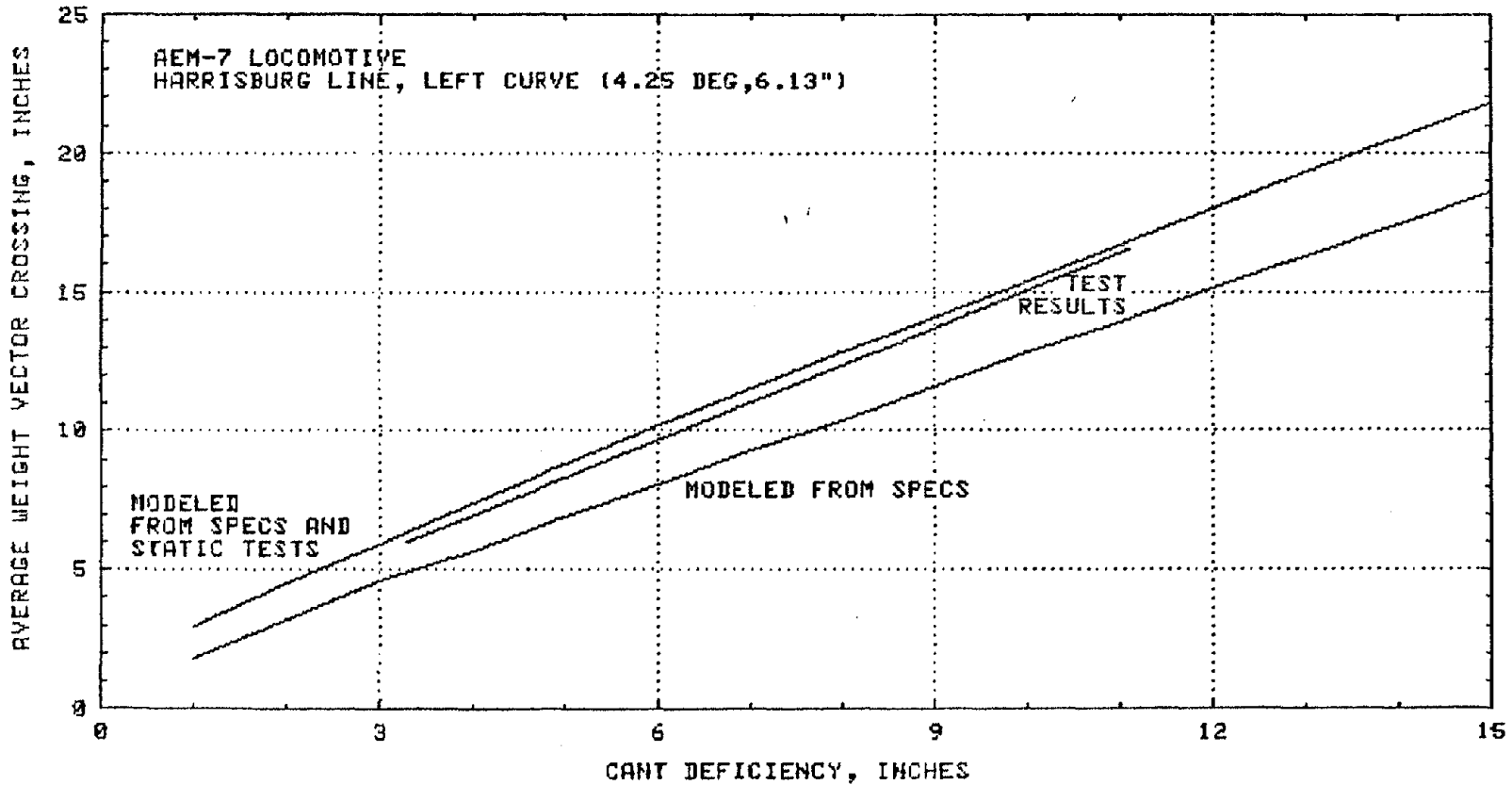


FIGURE 8-15

COMPARISON OF STEADY STATE WEIGHT VECTOR INTERCEPT PREDICTIONS TO TEST RESULTS FOR AEM-7 LOCOMOTIVE IN RIGHT HAND CURVE

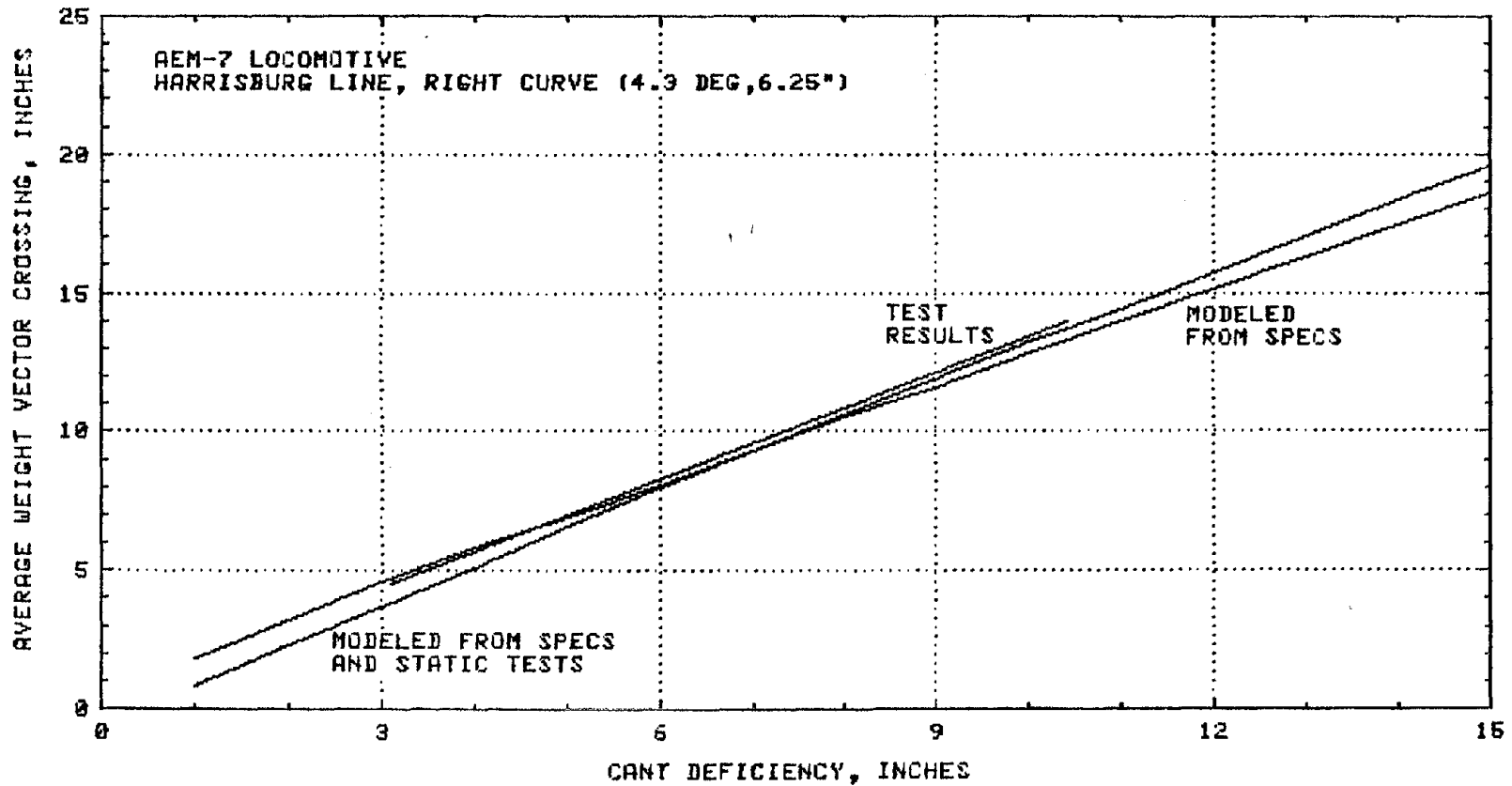
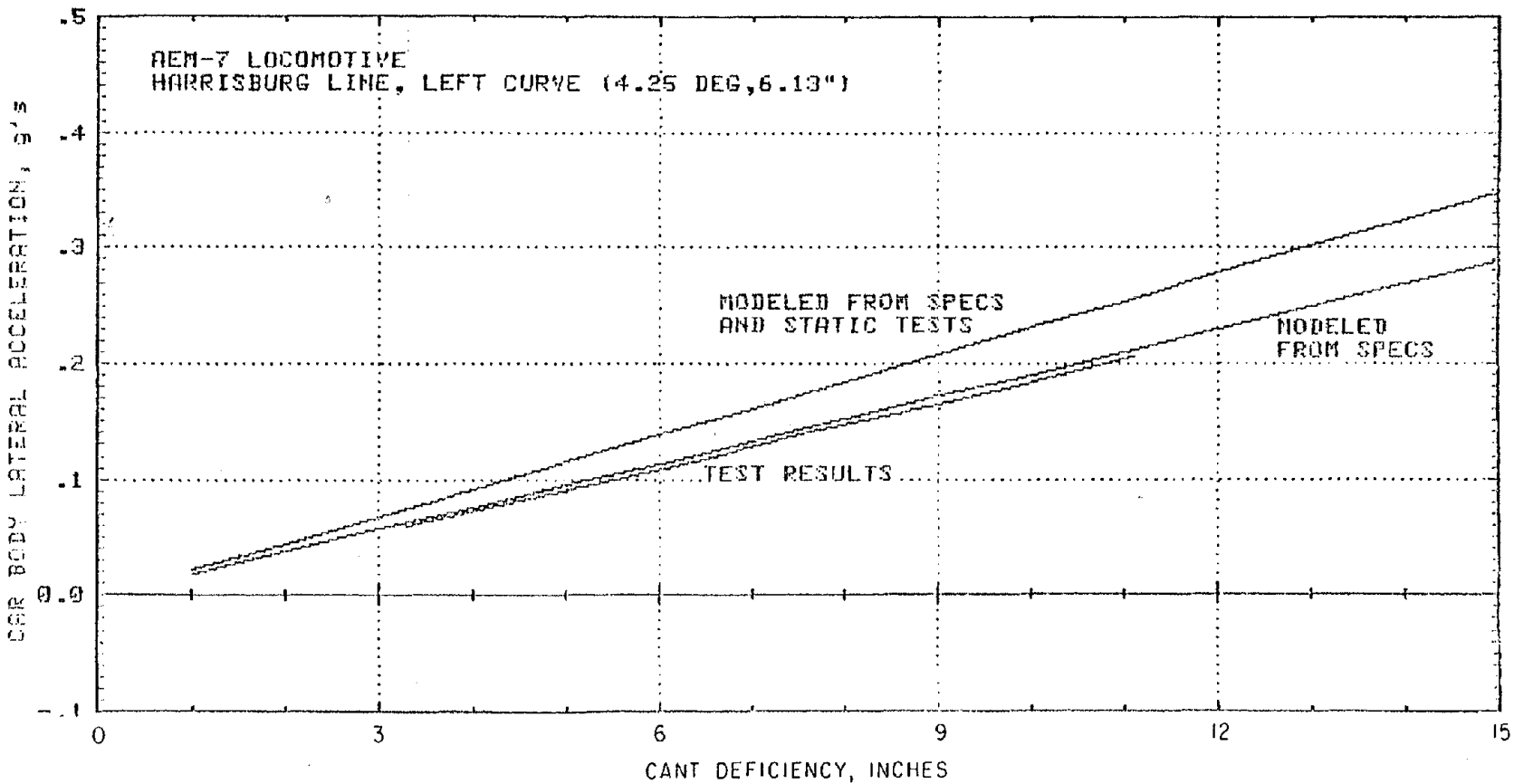


FIGURE 8-16

COMPARISON OF STEADY STATE CAR BODY LATERAL ACCELERATION PREDICTIONS TO TEST RESULTS FOR AEM-7 LOCOMOTIVE IN LEFT HAND CURVE



8-29

Reproduced from
best available copy

FIGURE 8-17

COMPARISON OF STEADY STATE CAR BODY LATERAL ACCELERATION PREDICTIONS TO TEST RESULTS FOR AEM-7 LOCOMOTIVE IN RIGHT HAND CURVE

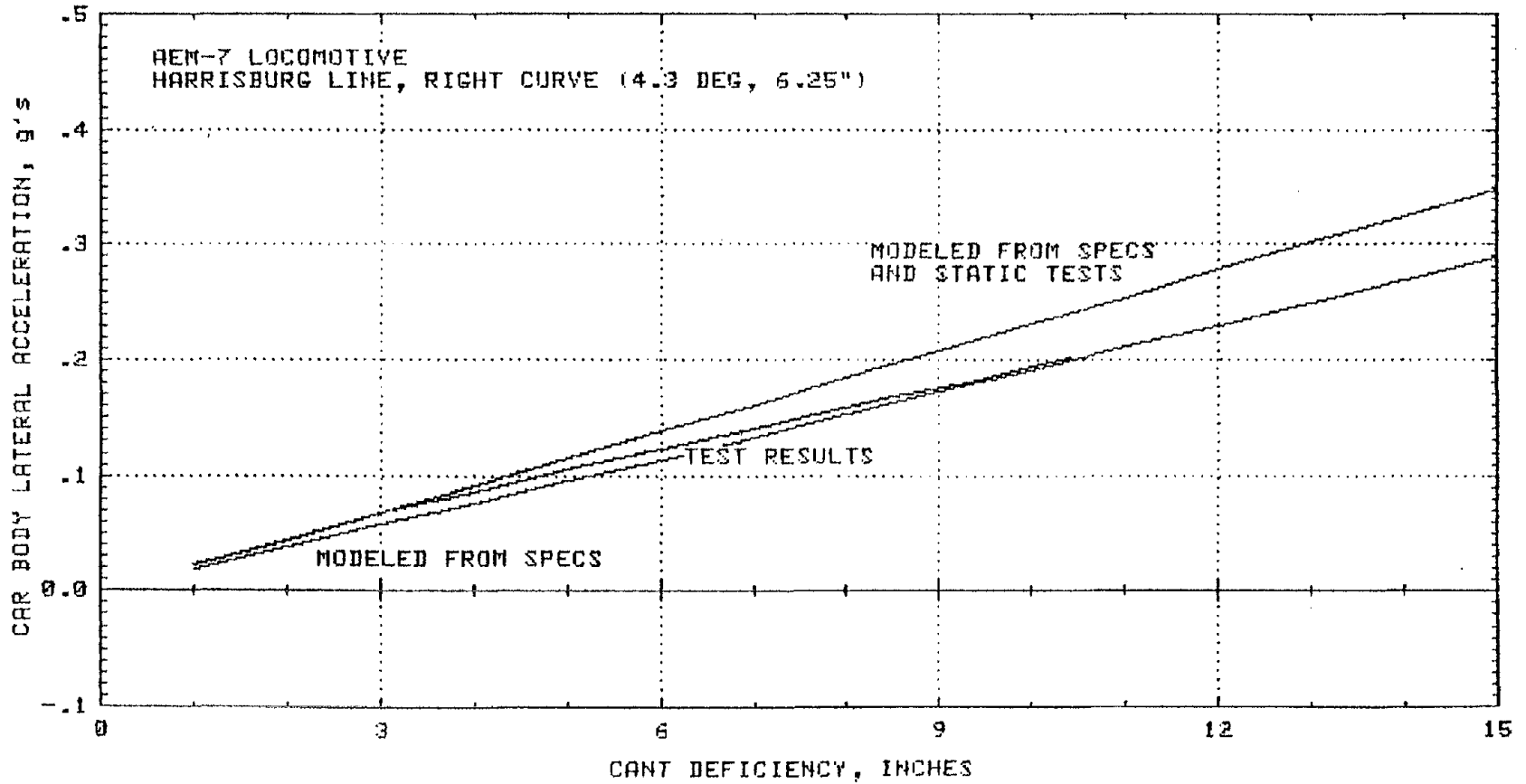


FIGURE 3-13

COMPARISON OF STEADY STATE NET TRUCK LATERAL FORCE PREDICTIONS TO TEST MEASUREMENTS OF HIGH RAIL SIDE TRUCK LATERAL FORCE FOR AEM-7 LOCOMOTIVE IN LEFT HAND CURVE

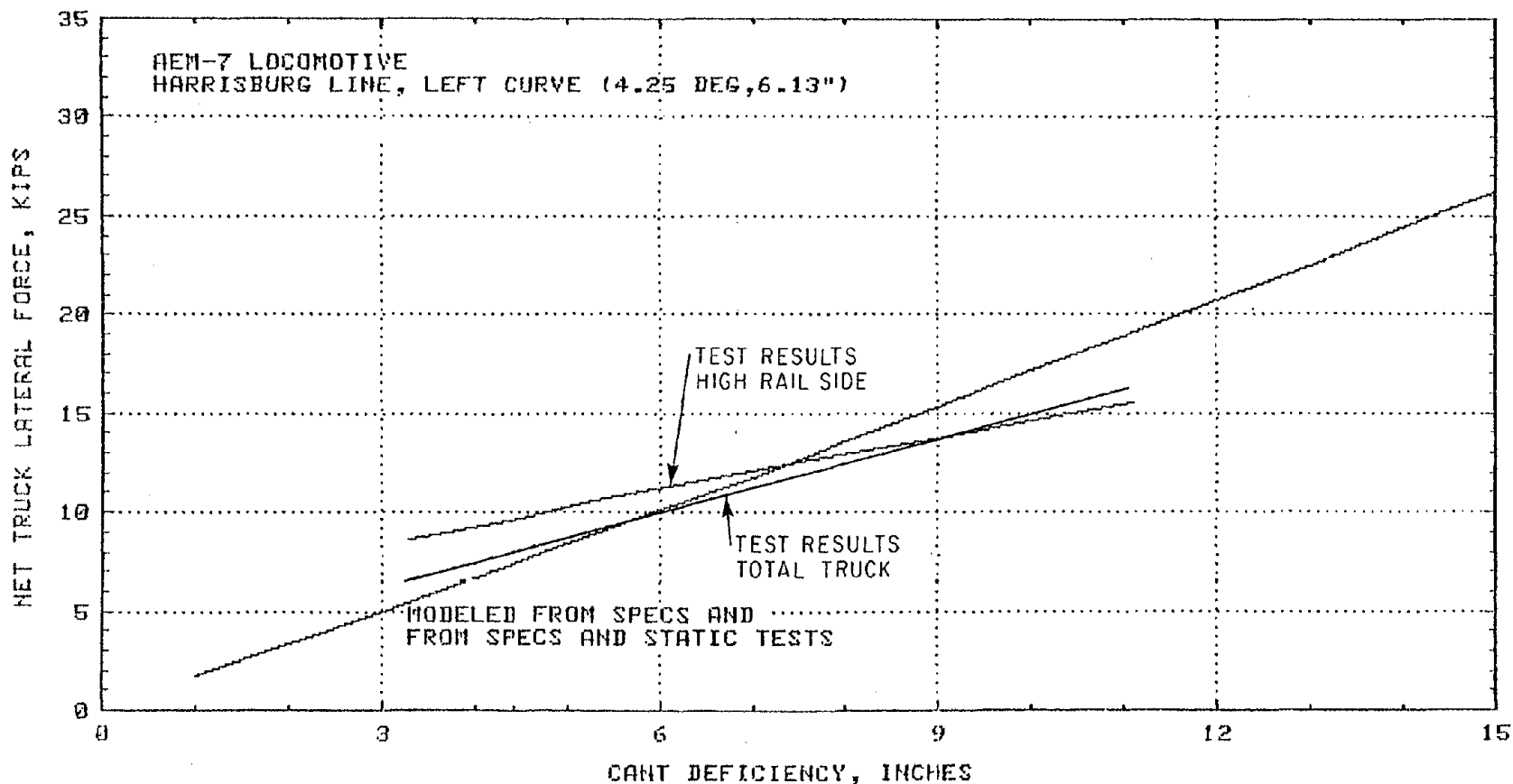
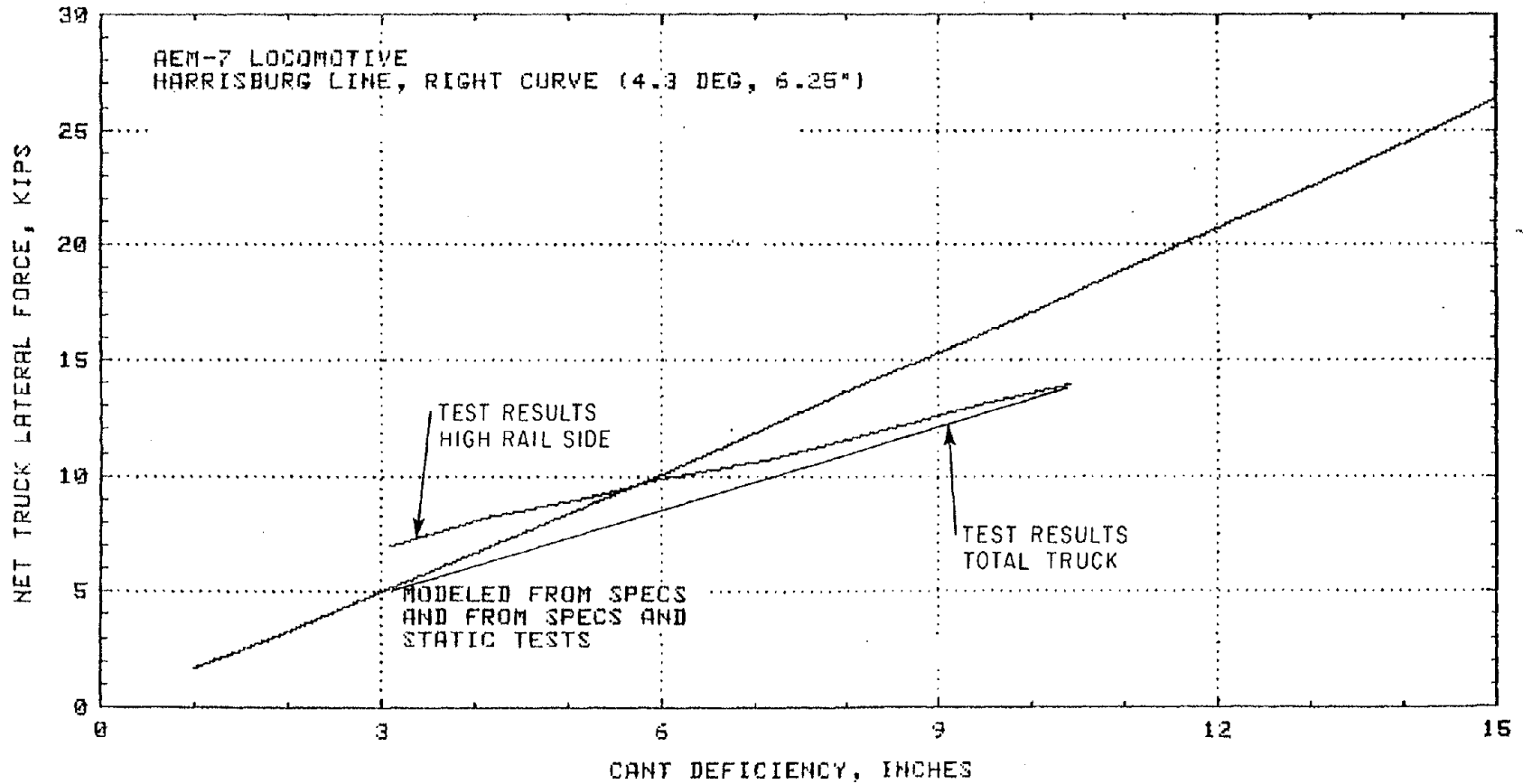


FIGURE 8-19

COMPARISON OF STEADY STATE NET TRUCK LATERAL FORCE PREDICTIONS TO TEST MEASUREMENTS OF HIGH RAIL SIDE TRUCK LATERAL FORCE FOR AEM-7 LOCOMOTIVE IN RIGHT HAND CURVE



9.0 GENERAL CONCLUSIONS

Several general conclusions can be reached about modern passenger equipment curving at high cant deficiency and about test methods for determining maximum safe cant deficiencies.

1. For simple unperturbed curves, the maximum cant deficiency of light weight vehicles with two axle trucks is determined by steady state side to side weight transfer (vehicle overturning).
2. The suspension roll center height, roll stiffness, and lateral suspension travel as well as center of gravity height determine steady state weight transfer.
3. A small number of curves on the Northeast Corridor have perturbations that cause transient weight transfer sufficient to lower the safe cant deficiency below the limit imposed by steady state vehicle overturning criteria.
4. Switches are commonly present at or near the exceptionable curves. Undergrade bridges are present at most of the others.
5. A lateral wind speed of 56 mph, the maximum for a 10 year mean recurrence interval at Boston measured 15 ft above the ground, is appropriate for conservative lateral force computations for vehicles running on the NEC. The effect of this lateral wind speed was included in the vehicle overturning and lateral track shift safety criteria.
7. The overturning safety of the coaches limit the safe cant deficiency of a consist due to the proportionately greater "billboard" effect at the maximum lateral wind speed allowance.
8. Except at a few unusually harsh curves, the LRC train can operate safely at 9 inches cant deficiency while maintaining less than 0.1g lateral acceleration at the coach floor (the AAR Ride Comfort Criteria).
9. An AEM-7 Locomotive towing standard Amcoaches can operate safely at 8 inches cant deficiency except at unusual curves. The steady state lateral acceleration in the coach is about 0.15g which is rated as strongly noticeable by the AAR standards.

10. It may be possible to reach critical wheel L/V ratios at under 110 mph at some switches on tangent track south of New York.
11. Wheelsets instrumented to measure force have been sufficiently developed as a practical means for making direct determinations of operating safety.
12. Operating safety criteria involving transient measurements have been interpreted conservatively because literature concerning transient phenomena is still sketchy.
13. The simple quasistatic curving model presented in this paper is useful for estimating the cant deficiency limits of passenger vehicles on relatively good track, especially when "as installed" measurements of suspension characteristics are included.

10.0 REFERENCES

1. Dean, F. E., and Ahlbeck, D. R., "Criteria for High Speed Curving of Rail Vehicles," ASME Paper No. 79-WA/RT-12, December 1979.
2. Ahlbeck, D. R., and Harrison, H. D., "An Evaluation of the Canadian LRC Train from Wayside Track Load Measurements on Curved and Perturbed Tangent Track," Report to Amtrak, May 1977.
3. Private conversation with Dr. F. B. Blader, The Analytic Sciences Corporation.
4. Anon., "Load Assumptions and Safety Margins for Rail Vehicles," publication of the study group Leichtbau der Verkehrsfahrzeuge and the Association of German Locomotive Manufacturers, 2nd Edition, 1970.
5. Kunieda, M., "Several Problems About Rolling Stock Which Can Run on Curves at High Speeds," Quarterly Reports, JNR Railway Technical Research Institute, Vol. 13, No. 1, 1972, pp. 1-7.
6. Anon., "Draft Final Report on Preliminary Design of Passive Tilt System for Amcoach," Japan Railway Technical Service report to FRA, May 1981.
7. Yokose, K., "A Theory of the Derailment of Wheelset," Quarterly Report, RTRI, Vol. 7, No. 3, 1966, pp. 30-34.
8. Matsudaira, T. M., "Dynamics of High Speed Rolling Stock," JNR Quarterly Report (Special Issue), 1962.
9. Koffman, J. L., "Four-Wheel Wagon Suspensions," Railway Gazette, No. 7, 1969, pp. 823-828.
10. Koffman, J. L., "Limitations of the Three-Piece Bogie," Railway Gazette, May 15, 1970, pp. 399-384.
11. Swenson, C. A., and Smith, K. R., Development and Use of Instrumented Locomotive Wheelsets, pre-print presented at International Conference on Wheel/Rail Load and Displacement Measuring Techniques, January 1981, at TSC.
12. Dean, F. E. and Ahlbeck, D. R., "Criteria for the Qualification of Rail Vehicles for High Speed Curving," a working paper for the Improved Passenger Equipment Evaluation Program, Federal Railroad Administration, October 1977.

13. Pocklington, A. R., "The B. R. Load Measuring Wheel," preprint presented at International Conference on Wheel/Rail Load and Displacement Measuring Techniques, January 1981 at TSC.
14. Koffman, J. L., "Higher Speeds through Curves," Railway Gazette, January 1970, pp. 60-64.
15. Anon., "Capability of Fasteners to Resist Rail Overturning," AAR Research Center, Report No. ER-77, November 1967.
16. Lawson, K. L., et al, "Northeast Corridor High Speed Rail Passenger Service Improvements Study - Task 9, Technical and Economic Analysis of Vehicle/Right of Way Systems, Vol. I," Report No. FRA-ONECD-73-9, August 1975.
17. Sonnevile, R. and Bentot, A., "Elastic and Lateral Strength of the Permanent Way," Bulletin of the International Railway Congress Association, November 1969, pp. 685-716.
18. Manual - Measuring Wheels for Amtrak, Swedish State Railways (SJ).
19. Instrumented Locomotive Wheels for Continuous Measurements of Vertical and Lateral Loads, Modransky, Donnelly, Novak, and Smith, ASME 79-RT-8, February 1979.
20. Anon., "Passenger Ride Comfort on Curved Track," AREA Committee Report, AREA Bulletin 516, Vol. 55, 1954, pp. 125-214.
21. Anon., "Task 19.2-Review of Lengths and Comfort Criteria for Spirals," Interim Report, Bechtel Corporation to Office of Northeast Corridor Development, FRA, December 1975.
22. Operational Test Plan for the LRC Cant Deficiency Test.
23. Cant Deficiency Test Events Report, ENSCO Report No. DOT-FR-81-08, July 1981.
24. AASHTO Standard Specifications of Structural Support for Highway Signs, Luminaires and Traffic Signals.

APPENDIX A
TEST DATA SUMMARY

A-i

CANT DEFICIENCY TEST RESULTS REPORT
INDEX TO APPENDIX A - TEST DATA SUMMARY

- Volume I - LRC Coach Data Summary
- Volume II - LRC Locomotive Data Summary
- Volume III - Amcoach Data Summary
- Volume IV - AEM-7 Locomotive Data Summary
- Volume V - NEC (New Haven - Providence) Curve Severity Data Summary for LRC Locomotive and LRC Coach at High Speed
- Volume VI - NEC (New Haven - Providence) Curve Severity Data Summary for LRC Locomotive and Amcoach at Track Speed
- Volume VII - NEC (New Haven - Providence) Curve Severity Data Summary for Amcoach at High Speed
- Volume VIII - NEC (New York - Washington) Curve Severity Data Summary for AEM-7 Locomotive at High Speed

APPENDIX B
QUASISTATIC CURVING MODEL

APPENDIX B

The simple quasistatic curving model shown in Figure B-1 was used to calculate weight vector intercept, vertical wheel force, total truck lateral force and lateral acceleration in the floor plane for comparison to the actual measurements. It takes into account the separate masses of the truck assembly (mass n) and the body (mass m) in a half vehicle representation. The suspension system is represented by an effective roll center which translates laterally with the body and has a roll stiffness, K_{θ} . The lateral stiffness considered at the secondary suspension is designated K_L . A computer program listed in this appendix along with a sample output was used for the convenient calculation of the above quantities as a function of cant deficiency. Vehicle constants obtained from manufacturers specifications and also from on site static experiments were used in the model. The constants for each vehicle from each source are listed in Appendix C.

The following terms are used in the quasistatic curving calculations:

- n = truck mass
- m = body mass
- V = speed in ft/sec
- S = crosslevel in inches
- D = curvature in degrees
- $r = 5730/D$ is the curve radius in feet
- $\theta = \sin^{-1} (S/60)$ is crosslevel angle
- $\alpha = \tan^{-1} (V^2/rg)$ is the deviation of the resultant force vector for the vertical axis
- ϕ = roll angle of the body
- $(\alpha - \phi)$ = angular cant deficiency
- $u = 60 \sin (\alpha - \phi)$ is the cant deficiency in inches
- K_L = lateral suspension stiffness in lb/in
- K_{ϕ} = overall roll rate in ft-lb/degree

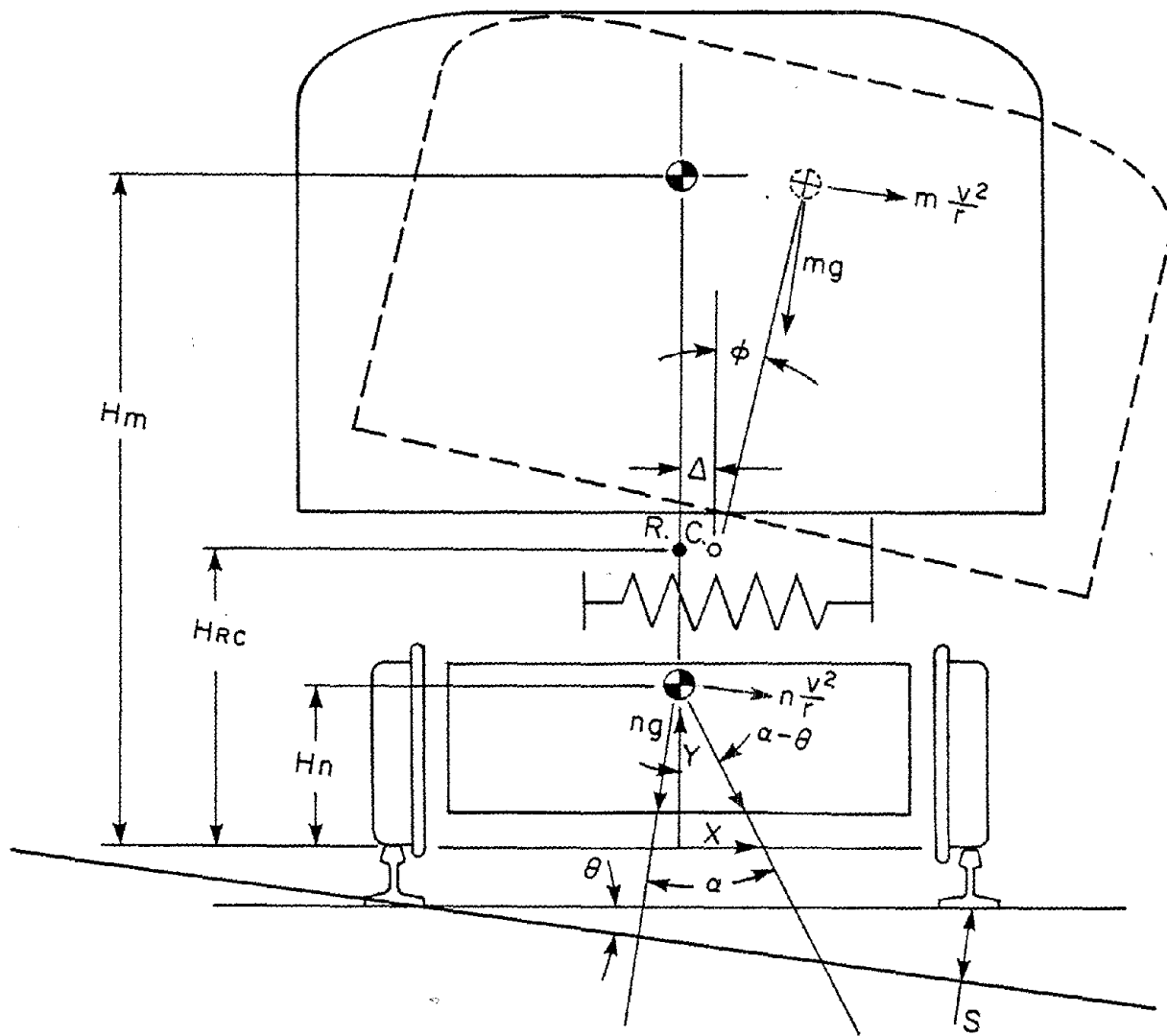


Figure B-1. Quasistatic Curving Model

The dimensions below are referenced to the track center line in the plane of the railheads:

- H_n = height of truck c.g., vehicle at rest
- X_n = lateral location of truck c.g.
- Y_n = vertical location of truck c.g.
- H_m = height of body c.g., vehicle at rest
- X_m = lateral location of body c.g.
- Y_m = vertical location of body c.g.
- H_{RC} = height of roll center

Figure B-2 illustrates the computation of the height of the effective roll center given by:

$$H_{RC} = H_S - A = H_S - \left[\frac{\frac{H_m - H_S + B}{L_p^2 K_p}}{\frac{H_m - H_S + B}{L_p^2 K_p} + \frac{2(H_m - H_S)}{L_s^2 K_s}} \right] B$$

where

- H_S = the height of the top of the secondary springs
- B = the distance between the tops of the secondary and primary springs
- K_p = the rate in lb/in of the primary suspension at one wheel
- L_p = the lateral spacing of the primary springs
- K_s = the rate in lb/in of the secondary suspension at one side
- L_s = the lateral spacing of the secondary springs

The following equations are derived from the model and computed by the program:

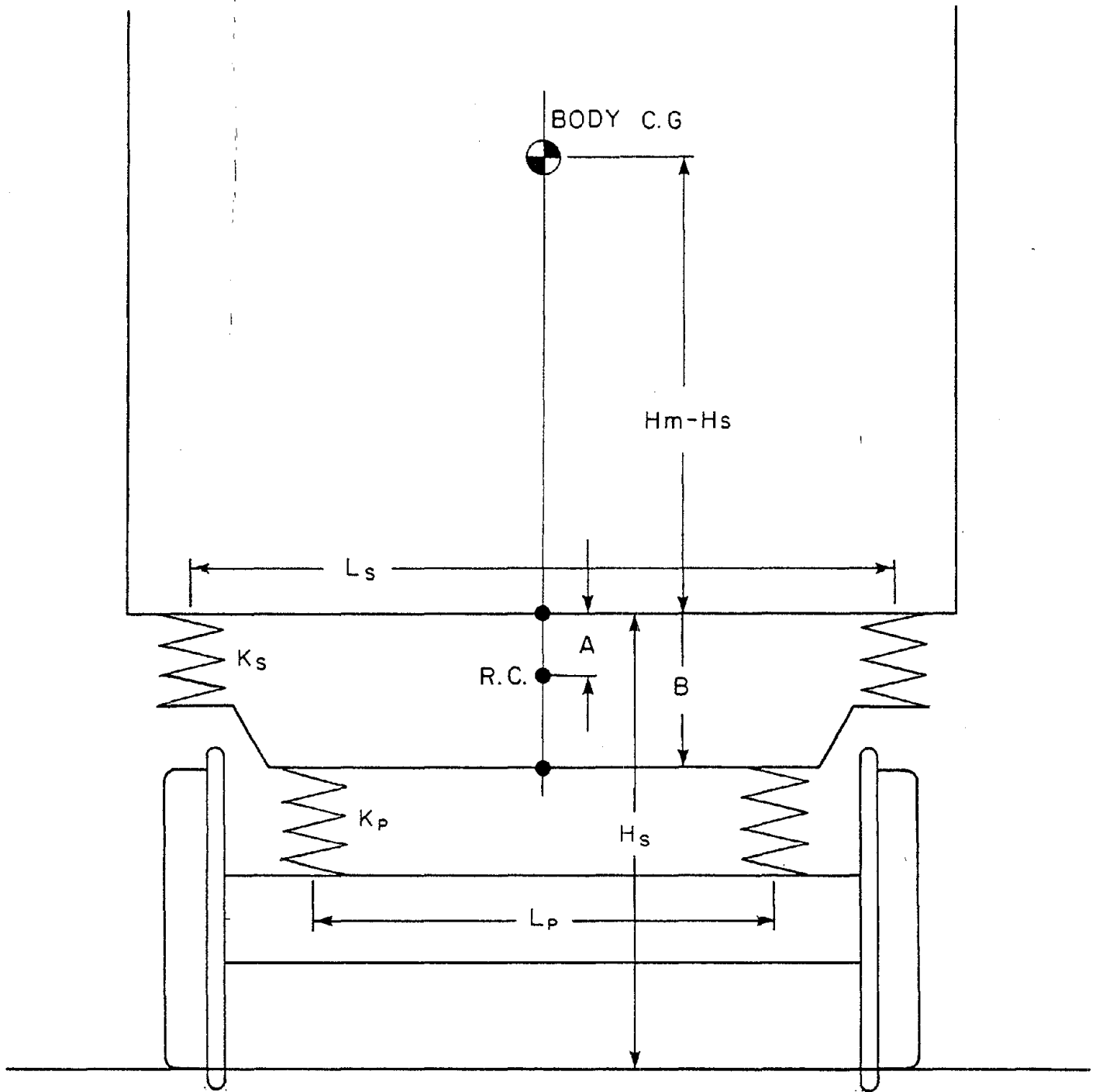


Figure B-2. Parameters for Effective Roll Center Height Calculation

LOCATION OF TRUCK C.G.

$$X_n = X_{on} \pm 1/2" \quad \begin{array}{l} + \text{ if } v^2/r > g \tan \theta \\ - \text{ if } v^2/r < g \tan \theta \end{array}$$

$$Y_n = H_n$$

LOCATION OF BODY C.G.

$$X_m = X_{om} \quad 1/2 + \frac{\frac{mV^2}{r} \cos \theta - mg \sin \theta}{K_L} + (H_m - H_{RC}) \sin \theta$$

where

$$\theta = \frac{(H_m - H_{RC}) \left(\frac{mV^2}{r} \cos \theta - mg \sin \theta \right)}{K_\phi}$$

but

$$\tan \alpha = \frac{v^2}{rg}$$

$$\therefore \frac{mV^2}{r} \cos \theta - mg \sin \theta = mg (\cos \theta \tan \alpha - \sin \theta)$$

and

$$\sin (\alpha - \theta) = \sin \alpha \cos \theta - \cos \alpha \sin \theta$$

$$\therefore \frac{\sin(\alpha-\theta)}{\cos \alpha} (\cos \theta) mg \sin \theta = \frac{mg \sin(\alpha-\theta)}{\cos \alpha} = \frac{mgu}{60 \cos \alpha}$$

So that

$$X_m = X_{om} \pm 1/2 + \frac{mgu}{60 K_L \cos \alpha} + (H_m - H_{RC}) \sin \phi$$

and

$$\phi = \frac{(H_m - H_{RC}) mgu}{60 \cos \alpha K_\phi}$$

$$Y_m = H_{RC} + (H_m - H_{RC}) \cos \phi$$

WEIGHT VECTOR INTERCEPT

$$VI = \frac{n[X_n + (Y_n) \tan (\alpha - \theta)] + m[X_m + (Y_m) \tan (\alpha - \theta)]}{n + m}$$

AVERAGE HIGH RAIL WHEEL LOAD

$$R_1 = 1/2 \left(\frac{30 + VI}{60} \right) (n + m) \left(g \cos \theta + \frac{V^2}{r} \sin \theta \right)$$

but

$$\tan \alpha = \frac{V^2}{rg}$$

$$\therefore R_1 = 1/2 \left(\frac{30 + VI}{60} \right) (n + m) g \cos \theta (1 + \tan \alpha \tan \theta)$$

AVERAGE LOW RAIL WHEEL LOAD

Similarly,

$$R_2 = 1/2 \left(\frac{30 + VI}{60} \right) (n + m) g \cos \theta (1 + \tan \alpha \tan \theta)$$

TRUCK LATERAL FORCE

$$F_{LT} = (n + m) \left(\frac{V^2}{r} \cos \theta - g \sin \theta \right) = \frac{(n + m)gu}{60 \cos \alpha}$$

ACCELEROMETER READING AT FLOOR PLANE

Floor angle = $\phi - \theta$

$$a_L = \frac{V^2}{r} \cos (\phi - \theta) + g \sin (\phi - \theta)$$

$$a_L = g \cos (\phi - \theta) (\tan \alpha + \tan (\phi - \theta))$$

for banking coach $\theta' = \theta + \theta_{\text{bank}}$

$$\therefore a_L = g \cos (\phi - \theta') (\tan \alpha + \tan (\phi - \theta'))$$

The following program in Basic performs the above calculations.
A sample output is included.

LIST

```
10 REM***QUASISTATIC CURVING MODEL TO PREDICT VECTOR INTERCEPT,  
11 REM***WHEEL FORCES,AND LATERAL ACCELERATION IN THE FLOOR PLANE  
12 REM***FORCES ARE EXPRESSED IN POUNDS,DISTANCE IN INCHES,  
13 REM***ACCELERATION IN g'S,AND ANGLES IN DEGREES  
20 PRINT "CROSSLEVEL";  
21 INPUT S  
30 PRINT "CURVATURE";  
31 INPUT D  
35 DIM V$(20)  
40 PRINT "ENTER VEHICLE IN QUOTES";  
41 INPUT V$  
50 PRINT "K sub phi ,ROLL RATE IN FT-LB/DEGREE";  
51 INPUT K1  
58 PRINT "FOR SINGLE STAGE SECONDARY LATERAL SUSPENSION"  
59 PRINT "ENTER ZEROS FOR STAGE 1 SPRING RATE AND COMPLIANCE !"  
60 PRINT "K sub L, LATERAL SPRING RATE IN LB/IN ,ENTER STG 1,STG 2";  
61 INPUT K2,K3  
65 PRINT "MAXIMUM LATERAL COMPLIANCE ,ENTER STG 1,STG 2";  
66 INPUT L1,L2  
70 PRINT "INPUT TRUCK WEIGHT COMA 1/2 BODY WEIGHT";  
71 INPUT W1,W2  
75 PRINT "WEIGHT OFFSET (POSITIVE TOWARD HIGH RAIL)";  
_76 INPUT D1
```

```

80 PRINT "HEIGHTS OF TRUCK C.G., BODY C.G., AND EFFECTIVE ROLL CENTER";
81 INPUT H1,H2,H3
90 LET T=S/60
91 LET T1=T*57.3
95 LET R=5730/D
100 PRINT
102 PRINT
110 PRINT "THE CURVE BEING MODELED HAS:"
120 PRINT "X-LEVEL, IN      ", "X-LEVEL, DEG.", "CURVATURE, DEG.", "RADIUS, FT"
130 PRINT S, T1, D, R
140 PRINT
141 PRINT
150 PRINT "THE VEHICLE BEING MODELED IS THE ";V$;" WITH THE CONSTANTS:"
160 PRINT "Ksub phi", "Ksub L#1", "Ksub L#2", "TRUCK WT.", "1/2 BODY WT."
165 PRINT K1, K2, K3, W1, W2
166 PRINT
170 PRINT "TRUCK C.G.", "BODY C.G.", "ROLL CNTR", "LAT. COMP.", "WT. DFST"
175 PRINT H1, H2, H3, L1;";";";L2, O1
180 LET G=32.2
185 PRINT
186 PRINT
187 PRINT
190 PRINT "CANT "; "SPEED "; "VECTOR "; "H VERT "; "L VERT ";
191 PRINT "TK LAT "; "ACCEL "; "THETA "; "ALPHA "; "PHI"

```



```

195 PRINT
200 FOR U=1 TO 15
210 LET V1=SQR((S+U)/(C.0007*D))
220 LET V2=V1*88/60
230 LET A=ATN((V2*V2)/(R*G))
240 LET A1=A*57.3
250 REM****COORDINATES OF TRUCK C.G.*****
260 LET D2=1/2
270 LET X1=D1+D2
280 LET Y1=H1
300 REM****COORDINATES OF BODY C.G.*****
310 LET D3=W2*U/(K2*60*COS(A))
312 IF D3<L1 THEN 330
314 LET D3=L1+(((W2*U)/(60*COS(A)))-K2*L1)/K3
320 IF D3>L2 LET D3=L2
330 LET P1=(H2-H3)*W2*U/(720*K1*COS(A))
340 LET P=P1/57.3
350 LET D4=(H2-H3)*SIN(P)
360 LET X2=D1+D2+D3+D4
370 LET Y2=H3+(H2-H3)*COS(P)
400 REM*****VECTOR INTERCEPT, V*****
410 LET V=(W1*(X1+Y1*TAN(A-T))+W2*(X2+Y2*TAN(A-T)))/(W1+W2)
420 REM****AVG HIGH RAIL WHEEL VERTICAL LOAD,F1*****
430 LET F0=.5*(W1+W2)*COS(T)*(1+TAN(A)*TAN(T))

```

```

440 LET F1=F0*(30+V)/60
450 REM*****AVG LOW RAIL VERTICAL LOAD,F2*****
460 LET F2=F0*(30-V)/60
470 REM*****NET TRUCK LATERAL FORCE,F3*****
480 LET F3=(W1+W2)*U/(60*COS(A))
490 REM*****LAT. ACCELERATION IN FLOOR PLANE*****
500 LET A2=COS(P-T)*(TAN(A)+TAN(P-T))
510 PRINT USING 520;U,V1,V,F1,F2,F3,A2,T1,A1,P1
520 IMAGE 2D.D,2X,3D.D,2X,2D.D,4X,3(5D,3X),D.3D,3(2X,2D.2D)
530 NEXT U
540 END

```

CROSSLEVEL?5.25
 CURVATURE?2.6
 ENTER VEHICLE IN QUOTES?"LRC LOCOMOTIVE, SPEC."
 K sub phi ,ROLL RATE IN FT-LB/DEGREE?22439
 FOR SINGLE STAGE SECONDARY LATERAL SUSPENSION
 ENTER ZEROS FOR STAGE 1 SPRING RATE AND COMPLIANCE !
 K sub L, LATERAL SPRING RATE IN LB/IN ,ENTER STG 1,STG 2?3200,20000
 MAXIMUM LATERAL COMPLIANCE ,ENTER STG 1,STG 2?1.5,2.6
 INPUT TRUCK WEIGHT COMA 1/2 BODY WEIGHT?38496,86904
 WEIGHT OFFSET (POSITIVE TOWARD HIGH RAIL)?0
 HEIGHTS OF TRUCK C.G.,BODY C.G.,AND EFFECTIVE ROLL CENTER?21.6,69.3,40.9

THE CURVE BEING MODELED HAS:

X-LEVEL,IN	X-LEVEL,DEG.	CURVATURE,DEG.	RADIUS,FT
5.25	5.01375	2.6	2203.85

THE VEHICLE BEING MODELED IS THE LRC LOCOMOTIVE, SPEC. WITH THE CONSTANTS:

Ksub phi	Ksub L#1	Ksub L#2	TRUCK WT.	1/2 BODY WT.
22439	3200	20000	38496.	86904.

TRUCK C.G.	BODY C.G.	ROLL CNTR	LAT. COMP.	WT. DFST
21.6	69.3	40.9	1.5	;2.6

CANT	SPEED	VECTDR	H VERT	L VERT	TK LAT	ACCEL	THETA	ALPHA	PHI
1.0	58.6	1.8	33359	29672	2101	0.019	5.01	5.94	0.15
2.0	63.1	3.0	34742	28380	4210	0.038	5.01	6.89	0.31
3.0	67.3	4.3	36128	27085	6329	0.058	5.01	7.82	0.46
4.0	71.3	5.4	37314	25991	8459	0.077	5.01	8.76	0.62
5.0	75.0	6.4	38421	24975	10601	0.096	5.01	9.69	0.77
6.0	78.6	7.4	39529	23958	12758	0.116	5.01	10.61	0.93
7.0	82.0	8.4	40638	22940	14931	0.135	5.01	11.53	1.09
8.0	85.3	9.3	41749	21921	17122	0.155	5.01	12.45	1.25
9.0	88.5	10.3	42860	20900	19333	0.174	5.01	13.35	1.41
10.0	91.5	11.3	43974	19878	21564	0.194	5.01	14.25	1.58
11.0	94.5	12.3	45088	18855	23817	0.213	5.01	15.15	1.74
12.0	97.4	13.3	46204	17830	26095	0.233	5.01	16.03	1.91
13.0	100.1	14.3	47322	16804	28397	0.252	5.01	16.91	2.08
14.0	102.8	15.3	48441	15776	30727	0.272	5.01	17.78	2.25
15.0	105.5	16.2	49562	14747	33085	0.292	5.01	18.64	2.42

APPENDIX C
VEHICLE CHARACTERISTICS

c-i

APPENDIX C
VEHICLE CHARACTERISTICS

The vehicle characteristics used in the quasistatic curving model in Appendix B and other characteristics of general interest are listed for each vehicle. The constants for the model are listed first. The value listed in or derived from the manufacturer's specifications is given first and a second value for some constants which was measured experimentally is also included:

The effective roll center as described in Appendix B was derived from the manufacturer's specifications by the following relation (see Figure B-2):

$$H_{RC} = H_s - A = H_s - \left[\frac{\frac{H_m - H_s + B}{L_p^2 K_p}}{\frac{H_m - H_s + B}{L_p^2 K_p} + \frac{2(H_m - H_s)}{L_s^2 K_s}} \right] B$$

where

H_s = the height of the top of the secondary springs

B = the distance between the tops of the secondary and primary springs

K_p = the rate in lb/in of the primary suspension at one wheel

L_p = the lateral spacing of the primary springs

K_s = the rate in lb/in of the secondary suspension at one side

L_s = the lateral spacing of the secondary springs

It was determined experimentally by:

$$H_{RC} = H_s - A = H_s - \frac{\phi_p}{\phi_p + \phi_s} B$$

where ϕ_p is the roll angle of the primary suspension measured with the vehicle parted on track having about 6 inches of cross-level, and ϕ_s is the secondary suspension roll angle measured under the same condition.

The overall roll rate K_ϕ (ft-lb/degree) was derived from the vehicle specifications as follows:

$$\frac{1}{K_\phi} = \frac{1}{K_{\phi p}} + \frac{1}{K_{\phi s}}$$

where the primary suspension roll rate,

$$K_{\phi p} = \frac{2L_p^2 K_p}{1375}$$

where:

L_p = the lateral spacing of the primary springs in inches

K_p = the rate in lb/in of primary suspension at one wheel

and the secondary suspension roll rate,

$$K_{\phi s} = \frac{L_s^2 K_s}{1375}$$

where

L_s = the lateral spacing of the secondary springs in inches

K_s = the rate in lb/in of the secondary suspension at one side of the truck.

K_ϕ was determined experimentally by parking the vehicle on track having a crosslevel angle θ and measuring the body roll angle ϕ . K_ϕ can be computed as:

$$K_{\phi} = \frac{(H_m - H_{rc}) mg \sin \theta}{l_{2\phi}}$$

where H_m is the body c.g. height and m is the body mass.

The weight offset at the instrumented truck was determined by measuring the weight vector intercept and averaging over several tangent sections. The weight offset is considered as a vehicle c.g. offset in a half vehicle model but it is possible that an opposite offset would be measured at the rear truck and the vehicle c.g. is actually on the centerline.

LRC LOCOMOTIVE

	<u>SPECIFICATION</u>	<u>OBSERVED</u>
Truck Weight, w_1 or W1	38,496 lb	
Half Body Weight, w_2 or W2	86,904 lb	
Truck c.g. Height, H_n or H1	21.6 in	
Body c.g. Height, H_m or H2	69.3 in	
Vehicle c.g. Height	54.7 in	
Effective Roll Center Height, H_{RC} or H3	40.9 in	41 in
Overall Roll Rate, K_ϕ	22,439 ft-lb/deg	8,130 ft-lb/deg
Secondary Lateral Spring Rate, K_L	3,200 lb/in to 1.5 in 20,000 lb/in to 2.6 in	2,710 lb/in to 3
Lateral Compliance	2.6 in	3 in
Weight Offset		.95 in Left
<u>Primary Suspension:</u>		
Wheel Rate, K_p	27,300 lb/in	
Lateral Wheel Rate	120,000 lb/in	
Lateral Spacing, L_p	79 in	
Spring Top Height, H_p		36 in
<u>Secondary Suspension:</u>		
Vertical Spring Rate per side, K_s	4,650 lb/in	
Vertical Spring Spacing, L_s	102 in	
Vertical Spring Top Height, H_s		45 in
Vertical Rate of Lateral Spring Per Side, K'_s	1,000 lb/in	
Lateral Spring Spacing, L'_s	46 in	
Truck Wheelbase	114 in	
Wheel Diameter	40 in	
Truck Spacing (Vehicle Wheelbase)	488 in	
Body Length	62 ft	
Body Height	11 ft	
Approximate Lateral Surface Area		682 ft ²
Height of Center of Wind Pressure		6-1/2 ft

LRC COACH

	<u>SPECIFICATION</u>	<u>OBSERVED</u>
Truck Weight, w_1 or W1	17,000 lb	
Half Body Weight, w_2 or W2	35,750 lb+6000 lb Load	
Truck c.g. Height, H_n or H1	18.5 in	
Body c.g. Height, H_m or H2	65.5 in	
Vehicle c.g. Height	51.9 in	
Effective Roll Center Height, H_{RC} or H3	29.1 in	
Overall Roll Rate, K_ϕ	4,360 ft-lb/deg	4,370 ft-lb/deg
Secondary Lateral Spring Rate, K_L	1,420 lb/in to 1.82 in 6,400 lb/in to 2.38 in	
Lateral Compliance	2.38 in	
Weight Offset	0	.58 in Right
<u>Primary Suspension:</u>		
Wheel Rate, K_p	5,750 lb/in	
Lateral Wheel Rate	75,000 lb/in	
Lateral Spacing, L_p	43.75 in	
Spring Top Height, H_p		16 in
<u>Secondary Suspension:</u>		
Vertical Spring Rate per side, K_s	1,065 lb/in	
Vertical Spring Spacing, L_s	88 in	
Vertical Spring Top Height, H_s	38 in	
Truck Wheelbase	97 in	
Wheel Diameter	30 in	
Truck Spacing (Vehicle Wheelbase)	678 in	
Body Length	85 ft	
Body Height	11 ft	
Approximate Lateral Surface Area		935 ft ²
Height of Center of Wind Pressure		6-1/2 ft

AMCOACH

	<u>SPECIFICATION</u>	<u>OBSERVED</u>
Truck Weight, w_1 or W1	13,710 lb	
Half Body Weight, w_2 or W2	38,475 lb+6000 lb Load	
Truck c.g. Height, H_n or H1	22.2 in	
Body c.g. Height, H_m or H2	75.3 in	
Vehicle c.g. Height	62.8 in.	
Effective Roll Center Height, H_{RC} or H3	39.2 in	
Overall Roll Rate, K_ϕ	10,700 ft-lb/in	7,460 ft-lb/in
Secondary Lateral Spring Rate, K_L	4,000 lb/in	7,500 lb/in
Lateral Compliance	1 in	0.9 in
Weight Offset	0	1.02 in Left
<u>Primary Suspension:</u>		
Wheel Rate, K_p	161,250 lb/in	
Lateral Wheel Rate	1,025,000 lb/in	
Lateral Spacing, L_p	46 in	
Spring Top Height, H_p	18	
<u>Secondary Suspension:</u>		
Vertical Spring Rate per side, K_s	1,850 lb/in	
Vertical Spring Spacing, L_s	90 in	
Vertical Spring Top Height, H_s	40 in	
Truck Wheelbase	102 in	
Wheel Diameter	36 in	
Truck Spacing (Vehicle Wheelbase)	714 in	
Body Length	85 ft	
Body Height		9 ft
Approximate Lateral Surface Area		765 ft ²
Height of Center of Wind Pressure		7-1/2 ft

AEM-7 LOCOMOTIVE

	<u>SPECIFICATION</u>	<u>OBSERVED</u>
Truck Weight, w_1 or W1	40,348 lb	
Half Body Weight, w_2 or W2	58,740 lb	
Truck c.g. Height, H_n or H1	31.2 in	
Body c.g. Height, H_m or H2	90.4 in	
Vehicle c.g. Height	66.3 in	
Effective Roll Center Height, H_{rc} or H3	34.6 in	36 in
Overall Roll Rate, K	32,260 ft-lb/deg	12,400 ft-lb/deg
Secondary Lateral Spring Rate, K_L	3,000 lb/in to 1 in	3,700 lb/in to 1 in
Lateral Compliance	2 in	2.5 in
Weight Offset	0	1.12 in Right
<u>Primary Suspension:</u>		
Wheel Rate, K_p	17,125 lb/in	
Lateral Wheel Rate	79,650 lb/in	
Lateral Spacing, L_p		76 in
Spring Top Height, H_p		25.5 in
<u>Secondary Suspension:</u>		
Vertical Spring Rate per side, K_s	5,595 lb/in	
Vertical Spring Spacing, L_s		101.5 in
Vertical Spring Top Height, H_s		38 in
Truck Wheelbase	96.5 in	
Wheel Diameter	51 in	
Truck Spacing (Vehicle Wheelbase)	307 in	
Body Length	50 ft	
Body Height		10 ft
Approximate Lateral Surface Area		500 ft ²
Height of Center of Wind Pressure		7-1/2 ft

APPENDIX D
SUMMARY REPORT ON WAYSIDE
MEASUREMENS - BATTELLE

D-1

Summary Report

on

LRC TRAINSET CANT DEFICIENCY TESTS
-- VEHICLE/TRACK DYNAMIC RESPONSE
FROM WAYSIDE MEASUREMENTS

to

ENSCO, INC.

from

BATTELLE
Columbus Laboratories

by

D. R. Ahlbeck and J. M. Tuten

January 9, 1980